ROLE OF STAT3 IN THE REGULATION OF MAMMALIAN PROTEASOME: Implications for Cancer and Proteasome Associated Disorders

Thesis submitted for the award of

DOCTOR OF PHILOSOPHY

In

BIOCHEMISTRY

By

JANAKIRAM REDDY VANGALA

July, 2014; Enrolment No. 09LBPH23

Department of Biochemistry
School of Life Sciences
University of Hyderabad
PO Central University, Gachibowli
Hyderabad 500 046
Telangana State, INDIA

ROLE OF STAT3 IN THE REGULATION OF MAMMALIAN PROTEASOME: Implications for Cancer and Proteasome Associated Disorders

Thesis submitted for the award of

DOCTOR OF PHILOSOPHY

In

BIOCHEMISTRY

UNIVERSITY OF HYDERABAD
HYDERABAD

By

JANAKIRAM REDDY VANGALA

July, 2014; Enrolment No. 09LBPH23

CENTRE FOR CHEMICAL BIOLOGY
CSIR - Indian Institute of Chemical Technology
Hyderabad- 500007, Telangana State.

2014

Dedicated to

My parents & Sisters

CERTIFICATE

This is to certify that research work presented in this thesis entitled **ROLE OF STAT3 IN THE REGULATION OF MAMMALIAN PROTEASOME: Implications for Cancer and Proteasome Associated Disorders** has been done by **Mr. VANGALA JANAKIRAM REDDY** under my supervision at Indian Institute of Chemical Technology (IICT), Hyderabad, India. This work is original and has not been submitted previously in part or full to any other university for any other degree or diploma.

Dr. Shasivardhan Kalivendi

(Supervisor)

DECLARATION

I, Vangala Janakiram Reddy, hereby declare that this thesis entitled **ROLE OF STAT3 IN THE REGULATION OF MAMMALIAN PROTEASOME: Implications for Cancer and Proteasome Associated Disorders** submitted by me is an original and independent research work carried out under the guidance of **Dr. Shasi vardhan Kalivendi**, at Indian Institute of Chemical Technology (IICT), Hyderabad. The results of this thesis have not been submitted previously in part or full to any other university for any other degree or diploma.

Date:

Name: Vangala Janakiram Reddy

Regd.No: 09LBPH23

Acknowledgements

First and foremost I would like to express my deepest gratitude for my supervisor, Dr. Shasivardhan Kalivendi. I have been amazingly fortunate to have a supervisor like him who gave me the freedom to explore. His constant guidance, cooperation and support assisted me in overcoming many a crisis related to matters both professional and personal. His immense patience with me throughout this period has been out of the ordinary. THANK YOU SIR.

I am indebted to Dr. Nishant Jain. This work could not have taken the present form without his support. I am very grateful for the training imparted by him which made me ready to combat situations. He is an excellent teacher to learn the basics of experimentation.

I would like to thank the past and present directors of IICT, Dr. J S Yadav and Dr. Lakshmi Kantam, for the excellent working atmosphere and infra structural facilities at centre for chemical biology.

I thank the Dean, Prof.A.S. Raghavendra and the Head of Department of Biochemistry, Prof. Shiva Kumar for allowing me to pursue this study.

I would like to thank the Head of Centre for Chemical Biology, Dr. Manika pal Bhadra for introducing me to Chemical Biology and always being so approachable. I am grateful for her constant support and encouragement and valuable suggestions, both personal and professional.

Thanks are also due to Dr. Srigiridhar Kotamraju and Dr. Anthony Addlagatta for their support and suggestions which bailed me out of tough situations. I request them to continue doing the same always. I thank Dr. Ramesh Ummani for his friendly nature valuable suggestions.

I owe deep sense of gratitude to Dr. Nagabhushana for his valuable trouble shooting tips and constructive suggestions during the writing of my paper. My sincere thanks to Dr. Dwijendra Reddy, Dr. Vijay Gupta and Dr. Vipul for providing vectors and help in writing the manuscript. I thank Rachna Jain for sequencing and providing the necessaries for plasmid isolations and Kunal, who was always ready to help with any doubts I had about the protocols.

I would like to thank both my past and present colleagues Dr. Deepthi, Madhuri, Deepa, Ravali, Durga Prasad, Madhumanti and Vishnu for their continuous support. Special thanks to Srikanth Dudem for being with me at all times to complete the project successfully. I am thankful to my former labmate and friend Shiva Nageshwar Rao for his financial aid during the end of my fellowship period.

I am grateful to Murthy and Supriya for fun filled lunches and everlasting moral support throughout the time inaddition to their help with chemical reagents and work. I thank Lakshminarayana Reddy, Santosh, Anver Basha for their critical suggestions and help in writing of this thesis. I also thank my seniors Dr. Suman, Dr. Avijeet, Dr. Shiva and my

colleagues at cellar Basha, Hema, Surekha for their moral support throughout this learning phase. A special word of gratitude to Suresh for teaching me Flowcytometry and Kazamuddin for all the administrative help.

Certainly playing all kinds of sports, facing the opponents with my ever energetic colleagues, their endless strategies and fun filled comments are one of the most memorable and joyful moments I have had during this period. I thank my unique team where each and every person at the same time is the captain, coach, player, sponsor and also the spectator. Thanks Abhinav, Pankaj, Bhanu, Bala Bhaskar, Raghunath, Pardes, Koteshwara rao (Sr), Santosh, Sathish, Raja, Sunil, Ravi, Tarun, Chandan, Rajesh, Laksmi Naryana, Loka Reddy, Utkarsh Reddy, Vijay and Koti (Jr) for all the fun. Special thanks to our team manager Venkateshwarlu (Saddanapu).

I wish to thank all the lab members of Dr. Srigiridhar, Dr. Anthony, Dr. Ramesh, Dr. Nishant, Dr. Manika pal Bhadra and Dr. Amitava Das who have helped create an amiable work environment which helped me carry out my work with ease.

I thank my friends Fathima, Poonam Sehgal and Suresh Kumar for their constant support and generosity with reagents. Fathima deserves special thanks for bearing my long sessions of stupidity and helping me in proof reading the thesis. No less Suresh has been my helpline for everything I've ever needed. I would like to thank my friends and seniors Sridevi, Balakrishna, Chintala, Arsani, Ramchandra, Kashyap, Saidulu, Shasi, Raju padia, Vijay, Jahangeer, Narasimha, Shyam, Vinay, Venkat Reddy and many more for their help. I also thank all the teaching and non-teaching faculty of Department of Biochemistry, University of Hyderabad for their timely help and cooperation.

I also greatly appreciate help from our lab boys Mr. Narender and Mr. Raju.

I am grateful to the almighty for imparting strength, perseverance and sagacity to go through this entire phase and indeed throughout my life as without his blessings I would not have come this far. No words can express my gratitude for the love, care and support shown by my ***BIG FAMILY*** *no matter what the situation.*

Last but not the least, I would like to thank ICMR for the fellowship.

Janaki Ram

Section		Page
List of Abbreviations		**i**
List of Figures		**iii**
Table of Nomenclature of 20S Proteasome Subunits		**vi**
Synopsis		**vii**
Chapter 1	**Introduction**	1
1.1	**Ubiquitin Proteasome System**	1
1.1.1	Ubiquitin and Ubiquitination	2
1.1.2	26S Proteasome	4
1.2	**Structure and Assembly of 26S Proteasome**	4
1.2.1	Structure of 20S Proteasome	4
1.2.2	19S RP (PA700)	6
1.2.3	Assembly of 20S Proteasome	7
1.2.4	Localization	8
1.2.5	Modifications of Proteasome Subunits	8
1.3	**Types of Proteasome**	9
1.3.1	Immunoproteasome	9
1.3.2	Thymoproteasome	10
1.4	**Biological Functions of UPS**	10
1.4.1	Inflammation and Auto Immunity	10
1.4.2	Neurological Disorders	11
1.4.3	Development	11
1.4.4	Differentiation	11
1.4.5	Regulation of Gene expression	12
a)	Transcriptional Regulation	12
b)	Translational Regulation	13
1.4.6	RNase Activity of Proteasome	13
1.4.7	Reprogramming of Proteasomes	13
1.4.8	Role of Proteasome in Cancer	14

1.5	**Inhibitors of Proteasome**	16
1.5.1	Types of Inhibitors	16
1.5.2	Mechanism of Apoptosis	17
1.6	**Resistance to Bortezomib**	18
1.6.1	Point Mutations of PSMB5	18
1.6.2	Overexpression of PSMB5	19
1.6.3	Altered Expression of Proteins	20
1.7	**Regulation of Proteasome**	20
1.7.1	Feedback Up-regulation of Proteasome	20
1.7.2	Basal Regulation of Proteasome	22
1.7.3	Nrf1 (NF-E2-related factor 1)	23
1.7.4	Nrf2 (NF-E2-related factor 2)	23
1.8	**EGFR (Epidermal Growth Factor Receptor)**	24
1.8.1	Structure of EGFR	24
a)	Extracellular Ligand-Binding Domain	24
b)	Transmembrane Domain	25
c)	Intracellular Domain	25
1.8.2	Activation of EGFR	25
1.8.3	EGFR Inactivation	26
1.8.4	Constitutive Activation of EGFR	27
1.8.5	Downstream Targets of EGFR	28
a)	Activation of MAPK/ERK1/2 Pathway	28
b)	Activation of PI3K/Akt Pathway	28
c)	Activation of PLC-γ	29
1.9	**STAT3 (Signal Transducer and Activator of Transcription)**	29
1.9.1	Activation of STAT3	29
a)	Tyrosine-705 Phosphorylation	30
b)	Serine-727 Phosphorylation	30
1.9.2	Negative Regulators of STAT3	31
a)	Tyrosine phosphatases	31
b)	Suppressors of Cytokine Signalling (SOCS) Proteins	31

c) Protein Inhibitors of Activated STATs (PIAS) 32
1.9.3 Role of STAT3 in Cancer 32

1.10 Back ground, Aims & Objectives 34

Chapter 2 Materials and Methods 36
2.1 Materials 37
2.1.1 Sources of Chemicals 37
2.1.2 Antibodies 37
2.1.3 Bacterial Strains 38
2.1.4 Cell Lines 38
2.1.5 Plasmids 39
2.1.6 Substrates 39
2.1.7 Media, Antibiotics and Chemical Stocks 40
2.2 Methods 42
2.2.1 Plasmid Isolation 42
2.2.2 Quantitation of Nucleic Acids 43
2.2.3 Agarose Gel Electrophoresis 43
2.2.4 Restriction Endonuclease Digestion 43
2.2.5 Gel Elution of DNA Fragments 43
2.2.6 Ligation 43
2.2.7 Preparation of Ultracompetent Cells 44
2.2.8 DNA Sequencing 44
2.2.9 RNA Isolation 44
2.2.10 Genomic DNA isolation 45
2.2.11 Polymerase Chain Reaction (PCR) 45
2.2.12 Reverse Transcription and Polymerase Chain Reaction (RT-PCR) 46
2.2.13 Quantitative Real-Time PCR (qRT-PCR) 47
2.2.14 Identification of Putative STAT3 Binding Sites in 20S Proteasome Subunits 48
2.2.15 Construction of Vectors for Expressing Short-hairpin RNA (ShRNA) 49

2.2.16	Generation of Adenoviruses Expressing STAT3	50
2.2.17	Mammalian Cell Culture	51
2.2.18	Transfection of DNA in Mammalian Cells	51
2.2.19	Immunofluorescence	52
2.2.20	Quantification of Proteins	52
2.2.21	SDS-Polyacrylamide Gel Electrophoresis (SDS-PAGE)	53
2.2.22	Western Blotting	53
2.2.23	β-Galactosidase Assay	54
2.2.24	Luciferase reporter (LUC) Assay	54
2.2.25	Sequence Analysis	54
2.2.26	Measurement of Caspase-3 Activity	55
2.2.27	Measurement of 20S Proteasome Activity	55
2.2.28	26S Proteasome Activity Assay	56
2.2.29	Measurement of Apoptosis by Flow Cytometry	56
2.2.30	Statistical Analysis	57
Chapter 3	**Regulation of PSMB5 and β-Subunits of Proteasome by STAT3**	58
3.1	**Introduction**	59
3.2	**Results**	60
3.2.1	Inhibition of activated STAT3 down regulated PSMB5 in DU 145 cells	60
a)	Effect of Stattic treatment on PSMB5 expression	60
b)	Effect of WP1066 on PSMB5 expression	61
c)	Effect of Resveratrol on PSMB5 expression	62
d)	Effect of STAT3 knockdown on PSMB5 expression	63
3.2.2	STAT3 inhibition coordinately down regulated the expression of a majority of 20S proteasome subunits in DU 145 cells	63

3.2.3 Suppression of pSTAT3 down-regulated PSMB5 in pSTAT3 constitutive cells 64
3.2.4 Proteasome subunits expression was unaltered by STAT3 inhibition in prostate normal and cancer cells devoid of constitutive pSTAT3 65
3.2.5 Suppression of pSTAT3 abrogated proteasome activities and cell viability in cells expressing constitutively active STAT3 67
3.2.6 Inhibition of pSTAT3 unaltered proteasome activities in prostate cells lacking constitutively active STAT3 69
3.2.7 Proteasome inhibitor induced apoptosis unaltered PSMB5 expression 70
3.2.8 Levels of proteasome activity and PSMB5 expression in cancer cell lines 70
a) PSMB5 expression correlates with intracellular levels of pSTAT3 70
b) Proteasome activities are higher in cells possessing constitutively active STAT3 71
3.2.9 Effect of exogenous expression of STAT3 on proteasome 72
a) Overexpression of STAT3 increased PSMB5 mRNA and protein levels 72
b) Enhanced proteasome activity by overexpression of STAT3 72
c) STAT3 dependent transactivation of PSMB5 promoter 73
3.2.10 Identification of STAT3 responsive sites in the consensus promoters of proteasome subunits 73

3.3 Discussion 73

Chapter 4 EGF-Induced Activation of Proteasome Subunits Through STAT3 77
4.1 Introduction 78
4.2 Results 79
4.2.1 EGF up-regulates the expression of PSMB5 79
4.2.2 EGF/ EGFR induced expression of PSMB5 requires STAT3 activation 79
4.2.3 Blockade of EGFR coordinately down-regulated the expression of proteasome subunits 81
4.2.4 PSMB5 protein levels are unresponsive to EGF in STAT3-negative PC-3 cells 82
4.2.5 Feedback regulation of proteasome subunits in prostate cancer cells 82
4.2.6 Bortezomib exacerbates STAT3 inhibitor-induced lose of proteasome expression, function and cellular apoptosis 83
4.3 Discussion 84

Summary of Results 88

References 90

Publications 121

List of Abbreviations

%	percent
µ	micron
°C	degrees Celsius
µg	microgram
µl	microliter
AMPK	AMP dependent kinase
ATP	adenosine triphosphate
BCIP	2-bromo, 3-chloro indolyl phosphate
bp	base pair
BSA	bovine serum albumin
CAT	chloramphenicol acetyl transferase
CD	cluster of differentiation 28
CDK	cyclin dependent kinase
cm	centimetre
CMV	cytomegalovirus
CR	cysteine rich
Cy3	indocarbocyanine
DAPI	4', 6-Diamidino-2-phenylindole dihydrochloride
DEPC	diethylpyrocarbonate
DMEM	Dulbecco's modified Eagle medium
DNase	deoxyribonuclease
DTT	dithiothreitol
ECL	enhanced chemiluminiscence
EDTA	ethylene diamine tetra acetic acid
EGF	epidermal growth factor
EGFP	enhanced green fluorescent protein
ERK	Extracellular signal regulated kinases
FBS	fetal bovine serum
FITC	fluorescein isothiocyanate
g	unit gravitational force
G1	first gap phase
GFP	green fluorescent protein
gm	gram
HCl	hydrochloric acid
HECT	homologous to the E6-AP carboxyl terminus
HEPES	(N-[2-Hydroxy ethyl] piperazine-N'-[2-ethane sulphonic acid])
hr	hour
HRP	horseradish peroxidase
IFN-γ	interferon-gamma
IGF-1R	insulin like growth factor -1 receptor
IL	interleukin
IPTG	isopropyl-beta-D-thiogalactoside
IR	insulin receptor
kDa	kilodalton
KEAP 1	kelch-like ECH-associated protein 1

LB	ligand binding
M	molar
mA	milliampere
MAPK	mitogen activated protein kinase
mg	milligram
min	minute
ml	milliliter
mm	millimeter
mM	millimolar
MOPS	3-[N-morpholino] sulphonic acid
mTOR	mammalian target of rapamycin
NLS	nuclear localization signal
nm	nanometer
OD_{260}	optical density at 260 nm
PAC	proteasome assembling chaperones
PAGE	polyacrylamide gel electrophoresis
PBS	phosphate buffered saline
PCR	polymerase chain reaction
PDGFR	platelet derived growth factor receptor
PMSF	phenyl methyl sulphonyl fluoride
PTK	protein tyrosine kinase
PTP	protein tyrosine phosphatase
PVDF	poly vinylidine difluoride
RING	really interesting new gene
RNA	ribonucleic acid
rpm	revolutions per minute
RT	reverse transcription
SDS	sodium dodecyl sulphate
TBST	Tris buffered saline containing tween-20
TCA	trichloroacetic acid
TEMED	N,N,N',N'-tetramethylene diamine
v	volume
V	volt
X-gal	5-bromo-4-chloro-3-indolyl-β-D-galactoside
IgG	immunoglobulin G

List of Figures

Chapter 1 Introduction

Figure 1.1 Schematic view of the Ubiquitin-Proteasome System

Figure 1.2 Schematic representation of the 19S, 20S and the formation of 26S proteasome

Figure 1.3 Assembly of 20S proteasome

Figure 1.4 Factors leading to the bortezomib resistance, a schematic view

Figure 1.5 Signalling pathways activated by EGFR

Figure 1.6 Activation and function of STAT3 in Cancer

Chapter 3 Regulation of PSMB5 and β-Subunits of Proteasome by STAT3

Figure 3.1 Dose and Time dependent inhibition of pSTAT3 down regulated PSMB5 expression

Figure 3.2 Inhibition of pSTAT3 down regulated PSMB5 expression

Figure 3.3 Resveratrol decreases the expression of PSMB5 in a dose dependent manner

Figure 3.4 Down regulation of PSMB5 by STAT3-ShRNA

Figure 3.5 Effect of STAT3 inhibition on mRNA and protein levels of 20S proteasome subunits

Figure 3.6 Effect of WP1066 on expression of 20S proteasome subunits

Figure 3.7 Stattic down regulated PSMB5 protein levels in pSTAT3 constitutive cell lines

Figure 3.8 WP1066 decreases protein levels of PSMB5 in STAT3 constitutively active cell lines

Figure 3.9 20S proteasome subunits were unaltered by STAT3 inhibitors in PC-3

Figure 3.10 Inhibition of pSTAT3 unaffected the 20S proteasome subunits in LNCaP

Figure 3.11 Inhibition of pSTAT3 don't effect the expression of 20S proteasome subunits in WPMY-1A

Figure 3.12 Inhibition of pSTAT3 abrogates proteasome activity in pSTAT3 constitutive cell lines

Figure 3.13 Inhibition of pSTAT3 decreases proteasome activity in STAT3 constitutively active cell lines

Figure 3.14 Inhibition of pSTAT3 induced Caspase-3 activity in pSTAT3 constitutive cells

Figure 3.15 WP1066 induced caspase-3 activity in pSTAT3 constitutive cells

Figure 3.16 Proteasome activities were unaltered due to pSTAT3 inhibition in prostate cells

Figure 3.17 Stattic induced Caspase-3 activity in prostate cells

Figure 3.18 Effect of proteasome inhibition on PSMB5 expression

Figure 3.19 High levels of PSMB5 in constitutively active STAT3 cells

Figure 3.20 Increased proteasomal activities in cancer cells

Figure 3.21 Exogenous expression of STAT3 induced PSMB5 expression

Figure 3.22 Increased PSMB5 promoter and activity by pSTAT3

Figure 3.23 Putative STAT3 binding sites in the promoter regions of 20S proteasome subunits

Chapter 4 EGF- Induced Activation of Proteasome Subunits Through STAT3

Figure 4.1 EGF induces the expression of PSMB5

Figure 4.2 Blockade of EGFR, STAT3 down-regulates EGF induced PSMB5 expression

Figure 4.3 EGF induced PSMB5 protein levels were unvaried due to ERK/MAP and PI3K/Akt inhibition

Figure 4.4 Blockade of EGFR down-regulates the expression of EGF induced various 20S proteasome subunits

Figure 4.5 Inhibition of EGFR down-regulated mRNAs of various 20S proteasome subunits

Figure 4.6	Lack of STAT3 impedes EGF-induced PSMB5 expression in PC-3 cells
Figure 4.7	Feed back induction of proteasome sub units are not regulated by STAT3
Figure 4.8	Inhibition of pSTAT3 unaltered the feedback induction of proteasome subunits
Figure 4.9	Feed back induction of proteasome sub units are regulated by STAT3
Figure 4.10	Synergistic inhibition of proteasome activities by Co treatments of proteasome and STAT3 inhibitors
Figure 4.11	Bortezomib enhanced pSTAT3 inhibition induced loss of PSMB5 and proteasome expression and function
Figure 4.12	Enhanced activation of apoptosis by pSTAT3 and proteasome inhibition
Figure 4.13	Proposed model of EGF/EGFR mediated regulation of PSMB5 and proteasome
Figure 4.14	Schematic representation on the synergistic role of STAT3 Inhibition in enhancing the anticancer effects of the proteasome inhibitors

TABLE OF NOMENCLATURE OF 20S PRTOEASOME SUBUNITS

Systematic Nomenclature	HUGO	Miscellaneous Nomenclature
α1	PSMA6	Iota
α2	PSMA2	C3
α3	PSMA4	C9
α4	PSMA7	C6
α5	PSMA5	zeta
α6	PSMA1	C2
α7	PSMA3	C8
β1	PSMB6	Y, delta
β2	PSMB7	Z
β3	PSMB3	C10
β4	PSMB2	C7
β5	PSMB5	X, MB1, epsilon
β6	PSMB1	C5
β7	PSMB4	N3, beta
β1i	PSMB9	LMP2, RING12
β2i	PSMB10	MECL1, LMP10
β5i	PSMB8	LMP7, RING10
β5t	PSMB11	

Synopsis

Introduction:

Ubiquitin Proteasome system (UPS) is the major proteolytic machinery that degrades long and short-lived proteins and is involved in a variety of cellular functions. Ubiquitin recognizes and presents target proteins to 26S proteasome for degradation. The 26S proteasome consists of 20S core proteasome complex responsible for proteolysis and 19S regulatory particle helps in recognition, deubuiquitination and transfer of targeted protein to 20S core particle. The 20S proteasome complex is made of outer two α rings and inner two β rings (αββα). Each α and β ring consists of 7 subunits i.e. α1-7, β1-7. α-subunits maintain the structure and each β-ring contains catalytically active subunits, such as, PSMB5 (β5), PSMB6 (β1), PSMB7 (β2) which possess chymotrypsin-like, caspase-like and trypsin-like activities respectively. These activities are stringently controlled and adjusted according to cellular requirements. However, despite the well characterized functions of mammalian proteasome the factors regulating the proteasome subunits remains unclear.

Inhibition of the catalytic activities of proteasome has been shown to induce apoptosis in various dividing cells. Bortezomib (velcade) is the first proteasome inhibitor approved by FDA and is being used in the treatment of multiple myeloma which principally inhibits chymotrypsin-like activity albeit inhibits other activities to a lesser extent. Most of the cancer cells have high levels of chymotrypsin like activity and studies in yeast have reported chymotrypsin-like activity as one of the major factor for cell survival. Cells treated with proteasome inhibitors for longer duration are known to gain resistance by synthesizing new proteasomes, a mechanism referred as feedback induction. Currently, bortezomib resistance is either attributed to mutations in PSMB5 or overexpression of the PSMB5 subunit. Hence, the mechanism of regulation of PSMB5 and other catalytically active subunits becomes imperative to identify the molecular basis of bortezomib resistance.

Previous studies have demonstrated that antioxidant response elements, such as, Nrf1 (TCFII) and Nrf2 are responsible for feedback induction or up-regulation of proteasome subunits in mammalian cells under the conditions of chronic inhibition of

proteasome or stress. However, the endogenous levels of proteasome subunits remain unaltered in mouse embryonic fibroblasts of *nrf1* and *nrf2*-disrupted mice. These observations suggest that, Nrf1 or Nrf2 largely regulate the feedback response to proteasome inhibition and there may be more than one mechanism to regulate the basal and feedback expression of the proteasome genes in mammalian cells.

Hence, the main objective of the present study is to identify the factors responsible for the regulation of proteasome subunits. This includes;

1. To determine the role of STAT3 in the regulation of proteasomal activity and expression.
2. To elucidate the molecular mechanism of EGF-induced activation of 20S proteasome subunits.

Chapter III: Regulation of PSMB5 and β-subunits of proteasome by STAT3.

STAT3 is a member of Signal Transducers and Activators of Transcription (STATs) and an important transcription factor that mediates signaling by numerous cytokines and growth factors. Persistent activation of STAT3 in malignant cells has been implicated in head and neck, breast and prostate cancers. Inhibition of phospho-STAT3 (pSTAT3) either by chemical inhibitors or shRNA targeting STAT3 has down-regulated various 20S proteasome subunits at both transcription and translation level in DU145 cells (prostate cancer cells with constitutive pSTAT3). pSTAT3 inhibition in cell lines expressing constitutively active STAT3, such as, A549, HeLa, MDA-MB-231 have also shown down-regulation of PSMB5, the catalytic subunit which is responsible for the chymotrypsin-like activity of proteasome. In contrast, STAT3 inhibition in cells that either do not express or with lower levels of pSTAT3 (either normal or cancer cells) did not result in the down-regulation of PSMB5. Reporter assays in which the expression of luciferase gene was driven under the control PSMB5 promoter was significantly increased in the presence of pSTAT3. Overexpression of STAT3 using Adenovirus (Ad-STAT3) in PC3 cells (where endogenous levels of STAT3 are absent) induced PSMB5 promoter and protein. Further, the presence of putative or canonical STAT3 binding sites have been identified by sequence analysis in the consensus promoter sequence of PSMB5. Moreover, a direct correlation was observed between the expression of proteasome activities, PSMB5 and pSTAT3. Inhibition of STAT3 significantly reduced chymotrypsin-like, trypsin-like and PGPH activities of proteasome and induced caspase-

3 activity in all the cell lines expressing constitutively active STAT3. However, proteasome activities were unaffected by STAT3 inhibition in normal prostate cells and prostate cancer cells possessing low or devoid of pSTAT3, but, induced apoptosis as measured by an increase in the caspase-3 activation. Furthermore, induction of apoptosis by proteasome inhibitors did not affect the expression of PSMB5 in DU145, suggesting that down-regulation of PSMB5 is not a general feature of apoptosis. The obtained results clearly demonstrate the indispensible role of STAT3 in regulating the expression of proteasome subunits, notably PSMB5.

Chapter IV: EGF-induced activation of proteasome subunits through STAT3:

EGFR is down regulated in normal prostate tissue by androgens, but, it is antagonistically regulated in androgen independent prostate cancers leading to the constitutive activation of EGFR. In addition, aberrant EGFR levels are found to be frequently associated with activated STAT3. Hence, we investigated whether EGF regulates PSMB5 protein expression in prostate cancer cells. EGF treatment significantly induced protein levels of PSMB5 along with an enhancement of pSTAT3 levels in a time-dependent manner in DU145 cells. In contrast, PSMB5 protein levels remain unchanged in response to EGF either in STAT3-negative (PC-3) or low levels of STAT3 (LNCaP) cells. Moreover, EGF-induced activation of PI3 kinase or ERK pathway did not affect PSMB5 expression in all the prostate cancer cells examined. Further, inhibition of either STAT3 or EGFR *per se* down-regulated the expression of PSMB5 and other β-subunits of 20S proteasome in pSTAT3 constitutive DU145 suggesting that STAT3 is required for EGF-induced proteasome sub-unit expression. Further diminished feedback induction of proteasome was observed in DU 145 suggests the pSTAT3 dependent regulation of proteasome. Finally, co-treatments employing STAT3 inhibitors along with bortezomib significantly enhanced cellular apoptosis and substantially decreased the proteasome expression and activities as compared to individual treatments alone. The observed results suggest that bortezomib and STAT3 inhibitors represent a synergistic combination and might prove as an effective regimen for the treatment of bortezomib resistance cancers; however, warranting further studies employing *in vivo* models.

Conclusions:

The results of the present study demonstrate for the first time the regulation of mammalian proteasome subunits by the oncogenic transcription factor, STAT3. A majority of β-subunits and few α-subunits of 20S proteasome were found to be regulated by STAT3. Importantly, PSMB5, which possess the chymotrypsin-like activity and also a known target of the proteasome inhibitor, bortezomib is directly regulated by STAT3. We have also identified a pivotal role of STAT3 even in EGF induced up-regulation of PSMB5. The above observations could provide new avenues to overcome the resistance of cancers towards bortezomib treatment. Also, the presented data aimed at understanding the basal regulation of the proteasome expression would improve our knowledge in understanding or / to develop new therapeutics for the treatment of cancer and other proteasome associated disorders.

CHAPTER 1

INTRODUCTION

1.1 Ubiquitin Proteasome System

Periodic degradation of proteins in various cellular organelles / compartments for performing a variety of cellular functions is as important as their synthesis for the survivability and development of cell. Proteolysis is essential to maintain the structural and metabolic integrity of the cell. The ubiquitin proteasome system (UPS) controls almost all basic cellular processes by degrading the short-lived regulatory proteins involved in cell cycle activation and progression, and degradation of various transcription factors involved in signal transduction pathways, immune responses, metabolism, development and differentiation. UPS also maintains the quality and homeostasis of proteins by degrading structurally aberrant proteins (Ciechanover, A. 2006; Tai, H. C. and Schuman, E. M. 2008; Varshavsky, 2005).

1.1.1 Ubiquitin and Ubiquitination

Ubiquitin is a 76 amino acid globular protein that is conserved in all eukaryotes and because it is expressed ubiquitously in both the cytosol and nucleus, it is referred as ubiquitin. It occurs either in free form or covalently bound to other ubiquitins (poly ubiquitin) and/or targeted proteins. Ubiquitin carries all the proteins targeted for proteasomal degradation to 26S proteasome (Stephen *et al*., 1996). Glycine 76 (G76) at the C-terminus of ubiquitin forms iso-peptide bond with ε-amino group of lysine (K) residue of the substrate protein. G76 is also involved in the formation of iso-peptide bonds between ubiquitin molecules or ubiquitin molecules and other proteins (Vijay-Kumar *et al*., 1985; Wilkinson *et al*., 1981). Ubiquitin has 7 lysine residues, poly-ubiquitin is formed when the C-terminal G76 of each ubiquitin is linked to a specific lysine residue of the previous ubiquitin (Chau *et al*., 1989). The attachment of ubiquitin to target protein is called ubiquitination. Ubiquitination of target protein is accomplished by multistep enzymatic reactions involving activation, conjugation of ubiquitin and ligation of ubiquitin to target protein. Ubiquitin activating enzyme (EI) initiates the ubiquitination by forming and transferring adenylated ubiquitin monomer to a conserved cysteine residue in the EI, which consumes 1 ATP molecule (Haas *et al*., 1982). This activated ubiquitin in a subsequent transthiolation reaction is transferred to an active site cysteine residue of ubiquitin conjugating enzyme (E2). E2-Ub transfers ubiquitin to

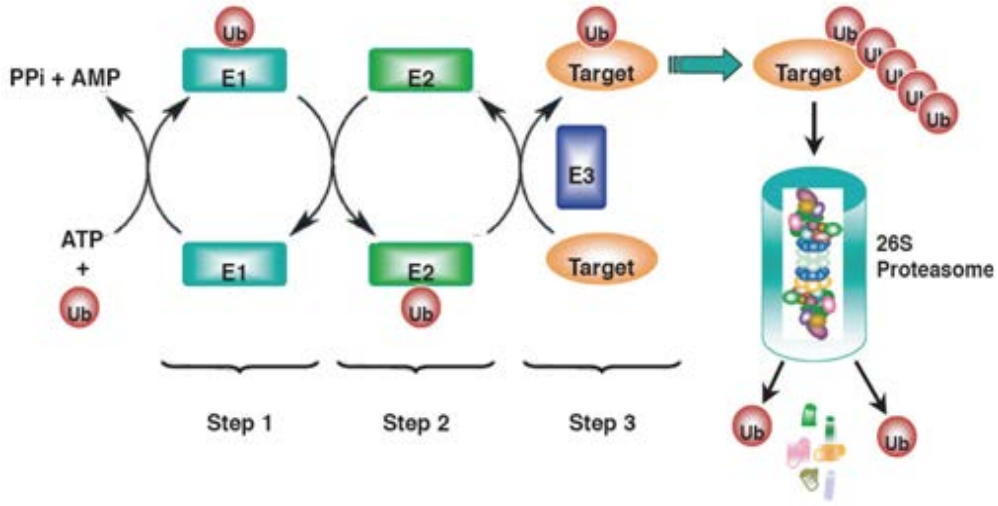

Figure 1.1: Schematic view of the Ubiquitin-Proteasome System.
Ubiquitin (Ub) is activated by covalent attachment to E1 enzyme in an ATP-dependent reaction (Step 1) and is subsequently transferred to an E2 (ubiquitin-conjugating) enzyme (Step 2). Ubiquitin is transferred from E2 to target substrate with or without the assistance of an E3 (ubiquitin ligase) enzyme (Step 3). E3s control the specificity of ubiquitination reactions. After several cycles of ubiquitination, the multi-ubiquitin chain bearing substrate is recognized by the 26S proteasome and targeted proteins are degraded leaving free ubiquitin molecules.

(Wang J, et al 2006; Cell Mol Immunol. Aug;3(4):255-61)

ubiquitin ligase (E3) and it is here that the ubiquitin is ligated to targeted protein by ubiquitin ligase (E3).

The N-terminus of E3 is highly variable and is responsible for specific substrate recognition and binding. The C-terminus is involved in the attachment and transfer of ubiquitin from E2-Ub to substrate protein to be degraded to form mono ubiquitinated protein. In case of HECT-domain containing E3 ligases, E2-Ub is transferred to target protein through thioester bond with E3 (E3-S-Ub), whereas, this transfer is direct without the formation of thioester bond in case of RING-domain E3 ligases (Lorick *et al*., 1999). Single E1 enzyme activates ubiquitin and interacts with all the E2 enzymes. In mammals, at least twenty five E2 enzymes are known to exist which define broader specificity (Sullivan & Vierstra, 1991). In the final stage, specificity of target protein is defined by a large (~500) heterogeneous population of E3 ligases. E3 ligases sequentially add ubiquitins to ubiquitin moiety of Ub-Protein complex to form poly-Ub chain. G76 of one ubiquitin forms isopeptide bond with K48 of previous ubiquitin (G76-K48). G76-K48-linked poly-Ub chains are important signals for proteasomal degradation (Chau *et al*., 1989). A minimum of four ubiquitin linked chains are essential for effective targeting of proteins for proteasomal degradation (Thrower *et al*., 2000). Other linkages like K63-G76 and mono ubiquitination are involved in non-proteolytic functions like regulation of transcription, DNA repair, endocytosis and activation of kinases (Hofmann *et al*., 1999).
These poly-Ub tagged proteins are recognized by 26S proteasome and targeted proteins are attached to 19S RP. Detachment of substrate protein from ubiquitin is essential to enter into 20S catalytic complex. Deubiquitinating enzymes (DUBs) are cysteine proteases which break the isopeptide bond after G76 residue resulting in deubiquitination. These proteases are located adjacent to proteasome. Some of 19S RP subunits also act as DUBs to remove ubiquitin from substrate proteins. UCH (Ubiquitin COOH-terminal Hydrolases) and USP (Ubiquitin Specific Proteases) are the two large groups of DUBs. These proteins dechain poly-Ub to ubiquitin monomers and thereby deubquitinate substrate proteins. The released ubiquitin monomers are re-used again for targeting of proteins for proteasomal degradation (Fig. 1.1).

1.1.2 26S Proteasome

26S proteasome is a large (2.5 MDa), ATP dependent multicatalytic protease complex responsible for the degradation of proteins by the ubiquitin proteasome system. 26S proteasome is made up of two sub-complexes. 20S proteasome (also called as catalytic core particle or CP) which is responsible for the catalytic degradation of targeted proteins and 19S regulatory particle (RP) attached to one or both ends of the 20S proteasome, which is responsible for the recognition and transfer of targeted proteins to 20S CP. Proteasome with one 20S CP and two 19S RP attached to both the ends of 20S is referred as 26S proteasome (Baumeister *et al*., 1998; Coux *et al*., 1996; Demartino & Gillette, 2007) (Fig. 1.2).

1.2 Structure and Assembly of 26S Proteasome

1.2.1 Structure of 20S Proteasome

20S proteasome is a 750 kDa barrel like structure with hollow space at the center. It is made up of four stackered rings of 2 outer and 2 inner rings of α and β respectively and are arranged in C2 symmetry. Each α and β rings are made up of 7 structurally similar subunits of sizes ranging from 21-35 kDa called as α1-α7 in α ring and β1-β7 in β ring. The subunits though structurally similar, perform common and different functions which are essential to maintain the integrity of proteasome structure and function. These rings are arranged in $\alpha_{1\text{-}7}\beta_{1\text{-}7}\beta_{1\text{-}7}\alpha_{1\text{-}7}$ (C2 symmetry) fashion. 20S CP consists of three internal chambers called αβ, ββ, αβ. The αβ chambers are located at the junctures of the α and β rings; the ββ chamber is confined to the β rings. The ββ chamber is catalytically active and is separated from cellular environment to prevent the uncontrolled degradation of proteins (Unno *et al*., 2002). The β ring contains the catalytic activities, namely, chymotrypsin-like activity (CT-L), caspase-like activity (PGPH: Post Glutamyl Peptidyl Hydrolase), trypsin-like activity (T-L). The subunits PSMB5 (β5), PSMB6 (β1) and PSMB7 (β2) are responsible for these activities respectively. All these activities of proteasome cleave both natural and synthetic peptides at the C-terminal side of hydrophobic, acidic and basic amino acids respectively. Two pairs of these proteolytic subunits reside in ββ chamber (Heinemeyer *et al*., 1997; Arendt & Hochstrasser, 1997).

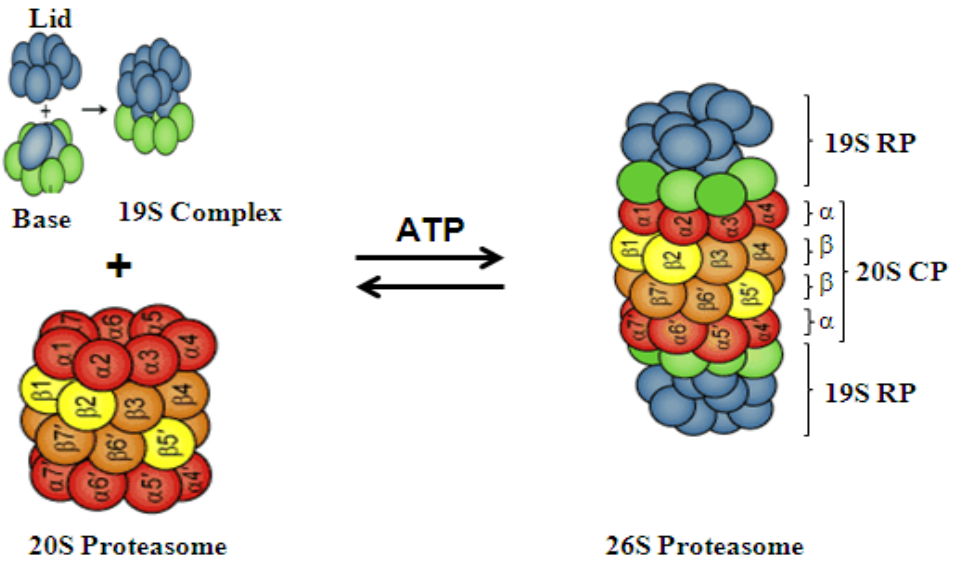

Figure 1.2: Schematic representation of the 19S, 20S and the formation of 26S proteasome.

The 20S proteasome is composed of a stack of four rings composed of seven subunits each. The two outer rings are made up of seven different α-subunits (marked by red), whereas, the two central rings are composed of seven different β-subunits (marked by orange). The proteolytic active sites of the 20S proteasome are located in the central β-rings at subunits β1, β2 and β5 (marked by yellow). 19S regulatory complexes are sub-divided into two distinct base and lid sub-complexes and composed of 11-12 non-ATPase (marked by blue) and six AAA-type ATPase subunits (marked by green). The 19S regulatory particle in the presence of ATP associates with 20S proteasome to form 26S proteasome.

(Boston Biochem).

In addition, the mammalian proteasome also has two more catalytic or proteolytic activities called SNaaP (Small Neutral aminoacid peptide cleavage), BrAAP (Branched chain aminoacid peptide cleavage) activity. The subunits responsible for these activities are not yet known (Orlowski *et al*., 1993). 20S proteasome processively generates oligo peptides of size in the range of 3-22 amino acids by degrading the target proteins in the catalytic chamber (ββ). These peptides are further hydrolyzed into smaller fragments and amino acids by oligo-peptidases, amino, carboxy peptidases present outside the proteasome. The α rings present at both sides of β rings control the activity of the catalytic chamber by preventing the penetration of non-targeted proteins in to the catalytic chamber (ββ) by narrowing the opening. Only the target proteins which are unfolded by 19S RP, unfolded abnormal proteins and proteins damaged by oxidative stress will enter into the catalytic chamber (DeMartino & Slaughter, 1999; Glickman *et al*., 1998; Liu *et al*., 2003a; Rechsteiner *et al*., 2000; Sorokin *et al*., 2005). The N-terminal extensions of α-subunits act as barriers for access to the active sites in ββ chamber (Groll *et al*., 1997; Smith *et al*., 2007). The α-subunits play important roles in assembly of the β-subunits to form 20S proteasome as well as recognition and attachment of 19S RP to the 20S proteasome. Proteasomes are present both in the cytosol and nucleus and undergo cell cycle dependent redistribution. Four of the α-subunits possess multiple nuclear localization signals (NLS), which assist in the localization to nucleus. All the β-subunits except β3, β4 contain prosequences or propeptides of varying length at their N-terminus. Prosequences helps in the correct orientation and arrangement of β-subunits during the formation or assembly of 20S proteasome and also prevent the premature catalytic activity of β subunits by hiding Thr. The prosequences also acts as signals for the localization of β-subunits during proteasome assembly. Once all the subunits are arranged, prosequences will be degraded and catalytically active Threonine will be exposed at the N-terminus. All these catalytically active subunits cleave the peptide bond by using their hydroxyl group of N-terminal threonine residue as nucleophile. Hence, the proteasome belongs to the class of N-terminal nucleophile hydrolases (Ntn-hydrolases) (Kisselev *et al*., 2000).

1.2.2 19S RP (PA700)

The catalytically active proteasomes are generally capped with regulatory particles (RP) on either or both ends of the assembled 20S proteasome. 20S CP alone can't degrade the ubiquitylated proteins. These regulatory particles performs the essential functions required for the degradation of targeted proteins like the recognition of polyubiquitylated targeted proteins, deubiquitylation and unfolding of proteins and transfers these unfolded proteins to 20S catalytic proteasome for the degradation by opening the narrow α ring. Constitutive 26S proteasome contains 19S RP (also called as PA700). 19S RP complex consists of approximately 20 different subunits of ATP dependent Regulatory particle of triple-ATPase (Rpt) subunits and ATP independent Regulatory particle of non- ATPase (Rpn) subunits. 19SRP contains 2 sub complexes namely lid and base. The lid complex consists of at least 9 non-ATPase subunits (Rpn3, Rpn 5, Rpn 6, Rpn 7, Rpn 8, Rpn 9, Rpn 11, Rpn 12 and Rpn 15). It is involved in the detachment of poly ubiquitin chain from the targeted protein by using Rpn 11 metallo-isopeptidase. This polyubiquitin chain is further deubiquitylated by other deubiquitylating enzymes (DUB) present adjacent or associated with 26S proteasome to monomeric ubiquitins (Glickman *et al*., 1998; Hanna & Finley, 2007; Hu *et al*., 2005a; Verma *et al*., 2002).

The base complex is also composed of ATP dependent (Rpt 1, Rpt 2, Rpt 3, Rpt 4, Rpt 5, Rpt 6) and independent (Rpn1, Rpn 2, Rpn 10, Rpn 13) subunits. The base complex captures the targeted proteins by recognising the polyubiquitin chains. Recognition and binding of polyubiquitin chain does not require energy. Rpn 10 and Rpn 13 of the base complex recognizes poly-ubiquitylated substrates and acts as receptors for the poly ubiquitin. Rpn 10 recognizes poly-ubiquitin chain with the help of C-terminal Ubiquitin Interacting Motif (UIM), whereas, Rpn 13 does it by its novel domain of pleckstrin-like receptor for ubiquitin (Pru) at N-terminus. Deubiquitylated client proteins must enter into catalytic core particle (20S proteasome) for degradation (Husnjak *et al*., 2008; Lam *et al*., 2002; Saeki & Tanaka, 2008; Schreiner *et al*., 2008). The proteolytic sites inside the 20S are guarded by the narrow opening (5nm) formed by N-terminal extensions of α-subunits to prevent the uncontrolled degradation of proteins. The ATPases of base sub-complex acts as molecular chaperone to unfold the proteins by

using ATP. The ATPases present in the base complex (Rpt1-6) forms a hexameric ring and help in the opening of the gate. Three of these ATPases, Rpt 2, 3, 5 contain a multiple conserved C-terminal hydrophobic-tyrosine-X (HbYX) motifs. These motifs facilitate the opening of the gate; however, binding of ATP is sufficient for opening the gate and its hydrolysis is not required (Liu *et al*., 2006; Rabl *et al*., 2008; Saeki & Tanaka, 2007; Smith *et al*., 2007).

1.2.3 Assembly of 20S Proteasome

All the subunits of 20S proteasome must be arranged in correct position to form the functionally active proteasome. Assembly of 20S proteasome starts with α-subunits assembly and the assembled α ring acts as a base for the assembly of β-subunits on it. α ring formation requires 4 extrinisic chaperones, viz., PAC1-PAC2 heterodimer and PAC3-PAC4 heterodimer (Proteasome Assembling Chaperones). Knock-down studies of PAC1 or PAC2 have shown that they are stable only in heterodimer forms and their absence results in aberrant α ring dimerisation (Hirano *et al*., 2005). PAC1-PAC2 with the help of PAC3-PAC4 starts the α-ring formation and prevent the formation of off-pathway products (αα ring dimers). PAC1-PAC2 complex binds to proteasome precursors and is degraded by proteasome itself when matured and functionally active protesome is formed. PAC3-PAC4 complex helps in the correct arrangement of α-subunits during α-ring formation (Murata *et al*., 2009). β-subunits are added to α-ring sequentially. Knock-down studies of individual β-subunits inferred that β2 subunit initiates the formation of β ring followed by β3, β4, β5, β6, β1 and finally β7 (Hirano *et al*., 2008). hUmp1 (human Ubiquitin mediated proteolysis, proteassemblin or POMP) bind with β2 and recruits it to α ring. hUmp1 also binds to proteasome precursors and undergoes degradation after the formation of mature proteasome (Ramos *et al*.,1998; Witt *et al*., 2000). Pro-peptides and C-terminal sequences of β-subunits acts as intramolecular chaperones in correcting the orientation of β-subunits and recruitment of subsequent β-subunits. Propeptides of β2 are essential for the recruitment of β3 subunit (De *et al*., 2003; Shinde & Inouye, 2000). All the subunits except β7 are arranged in a ring like manner and this state of proteasome is referred as half-mer precursor. Finally, the C-terminal tail of β7 subunit inserts into a groove between β1 and β2 in the opposite half-

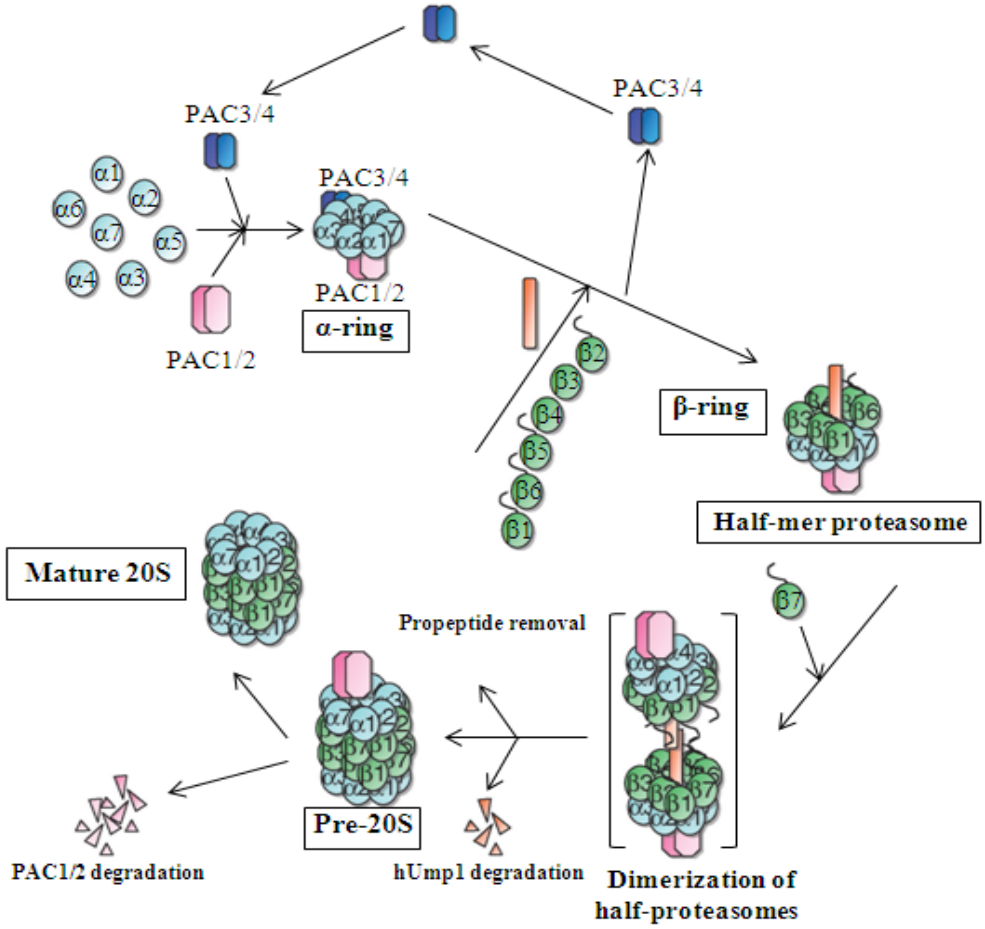

Figure 1.3: Assembly of 20S proteasome.
Heterodimeric complexes of PAC1–PAC2 and PAC3–PAC4 mediates α-ring formation. The binding of β2 and hUmp1 on the α-ring followed by sequential incorporation of the β-subunits except β7 results in half proteasomes. PAC3–PAC4, maintains the structural integrity of the intermediates until β3 is incorporated on the β-ring. Dimerization of half-mers (i.e., half-proteasomes lacking β7) is assisted by the C-terminal tail of β7 followed by removal of the pro-peptides of subunits (β1, β2, β5, β6 and β7). hUmp1 and PAC1–PAC2 degradation results in to mature 20S Proteasome.

(Tanaka K, 2009 *Proc Jpn Acad Ser B Phys Biol Sci.* 2009;85(1):12-36).

mer precursor resulting in the dimerization of half proteasomes followed by processing of β-subunits results in the catalytically active prtoeasome which eventually degrades hUmp1 and PAC1-PAC2 complex (Chen & Hochstrasser, 1996; Li *et al*., 2007; Marques *et al*., 2007). The complete assembly mechanisms of 19S as well as 26S are not well understood. However, studies have reported ATP-dependent chaperone activity of Hsp90 probably plays an important role in the assembly of 19S RP with 20S CP to form 26S proteasome (Imai *et al*., 2003) (Fig. 1.3).

1.2.4 Localization

Proteasomes are abundant in both cytosol and nucleus. Distribution of proteasome between cytosol and nucleus varies with cell types and their requirement. Liver cells have more cytosolic proteasomes, whereas, lung cells have predominantly nuclear proteasomes (Rivett *et al*., 1992). Rapidly growing cells show more proteasomes than non-dividing cells (Kumatori *et al*., 1990). Although some subunits of the proteasome possess nuclear localization signals, modifications on the subunits of proteasome might also signal the translocation of proteasomes from cytosol to the nucleus. However, the precise mechanism of intracellular distribution of proteasomes is not yet known (Benedict *et al*., 1995; Nederlof *et al*., 1995; Wang *et al*., 1997). Proteasomes are also observed extracellularly and enhanced proteasome levels found in the blood serum of leukemia, myeloma, and carcinoma patients may be because of increased secretion of proteasomes by the tumor cells (Wada *et al*., 1993).

1.2.5 Modifications of Proteasome Subunits

26S Proteasome subunits have been shown to undergo post translational modifications to modulate the function and localization of proteasome. Phosphorylation of α1, α2, α3, β2, β3 and β7 subunits have been shown to increase chymotrypsin-like and caspase-like activities of proteasome *in vitro* (Zong *et al*., 2006). Phosphorylation of α2 on Tyr120 has been shown to act as a nuclear localization signal for the proteasome (Benedict *et al*., 1995). Phosphorylation of α7 stabilizes the association of 20S CP with 19S RP, whereas, dephosphorylation of α7 results in the immunoproteasome formation by enhancing the association of 20S CP with PA28 α/β (11S REG) (Bose *et* al., 2004). S-

glutathionylation of cysteine residues in various subunits of 20S CP has been shown to inhibit chymotrypsin and trypsin-like activities without effecting caspase-like activity (Demasi *et al*., 2003). Though N-myriostylation was observed in 19S, its significance is not yet known (Wang *et al*., 2007). Glycosylation of 19S RP has been shown to reduce the ATPase activity (Zhang *et al*., 2003).

1.3 Types of Proteasome

1.3.1 Immunoproteasome

Higher vertebrates have a special type of proteasome that helps in the processing of antigens for adaptive or acquired immune response called as Immunoproteasome. It is different from standard or constitutive proteasome in having subunits β1i, β2i, β5i in place of β1, β2, β5 and 11S RP (PA28) instead of 19SRP (PA700). IFN-γ induces the Immunoproteasome formation. Immunoproteasome processes intracellular peptides that include virus, pathogens and tumours and present them to MHC class I peptides on the cell surface. These are recognized by CTL (Cytotoxic T-Lymphocytes) and kill those cells. IFN-γ also alters the proteolytic activities of immunoproteasome. Increased chymotrypsin and trypsin-like activities and decreased caspase-like activity have been reported in immunoproteasome. It generates peptides of size 6-8 amino acids having more of basic and hydrophobic amino acids containing at C-terminus, which favors MHC class I peptide binding groove for proper recognition (Kloetzel, 2001; Rock *et al*., 2002; Tanaka & Kasahara, 1998). Similar to 19S RP, immunoproteasome also has activator called PA28 (11S regulator). It is made up of PA28α, PA28β, PA28γ sub-complexes. PA28α and PA28β forms heterodimeric complexes and are present in cytosol, whereas, PA28γ forms homopolymeric complexes and is present in the nucleus and activates the respective immunoproteasomes. PA28γ is involved in the degradation of p53 via mdm2 mediated proteasomal degradation. It also promotes the degradation SRC-3 (steroid receptor co-activator 3) which is an oncogene and is highly expressed in breast cancer (Li *et al*., 2006; Tanahashi *et al*., 1997; Wojcik *et al*., 1998; Zhang *et al*., 2008).

1.3.2 Thymoproteasome

In addition to the β5, β5i, studies identified a catalytic subunit β5t which is expressed only in cortical thymic epithelial cells. The β5t subunit along with β1i, β2i forms a proteasome called Thymoproteasome. It is implicated in the positive selection of developing thymocytes. Thymoproteasome shown less chymotrypsin-like activity, whereas, no change was observed in trypsin and caspase-like activities (Murata *et al*., 2007 & 2008).

1.4 Biological functions of UPS

1.4.1 Inflammation and Auto Immunity

UPS plays an important role in the immune protection of organism. First, it is involved in the processing of antigens in antigen presenting cells. Second, it regulates the transmission of signals from T cell antigen receptor and CD28 co-stimulatory molecule. Third, it regulates the activation of NF-kB which is a key regulator of genes involved in inflammation. UPS activates NF-kB in two steps, first it processes p105 and p100 to generate p50 (NF-kB1) and p52 (NF-kB2). These are further dissociated from inhibitors of NF-kB (IkBs) to form active transcription factors p50 and p52 by UPS dependent degradation of Ikb, which translocates to the nucleus and activates NFkB target genes. Abnormal activation of TH2 (T-Helper 2) leads to the JunB dependent transcription of various interleukins such as IL-4, IL-5, IL-9, IL-10 and IL-13 which result in asthma and allergic reactions (Hartenstein *et al*., 2002; Li *et al*., 1999). Itch is an E3 ligase that targets JunB to UPS for degradation. Mice lacking the itch demonstrated various types of allergies (Gao *et al*., 2004; Venuprasad *et al*., 2006). Rheumatoid arthritis is an autoimmune disease characterized by chronic synovial tissue inflammation which results from the activation of NFkB. Proteasome inhibitors have been demonstrated in mitigating inflammation and allergy by inhibiting NFkB (Firestein, 2004; Tsao *et al*., 1997).

1.4.2 Neurological Disorders

Formation of large protein aggregates is a specific feature of neurodegenerative diseases along with loss of function and reduction in neuronal cells. Most of these aggregates contain Ub and proteasomes (Sieradzan *et al*., 1999). It has been observed that impairment in the proteasomal activity leads to the generation of protein aggregates. Correlation between the disease development and dysfunction of UPS has been shown in inheritable Parkinson's and Alzheimer's diseases. Nonetheless, the exact relationship between neurological disorders and UPS is still under investigation. (Bence *et al*., 2001; Emmanouilidou *et al*., 2010; Zhang *et al*., 2008a).

1.4.3 Development

Initiation of early embryonal mitosis and development in rodents requires differentially regulated expression of distinct subunits of 19S RP and proteasomal degradation of cell cycle regulatory proteins (Josefsberg *et al*., 2001: Kawahara *et al*, 2000). Changes in the molecular assembly and proteolytic activities of some subunits of the 26S proteasome was observed during completion of meiosis in vertebrates (Josefsberg *et al*., 2000; Reverte *et al*., 2001). It is also reported that 26S proteasome is essential for rat oocyte maturation.

1.4.4 Differentiation

Withdrawal of cells from cell cycle is essential for the differentiation of eukaryotic cells. This process is accomplished by inactivation or down-regulation of CDKs (cyclin dependent kinases) during G1-phase of cell cycle. CDKs associate with CKI (cyclin dependent kinase inhibitors) which inhibit the activity of CDKs. CKIs (p21 WAF1/CIP1, p27KIP1, p57KIP2, p19INK4d) are known substrates of proteasome. Proteasomal degradation of cell cycle regulators, p21 WAF1/CIP1 and cyclin D1 resulted in the differentiation of mouse and human cells (Bernardi *et al*., 2000: Di Cunto *et al*., 1998; Negishi *et al*., 2001: Spinella *et al*., 1999). Retinoic acid induced neuronal differentiation of human multipotent embryonal stem cells requires inhibition of proteasome mediated degradation of p27KIP1 (Baldassarre *et al*., 2000). Nonetheless, proteasomes regulate the differentiation of eukaryotic cells either positively or negatively.

1.4.5 Regulation of Gene expression

Proteasomes have been reported to control the expression of genes through chromatin modifications, transcription, mRNA stability and translation. Proteolytic and non-proteolytic activities of proteasomes are reported to be responsible for these processes.

1.4.5a Transcriptional Regulation

Proteolytic activities of the proteasome regulate activation of a large number of transcription factors either by processing or degradation of inhibitory proteins associated with them. This process is termed as regulated ubiquitin/proteasome-dependent processing. Mammalian NFkB and yeast SPT23 and MGA2 are controlled by this process (Rape & Jentsch, 2004). Inhibition of proteasomal activities in yeast demonstrated the inability of transcription activators to recruit RNA pol-II to promoters (Lipford *et al*., 2005). Further, in yeast accurate termination of transcription also depends on the active proteasome (Gillette *et al*., 2004). Estrogen receptors (ER) belong to nuclear hormone receptors family which associates with SRCs (Steroid Receptor Coactivator) and activates or regulates downstream target gene transcription. SRCs have been shown to interact directly with LMP2 of immunoproteasome. It has been shown that association of LMP2 with SRCs is essential for the cyclic association of ER regulated transcription complexes on ER target promoters. Proteolytic activities of the proteasome regulates glucocorticoid hormone receptor (GR)-dependent gene transcription by proteolytic cleavage and recycling of receptor/transcriptional-DNA complexes (kinyamu *et al*., 2007). In addition to this, inhibition of proteasome modified the chromatin by increasing trimethyl histone H3K4 levels on GR-regulated promoter regions and accumulated phosphorylated RNA pol II at GR-target genes leading to the enhanced transcription (Kinyamu & Archer, 2007). Proteasomes also degrades elongating RNA pol II and prevents the transcription during DNA damage (Krogan *et al*., 2004; Reid & Svejstrup, 2004; Somesh *et al*., 2005).

Mutants of 19S RP subunits SUG1 (Rpt6), SUG2 (Rpt4) in yeast inhibited the elongation of transcription which could be restored by the addition of 19S complex (Ferdous *et al*., 2001).

1.4.5b Translational Regulation

eIF4G and eIF3a are the components of eukaryotic translation initiation complex. eIF4F and eIF3 are selectively degraded by the UPS. This process inhibits the assembly of ribosomal pre-initiation complexes on different cellular and viral mRNAs leading to the inhibition of translation. In line with the above findings, inhibition of proteasomal activities restored the initiation of translation by preventing the degradation of eIF4F and eIF3. Proteasomes are also involved in the transcription of ribosomal protein genes (Auld & Silver, 2006). These findings provide a direct link between protein synthesis and protein degradation in maintaining cellular protein homeostasis.

1.4.6 RNase Activity of Proteasome

Previous studies have shown that proteasomes have endoribonuclease activity and the subunits possessing this activity are α5/zeta and α1/iota (Petit *et al*., 1997). Though both 26S and 20S proteasomes possess RNase activity, they differ in type of RNA to be degraded and their dependence on divalent cations. 20S proteasome is active only in the presence of divalent cations, whereas, 26S is active both in the presence or absence of divalent cations (Evteeva *et al*., 2000; Mittenberg *et al*., 2002). Phosphorylation of 26S proteasome subunits is essential for RNase activity. Studies have shown that RNase activity of proteasome is differentially regulated during differentiation and apoptosis (Mittenberg *et al*., 2007).

1.4.7 Reprogramming of Proteasomes

To perform a wide variety of cellular functions and to meet the requirements of cells, proteasomes undergoes modification or reprogram its subunit composition and alter their proteolytic activities. During immune response to pathogens, IFN-γ, TNF-α treatment causes the changes in the catalytic activities of the proteasome by replacement of constitutive catalytically active subunits β1, β2 and β5 with LMP2, LMP10 and LMP7

respectively. Further, PA28 α/β replaces 19S RP and causes efficient processing of antigenic peptides (Groettrup *et al*., 2001). IFN-γ also stimulates trypsin-like and chymotrypsin-like activities (Akiyama *et al*., 1994). It was also reported that IFN-γ decreases the phosphorylation of proteasome subunits (Rivitt *et al*., 2001).

Induction of erythroid differentiation of K562 (human proerythroleukaemic cells) by hemin is accompanied by redistribution of proteasomes to cytosol, changes in the phosphorylation state of several proteasome subunits and changes in the endoribonuclease activity of proteasomes (Mittenberg *et al*., 2002 & 2007). Enzymatic activities and subunit composition of proteasomes were also changed in K562 cells during apoptosis. Trypsin and chymotrypsin-like activities of proteasome were increased in doxorubicin induced apoptotic cells of K562 compared to untreated cells (Tsimokha *et al*., 2006 & 2007).

1.4.8 Role of Proteasome in Cancer

A large number of oncogenes and tumor suppressor proteins were shown to be the targets of UPS and malfunction of UPS has been reported to either enhance the oncoprotein activity or reduce the function of tumor suppresser proteins in variety of cancers. Hypoxia inducible factors (HIF) mediate the response to hypoxic conditions by activating the expression of genes that promotes angiogenesis such as VEGF (Vascular Endothelial Growth Factor). Under normal conditions (normoxic) the HIFs are inactive due to hydroxylation of two proline residues and this form of protein is recognized by E3 ligases and present them for degradation by proteasome. VHL (Von Hippel-Lindau) is a E3 ligase responsible for the recognition and presentation of HIF to proteasome under normoxic conditions (Ivanov *et al*., 2001; Jaakkola *et al*., 2001). Mutations in VHL gene makes it unable to recognize and target HIF for degradation and leads to cancer (Clifford *et al*., 2001). Moreover, increased HIF and VEGF in VHL mutated cells has been observed in renal carcinomas (Iliopoulos *et al*., 1996; Siemeister *et al*., 1996; Turner *et al*., 2002; Yang *et al*., 2003).

β-catenin in association with other proteins activates the transcription of cyclin D1 and MYC (Crawford *et al*., 1999; He *et al*., 1998; Tetsu & McCormick, 1999; Uthoff *et al*., 2001). β-catenin is regulated by phosphorylation of N-terminal serine and

threonine by casein kinase I (CKI). The phosphorylated β-catenins are ubiquitinated and undergoes proteasomal degradation. APC is responsible for presenting the β-catenin to CKI for N-terminal phosphorylation. In most of the colon cancers APC gene undergoes mutations resulting in the C-terminal truncated protein, which no longer recognizes β-catenin (Miyoshi *et al*., 1992; Powell *et al*., 1992). In some cases, β-catenin itself undergoes mutations at phosphorylation sites preventing it from degradation by UPS and this leads to cancer (Sparks *et al*., 1998).

p53 is a tumor suppressor gene that responds to DNA damage, stress and activates apoptosis and cell cycle arrest. p53 is a target of UPS. It regulates itself by synthesising mdm2, an E3 ligase which ligates p53 to proteasome for degradation. Amplification of mdm2 results in the suppression of p53 in a variety of sarcomas (Momand *et al*., 1998). Human Papilloma Viruses (HPV) causes cervical carcinoma by manipulating the UPS to degrade the p53. High risk HPV produces E6 which binds to E6-AP, which is a ubiquitin ligase (E3). HPV E6 binds to N-terminal of E6-AP (E6-E6AP) and alters its substrate specificity. The N-terminal substrate binding domain of E6-AP of E6-E6AP binds to p53 and transports it to proteasome for degradation (Scheffner *et al*., 1993).

Control of cell cycle is crucial to prevent transformation of a cell into a cancer cell. Periodic turnover of cyclins and cyclin dependent kinases regulates the cell cycle. Cyclin E levels are high at G1-S transition and it activates CDK2. CycE/CDK2 complex is essential for cells to enter genome duplication phase (S phase). p27 is a tumor suppressor gene which interacts with cdk2/cycE and cdk2/cycD complexes and prevents cell cycle progression (Pagano *et al*., 1995; Shirane *et al*., 1999) and this protein also happens to be a substrate of UPS. Skp2 (S phase kinase protein) is a ubiquitin ligase which ligates p27 to the UPS for degradation results in cell cycle progression to S-phase (Carrano *et al*., 1999; Sutterluty *et al*., 1999; Tsvetkov *et al*., 1999). Low levels of p27 has been reported in various malignancies such as breast, prostate, lung, ovarian, colon, lymphoma and brain (Loda *et al*., 1997; Moller, 2000; Slingerland & Pagano, 2000). Cyclin A and B are also regulated by UPS. Anaphase promoting complex/cyclosome (APC/C) acts as ubiquitin ligase (E3) to target them for proteasomal degradation.

1.5 Inhibitors of Proteasome

Given their indispensable role for cell survival, inhibition of proteasome has been a promising target for anticancer therapy although this approach can also be used for other disorders or diseases. Since proteasome is a multicatalytic enzyme complex and all active sites cleave peptide bonds by similar N-terminal hydrolase reaction, inhibitors of one type of activity also inhibit other activities at higher concentrations (Kisselev *et al*., 2006). Earlier studies carried out in yeast and human cells demonstrated that all three catalytic activities are important for cells albeit chymotrypsin like activity was found to be vital (Arendt & Hochstrasser, 1997; Chen & Hochstrasser, 1996; Heinemeyer *et al*., 1997). All of the natural product inhibitors and most of the synthetic proteasome inhibitors primarily target the chymotrypsin-like activity of proteasome. Cancer cells or dividing cells requires high levels of protein synthesis and degradation than their normal cell counterparts or non-dividing cells. This property makes the proteasome inhibitors selective for cancer cells over normal cells, thus reducing the toxicity concerns of normal cells (Adams, 2004; Kisselev & Goldberg, 2001).

1.5.1 Types of Inhibitors

Proteasome inhibitors are structurally diverse. Most of the proteasome inhibitors are peptide based ligand mimetics or transition state analogs of enzyme catalyzed reactions. They inhibit proteasomes reversibly or irreversibly by formation of a covalent or non covalent adduct between the inhibitor and the catalytic site of the enzyme.

Peptide Aldehydes are the first inhibitors of proteasome to be developed. They inhibit proteasome by forming hemiacetal bond with hydroxyl group of catalytic threonine residue and are rapidly reversible due to oxidation of aldehydes. MG132 is the well studied drug of this group (Adams *et al*., 1998).

Peptide Boronates are much more potent inhibitors of proteasome compared to aldehydes and dissociates more slowly from proteasome. They also share the mode of inhibition with peptide aldehydes by forming tetrahedral adducts with active site threonines, which are further stabilized by a H- bond between N-terminal amino group of threonine and one of the hydroxyl groups of boronic acid. Due to this H-bond they do not inhibit serine proteases (Adams *et al*., 1998). Bortezomib had been using as front line

treatment for relapsed and refractory multiple myeloma and few of the inhibitors of this class, such as, CEP-18770 and MLN2238 are under clinical trials (Kupperman *et al*., 2010; Piva *et al*., 2008).

Peptide α, β-Epoxyketones are the most specific and potent proteasome inhibitors known to date. They form an irreversible morphilino ring with N-terminal threonine of catalytic site. Carfilzomib has been approved for the treatment of relapsed and refractory multiple myeloma. An example in this class of inhibitor includes, ONX-0912 which is presently under clinical trials (Zhou *et al*., 2009).

β-Lactones are less specific and less potent inhibitors than epoxoketones. They inactivate proteasome by esterfying the catalytic threonine hydroxyl group (Groll *et al*., 2006). All β-Lactone adducts are slowly hydrolyzed by water and lead to the reactivation of proteasomes (Dick *et al*., 1997). Marizomib belongs to this class of inhibitors and is presently under clinical trials.

Peptidyl vinly sulfones are irreversible inhibitors of proteasome which covalently modify the catalytic threonine residue in all the active β-subunits of proteasome (Groll *et al*., 2002). Other classes of proteasome inhibitors such as cyclic peptides, non cyclic peptides, peptide isosteres, non specific proteasome inhibitors, allosteric inhibitors and site specific proteasome inhibitors were limited to laboratory studies due to relative lack of potency, specificity or stability (Kisselev *et al*., 2012).

1.5.2 Mechanism of Apoptosis

Although the precise mechanism(s) of action of proteasome inhibitors are not yet fully defined, there are a number of pathways that appear to be important in their selectivity towards malignant cells. Induction of apoptosis by proteasome inhibition is mediated through several mechanisms such as inhibition of NFκB activity, altered degradation of cell cycle related proteins, altered proapoptotic and anti-apoptotic protein balance, endoplasmic reticulum stress, inhibition of angiogenesis and DNA repair. The choice of mechanism appears to be dependent on type of cell and drug (Daniel *et al*., 2005; Richardson *et al*., 2003).

Bortezomib is the first proteasome inhibitor that has been using as frontline drug for multiple myeloma. However, limited activity of bortezomib in solid tumors, development of resistance, dose dependent peripheral neuropathy, stability and intravenous administrations prompted the development of structurally distinct second generation inhibitors of proteasome. These include CEP-18770, MLN2238, Carfilzomib, ONX-0912 and Marizomib. Carfilzomib has been approved for multiple myeloma which has shown prominent results than bortezomib. These second generation drugs although superior in selectivity, exhibit dose-limited toxicity (Kisselev *et al*., 2012).

1.6 Resistance to Bortezomib

Various bortezomib resistant cell lines were developed by continuous or repeated exposure of bortezomib in order to study the cellular basis of bortezomib resistance. Several studies reported the presence of point-mutations or overexpression of the PSMB5 subunit which is responsible for chymotrypsin-like activity and happens to be the principle target of bortezomib.

1.6.1 Point Mutations of PSMB5

G322A, C323T, C326T point mutations of PSMB5, which results in the substitution of Ala49Thr, Ala50Val in the functional PSMB5 (Ala108Thr, Ala109Val in proPSMB5) were reported in Bortezomib-resistant lymphoblastic lymphoma/leukemia cells called JurkatB (Lu *et al*., 2008). Oerlemans *et al*. (2008); Ri *et al*.(2010) also confirmed G322A PSMB5 mutations in bortezomib resistant human monocytic/macrophage THP1/BTZ cells, bortezomib-resistant MM cell lines KMS-11/BTZ and OPM-2/BTZ respectively. Franke *et al*. (2012) identified G322A, C323T and G247A (Thr21Ala) PSMB5 mutations in bortezomib-resistant MM cell line 8226/BTZ, G322A, C323T, G332T (Cys52Phe) mutations in acute lymphoblastic leukemia cell line CEM/BTZ and G312T (Met45Ile), A310G (Met45Val) in human monocytic/macrophage THP1/BTZ cells. De Wilt *et al*. (2012) proved that bortezomib resistance of Non-Small-Cell Lung Carcinoma (NSCLC) cell lines is associated with Ala49Thr, Met45Val and Cys52Phe mutations in PSMB5.

Bortezomib binds with PSMB5 and inhibits the chymotrypsin-like activity of proteasome. Most of these mutated residues are around the S1 specificity pocket (binding

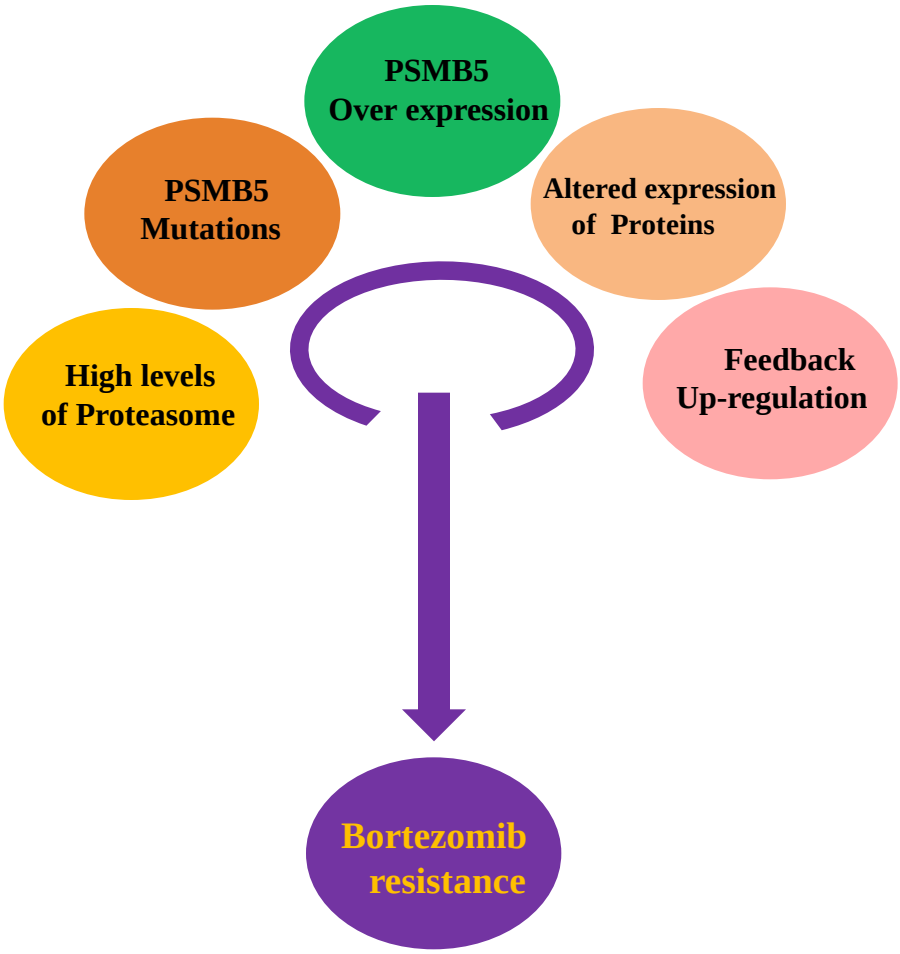

Fig 1.4: Factors leading to bortezomib resistance, a schematic view.

site) of the PSMB5 which is responsible for recognizing the peptide bond of substrate. Ala49 and Ala50 of PSMB5 directly interacts with bortezomib by strong H-bonding at binding site of PSMB5, whereas, Cys52 and Met45 are in close proximity to the binding site of bortezomib. Mutation of these amino acids causes the conformational changes of PSMB5 binding site that prevent binding of bortezomib to PSMB5 and confer varying degrees of resistance. Ala49Thr, Ala50Val are involved directly and Cys52Phe, Met45Ile, Met45Val are involved indirectly in preventing the bortezomib binding to PSMB5 (De Wilt *et al*., 2012; Franke *et al*., 2012; Lu *et al*., 2008 & 2009; Oerlemans *et al*., 2008; Ri *et al*., 2010). However, studies on patients of relapsed or refractory myeloma from bortezomib did not show any mutations (Lu *et al*., 2011; Politou *et al*., 2006) in PSMB5.

1.6.2 Overexpression of PSMB5

Studies of Lu *et al*. (2010) in jurkatB cells revealed the increased expression of PSMB5 and chymotrypsin-like activity. Increased expression of PSMB5 was also reported in patients of multiple myeloma treated with bortezomib (Lu *et al*., 2011). Findings of Balsas *et al*. (2012) on multiple myeloma cells displaying resistance to bortezomib (8226/7B) have shown overexpression of PSMB5 both at the mRNA and protein levels without possessing mutations. These cells also displayed nearly double the quantity of DNA per cell. However, these cells (8226/7B) were as sensitive as parental cells to other chemotherapeutic agents.

Bortezomib-sensitive human acute myeloid leukemia cell line HL-60 (HL-60a) proteasomal activity profiling revealed an up-regulation of levels of active subunits and activities of proteasome in contrast to control cells. Increased expression of catalytic subunits influenced the sensitivity of hematologic maliganancies towards bortezomib (Kraus *et al*., 2007). Higher basal levels of proteasome activity and subunit expression was reported to be associated with intrinsic and acquired resistance to bortezomib in NSCLC (De wilt *et al*., 2012) and HT-29 adenocarcinoma cells (Suzuki *et al*., 2011). Taken together, these findings demonstrate that intrinsic bortezomib resistance is mainly associated with high basal levels of proteasome activity, increased proteasome subunit expression (PSMB5) or emergence of mutant PSMB5 (β5).

1.6.3 Altered Expression of Proteins

Studies in bortezomib resistant diffuse large B- cell lymphoma cell line (SUDHL-4) and bortezomib sensitive cell line (SUDHL-6) reported differential expression of genes following bortezomib treatment. Increased expression of heat shock proteins, specifically HSP27 was identified as a mediator of bortezomib resistance in SUDHL-4. Further, higher expression of TCF-4 (transcription factor 4), cyclin D1 and c-myc were reported in SUDHL-4 cells (Chauhan *et al*., 2003; McConkey & Zhu, 2008; Shringarpure *et al*., 2006). High levels of HSP27 were also reported in bortezomib resistant HT-29 cells (Suzuki *et al*., 2011). Enhanced levels of β-catenin were found to be associated with bortezomib resistance in myeloma cell lines.

Elevated IGF-1 secretion and activation of IGF-1R was reported to be responsible for bortezomib resistance in various cell lines. Further, inhibition of IGF-IR increased the sensitivity to bortezomib in these cells. Over expressed c-met enhanced bortezomib resistance through activation of Akt/mTOR in human multiple myeloma cells (Que *et al*., 2012). Similarly increased levels Akt/mTOR conferred resistance to bortezomib in mantle cell lymphoma (Kim & Park, 2012). High degree of resistance was developed in Rad (Ras associated with diabetes) expressed cells (Yeom *et al*., 2012).

In addition to the above mechanisms, elevated synthesis of proteasome subunits following inhibition of proteasome or stress conditions, referred as, feedback up-regulation of proteasome is associated with resistance to bortezomib or proteasome inhibitor treatment (Fig.1.4).

1.7 Regulation of Proteasome

1.7.1 Feedback Up-regulation of Proteasome

Early studies in yeast (*Saccharomyces cerevisiae*) identified Rpn4 as a transcriptional activator of proteasome genes. An Rpn4 binding site, a 9 bp (5'-GGTGGCAAA-3') known as PACE (proteasome associated control element) was observed in promoter regions of 26 out of 32 proteasome genes suggesting the concerted regulation of proteasome. Deletion of PACE in one of the proteasome genes markedly

decreased the levels of assembled and active proteasome in the cell. Rpn4 itself is degraded by proteasome and inhibition of proteasome in yeast further up-regulated proteasome expression, an observation which lead to the formulation of a negative feedback circuit for the proteasome homeostasis (Ju *et al*., 2004; Mannhaupt *et al*., 1999; Wang *et al*., 2008; Xie & Varshavsky, 2001). Various stress conditions are known to activate Rpn4 in yeast (Hahn *et al*., 2006). Although bioinformatics analysis reported lack of structural homologs for Rpn4 and PACE in higher eukaryotes, proteasome regulators share functional similarities with yeast. Knock-down of individual proteasome subunits in *Drosophila* cells or inhibition of proteasome activity by MG132 resulted in the 5′-untranslated region dependent up-regulation of other subunits of proteasome suggesting the concerted feedback regulation in higher eukaryotes (Lundgren *et al*., 2005). In addition, inhibition of proteasome or stress induces coordinated up-regulation of proteasome genes in mammalian cells (Meiners *et al*., 2003). Recent studies suggested that Nrf1 and Nrf2, members of CNC-bZIP (cap 'n' collar basic leucine zipper) family of transcription factors which are principally involved in antioxidant response are reported to be involved in the feedback up-regulation of proteasome subunits during proteasome inhibition. Nrf1 and Nrf2 binds to a common sequence (5'-TGAnnnnGC-3') called ARE (anti oxidant response element) in the promoter regions of target genes and activate their transcription (Itoh *et al*., 1997; Johnsen *et al*., 1996; Myhrstad *et al*., 2001). It was observed that almost all proteasome genes contain AREs, though many do not display complete sequence identity with consensus sequence (Rushmore *et al*., 1991). Although both Nrf1 and Nrf2 bind to the same sequence, Nrf1 appeared to activate the proteasome gene expression with higher efficiency (Steffen *et al*., 2010).

Inhibition of proteasome by MG132 lead to the Nrf2 mediated feedback induction of proteasome genes in human skin fibroblast cells (Kraft *et al*., 2006). Increased expression of proteasome genes was reported in the liver of wild type, but not in $Nrf2^{-/-}$ mice treated with antioxidant 3H-1,2-dithiole-3-thione (D3T), a known activator of Nrf2 suggesting the involvement of stress and Nrf2 in proteasome genes up-regulation (Kwak *et al*., 2003). Further, induction of proteasome subunit, PSMB5, by 3-methylcholanthrene (3-MC) requires the presence of ARE and is mediated by Nrf2 in murine neuroblastoma Neuro2A cells (Kwak & Kensler, 2006). Increased proteasome subunit expression and

proteasome activity in samples obtained from colon cancer patients attributed to higher nuclear levels of Nrf2 (Arlt *et al*., 2009). Furthermore, in human skin fibroblasts, Nrf2 was shown to be responsible for inducing proteasome activity in response to a low dose of MG132 (Kraft *et al*., 2006). Studies on mouse embryonic fibroblasts revealed that Nrf1 but not Nrf2 is required for the feedback induction of proteasome genes in response to proteasome inhibitors (Radhakrishnan *et al*., 2010). It is possible that the transcription factors required for the feedback proteasome gene expression are cell type dependent: The feedback regulation is regulated by Nrf1 in some cell types and by Nrf2 in others.

1.7.2 Basal Regulation of Proteasome

Rpn4 has been shown to control both basal and stress induced proteasome expression in yeast (Dohmen *et al*., 2007). Neither Nrf1 nor Nrf2 appears to play a major role in the basal expression of proteasome genes in mammalian cells. Both $Nrf1^{-/-}$ and $Nrf2^{-/-}$ MEFs and the hepatic cells of $Nrf2^{-/-}$ mice display similar endogenous levels of proteasome subunits as their wild-type counterparts (Kwak *et al*., 2006; Radhakrishnan *et al*., 2010). In contrast, the expression levels of a subset of proteasome genes are down-regulated in the neuronal cells of $Nrf1^{-/-}$ knockout mice (Lee *et al*., 2011). Further, impaired basal and induced expression of proteasome genes and diminished proteasome activities were reported in liver-specific knockout of $Nrf1^{-/-}$ in mice (Lee *et al*., 2013).

Low expression levels of a large number of proteasome genes in $Hsf2^{-/-}$ mouse embryonic fibroblast as compared to their wild type counterparts suggests the involvement of HSF (heat shock factor 2) in the basal regulation of proteasome genes (Lecomte *et al*., 2010). Recent study has shown NF-Y transcription factor dependent basal regulation of proteasome genes requires CCAAT box in their promoters, demonstrating that proteasome genes lacking this box are regulated by other transcription factors (Haiming *et al*., 2012). These observations suggest that there may be two distinct mechanisms that regulate proteasome genes expression in mammalian cells, one for the basal level and the other for the feedback up-regulation.

1.7.3 Nrf1 (NF-E2-related factor 1)

It is highly conserved throughout evolution and several different Nrf1 isoforms were detected in cells due to alternative first exons, differential splicing and alternate polyadenylation sites. Amongst them, p120 and p65 isoforms of Nrf1 are predominant and extensively studied. The p120-Nrf1 is localized primarily to ER through N- terminal amino acids as an integral membrane protein, where it is proteolytically cleaved to form the active p95 form, which translocates into the nucleus and bind to the electrophile response element (EpRE, also referred as antioxidant response element or ARE) and induces antioxidant enzyme production. The nuclear p65-Nrf1 isoform contains DNA and Maf binding domains. Due to the absence of transactivation domain p65-Nrf1 does not activate antioxidant response, which makes it a competitive inhibitor of Nrf1 and Nrf2. In addition, Nrf1 contains a Neh2-like domain with complete conservation of the DLG and ETGE motifs important for Keap1 binding. The Neh2 domain of Nrf2 binds Keap1, which regulates Nrf2 stability. Although Nrf1 has also been shown to interact with Keap1, the biological significance of this interaction remains to be determined. Despite the importance of Nrf1 in proteasome biology and its potential as an anti-cancer target, a thorough understanding of the molecular mechanism behind its regulation and activation is currently lacking (Chepelev *et al*., 2011; Madhurima *et al*., 2010).

1.7.4 Nrf2 (NF-E2-related factor 2)

A potent transcriptional activator and plays a central role in the inducible expression of many cytoprotective genes in response to oxidative and electrophilic insults (Itoh *et al*., 1997; Motohashi & Yamamoto, 2004). Under normal conditions Nrf2 is inactive and constantly degraded by proteasome. During stress, it gets activated and translocates to the nucleus and induces the expression of genes involved in glutathione synthesis (Glutamate-cysteine ligase-catalytic, glutamate cysteine ligase-modifier), elimination of ROS (thioredoxin reductase 1, peroxiredoxin 1) and detoxification of xenobiotics (Glutathione S-transferase, NAD(P)H dehydrogenase quinone1). Under basal conditions Nrf2 binds with cytosolic repressor, Keap1, through Neh2 domain. Cullin3, an Ub-ligase (E3) recognizes keap1 and binds to keap1/Nrf2 complex and degrades Nrf2,

which contains degron sequence in Neh2 domain. Keap1 is a cysteine rich protein and under oxidative stress some of the cysteines undergo oxidation impeding its ability to bind Nrf2, thus leading to the activation of Nrf2 and its translocation to the nucleus. In the nucleus small bZIP factors, such as, Maf F, Maf G Maf K form individual heterodimers with Nrf1 and Nrf2 (Itoh *et al.*, 1995; Johnsen *et al.*, 1996 & 1998). These activated heterodimers binds to promoters containing ARE sequence (TGANNNNGC) and activates them. Recent studies revealed EGF/EGFR mediated regulation of Nrf2 thorugh PI3, AKT and ERK pathway involving ROS (Papaiahgari *et al*., 2006).

1.8 EGFR (Epidermal Growth Factor Receptor)

The EGF receptor family is a member of the large family of receptor tyrosine kinases (RTKs), which activates a wide range of biological responses including mitogenesis, migration, differentiation and apoptosis. EGFR (HER1/ErbB-1) is one of the members of the EGFR family consisting of four members including EGFR (HER1/ErbB-1), HER2 (ErbB-2/neu), HER3 (ErbB-3) and HER4 (erbB-4). It is a 170 kDa Type-I transmembrane glycoprotein receptor comprising of three major functional domains. The N-terminal extracellular ligand-binding domain, a hydrophobic transmembrane domain and a intracellular C-terminal tyrosine kinase domain. All the other members share structural similarity with EGFR (Wells, 1999; Yarden *et al*., 2007).

1.8.1 Structure of EGFR

1.8.1a Extracellular Ligand-Binding Domain

The extracellular region of EGFR contains four domains (I-IV). Domains I (LB1) and III (LB2) are each about 160 amino acids in length and together they bind to activating ligands. Domains II (CR1) and IV (CR2) are cysteine rich domains and both of them have around 150 amino acids, held together by one or two disulfide bonds in inactive state. Ligand binding to domains I and III induces a conformational change in the domain II resulting in the exposure of a loop from domain II which further interacts with domain II of another ligand bound EGFR or EGF receptor family member leading to

dimerisation (Bublil & Yarden, 2007; Hubbard, 2009; Jura *et al*., 2009, Wilson *et al*., 2009).

1.8.1b Transmembrane Domain

The EGFR passes the cell membrane through a single α-helical domain consisting of 23 amino acids. Schlessinger, 2002 have reported additional role of transmembrane domain in the regulation of receptor dimerisation.

1.8.1c Intracellular Domain

It comprises of three domains, a juxtamembrane region (JM), a tyrosine kinase domain (TKD) and a carboxy-terminal regulatory region (CT). Various regulatory functions have been attributed to juxtamembrane region such as regulation of down-stream proteins (Castagnino *et al*., 1995), ligand dependent receptor internalization (Kil & Carlin, 2000). Tyrosine kinase domain is the catalytic domain responsible for the auto phosphorylation of tyrosine residues at CT region. Receptor dimerisation promotes the trans-phosphorylation of key tyrosine within the juxtamembrane domain that disrupts the auto-inhibitory conformation and lead to activation of TKD. The CT region contains numerous tyrosine residues which undergo phosphorylation by activated TKD. The CT region also contains several serine/threonine residues that are phosphorylated by down-stream kinases which are part of the EGFR activation. The CT also regulates the activity of TKD by inhibiting its kinase activity (Bose & Zhang, 2009;Hubbard, 2009; Schlessinger, 2000).

1.8.2 Activation of EGFR

Cognate ligand binding to the EGFR triggers dimerisation of ligand bound receptors. EGFR may dimerise with either EGFR (homo dimer) or other members of EGFR family such as Her2, Her3, Her4 (hetero dimer). The dimerization results in the activation of tyrosine kinase activity of the receptors resulting in autophosphorylation of specific Tyrosine (Y) residues (Y 1173, 1148, 1086, 1068 and 992) in the C-terminal end of EGFR. Phosphorylation of tyrosine residues creates binding sites for src homology 2 (SH2) and phosphotyrosine-binding (PTB) domain containing proteins and facilitates

signal transduction. The EGFR phospho-tyrosine may directly recruit these proteins or indirectly via binding to other docking proteins such as Grb2. In addition to auto-phosphorylation, EGFR is also trans-phosphorylated by other tyrosine kinases (such as Src) providing the required docking site for the adaptors and modifiers. In addition, EGFR has been shown to interact with various ligands, such as, EGF, transforming growth factor-α (TGF-α), heparin-binding EGF, amphiregulin, betacellulin (BTC), epiregulin and neuregulin G2β (Gandhi *et al*., 2009; Gazdar & Minna, 2008; Morandell *et al*., 2008; Shtiegman *et al*., 2007; Wells, 1999).

Previous studies reported the accumulation of EGFR in nucleus. In contrast to canonical pathway, activated EGFR escapes internalization and translocates to nucleus and acts as a transcriptional co-factor due to lack of DNA binding domain. Nuclear EGFR has been shown to co-operate in the up-regulation of several genes involved in cell cycle progression like, iNOS, COX-2 and TWIST. Although numerous studies substantiate the nuclear localization of EGFR, the precise mechanism of its translocation is not known (Husvik *et al*., 2009; Lo *et al*., 2006a; Lo *et al*., 2010; Xu *et al*., 2009).

Activated EGFR recruits a number of down-stream signaling molecules, leading to the activation of several major pathways that are important for tumor growth, progression and survival. The major EGFR down-stream intracellular signal transduction pathways include components of the Ras-mitogenactivated protein kinase (MAPK), phosphatidyl inositol 3-kinase (PI3K)-Akt, JAK2-STAT3, PLCγ-PKC and phospholipase D pathways (Alroy I & Yarden Y, 1997; Grant *et al*., 2002; Wells, 1999; Yarden & Sliwkowski 2001; Yarden & Shilo, 2007) (Fig. 1.5).

1.8.3 EGFR Inactivation

In resting cells EGFR resides in lipid rafts of the cell membrane enriched in caveolins and cholesterol. Following ligand binding, EGFR exits these domains in Src dependent manner. The ligand bound receptor within the lipid rafts associate to coat adaptors, such as, adaptor protein 2 (AP2) and Eps15 involved in the endocytic machinery. EGFR endocytosis takes place through clathrin-coated pits (CCPs), cavoelae mediated endocytosis (CavME), or via macro-pinocytosis and finally fuses with lysosomes. EGF dependent activation induces CCPs mediated EGFR endocytosis, IR

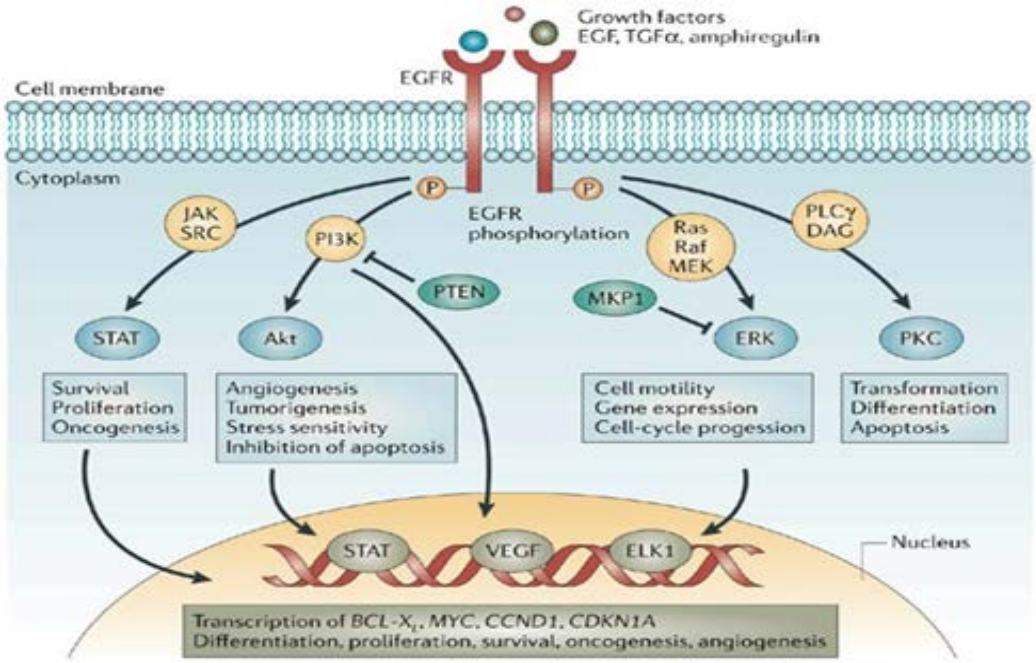

Figure 1.5: Signaling pathways activated by EGFR.
Activated EGFR upon binding of ligand recruits SH2-domain containing proteins and activates them. This further activates STAT, Akt, ERK and PLCγ leading to the activation of various cell survival pathways. The function of each pathway is highlighted in the coloured boxes. Two inhibitors (PTEN and MKP1) are shown to inhibit PI3K and MAPK pathway respectively.

(Mukesh K. Nyati et al 2006. *Nature Reviews Cancer* **6**, 876-885).

induces EGFR CavMe endocytosis (Oved & Yarden, 2002; Zwang & Yarden, 2009). In addition, the phosphorylation of threonine 654 and serines1002, 1046 and 1047 have been associated with a decrease in the ability of EGF to stimulate receptor dimerisation, tyrosine kinase activity, phosphatidylinositol turnover and receptor internalization (Schuh *et al*., 1994).

1.8.4 Constitutive Activation of EGFR

Elevated levels of EGFR expression have been correlated with increased survival in many cancer types including head and neck, bladder, ovarian, cervical and esophageal. Due to the overwhelming network of signal transduction pathways that are involved in EGFR mediated cell signaling either directly or indirectly, EGFR is a major player in various types of cellular functions. Since EGFR is involved in cell proliferation, survival and motility through its down-stream kinases, uncontrolled regulation of EGFR is associated with many human cancers. Several studies have reported that modulation of EGFR-ligand system and mutations in EGFR are the prime causes for constitutive activation of EGFR in several cancers.

The modulation of EGFR-ligand can be achieved by any or all of the following mechanisms.

I) Autocrine production of EGFR ligand TGF-α has been associated with EGFR actvation in various cancers. In addition it has also been shown that TGF-α induced EGFR avoids endocytosis mediated degradation resulting in the constitutive activation of EGFR.

II) Due to the presence of numerous receptors at the membrane, ligand independent spontaneous receptor dimerisation induces constitutive activation of EGFR (Arteaga, 2002).

III) Increased activity of EGFR promoter, deregulation at translational, post translational levels and gene amplification of EGFR has been observed in various cancers that express high levels of EGFR (Gazdar & Minna, 2008; Kersting et *al*., 2008).

In addition to the above mechanisms, various deletion and point mutations in different domains of EGFR have been reported to play a significant role in the constitutive activation of EGFR in various cancers (Sharma & Settleman, 2009).

1.8.5 Downstream Targets of EGFR

1.8.5a Activation of MAPK/ERK1/2 Pathway

Auto-phosphorylation of activated EGFR promotes the binding of growth factor receptor-bound protein 2 (Grb2) to EGFR directly through Src Homology 2 domain (SH2) or indirectly mediated by the binding of EGFR to Shc that then recruits Grb2 (Grant *et al*., 2002). The other domains of Grb2 bind continuously to a guanine nucleotide exchange factor called SOS (Son of Sevenless). This translocated Grb/SOS complex promotes the interaction of Ras with SOS resulting in the activation of Ras by replacing GDP with GTP. Activated Ras recruits Raf to the membrane and activates it by phosphorylation. Raf phosphorylates and activates serine/threonine protein kinases MEK1 and MEK2 which subsequently phosphorylate ERK1 and ERK2 on tyrosine/threonine residues (Crews *et al*., 1992; Dent *et al*., 1992; Kyriakis *et al*., 1992). Activated ERK1/2 phosphorylates numerous substrates in all cellular compartments thereby regulating proliferation, differentiation and cell survival (Aktas *et al*., 1997; Blanchard *et al*., 2000; Liu *et al*., 1995).

1.8.5b Activation of PI3K/Akt Pathway

Class I PI3K are cytoplasmic heterodimers composed of a catalytic subunit (p110) and an adaptor protein (p85), which contains two SH2 and one SH3 binding domain. Through SH2 domains PI3K binds to phophorylated EGFR and gets activated and converts phosphatidylinositol-4,5-bisphosphate (PIP2) to the second messenger phosphatidylinositol-3,4,5-triphosphate (PIP3) (Djordjevic *et al*., 2002). PIP3 serves as a docking site for subsets of proteins containing pleckstrin homology domains which are recruited to the plasma membrane and are activated. The most characterized target of this secondary messanger is the serine/threonine kinase Akt. Translocation of Akt to the membrane brings it close to upstream regulatory kinases such as the phosphoinositide dependent kinase 1 (PDK1) that phosphorylates Akt on Thr 308 (Nicholson & Anderson, 2002), which is necessary for Akt activation. However, maximal activation requires additional phosphorylation at Ser473 by the rapamycin-insensitive mTOR complex (mTORC2) (Sarbassov *et al*., 2005). Once fully activated, Akt localizes both in the

cytosol and the nucleus where it mediates survival, evasion of apoptosis, sustained angiogenesis and replicative potential (Liang *et al*., 2002).

1.8.5c Activation of PLC-γ

Phospholipase C- γ (PLC-γ) directly binds to the activated EGFR at Y1173 and Y992 residues and is consequently activated by phosphorylation on Y771and Y1254 by EGFR. Activated phospholipase C-γ catalyses the hydrolysis of PIP2 resulting in the accumulation of secondary messengers IP3 and 1,2 diacylglycerol (DAG). The cellular role of IP3 is to release calcium while DAG acts as a cofactor in the activation of the protein kinase C (PKC) kinase. Therefore, EGFR can activate Ca^{2+}-dependent pathways and activates other signaling pathways through the indirect activation of PKC (Dengjel *et al*., 2007; Marmor *et al*., 2004).

1.9 STAT3 (Signal Transducer and Activator of Transcription)

STAT3 is a member of STAT family which modulates the transcriptional regulation of diverse genes involved in cell proliferation, differentiation, apoptosis, angiogenesis, metastasis and immune responses. Persistent activation of STAT3 amongst mammalian STAT family members is frequently detected in majority of human cancer cell lines and tumor tissues. These include breast cancer, lung cancer, pancreatic cancer, head and neck cancer, prostate cancer, ovarian cancer, melanoma, leukaemias, and lymphomas.

1.9.1 Activation of STAT3

STAT3 present in cytoplasm remains in the inactive form. Activation of STAT3 requires phoshphorylation of conserved tyrosine 705 (Y705) followed by the formation of pSTAT3 homodimer through the interaction of SH2 domain of pSTAT3 monomer with Y705 residue of its partner. Nuclear localization signals (NLS) present in the coiled-coil domain and dimer dependent DNA binding domain (DBD) interacts with importins. These active dimers are carried to the nucleus through nuclear pore complex (NPC) where they bind to specific DNA sequences in the target genes and regulate their transcription. However, non-phosphorylated STAT3 are reported to enter nucleus at much lower speed than the active STAT3 dimers. Further, phosphorylation of serine

(S727) in the transactivation domain of STAT3 dimer increases the efficiency of its transcriptional activity.

1.9.1a Tyrosine-705 Phosphorylation

STAT3 is activated by phosphorylation of a single tyrosine residue located at position 705. Various tyrosine kinases are reported to be responsible for the activation of STAT3. These include receptors with intrinsic tyrosine kinase activity (RTK) such as epidermal growth factor receptor (EGFR), vascular endothelial growth factor receptor (VEGFR), platelet derived growth factor receptor (PDGFR), and colony stimulating factor-1 (Garcia *et al*., 1997). All these receptors underogo phosphorylation with the help of receptor associated tyrosine kinase (RTK) activity after ligand binding. These phosphorylated receptors docs to SH2 domain of inactive STAT3 followed by phosphorylation of Y705 of STAT3.

Signaling events initiate when ligands such as cytokines (IL-6) bind to and activate their cell surface receptors, typically by inducing receptor aggregation. Cytokine receptors, such as, IL-6 receptors (IL-6R) which lack intrinsic tyrosine kinase activity recruit the Janus kinase 2 (JAK2) posessing tyrosine kinase activity (TK) to mediate activation of STAT3 (Ihle, 1996). Following ligand binding, the receptor-associated JAK2 becomes activated by auto-phosphorylation and subsequently phosphorylate tyrosine residues within the receptor cytoplasmic tails. The receptor phospho-tyrosines serve as docking sites for recruitment of inactive cytoplasmic STAT monomers through interaction with the SH2 domain in STAT3 followed by JAK2 mediated Y705 phosphorylation of STAT3 and further translocation to nucleus (Seidel *et al*., 1995). In addition, non-receptor tyrosine kinases, such as, Src and abl also catalyse the tyrosine phosphorylation of STAT3 directly in the absence of ligand induced receptor signaling.

1.9.1b Serine-727 Phosphorylation

Tyrosine phosphorylation of STAT3 constitutes an early event in the activation of STAT3 that is required for their dimerization and DNA-binding activity. In addition, phosphorylation of a Ser-727 residue in the C-terminal transcriptional activation domain in STAT3 enhances its transcriptional activity (Wen *et al*., 1995). Bromberg *et al*. (1998)

and Turkson et al. (1999) further confirmed that phosphorylation of Ser-727 is essential for Src mediated transformation.

Numerous studies reported that various serine kinases, such as, members of MAPK family (p38MAPK, ERK, JNK), PKCδ, mTOR and NLK have been involved in phosphorylation of STAT3 at serine position 727 (Yokogami *et al*., 2000; Turkson *et al*., 1999; Chung *et al*., 1997b; Jain *et al*., 1999; Kojima *et al*., 2005). These studies demonstrated convergence of tyrosine and serine kinases in STAT3 activation. Additionally, STAT3 is also acetylated on a single lysine residue located at position 685 by histone acetyl transferase p300. This acetylation appears to regulate both transcriptional activity and homodimer stability (Yuan *et al*., 2005).

1.9.2 Negative Regulators of STAT3

1.9.2a Tyrosine Phosphatases

Since, phosphorylation of tyrosine and serine residues of STAT3 are essential for its activation, various tyrosine and serine phosphatases have been shown to play an important role in the inactivation of STAT3. Protein tyrosine phosphatases (PTPs), such as, SH2- domain containing SHP-1 and SHP-2, phospho-tyrosine phosphatase 1B (PTP1B) and T cell- protein tyrosine phosphatise (TC-PTP) have been implicated in the regulation of STAT3. SHP-2 by virtue of its two SH-2 domains, associates with phospho-Y-sites of growth factor receptors, cytokine receptors, gp130, JAKs, members of the Src family of tyrosine kinases (SFKs), STAT3 and dephosphorylates them. The nuclear PTP TC45 is reported to be important in the termination of STAT3-mediated transcriptional activation (Han *et al*., 2006; Herrmann *et al*., 2007). In addition to these, dual specificity phosphatases, such as, PP2A and PP2B have been reported to dephosphorylate serine and tyrosine phosphorylated STAT3 in smooth muscle cells (Liang *et al*., 1999).

1.9.2b Suppressors of Cytokine Signalling (SOCS) Proteins

The family of SOCS (SOCS 1-7) proteins are classical feedback inhibitors of STATs family. They contain a central SH-2 domain flanked by SOCS box domain. The SOCS SH-2 domain binds to pY-containing motifs such as in JAKs, gp130 and cytokine

receptor chains and the SOCS box domain binds to an E3 Ubiquitin ligase complex that can target these for proteasome mediated degradation. SOCS3 inhibits the STAT3 signaling by any of the following mechanisms: a) Binding and inhibition of activated receptors. b) Competing with STAT3 for pY-binding sites on activated receptors. c) Targeting signalling molecules and STAT3 for proteasomal degradation (Croker BA *et al*., 2008; Endo *et al*., 1997; Minamoto *et al*.,1997 ; Nicola *et al*., 1999; Starr *et al*., 1997; Wormald & Hilton, 2004). SOCS3 can also be up-regulated independent of STAT3 through cAMP (Naviglio *et al*., 2010; Woolson *et al*., 2009).

1.9.2c Protein Inhibitors of Activated STATs (PIAS)

This family of proteins have been reported in the regulation of STATs and other transcription factors. PIAS3 binds specifically to the activated STAT3 and blocks its DNA-binding activity and transcriptional activation (Chung *et al*., 1997a). In contrast to SOCS these are nuclear localised. In addition, PIAS mediated gene regulation involves recruitment of transcriptional corepressors, promoting protein sumoylation and targeting them for proteasomal degradation (Shuai & Liu, 2005). However, the role of sumoylation in STAT3 regulation needs further investigation.

1.9.3 Role of STAT3 in Cancer

Malignant transformation of cells by various protein tyrosine kinases, oncogenes and viruses is mediated through STAT3 activation (Frank, 2007). Bromberg *et al*. (1998) and Turkson *et al*. (1998) showed that transformation of cells by src protein kinase is mediated through the activation of STAT-3. Bromberg *et al*. (1999) demonstrated activation of STAT3 alone induces transformation and referred it as oncogene.

In addition to cellular transformation, STAT3 has also been linked with proliferation and survival of tumor cells. Up-regulation of growth promoting genes such as c-myc (Kiuchi *et al*., 1999), cyclin D1 (Masuda *et al*., 2002) and pim-1(Shirogane *et al*., 1999) by STAT3 was reported to be responsible for cell proliferation. Increased levels of cell survival gene products such as bcl-xl (Karni *et al*., 1999), bcl-2 (Zushi *et al*., 1998), survivin (Mahboubi *et al*., 2001), Mcl-1(Liu *et al*., 2003b) and down-

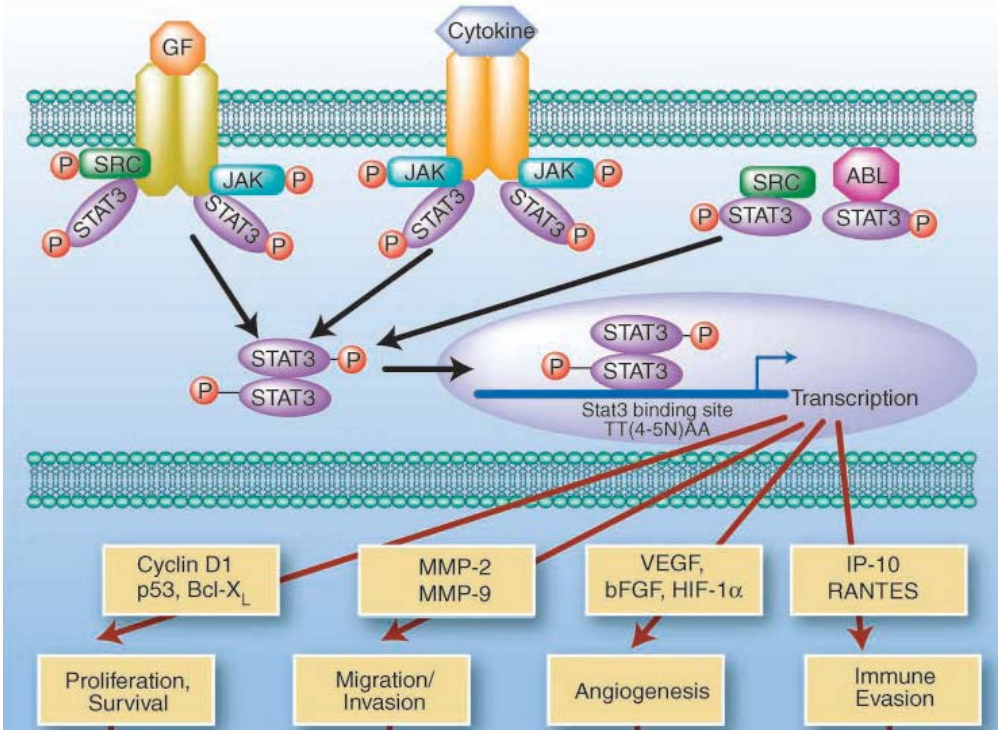

Figure 1.6: Activation and function of STAT3 in Cancer.
Cytoplasmic STAT3 recruited to phospho-tyrosine motifs within complexes of growth factor receptors (e.g., epidermal growth factor receptor), cytokine receptors (e.g., IL-6 receptor), or non-receptor tyrosine kinases (e.g., Src and BCR-ABL) through their SH2 domain. STAT3 is then phosphorylated on a tyrosine705 residue by activated tyrosine kinases in receptor complexes. Phosphorylated STAT3 forms homodimer and translocates to the nucleus. In the nucleus, activated STAT3 dimers bind to specific promoter regions and regulates the expression of genes that are critical for cell transformation and metastasis.
Abbreviations: GF, growth factor; JAK, Janus-activated kinase; P, phosphorylated tyrosine residue; Bcl-xL, Bcl-2-like 1; bFGF,basic fibroblast growth factor; HIF-1a,hypoxia-inducible factor-1a; RANTES,regulated upon activation/normalT-cell expressed and secreted; IP-10,IFN-γ, inducible protein-10.
(Suyun Huang, 2007. *Clin Cancer Res* ;13:1362-1366).

regulation of pro apoptotic factors such as p53 (Niu *et al*., 2005) and Fas (Ivanov *et al*., 2001) by STAT3 inhibits the apoptosis.

Several studies demonstrate that STAT3 plays a crucial role in complex multistep cellular invasion process by regulating the expression of matrix metalloproteinases (MMPs). Constitutively activated STAT3 have been shown to up-regulate the expression of MMP-2, MMP-1 and MMP-9 directly (Dechow *et al*., 2004; Itoh *et al*., 2006; Xie *et al*., 2004). Similarly, over-expression of STAT3 correlated with cellular invasion and metastasis in cutaneous squamous cell carcinoma (Suiqing *et al*., 2005). Targeting STAT3 blocks tumor growth, invasion and metastasis in a pancreatic cell lines (Wei *et al*., 2003).

Cellular migration is a central step for many biological processes including embryogenesis, cell invasion, and cancer metastasis. STAT3 demonstrated a crucial role in wound healing and migration of keratinocytes (Sano *et al*., 1999). Metastasis of human melanoma to brain is regulated by STAT3 (Xie *et al*., 2006). Similarly, over-expression of STAT3 increased migration potency of human prostate epithelial cells (Azare *et al*., 2007).

Formation of new blood vessels from pre-existing vasculature is called angiogenesis and this process is essential for tumor metastasis and proliferation. Vascular endothelial growth factor (VEGF) is the most potent inducer of angiogenesis and is the direct transcriptional target of STAT3. Constitutive activation of STAT3 up-regulates VEGF and induces angiogenesis in endothelial cells (Bartoli *et al*., 2003; Yahata *et al*., 2003) melanoma (Niu *et al*., 2002) and pancreatic cancer cells (Wei *et al*., 2003).

STAT3 activation has a major role in protecting the tumor cells from body's immune surveillance during their transit through circulation by modulating the secretion of various inflammatory factors, such as, IL6 and TNFα that act as immuno suppressors (Nguyen *et al*., 2009). STAT3 activation in tumor micro-environment also reduces the activity of NK cells, thereby protecting tumor cells during circulation (Wang *et al*., 2004). Collectively, all the above studies demonstrate an important role of STAT3 in the initiation and development of cancer (Fig.1.6).

1.10 Back ground, Aims & Objectives

The quality control of cellular proteins and their appropriate turnover rate is essentially controlled by the 26S proteasome, which is a large multicatalytic protease complex comprised of 20S catalytic particle and 19S regulatory particle. The chymotrypsin-like (PSMB5), trypsin-like (PSMB7) and caspase-like (PSMB6) activities which govern the overall function of proteasome reside in the 20S core particle. Targeting the protein degradation pathway using proteasome inhibitors has been shown as a viable anticancer strategy by earlier studies. Bortezomib is the first proteasome inhibitor approved for the treatment of relapsed multiple myeloma and mantle cell lymphoma that targets the PSMB5 subunit. Although, introduction of bortezomib resulted in significant clinical success, incidence of drug resistance has been the major conundrum in clinics.

Studies in various bortezomib resistant cells identified mutations in the PSMB5 subunit, over-expression of PSMB5 and proteasome or feedback up-regulation of proteasome as the major factors governing resistance to bortezomib. Earlier studies reported proteasome inhibitors induced activation of Nrf1, Nrf2 resulting in the feedback induction proteasome subunits including PSMB5 in cell line specific manner, although with greater sensitivity to Nrf1. However, knock out studies of $Nrf1^{-/-}$ and $Nrf2^{-/-}$ revealed their limited role in the basal expression of proteasome subunits. Earlier studies identified HSF and NF-Y dependent basal regulation of proteasome in mouse embryonic fibroblasts and human breast cancer cells. However, the transcription factors regulating the basal expression of proteasome in cancers are largely unknown.

In addition, up-regulation of IGF-1/IGF-1R, IL-6 and various growth promoting pathways were reported in bortezomib resistant cell lines. Inhibition of IGF-1/IGF-1R, Nrf1, NF-Y increased the sensitivity of cancer cells to proteasome inhibitors. Thus, targeting the transcription factors that regulate the expression of proteasome or involved in bortezomib resistance appears to be a promising strategy to improve the treatment regimen. Hence, it is important to study the basal regulation of proteasome in cancer to gain mechanistic insights.

Hence, in the present study we have focused on the regulation of human 20S proteasome in cancer. The main objectives include:

1. To delineate the role of STAT3 in the regulation of proteasomal activity and expression.
2. To elucidate the molecular mechanism involved in EGF-induced activation of 20S proteasome subunits.

CHAPTER 2

MATERIALS AND METHODS

2.1 Materials

2.1.1 Sources of Chemicals

Acrylamide, bis-acrylamide, Agarose, APS, β-mercaptoethanol, BPB, BSA fraction V, calcium chloride, DEPC, DMSO, DTT, ethidium bromide, EDTA, formamide, Glycine, HEPES, IPTG, kanamycin, NaCl, $NaHCO_3$, penicillin, PIPES, PMSF, Ponceau S, propidium iodide, purified 20S proteasome fraction, Resveratrol, RNase A, Sodium dodecyl sulphate (SDS), streptomycin, TEMED, Tris base, Triton X-100, Trypsin-EDTA, Tween-20, X-gal were all obtained from Sigma. Spectra multicolour molecular weight marker proteins for SDS-PAGE, DNA markers and PCR reagents were from Fermentas. Lipofectamine 2000, Trizol Reagent, Superscript II first strand cDNA synthesis kit, DMEM, DPBS, FBS, F12, MEM and RPMI were obtained from Invitrogen. 324674, MG132, EGF, Epoxomicin, LY294002, PD98059, Stattic V, VEGF and WP1066 were from Calbiochem. Bortezomib was from Natco pharma, India. 5X RLB (reporter lysis buffer) for reporter assays, Luciferase assay substrate and buffer were obtained from Promega. Hybond C, Hybond N, and Hybond N^+ membranes were purchased from Amersham Life Science. Western lighting chemiluminescence reagent was from Perkin Elmer Life Science. Columns for preparing transfection grade DNA were from Qiagen or Life Technologies. Restriction enzymes, T4 DNA ligase were from New England Biolabs and Fermentas. Tryptone, agar and yeast extract were from Himedia Laboratories and Blotto was from Santacruz. Whatmann filter papers were from Whatmann International Ltd; X-ray films were from Konica Corporation or Kodak. Other reagents were from local suppliers like Qualigens, SRL, SD fine-chemicals Ltd., and Merck India Ltd. and were of analytical grade.

2.1.2 Antibodies

Rabbit polyclonal anti-Bcl-2 antibody was from Santa Cruz biotechnology. Rabbit polyclonal PSMB5 antibody, rabbit polyclonal anti-PSMB3, rabbit polyclonal anti-FLAG, rabbit polyclonal anti-ubiquitin, mouse monoclonal anti-α tubulin antibody and mouse monoclonal anti-GFP antibody were from Sigma-Aldrich.

Rabbit polyclonal anti-AKt, anti-EGFR, anti-ERK1/2, anti-STAT1, anti-STAT3, anti-pAKt, anti-pEGFR, anti-pERK1/2, anti-pSTAT1 and anti-pSTAT3 were obtained

from Cell Signalling Technologies. Rabbit polyclonal 20S antibody and anti 20S core subunits sampler pack were from Enzo life sciences. Secondary antibodies for Western blotting and immunofluorescence were from Amersham Life Science, Sigma-Aldrich respectively.

2.1.3 Bacterial Strains

***E. coli* DH5α :** F' end A1 hsd R17 (r_{k-} , M_{k-}) sup E44 thi-1 rec A1 gyr A96 (NaI^r) rel A1 Δ (lac ZYA-arg F) $_{u169}$ (ϕ80 lac Zδ M15) strain of *Escherichia coli* was used for all transformations, plasmid isolations and for selection of recombinant clones.

2.1.4 Cell Lines

The cell lines used in this study and their tissue types, growth medium are listed below.

S.NO	Name of cell line	Description of cell line	Growth medium
1	A549	Human lung carcinoma	DMEM
2	MRC5	Human lung fibroblast	MEM
3	DU-145	Human prostate carcinoma	MEM
4	HeLa	Human cervical adeno carcinoma	DMEM
5	HEK293T	Human Embryonic kidney cells	DMEM
6	LNCap-FGC	Human prostate carcinoma	RPMI
7	MDAMB-231	Human breast carcinoma	MEM
8	PC-3	Human prostate carcinoma	F12K
9	WPMY-1A	Human prostate cells	DMEM
10	HePG2	Human hepato carcinoma	MEM
11	MCF-7	Human breast carcinoma	MEM

2.1.5 Plasmids

a) The mU6-pro vector contains the mouse U6 snRNA promoter (RNA polymerase III) with a Bbs I cloning site arranged to allow insertion of the shRNA template sequences after the first nucleotide of the U6 snRNA. The vector has a GFP insert that can be released with Bbs I and Xba I and the hairpin oligonucleotide can be subsequently cloned in its place. This vector was a gift to Dr. Jyotsna Dhawan of CCMB from Dr. David L. Turner, University of Michigan and has been described in (Yu *et al.,* 2002). STAT3 shRNA cloned in mU6Pro vector which targets nucleotides 922 – 938, 2276 – 2296 of STAT3 mRNA (NM_139276.2).

b) pGL3-Basic and promoter vectors were from Promega. pGL3-Basic vector lacks eukaryotic promoter and enhancer sequences and was used to clone putative promoter sequences upstream of a Luciferase (Luc) reporter gene. pGL3-PSMB5 consists of putative promoter sequence of PSMB5 can be excised by KpnI and XhoI digestion.

c) pRC-CMV-FLAG-mSTAT3 plasmid has the mouse wild-type STAT3 cDNA down-stream of CMV promoter was a kind gift from Dr. Vijay Gupta, Scripps Research Institute.

d) pCMV-SPORT-βGal containing the *E.coli* β-Galactosidase gene under a CMV promoter was from Invitrogen.

e) pEGFP-C1 vector contains enhanced GFP in which proteins of interest can be expressed as a fusion to the GFP C-terminus. This plasmid was from Clontech.

f) pTZ75R/T was used for cloning of PCR products. This plasmid was part of the InsTA PCR Cloning Kit purchased from Thermo Scientific (Fermentas).

2.1.6 Substrates

All fluorogenic substrates for proteasome and caspase activities were obtained from Sigma-Aldrich.

Suc-Leu-Leu-Val-Tyr-AMC	Chymotrypsin-like activity
Z-Ala-Arg-Arg-AMC	Trypsin-like activity
Z-Leu-Leu-Glu-AMC	Caspase-like activity (PGPH)
Ac-Asp-Glu-Val-Asp-AMC	Caspase-3 activity

2.1.7 Media, Antibiotics and Chemical Stocks

β-Gal assay buffer (2X): A solution of 1.33 mg/ml ONPG, 2 mM $MgCl_2$ and 100 mM β-mercaptoethanol was made in 200 mM sodium phosphate buffer (pH 7.3), and stored in aliquots at -20°C.

1M DTT: 3.09 g of DTT was dissolved in 20 ml of 0.01 M sodium acetate (pH 5.2), sterilized by filtration and stored as aliquots in -20°C.

1X PBS: 137 mM NaCl, 2.7 mM KCl, 4.3 mM Na_2HPO_4 and 1.4 mM KH_2PO_4. A 10X stock solution was prepared in double distilled water, pH adjusted to 7.4 with HCl and autoclaved.

1X TBE: 89 mM Tris base, 89 mM boric acid and 1 mM EDTA were dissolved in double distilled water. 10X stock solution prepared was filtered, autoclaved and stored at room temperature.

30% acrylamide solution: 29.2 g of acrylamide and 0.8 g of N, N'-methylene bis-acrylamide were dissolved in double distilled water, made up to 100 ml and stored at 4°C in an amber-coloured bottle.

6X Agarose gel loading buffer: 0.25% bromophenol blue and 0.25% xylene cyanol in 30% glycerol.

Amido-black staining solution: 0.1% amidoblack 10B, 25% isopropanol and 10% acetic acid in water.

Amido-black de-staining solution: 25% Isopropanol and 10% acetic acid in water.

Ampicillin: 1000X stock solution was made by dissolving 100 mg ampicillin per ml of sterile double distilled water.

Kanamycin: 1000X stock solution was made by dissolving 50 mg kanamycin per ml of sterile double distilled water.

Buffer saturated phenol: Melted phenol was mixed with equal volume of 0.5M Tris-HCl pH 8.0 and 0.1% 8-hydroxyquinoline and mixed well. The upper aqueous phase was removed and the process repeated with 0.1M Tris-HCl pH 8.0. This step was repeated till the pH of the aqueous solution was equilibrated to 8.0. It was mixed with 0.1 volume of 0.1M Tris-HCl (pH 8.0) and stored in amber-colored bottle at 4°C.

Chloroform:Isoamyl alcohol: 24:1 (v/v) chloroform:isoamyl alcohol mixture was prepared.

DEPC water: Water for RNA isolation was treated with 1% DEPC, left overnight and subsequently autoclaved to remove excess DEPC.

DMEM (1X): 13.4 g of DMEM and 3.7 g of $NaHCO_3$ was dissolved in milli-Q water to make 1 litre of the medium. The pH was adjusted to 7.4 using HCl and subsequently filter sterilized.

MEM (1X): 13.4 g of MEM and 2.6. g of $NaHCO_3$ was dissolved in milli-Q water to make 1 litre of the medium. The pH was adjusted to 7.4 using HCl and subsequently filter sterilized.

RPMI (1X): 13.4 g of RPMI and 2.6. g of $NaHCO_3$ was dissolved in milli-Q water to make 1 litre of the medium. The pH was adjusted to 7.4 using HCl and subsequently filter sterilized.

F-12k (1X): 13.4 g of F-12k and 1.8. g of $NaHCO_3$ was dissolved in milli-Q water to make 1 litre of the medium. The pH was adjusted to 7.4 using HCl and subsequently filter sterilized.

Ethidium Bromide: 10 mg/ml solution in water.

LB Agar: LB media reconstituted with 1.5% Bactoagar was used for pouring LB plates.

Luria-Bertani (LB) broth: 1% Bactotryptone, 1% NaCl and 0.5% Bacto-yeast extract were dissolved in double distilled water. pH was adjusted to 7.4 using 10N NaOH and then autoclaved.

Mountant: 90% glycerol, 10% antifade solution (10 mg/ml para-phenylene diamine hydrochloride in 10X PBS) and 0.5μg/ml DAPI (from 5 mg/ml stock) in 1X PBS.

Penicillin, streptomycin, kanamycin: 600 mg penicillin, 1000 mg kanamycin, 500 mg streptomycin were dissolved in 100 ml 1X PBS and filter sterilized to make a 100X stock which was stored frozen at -20°C. 1X antibiotic solution was used in all tissue culture media.

Ponceau S: A 10X stock of ponceau S was made containing 2% ponceau S, 30% trichloroacetic acid and 30% sulfosalisylic acid in water. For use with PVDF membranes, 1X solution of 0.1% Ponceau S in 5% acetic acid solution was used.

RNase A: 20 mg/ml stock solution was made in 15 mM NaCl and 10mM Tris (pH 7.5). It was then boiled for 15 minutes and cooled slowly to room temperature. The stock was then aliquoted and stored at -20°C.

SDS-PAGE sample buffer (3X): 180mM Tris-Cl pH 6.8, 6% SDS, 15% glycerol, 7.5% β-mercaptoethanol and 0.01% bromophenol blue in double-distilled water and stored at -20°C.

Tris EDTA pH 8.0 (TE): 10 mM Tris HCl (pH 8.0) and 1 mM EDTA (pH 8.0).

Trypsin EDTA: 0.125% trypsin (cell culture grade) and 0.1% EDTA was dissolved in 1X PBS, filter sterilized and stored at -20°C.

2.2 Methods

2.2.1 Plasmid Isolation

Plasmid DNA miniprep was carried out by boiling lysis method as described by Sambrook *et al.,* 1989 with certain modifications. Restriction digestion of plasmids for screening purposes was carried out after the RNase treatment. In order to prepare plasmids for sequencing purposes, an alternate method of plasmid purification from technical manual of the ABI prism 3700 sequencer was used. By this method, 3 ml of overnight grown bacterial culture was pelleted and re-suspended in 100 µl of double-distilled water. 100 µl of lysis buffer (100 µl of 10% SDS, 20µl of 0.5M EDTA and 10 µl 10N NaOH made up to 1ml with water) was added and the tube was kept in boiling water for 2 minutes. 50 µl of 1M $MgCl_2$ was added to these, mixed and kept on ice for 2 minutes. The mixture was spun at a maximum speed in a micro-centrifuge for 2 minutes. 50 µl of 5M potassium acetate was added to the supernatant and kept on ice for 2 minutes. The tube was then spun at maximum speed for 2 minutes and the supernatant transferred to a separate tube. DNA was precipitated by adding 600 µl of isopropanol followed by 2 minutes incubation on ice. The tube was then spun at maximum speed for 2 minutes to pellet the plasmid DNA. The pellet was washed with 1 ml of 70% ethanol and air-dried. The pellet was subsequently re-suspended in 100 µl of TE pH 8.0 containing RNase A.

Plasmids for transfections were prepared using QIAGEN-tip20 (miniprep) and QIAGEN-tip 100 (midiprep) columns or using the GibcoBRL CONCERT High Purity plasmid columns according to manufacturer's instructions. The protocol involves alkaline lysis of cells followed by column purification of DNA that yields high purity plasmids with relatively low levels of impurities.

2.2.2 Quantitation of Nucleic Acids

The nucleic acid concentration was determined by measuring the absorbance at 260 nm (Maniatis *et al.,* 1982). Empirical relationship of 50 μg of double stranded DNA, 33 μg of single stranded DNA or 40 μg of single stranded RNA was taken to be equal to 1.0 OD_{260}. Purity of the preparation was estimated using ratio of absorbance at 260 nm to 280 nm.

2.2.3 Agarose Gel Electrophoresis

DNA and RNA samples were mixed with 6X loading dye (so as to make it 1X) and were resolved, using 0.8-1.2% agarose gels made in 1X TBE buffer. 0.25 μg/ml ethidium bromide was added to gels during preparation for visualizing DNA.

2.2.4 Restriction Endonuclease Digestion

Plasmid DNA (1-2.5μg) was digested with 1-2.5 units of restriction enzyme in a compatible buffer in a 20 μl final volume, as per manufacturers instructions. Digested products were visualized by resolving in an agarose gel along with appropriate DNA markers.

2.2.5 Gel Elution of DNA Fragments

The GeneClean purification kit from Bio101 was used to purify DNA by gel elution. Eluted DNA was used for further protocols such as ligation.

2.2.6 Ligation

DNA fragments obtained after gel purification of PCR products or restriction digests were ligated using T4 DNA ligase at 22°C (for blunt ended cloning) or 16°C for 8

hrs to overnight. A molar ratio of vector to insert of 1:3 was generally used. When using the pTZ75R/T vector for cloning PCR products, the protocol suggested in the product literature was followed.

2.2.7 Preparation of Ultracompetent Cells

The method of Inoue *et al.,* 1990 was used for high efficiency ultra-competent cells. Pre-inoculum of *E.coli* DH-5α strain from a single colony was grown overnight in 10 ml of LB at 37°C. 0.1% inoculum of this culture was added to 250 ml LB medium in a 2-litre flask and kept under vigorous shaking at 18°C till absorbance reached about 0.6. The culture was kept on ice for 10 min and the cells harvested by centrifuging at 2500 g for 10 min at 4°C. The cell pellet was resuspended in 80 ml of ice-cold filter sterilized PIPES buffer (10 mM PIPES, 15 mM $CaCl_2$, 250 mM KCl, 55 mM $MnCl_2$ pH 6.7) and placed on ice for 10 min. Cells were re-centrifuged and gently resuspended in 10 ml of PIPES buffer with 7% DMSO. The cells were kept on ice for about 10 min, aliquoted and snap frozen using liquid nitrogen for storage at -80°C.

2.2.8 DNA Sequencing

ABI Prism Model 3700 DNA Analyzer or Model 3730 DNA Analyzer was used for all DNA sequencing reactions. 200 ng of plasmid DNA and 2.5-5 pmoles of primer was constituted in a volume of 3.2 µl and mixed with 1.8 µl of the big-dye terminator sequencing kit (Perkin-Elmer). PCR was carried out in the Gene Amp PCR System 9600 Thermal Cycler with denaturation at 96°C for 10 sec, annealing at 50°C for 5 sec and extension at 50°C for 4 min, for a total of 35 cycles and a final extension was done for 5 minutes. DNA was ethanol precipitated and washed with 70% ethanol. The samples were then resuspended in 10 µl High-dye-formamide (Perkin-Elmer) and 5 µl of this was loaded in the capillaries.

2.2.9 RNA Isolation

RNA was prepared using TRIZOL reagent (monophasic mixture of phenol and guanidium isothiocyanate (GITC)). Cells were lysed by addition of 1 ml of TRI regent to

1×10^7 cells and allowed to stand for 5 min at room temperature to allow complete dissociation of nucleoprotein complexes. To this 0.2 ml of chloroform was added and kept at room temperature for 10 min after vigorous shaking. It was then centrifuged at 12000g for 15 min at 2-8^{0}C. Centrifugation separated the mixture into 3 phases: a red organic phase (protein), an interphase (DNA) and colourless upper aqueous phase (RNA). Carefully transferred upper RNA layer into a fresh tube, then 0.5 ml of isopropanol was added and inverted few times before incubating at room temperature for 10 min. After incubation, spun down at 12000g for 10 min under cold conditions resulted in the precipitation of RNA. After removing the supernatant the RNA pellet was washed with 75% ethanol to remove salts and proteins and spun-down at 12000g for 5 min. RNA pellet was allowed to dry at room temperature after removing supernatant. The RNA pellet was solubilised in 20 µl of DEPC treated water and quantified by using spectrophotometer as described earlier. Purity of RNA was checked by ratio of 260/280. RNA with 260/280 > 1.8 was used for further experiments.

2.2.10 Genomic DNA isolation

After removing upper aqueous layer (RNA) 0.3 ml of 100% ethanol was added to remaining phases and incubated at room temperature for 5 min after mixing by invertion. To precipitate the DNA, the mixture was centrifuged at 2000g for 5 min at 2-8^{0}C. Supernatant containing protein was removed and the DNA pellet was washed twice with 10% ethanol solution containing 0.1 M trisodium citrate after an incubation of 30 min each time at 2000g for 5 min. Then, the DNA pellet was incubated with 1.5 ml of 75% ethanol at room temperature for 20 min and spun-down at same speed as above. After drying the DNA pellet 8 mM NaoH was added to get a final concentration of 300 ng / µl. Purity and quantification of DNA was done by using spectrophotometer as described earlier.

2.2.11 Polymerase Chain Reaction (PCR)

PCR was done in a reaction mix containing 1X PCR buffer (10 mM Tris-HCl pH 9.0, 50 mM KCl, 1.5 mM $MgCl_2$, 0.01% gelatin- Taq buffer 10A from Bangalore Genei), 250 mM each of the dNTPs, 200 ng primers and 1.5 units of Taq DNA polymerase. After

an initial denaturation at 94°C for 2 min required number of cycles was carried out. Each cycle consisted of denaturation at 94°C for 30 sec, annealing at 4°C below melting temperature of the primer for 1 min and extension at 72°C for 1 min. A final extension for 7 min was given at 72°C for completion of elongation products.

2.2.12 Reverse Transcription and Polymerase Chain Reaction (RT-PCR)

RT reaction was carried out using the Superscript II first strand cDNA synthesis kit (Invitrogen) according to the manufacturers recommended protocol. 2 μg of total RNA was used as the template and oligo-dT was used as primers for reverse transcription in 20 μl reaction volume. The RNA was annealed with 500 ng of oligo-$dT_{(12-18)}$ at 65^0C for 5 min in a 10 μl reaction volume. This was incubated at 42^0 C for 2 min in a reaction mix containing 1X RT buffer (20 mM Tris-HCl pH 8.4, 50 mM KCl), 5 mM $MgCl_2$, 10 mM DTT, 500 μM of each dNTP and 40 units of RNase inhibitor. The reverse transcription was carried out at 42^0 C for 50 min using 50 units of Superscript II RT enzyme. The reaction was stopped by incubation at 70^0C for 15 min. The reverse transcription product was used as template for semi-quantitative PCR reactions. The primers used for RT-PCR are listed below:

PRIMER	SEQUENCE	Amplicon size (bp)	T_m, No. of cycles
PSMA1-F	5'- CAGGGCAGGATTCATCAAAT -3'	431	56^0C, 28
PSMA1-R	5'- GACATGGCTCTGCAGTCAAA -3'		
PSMA2-F	5'- TGAATATGCTTTGGCTGCTG -3'	539	56^0C, 28
PSMA2-R	5'- GCCCTTCAAAGCTTTCCTTT -3'		
PSMA3-F	5'- TGCTATGAAGGCTGTGGAAA -3'	403	56^0C, 26
PSMA3-R	5'- CGGCAGGTCATTTCTTTCAT -3'		
PSMA4-F	5'- TTTTGCTTGCAGCAGAGAGA -3'	385	56^0C, 27
PSMA4-R	5'- GCTGCAGCGCTATTATTTCC -3'		
PSMA5-F	5'- CCATGAGTGGGCTAATTGCT -3'	407	56^0C, 27
PSMA5-R	5'- GCATTCAGCTTCTCCTCCAT -3'		

PSMA6-F	5’- CAGGGTGGCCTTACATCAGT -3’	355	56^0C, 27
PSMA6-R	5’- ATACCTGAGGGCCTTGCTCT -3’		
PSMA7-F	5’- AGTGCGGAAGATCTGTGCTT -3’	260	56^0C, 27
PSMA7-R	5’- AGAGCCTAGGAGTGCCATCA -3’		
PSMB1-F	5’- TTTCGCCCTACGTTTTCAAC -3’	559	56^0C, 27
PSMB1-R	5’- TACAGCCCCCTTTCCTTCTT -3’		
PSMB2-F	5’- AAGGCCCCGACTATGTTCTT -3’	510	56^0C, 25
PSMB2-R	5’- AGGTTGGCAGATTCAGGATG -3’		
PSMB3-F	5’- GAAGGGGAAGAACTGTGTGG -3’	553	56^0C, 27
PSMB3-R	5’- CCTGGTGGTGATTTTGTCCT -3’		
PSMB4-F	5’- TCAGTCCTCGGCGTTAAGTT -3’	456	56^0C, 27
PSMB4-R	5’- GCTTAGCACTGGCTGCTTCT -3’		
PSMB5-F	5’- CCATACCTGCTAGGCACCAT -3’	404	56^0C, 25
PSMB5-R	5’- GCACCTCCTGAGTAGGCATC -3’		
PSMB6-F	5’- CCTATTCACGACCGCATTTT -3’	329	56^0C, 22
PSMB6-R	5’- TCCCGGTAGGTAGCATCAAC -3’		
PSMB7-F	5’- GCAACTGAAGGGATGGTTGT -3’	241	56^0C, 22
PSMB7-R	5’- AAACTAGGGCTGCACCAATG -3’		
Bcl2-F	5'- CTACGAGTGGGATGCGGGAGATGT -3’	473	56^0C, 28
Bcl2-R	5’- GGTGCCGGTTCAGGTACTCAGTCATC -3’		
18S- F	5’- CCTGCGGCTTAATTTGACTC -3’	168	56^0C, 18
18S- R	5’- ATGCCAGAGTCTCGTTCGTT -3’		

2.2.13 Quantitative Real-Time PCR (qRT-PCR)

ABI prism 7500 model system was used to perform Real Time PCR. Primers specific for real-time PCR were designed and conditions were optimized to generate >95 % PCR efficiency. Dissociation curve analysis was performed after the last cycle to confirm amplification of a single product. Each sample was run in triplicate in a final volume of 25 µl containing 30 ng of cDNA, 10 pmol of each primer, and 12.5 µl of SYBR® Green 2X PCR master mix. The PCR consisted of denaturation at 95^0C for 15 sec, annealing at 56^0c for 30 sec and extension at 72^0C for 30 sec for 40 cycles. During

PCR, fluorescence accumulation resulting from DNA amplification was analyzed using the sequence detector software (Applied Biosystems) at extension step. Comparative Ct method was used to quantify the target genes abundance. RQ Manager 1.2 (Applied Biosystems) was used to compile data from all plates and compare expression levels. The threshold cycle (Ct) was defined as the fractional cycle number at which the fluorescence exceeds the given threshold. Transcript abundance of genes were normalized to that of 18S RNA. The obtained data were translated into the log2 scale. The real time results are presented as fold change in expression relative to control using target gene Ct values normalized to that of 18S RNA gene Ct values based on the $2^{-\Delta\Delta Ct}$ method (Livak and Schmittgen, 2001). Primers employed for Real-Time PCR are listed below.

PRIMER	SEQUENCE	Amplicon size (bp)	Tm, No. of cycles
PSMB3-F	5'-GAGAAACGGTTTGGCCCTTA-3'	169	58^0C, 40
PSMB3-R	5'-GGGACTCACACATTCCGTAC-3'		
PSMB5-F	5'-GTTCTGGCTCTGTGTATGCA-3'	152	58^0C, 40
PSMB3-R	5'-CACGTGGTAGAGGTTGACTG-3'		
PSMB6-F	5'-GGACTCCAGAACAACCACTG-3'	160	58^0C, 40
PSMB3-R	5'-TTCAATGCTGTGGAAACCGA-3'		
PSMA1-F	5'-TTCCAAACCTGTCCATCTGC-3'	167	58^0C, 40
PSMA1-R	5'-GGAAGCGTCTCTCTTAAGGC-3'		

2.2.14 Identification of Putative STAT3 Binding sites in 20S Proteasome Subunits

The genomic location and sequence of human 20S proteasome subunits genes were determined using the human genome blast at NCBI. Using the NCBI software Spidey, intron-exon structure of the gene was determined. Presence of STAT-3 binding sites was determined in these sequences using the MatInspector 2.2 software (Genomatix) with a stringency level of 0.6 for both core and matrix.

2.2.15 Construction of Vectors for Expressing Short-hairpin RNA (ShRNA)

The shRNAs targeting STAT3 were constructed using mU6 promoter based vector. The desired synthetic oligonucleotides targeting the nucleotide sequences of STAT3 (NM_139276.2) were annealed and cloned into the BbsI-XbaI digested mU6 pro. The oligonucleotides were designed so as to encode short-hairpin RNAs (shRNA) with a duplex length of 21 nucleotides (nt) and a 9-nt loop. The sequence representing the anti-sense strand was put before that representing the sense strand in the oligonucleotides. 2 μg of complementary oligo nucleotides were annealed by incubation at 65^0C for 5 min in a buffer containing 10mM Tris pH 8.0 and 50mM NaCl, followed by slow cooling at room temperature (total volume- 40 μl). These oligonucleotides were designed to have overhangs of Bbs I site at the 5' end and Xba I site at the 3' end to enable cloning into the mU6pro vector between Bbs I and Xba I sites. mU6pro vector expressing shRNA of unrelated sequence of the same length used as control.

Hairpin siRNA template:

TTTGNNNNNNNNNNNNNNNNNNNNNNNNNNNNNNNNNNNNNNNTTTTT

NNNNNNNNNNNNNNNNNNNNNNNNNNNNNNNNNNNNNNNAAAAAGATC

Cloning vector with Bbs1/Xba1 overhangs:

4170 4180 770 780 790 800

…TCCCTTGGAGAAAAGCCTTG CTAGATTCTGCAGCCCTATAGTGAGTCGTATTACG…

AGGGAACCTCTTTTCGGAACAAAC TAAGACGTCGGGATATCACTCAGCATAATGC

The positive clones were identified by colony PCR and the sequence was confirmed by sequencing. The oligonucleotides used for cloning shRNA in the study are listed below.

PRIMER	SEQUENCE	ShRNA
Sh-STAT3-A1	5'tttgCAATGGAGTACGTGCAGAAGAttcaagagaTCTTCTGCACGTACTC CATTGttttt 3'	Sh-STAT3-1
Sh-STAT3-A2	5'ctagaaaaaCAATGGAGTACGTGCAGAAGAtctcttgaaTCTTCTGCACGTA CTCCATTG 3'	
Sh-STAT3-B1	5'tttgAGGAGGAGGCATTTGGAAAGTttcaagagaACTTTCCAAATGCCTC CTCCTttttt 3'	Sh-STAT3-2
Sh-STAT3-B2	5'ctagaaaaaAGGAGGAGGCATTTGGAAAGTtctcttgaaACTTTCCAAATGC CTC CTCCT 3'	

2.2.16 Generation of Adenoviruses Expressing STAT3

Adenoviral vectors were generated using the AdEasy™ adenoviral vector system from Stratagene. The cDNA was isolated from the pRC-CMV-FLAG-mSTAT3 plasmid by PCR and was cloned into the Kpn1/Xho1 of pAdtrack-cytomegalovirus (CMV) plasmid co-expressing green fluorescent protein as marker to monitor infection efficiency. The cDNA is under the control of the CMV promoter terminated by the simian virus 40 (SV40) polyadenylation signal, resulting in pAd-STAT3. The pAdTrack-CMV plasmid was utilized as a control vector. Both pAd-STAT3 and pAdTrack-CMV were linearized by Pme1 digestion, ethanol precipitated and resuspended in 10 µl of water. Electro competent BJ5183 cells which harbors Adeasy-1 were prepared as described and stored at -80^{0}C. 20 µl of BJ5183 were electroporated at 2,500 V, 200 Ω and 25 µF with 1 µg of linearized pAd-STAT3 or pAdTrack-CMV. Recombinant adenoviral DNAs were produced by homologous recombination of Pme1 digested pAd-STAT3 or pAdTrack-CMV with pAdeasy-1 plasmid (adenoviral) contained in the AdEasier-1 cells (*E.coli* BJ5183). The transformants were selected on kanamycin plate. Small colonies were patched on both kanamycin, streptomycin plates. The colonies which grew on both kanamycin and streptomycin plates were selected for further screening for recombination. After screening for the recombinants by Pac1 digestion, the plasmids containing positive inserts were transformed in *E.coli* DH5α to increase the yield of the plasmids. Recombinant adenoviral vector DNA (2µg), digested with PacI and ethanol precipitated was used for transfection of Hek293T cells in a 35mm dish. A transfection mix was prepared by adding 2µg of linearized plasmid DNA and 4 µl of

Lipofectamine 2000 (Invitrogen) and transfections were carried out according to the manufacturer's instructions. Transfections and production of virus were monitored by GFP expression. After 7 to 10 days post-transfection, cells were scraped off along with the medium, lysed by three cycles of freezing in liquid nitrogen and rapid thawing at 37°C. Lysed cells along with medium was centrifuged at 3000 rpm for 10 minutes at room temperature to pellet the cell debris, the supernatants containing the viruses were aliquoted and stored at -80^{0}C. These harvested viral supernatants were used to infect 50,000 HEK293T cells. The least volume of viral supernatant capable of completely infecting cells was employed for further amplification in HEK293T cells. High titers of viruses were generated by infecting sub-confluent HEK293T cells plated in a 60mm dish. After 40-48h of infection viral supernatants were prepared as mentioned above. Infections were carried out in PC-3 cells at MOI (Multiplicity of Infection), which resulted in 100% infection.

All the procedures involved in the generation and production of recombinant adenoviruses were performed under the conditions of Biosafety Level 2 (BL2) and wastages containing adenoviruses were disinfected with chlorine bleach.

2.2.17 Mammalian Cell Culture

Cell lines were maintained in respective medium containing 10% FBS with penicillin, streptomycin and kanamycin at 37^0 C in a humidified 5 % CO_2 containing incubator. Sub-culturing was done by incubating the cells with trypsin-EDTA solution after rinsing with sterile 1X PBS. Detached cells were re-suspended in 1:3 ratio. For storage of cells 10% DMSO containing growth medium was added to equal volume of cells after trypsinization and allowed to freeze slowly at – 80^{0}C for 30 min and kept at liquid nitrogen for long time storage.

2.2.18 Transfection of DNA in Mammalian Cells

Cells were transfected with required plasmids using Lipofectamine 2000 reagent according to the manufacturer's instructions. Cells were trypsinized and required numbers were plated in antibiotic free medium the day before transfection. Plasmids (total of 500 ng per 12 well plate and 2 μg for each 35 mm dish) and Lipofectamine 2000

(1 µl for coverslips and 4 µl for 35 mm dishes) were diluted in serum and antibiotic-free DMEM, mixed, incubated for 30 minutes at room temperature and added on to the cells. Transfections were stopped after 5 hrs by replacing transfection medium with complete DMEM.

2.2.19 Immunofluorescence

For immunofluorescence, the cells were grown on cover slips and processed as described by Radha *et al.,* 1994. The cells, after required treatments or transductions, were washed with PBS and fixed with 3.7% formaldehyde in 1X PBS (pH 7.4) for 10 min at room temperature. They were then permeabilized using 0.5% Triton-X 100 and 0.05% Tween-20 in 1XPBS for 6 minutes at room temperature. The cells were then washed and incubated with PBS containing 2% BSA for 1 hr at room temperature for blocking. They were then incubated for 4 hr with primary antibody that is diluted in PBS (anti-FLAG 1:100) containing 2% BSA. After washing with PBS, cells were incubated with fluorophore-conjugated secondary antibody (anti-TRITC 1: 500) in blocking solution for 1 hr at room temperature. The cells were again washed with PBS and mounted on glass slides in vectashield mounting medium containing DAPI to stain nuclei. Localization was observed using LSM510 META confocal laser scanning microscope equipped with a ×63 objective (Carl Zeiss).

For bright field images after treatment cells were directly observed under Olympus microscope and images were captured. The cells were observed using an Olympus BX60 fluorescence microscope and images were captured with a CCD and analysed using the Image-Pro software.

2.2.20 Quantification of Proteins

For quantifying proteins from the lysate used for enzyme activity determinations, Bradford method was employed and amido black method was used for Western blotting procedures. 1 mg/ml of BSA was employed to generate standard curve. Briefly, the clarified cell lysates were diluted to 10 µl with water and 100 µl of Bradford reagent was added to this in a 96 well plate. Commassie G-250 in Bradford reagent binds with positive amino acids and gives dark blue color. After keeping in dark for 5 minutes with

constant shaking readings were taken at 595 nm and quantification of proteins was done from standard graph. For amido black method, cell lysates collected in 1X sample buffer were heated at 100 ^{0}C for 10 min and 1 µl of each sample was loaded on nitro cellulose membrane. After air-drying for 10 min, amido black solution was added for 10 min followed by washing with destaining solution to remove background stain. Band intensities were quantified with densitometric analysis using syngene gel doc.

2.2.21 SDS-Poly Acrylamide Gel Electrophoresis (SDS-PAGE)

SDS-PAGE, as described by Laemmli, 1970, was carried out using a discontinuous buffer system. Stacking gel (0.125 M Tris-HCl pH 6.8, 5% acrylamide and 0.1% SDS) and the resolving gel (0.375 M Tris HCl pH 8.8, 10 or 12 % acrylamide and 0.1% SDS) were polymerised using TEMED and 10 % ammonium per sulphate . The gels were run using buffer containing 0.025M Tris, 0.192M glycine and 0.1% SDS at 20 mA constant current. After stacking of proteins at the resolving front and subsequent entry into the resolving gel, current was increased to 30 mA till the end of the run.

2.2.22 Western Blotting

Proteins resolved using the SDS-PAGE gel were blotted onto nitrocellulose membranes (Hybond C from Amersham or Immobilon P from Millipore) using the semidry apparatus (Pharmacia). The semidry transfer buffer containing 39 mM glycine, 48 mM Tris-HCl, 0.0375% SDS and 20% methanol was used and transfer was carried out at constant current at 0.8 mA / cm^2 for 1-2 hrs. After transfer, the proteins were stained using ponceau S solution and the positions of molecular weight markers were marked using pencil. Subsequently, blots were incubated in 5% Blotto (Santacruz) in TBST (10 mM Tris HCl pH 8.0, 150 mM NaCl, 0.05% Tween-20) for 1 hr at room temperature. The blots were then incubated with the required dilution of primary antibody in 0.5% Blotto in TBST for 1-2 hrs at room temperature or overnight at 4^0 C. Non-specifically bound primary antibody was removed by three 5-minute washes with TBST. Subsequently, blots were incubated with appropriate dilution of secondary antibody in 0.5% Blotto in TBST for 60 minutes. After three washes with TBST, blots were processed for enhanced chemilumunescence (ECL) detection. ECL was done using the

Western lighting chemiluminescence reagent from Amersham and different exposure times were given to get the right intensity of the signal.

2.2.23 β-Galactosidase (β-Gal) Assay

The assay for β-galactosidase activity in cell extracts was performed according to the method described in Promega protocols and applications guide. For each assay 20 µl of lysate was diluted to 100 µl with 1X RLB (Reporter Lysis Buffer). Equal volume of 2X β-galactosidase assay buffer was added and the tube was incubated at 37^0C until yellow colour developed (5-10 min). The reaction was stopped by the addition of 400 µl of 1M Na_2CO_3 and the absorbance was measured at 420 nm. Values shown are the mean ± SD of at least three independent experiments. $p< 0.05$ were considered as significant.

2.2.24 Luciferase Reporter (LUC) Assay

Lysates from cells transfected in 35 mm dishes were made using 1X RLB (Promega). 200 µl of 1X RLB was added to each well after initially removing the medium and rinsing the cells with 1X PBS. The plate was kept in a shaker for 15 min and the cells were subsequently scraped using a cell lifter. Repeated pipetting was done to obtain a suspension and the debris was pelleted down by centrifugation at 10,000 rpm for 2 min under cold conditions. The supernatant was used for LUC assays and β-galactosidase assays. Generally, a reaction containing 100 µl of LUC assay buffer with substrate, 20 µl lysate and the volume was made up to 150 µl with 1X RLB. The amount of luminiscence from reaction mix was measured at 37^0C using Tecan multimode reader. The obtained luminescence values were normalized with β-gal assays and represented as fold change or relative Luc activity compared to control. Values shown are the mean ± SD of at least three independent experiments. $p< 0.05$ were considered as significant.

2.2.25 Sequence Analysis

NCBI programs BLASTn and BLASTp were used to analyze sequence similarity and database search. Bl2seq was used to align two nucleotide sequences based on their similarity (http://www.ncbi.nlm.nih.gov/BLAST/). WebCutter 2.0 was used for analyzing

restriction enzyme sites. MatInspector v2.2 (http://www.genomatix.de/cgi-bin/matinspector/matinspector.pl) was used for identifying STAT3 binding sites in genomic sequences. Genomic sequence alignment with mRNA to identify intron-exon organization was carried out using Spidey at NCBI (http://www.ncbi.nlm.nih.gov/spidey/). Sequence Manipulation Suite was used to arrange and reverse complement sequences (http://www.ualberta.ca/~stothard/javascript/).

2.2.26 Measurement of Caspase-3 Activity

Following treatments, cell pellet was washed twice with phosphate-buffer saline and suspended in lysis buffer (50 mM HEPES, (pH 7.4) with 5 mM CHAPS and 5 mM DTT) for 15 min on ice. Subsequently, cells were centrifuged for 15 min at 14000g in cold conditions. Supernatant was added to assay buffer (20 mM HEPES -pH 7.4, 2 mM EDTA, 0.1% CHAPS and 5 mM DTT) containing 40 µM of caspase-3 substrate, Ac-DEVD-AMC). The incubation was for duration of 1 hr with readings recorded at an interval of 5 min. Fluorescence released by AMC was measured at 360 nm and 460 nm excitation and emission respectively. Values are normalized to protein concentration and expressed as a fold change of activity relative to DMSO control. Values shown are the mean ± SD of at least three independent experiments.

2.2.27 Measurement of 20S Proteasome Activity

Following the termination of experiment, cells were washed and collected in DPBS by centrifugation at 3000 rpm/5 min under cold conditions. Pellet was suspended in lysis buffer containing 0.5 mM DTT, 0.1 % Triton X-100 in DPBS for 10 min on ice and centrifuged at 13,200 rpm/10 min in cold conditions. Supernatant (cell lysate) containing 20S proteasome was collected. 20 µg of supernatant was used for assay. Peptidase activities of proteasome were measured by the addition of 50 µM of fluorogenic peptides Suc-Leu-Leu-Val-Tyr-AMC (for chymotrypsin-like), Z-Ala-Arg-Arg-AMC (for trypsin-like), Z-Leu-Leu-Glu-AMC (for caspase-like activity) separately to assay buffer containing supernatant. The assay buffer is composed of 50 mM Tris-HCl (pH 7.8), 20 mM KCl, 5 mM MgCl2, and 1 mM DTT was added to cell lysate. The mixture was incubated for 1 hr with readings recorded for every 5 min at 37^0C. Later, the

reaction was stopped by addition 125 mM sodium borate buffer (pH 9.0) containing 7.5% ethanol. Different peptidase activities cleave their respective peptide substrates to release free fluorescent AMC. The released fluorescence was measured by using 360 nm/460 nm excitation and emission wavelengths respectively in EnSpire multimode plate reader (Perkin Elmer). Enzymatic activities were normalized to protein concentration and expressed as percentage of activities relative to DMSO control. Values shown are the mean ± SD of three independent experiments.

2.2.28 26S Proteasome Activity Assay

Cells were lysed using lysis buffer 50 mM Tris, pH 7.4, 2 mM DTT, 5 mM $MgCl_2$, 2 mM ATP and 250 mM sucrose on ice for 10 min. Supernatant was collected after centrifugation in cold condition at 13,200rpm / 10 min. 20 µg of supernatant was added to assay buffer containing 50 µM fluorogenic proteasome substrates. The assay buffer is as same as lysis buffer except sucrose. Proteolytic activities were measured and expressed as similar to 20S proteasome activity.

2.2.29 Measurement of Apoptosis by Flow Cytometry

Fluorogenic propidium iodide (PI) binds to nucleic acids. Since, apoptotic cells demonstrate low levels of DNA content or condensed nucleus, they exhibit less fluouroscence by propidium iodide. Flow cytometry was used to measure the red fluorescence emitted by propidium iodide. Follwoing treatments, cells were collected by trypsinization and resuspended in 0.5 ml of PBS and fixed with 4.5 ml of 70% ethanol under cold conditions for 10 min. Cells were spun down at 400g for 5 min and washed with PBS under cold conditions. Cell pellet was suspended in 1 ml of DNA staining solution containing 0.002% of propidium iodide, 0.02% of DNase free RNase in PBS and incubated for 1 hr at room temperature in the dark. The DNA contents of 20,000 events were measured by flow cytometer (DAKO CYTOMATION, Beckman Coulter, Brea, CA). Histograms were analyzed using Summit Software.

2.2.30 Statistical Analysis

Data was analyzed using Student's *t*-test to make statistical decisions between different treatment conditions and number of replicates. The hypothesis was tested at a level of significance of 0.05 (p= 0.5), employing the software designed by Microsoft, termed as Excel.

CHAPTER 3

REGULATION OF PSMB5 & β-SUBUNITS OF PROTEASOME BY STAT3

3.1 Introduction

The ubiquitin-proteasome system facilitates degradation of regulatory and abnormal proteins. Polyubiquitinated proteins are targeted for degradation by the 26S proteasome. Aberrations of this pathway lead to pleiotropic defects in all aspects of cell function. Because of their indispensable role, inhibitors of the proteasome are routinely used as antineoplastic agents in clinics (Coux *et al*., 1996; Goldberg, 2003; Demartino & Gillette, 2007; Tanaka, 2009). Most of the proteasome inhibitors target the chymotrypsin-like activity of PSMB5, although they co-inhibit the caspase-like and/or trypsin-like activity at higher concentrations. Bortezomib, a peptide boronic acid congener, is used clinically as a frontline therapy for multiple myeloma as a single agent or in combination with standard therapies. Bortezomib binds and inhibits the chymotrypsin-like activity of the PSMB5 subunit. However, resistance to bortezomib develops in a majority of patients, thereby limiting its clinical efficacy (Adams, 2004; Chen *et al*., 2011; Kisselev *et al*., 2012). Hence, elucidation of the mechanism of regulation of PSMB5 is imperative to identify the molecular basis of bortezomib resistance.

Suppression of the proteasome activity or autophagy in mammalian cells by pharmacological inhibitors results in the induction of PSMB5 and other proteasome genes in a concerted manner (Meiners *et al*., 2003; Wang *et al*., 2013). Nrf1 and Nrf2 are key transcription factors involved in the up-regulation of proteasome genes in response to proteasome inhibition. Under normal conditions, Nrf1 undergoes endoplasmic reticulum-mediated degradation, whereas, Keap1-bound Nrf2 is degraded by the ubiquitin-proteasome system. In response to proteasome inhibition, these transcription factors translocate to the nucleus and form heterodimers with Maf proteins. The Nrf1/Maf or Nrf2/Maf heterodimers transactivate proteasome genes through the antioxidant response elements in the promoters (Kwak *et al*., 2006; Radhakrishnan *et al*., 2010; Steffen *et al*., 2010). Brain specific, conditional knockout mice of Nrf1 exhibit a coordinated down-regulation of the basal levels of various proteasomal genes (Lee *et al*., 2011). Conversely, endogenous levels of proteasome subunits remain unaltered in mouse embryonic fibroblasts of *nrf1*- and *nrf2*-disrupted mice (Radhakrishnan *et al*., 2010). Therefore, on the basis of these observations, Nrf1 or Nrf2 largely regulate the feedback response to proteasome inhibition and contribute minimally to the basal expression of proteasome

genes. However, the transcription factors that regulate the basal level expression of proteasome subunits are largely unknown (Xie, 2010).

Neoplastic growth is frequently associated with increased proteasome activity and subunit expression to maintain protein homeostasis (Bazzaro *et al*., 2006; Chen & Madura, 2005; Kraus *et al*., 2007; Ren *et al*., 2000; Wyke *et al*., 2004). Because of their stringent mode of activation, Nrf1 and Nrf2 are unlikely to promote the increased proteasome subunit expression in malignancies unless they are deregulated. Accordingly, colon tumors showed a gain of proteasome activity because of increased nuclear localization of Nrf2 (Arlt *et al*., 2009). Thus, to cope with increased proteasome function in malignancies, it is plausible that the proteasome genes are regulated coordinately by oncogenic transcription factor(s).

In this study, we investigated the mechanisms underlying increased proteasome subunit expression and activity in mammalian cell lines harboring oncogenic STAT3 protein.

3.2 Results

3.2.1 Inhibition of activated STAT3 down-regulated PSMB5 in DU 145 cells

3.2.1a Effect of Stattic treatment on PSMB5 expression

Earlier studies have shown that Bortezomib treatments of HNSCC cell lines lead to a significant up-regulation of total and phosphorylated STAT3 (Li *et al*., 2009). In another study, bortezomib-resistant clones of human monocytic cells, THP1 cell line manifested a marked increase in PSMB5 protein levels (Oerlemans *et al*., 2008). These observations suggest a possible role of STAT3 in the regulation of PSMB5 expression. To explore this, we opted for DU 145 cells, which harbor aberrantly high levels of activated STAT3. DU 145 cells were treated with Stattic, an inhibitor of pSTAT3 at different concentrations 1, 2.5, 5, 7.5, 10 µM for 24 h (Schust *et al*., 2006). Stattic treatments resulted in the down-regulation of PSMB5 protein levels in a dose dependent manner while tubulin remained constant. A significant decrease in the protein levels of PSMB5 was evident at 2.5 µM of Stattic and there was further decrease in PSMB5 levels with increasing concentrations. PSMB5 levels were almost undectable at 10 µM of Stattic

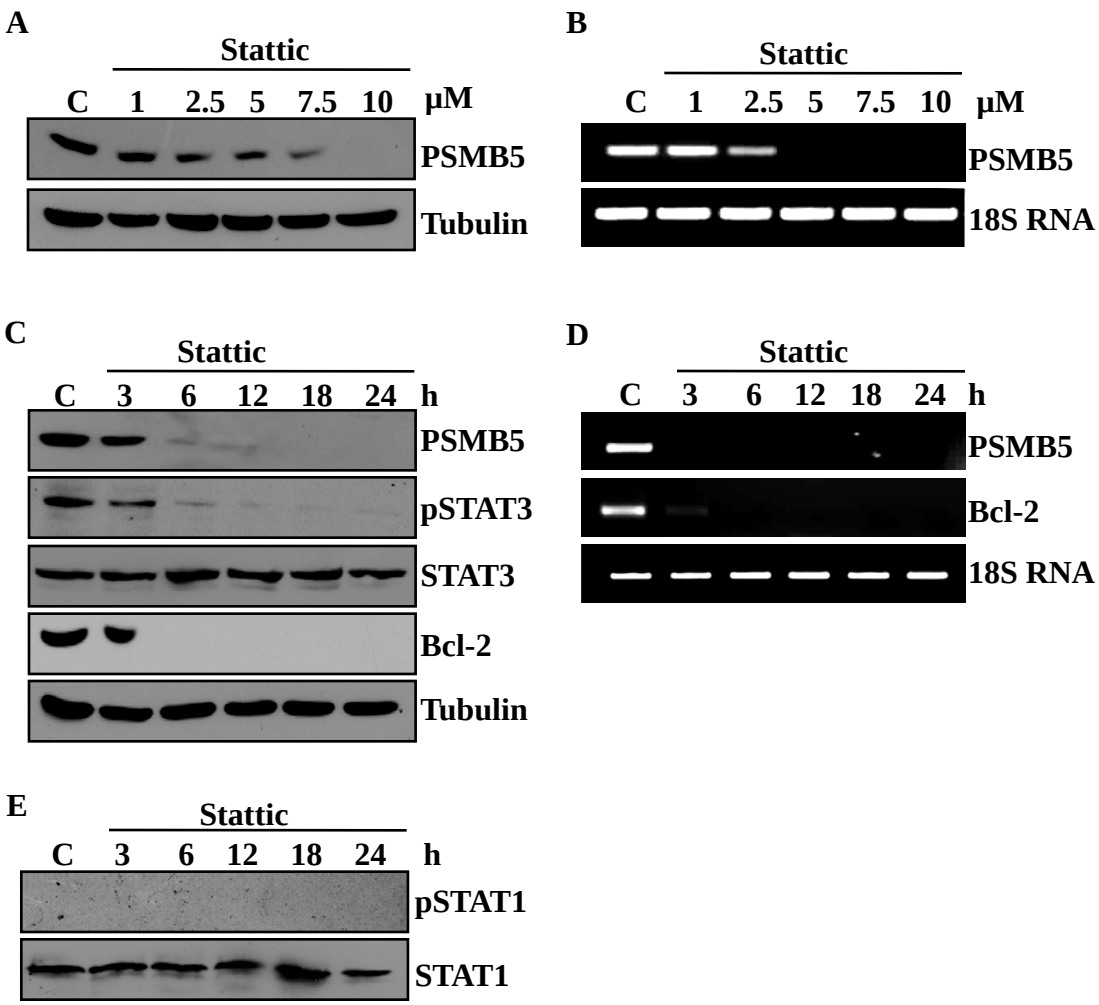

Figure 3.1: Dose and Time dependent inhibition of pSTAT3 down regulated PSMB5 expression.

Panel A, Panel B, DU 145 cells were treated with different concentrations of Stattic as indicated for 24 h: *Panel C, Panel D, Panel E*, DU 145 cells were treated for indicated time points with Stattic (10 μM). *Panel A, Panel C,* Subsequently cells were harvested and antibodies were employed to detect PSMB5, pSTAT3, STAT3, Bcl-2; *Panel E* pSTAT1 and STAT1. Tubulin used as loading control. *Panel B, Panel D,* Total RNA was isolated by Trizol and subsequently semi quantitative RT-PCR was performed to analyze the PSMB5, Bcl2. 18S RNA used as loading control.

treatment (Fig. 3.1A). Next, we analyzed the mRNA levels of PSMB5 under similar treatment conditions. PSMB5 mRNA levels were also down-regulated in dose dependent manner while 18S RNA levels, which was employed as loading control were unaltered (Fig. 3.1B).

Based on the above observations, we have treated DU 145 cells with Stattic at 10 µM concentrations for 3, 6, 12, 18, 24 h. Stattic treatments resulted in the down-regulation of PSMB5 protein in a time dependent manner. The decrease in PSMB5 levels was evident as early as 3 h time period and the levels were hardly detectable from 12h onwards following Stattic treatment (Fig. 3.1C). To validate these results and any non-specific effects of inhibitor, we further checked the levels of STAT3, pSTAT3, Bcl-2, tubulin from same lysates. Stattic treatments resulted in the down-regulation of STAT3 tyrosine phosphorylation (phospho-STAT3-Y705) from 3 h and the same was undetectable from 12 h onwards, whereas, total STAT3 protein levels remained constant in control and all the treatments. The protein levels of Bcl-2, a target of STAT3, also decreased significantly by 3 h following Stattic treatment and from 6 h onwards Bcl-2 levels were undectable, whereas tubulin which was employed as a loading control, remained the same during the course of treatment (Fig. 3.1C). Further, we explored the mRNA levels of PSMB5 following inhibition of pSTAT3 in DU 145 cells. Results demonstrate that STAT3 inhibition by Stattic (Fig. 3.1D) drastically reduced the mRNA levels of PSMB5, Bcl-2 while 18S RNA remained unchanged. Moreover, the decrease in protein levels was preceded by mRNA levels of PSMB5 and Bcl-2 in pSTAT3 inhibited DU 145 cells.

Since STAT3 shares a close structural similarity with STAT1, to validate the specificity of STAT3 inhibitor, Stattic treated DU 145 cells were analyzed for phospho-STAT1-Y701 levels. Notably, the tyrosine phosphorylated STAT1 levels were undetectable in DU 145 cells and total STAT1 levels remain unchanged in treated and control cells (Fig. 3.1E).

3.2.1b Effect of WP1066 on PSMB5 expression

In order to validate our observations with Stattic, DU 145 cells were treated with another STAT3 inhibitor, WP1066 at different concentrations 1, 2.5, 5, 7.5, 10 µM for 24

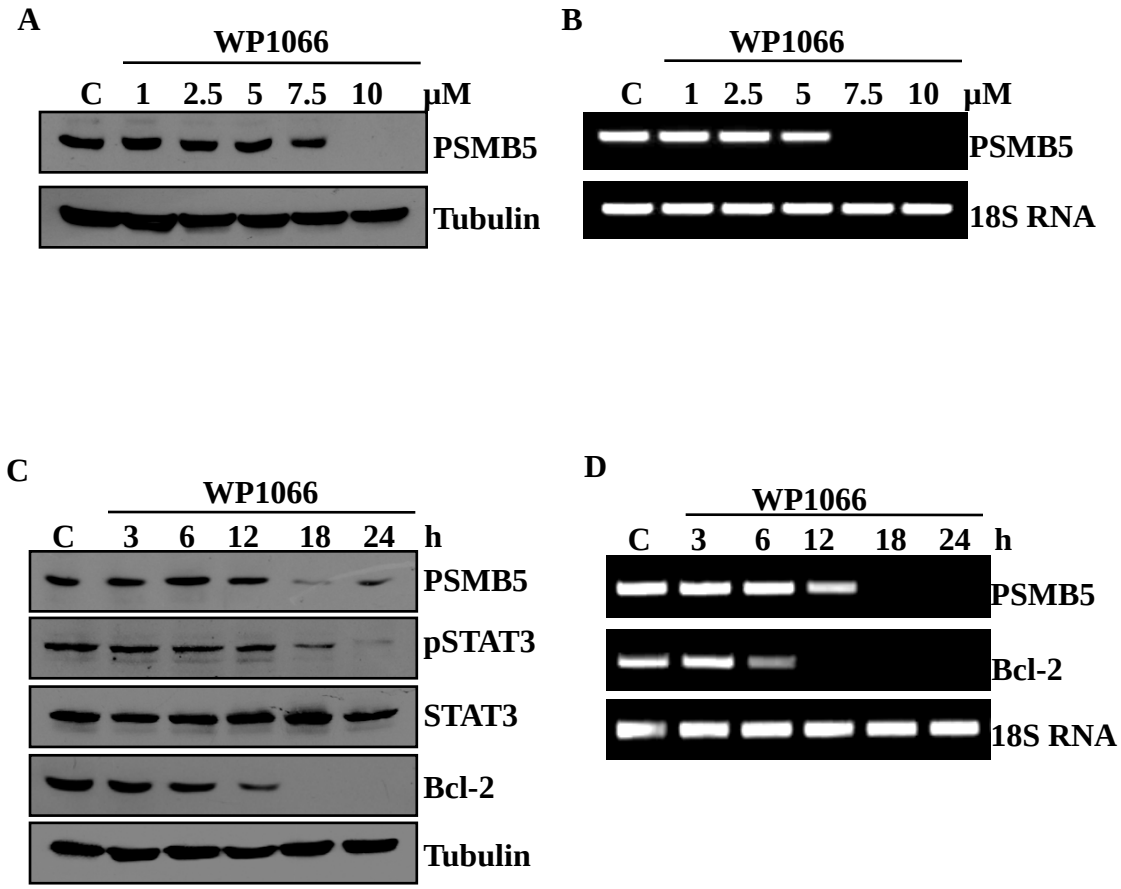

Figure 3.2: Inhibition of pSTAT3 down regulated PSMB5 expression.

Panel A, Panel B, DU145 cells were treated with different concentrations of WP1066 as indicated for 24 h: *Panel C, Panel D,* Cells were treated for indicated time points with Stattic (10 µM). *Panel A, Panel C,* Subsequently cells were harvested and antibodies were employed to detect PSMB5, pSTAT3, STAT3 and Bcl-2. Tubulin was employed as loading control. *Panel B, Panel D,* Total RNA was isolated by Trizol and subsequently semi quantitative RT-PCR was performed to analyze the PSMB5, Bcl2. 18S RNA used as loading control.

h (Iwamaru *et al*., 2007). WP1066 treatments resulted in a dose dependent down-regulation of PSMB5 protein levels while the levels of tubulin, which was employed as a loading control remained constant. The decrease in the protein levels of PSMB5 was evident from 5 μM and a further decrease at 7.5 μM and undetectable levels of PSMB5 was evident at 10 μM of WP1066 treatment (Fig. 3.2A). Next, under similar treatment conditions mRNA levels of PSMB5 were also decreased in a dose dependent manner while 18S RNA levels remained constant similar to Stattic treatments (Fig. 3.2B).

Further, DU 145 cells were treated with WP1066 at 10 μM for different time points same as Stattic treatment. Treatment with WP1066 resulted in significant reduction of PSMB5 protein levels by 18 h. Phospho-STAT3-Y705 levels also concomitantly decreased from 18 h of treatments. Bcl-2, known target of STAT3 was also down-regulated from 12 h onwards. Similar to Stattic, the protein levels of STAT3 and tubulin remained unchanged in WP1066 treated cells. The difference in the inhibition of phospho-STAT3-Y705 protein levels in Stattic and WP1066 treated cells is probably due to the efficacy of the inhibitors. The decrease of pSTAT3-705 levels correlated with decrease of PSMB5 protein levels (Fig. 3.2C). Furthermore, levels of mRNAs of PSMB5, Bcl-2 were also down-regulated similar to protein levels in WP1066 treatments (Fig. 3.2D).

3.2.1c Effect of Resveratrol on PSMB5 expression

Previous studies reported that Resveratrol inhibits Src tyrosine kinase activity and thereby blocks STAT3 protein activation in DU 145 cells (Kotha *et al*., 2006). To further confirm the STAT3 dependent PSMB5 subunit expression, we have employed resveratrol at 25, 50, 75, 100 μM concentrations for 24 h. Treatment of DU 145 cells with resveratrol suppressed phospho-STAT3-Y705, Bcl-2 levels in a dose-dependent manner with a profound potency at higher concentrations while total STAT3 and tubulin remain unaffected. Reduction in pSTAT3-Y705 was associated with decreased PSMB5 protein levels in resveratrol treated cells. Down-regulation of PSMB5 was evident from 50 μM followed by a further decrease at 75 μM and 100 μM concentrations of resveratrol (Fig. 3.3A). Next, analysis of mRNA levels of PSMB5 in resveratrol treatments shown dose dependent down-regulation along with Bcl-2, while 18S RNA levels remained constant

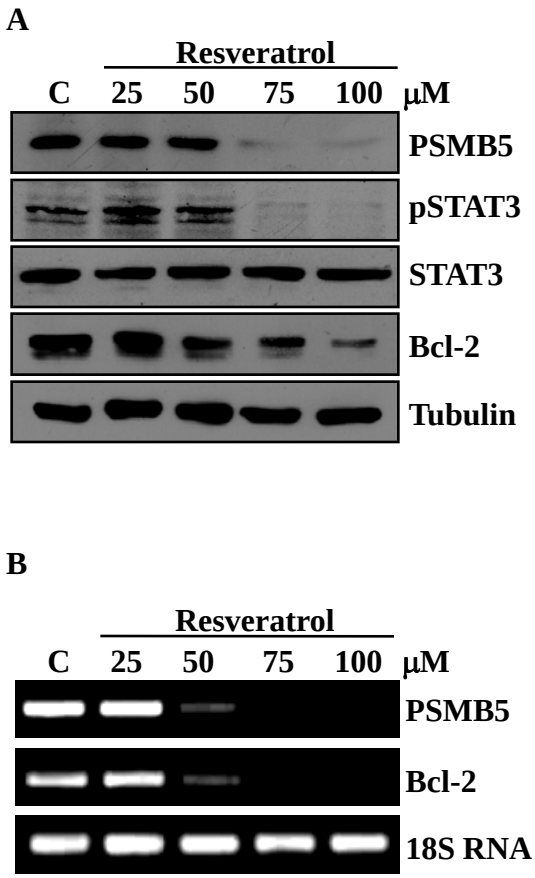

Figure 3.3: Resveratrol decreases the expression of PSMB5 in a dose dependent manner.

DU 145 cells were treated with indicated concentrations (25 μM-100 μM) of Resveratrol for 24 h. *Panel A,* Subsequently, immunoblot analysis was performed for PSMB5, pSTAT3, STAT3, Bcl-2 and Tubulin. *Panel B,* mRNA expression levels of PSMB5, Bcl-2 were analyzed with Semi quantitative RT-PCR. 18S RNA used as loading control.

indicating that STAT3 induced down-regulation of PSMB5 occurs at transcription level (Fig. 3.3B).

3.2.1d Effect of STAT3 knockdown on PSMB5 expression

To provide further evidence for the requirement of STAT3 in the regulation of PSMB5, we used a STAT3-directed short hairpin RNA (shRNA). Both the constructs of STAT3-shRNA significantly knocked down total STAT3 and pSTAT3-Y705 protein levels along with Bcl-2, while GFP and tubulin expression remain unchanged indicating uniform transfection and protein amount. Scrambled shRNA was used as control. In accordance with our earlier observations, knockdown of pSTAT3 protein resulted in lower PSMB5 protein levels along with Bcl-2 (Fig. 3.4A). Further, under similar experimental conditions, mRNA levels of PSMB5 and Bcl-2 were also corroborated with protein levels (Fig. 3.4B).

Taken together, pharmacological inhibition of pSTAT3, shRNA-mediated knock down of constitutive pSTAT3 down-regulated the PSMB5 protein and mRNA levels in DU 145 cells. Hence, the observed findings suggest that STAT3 activation plays an important role in the expression of PSMB5 in DU 145 cells.

3.2.2 STAT3 inhibition coordinately down-regulated the expression of a majority of 20S proteasome subunits in DU 145 cells

Previous reports demonstrated that proteasome genes are regulated coordinately through a common transcription factor (Kwak *et al*., 2006; Radhakrishnan *et al*., 2010; Steffen *et al*., 2010). Since, expression of PSMB5 was down-regulated by pSTAT3 inhibition (Fig. 3.1- Fig.3.4), we analyzed whether the other α and β-subunits of 20S proteasome are also coordinately regulated by pSTAT3. To test this assumption, we treated DU 145 cells dose-dependently with Stattic (5, 10 μM) for 24 h. It was observed that like PSMB5 protein, levels of β-subunits such as PSMB1, PSMB3, PSMB4, PSMB6, PSMB7 and α-subunit such as PSMA4 were decreased to undetectable levels at both 5 μM, 10 μM, whereas, PSMB2, PSMA1 levels were significantly reduced by Stattic treatments at both the concentrations and the effects were more profound at higher

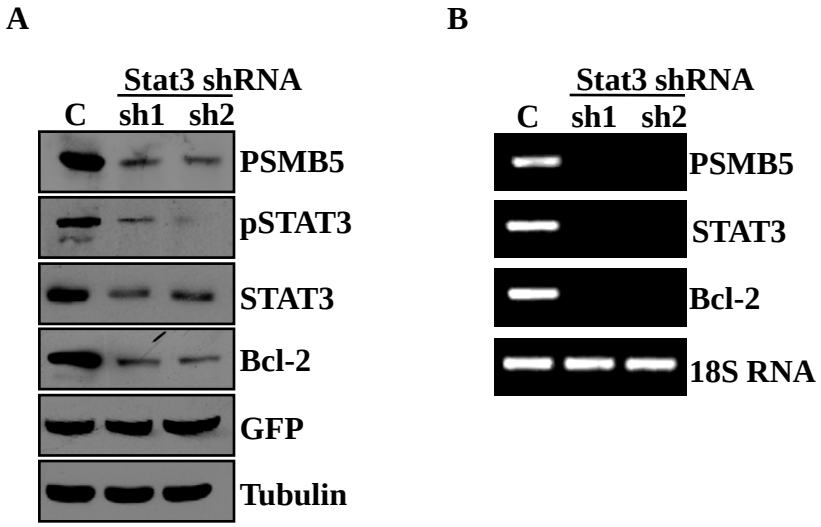

Figure 3.4: Down regulation of PSMB5 by STAT3-ShRNA.

DU145 cells were transfected with 2 μg of each STAT3-shRNA. After 48 h; *Panel A,* cells were harvested and expression of pSTAT3, STAT3, PSMB3, PSMB5 and Bcl-2 was analyzed with immunoblotting. Tubulin used as loading control. GFP used as transfection control. *Panel B,* mRNA levels of PSMB5, STAT3 and Bcl-2 was analyzed with Semi quantitative RT-PCR. 18S RNA was used as loading control.

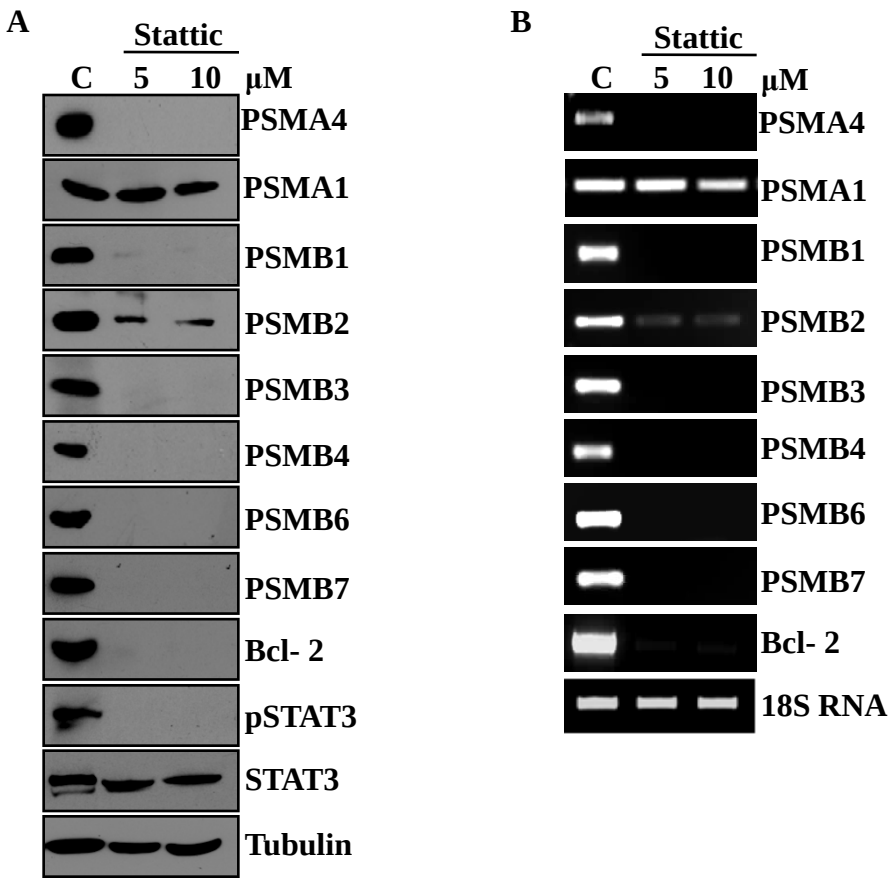

Figure 3.5: Effect of STAT3 inhibition on mRNA and protein levels of 20S proteasome subunits.

DU145 cells were treated with 5 μM, 10 μM concentrations of Stattic for 24 h. *Panel A*, Immunoblot analysis was performed for subunits of 20S proteasome, pSTAT3, STAT3, and Bcl-2. Tubulin was used as a loading control. *Panel B*, Total RNA was isolated and semi-quantitative RT-PCR analysis was performed for PSMA (α-subunits), PSMB (β-subunits). 18S RNA served as loading control.

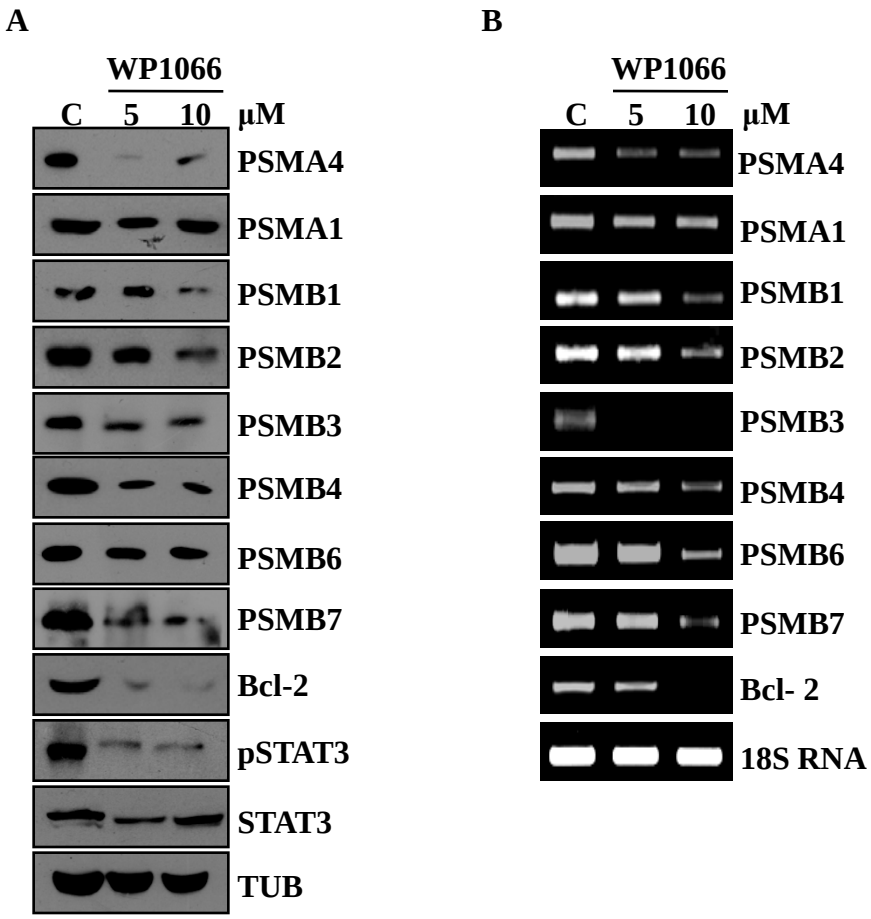

Figure 3.6: Effect of WP1066 on expression of 20S proteasome subunits. DU145 cells were treated at 5 µM, 10 µM concentrations of WP1066 for 24 h. *Panel A,* Under similar conditions of treatment immunoblot analysis was performed for subunits of 20S proteasome, pSTAT3, STAT3 and Bcl-2. Tubulin was used as a loading control. *Panel B,* mRNA levels of 20S proteasome subunits were analyzed using semi-quantitative RT-PCR. 18S was used as loading control.

concentration. Stattic also decreased the levels of pSTAT3-Y705 and Bcl-2 protein levels at both 5 µM, 10 µM, whereas, total STAT3 remained the same. Moreover the decrease in pSTAT3 was correlated with down-regulation of PSMA4, PSMB1, PSMB3, PSMB4, PSMB6 and PSMB7 (Fig. 3.5A). Next we sought to verify whether similar conditions of treatments would concertedly effect the expression of mRNA levels of α and β-subunits. Corroborating the results obtained at protein levels, the mRNA levels of α-subunits, β-subunits and Bcl-2 were also coordinately decreased in Stattic treated cells while 18S RNA levels remain unaffected (Fig. 3.5B).

To further validate these observations, DU 145 cells were treated with WP1066 at 5 µM, 10 µM concentrations for 24 h. Suppression of pSTAT3-Y705 by WP1066 also resulted in the down-regulation of 20S proteasome subunits. The levels of PSMB4, PSMB7, PSMB3 and PSMA4 were decreased, albeit to a lesser extent at both 5 µM, 10 µM which correlates with pSTAT3-Y705 and Bcl-2 levels, whereas, PSMB1, PSMB2 protein levels were decreased significantly in a dose dependent manner. PSMB6 levels were reduced to nearly 50% at both the concentrations, whereas, the protein levels of PSMA1 was moderately reduced at 5 µM, 10 µM of WP1066 (Fig. 3.6A). However, abrogation of proteasome subunits, pSTAT3-Y705 as in Stattic treatments was not observed in WP1066 treatments, suggesting that the residual pSTAT3-Y705 levels were probably the reason for the expression of moderate levels of proteasome subunit. Next, we determined whether similar conditions of treatments would concertedly effect the expression of mRNA levels of 20S proteasome α and β-subunits. Similar to the expression of protein levels, mRNA levels of 20S proteasome were substantially down-regulated in WP1066 treated DU 145cells (Fig. 3.6B).

Thus, taken together the above results suggest that blockade of activated STAT3 coordinately reduced the mRNA and protein levels of most of the α- and β-subunits of 20S proteasome in DU 145 cells.

3.2.3 Suppression of pSTAT3 down-regulated PSMB5 in pSTAT3 constitutive cells

In addition to DU 145, few other cell lines were also shown to express constitutively active STAT3, such as, A549, HeLa and MDA-MB-231 (Zhao *et al*., 2011; Zhou *et al*., 2010). Hence, we analyzed in these cell lines to know whether

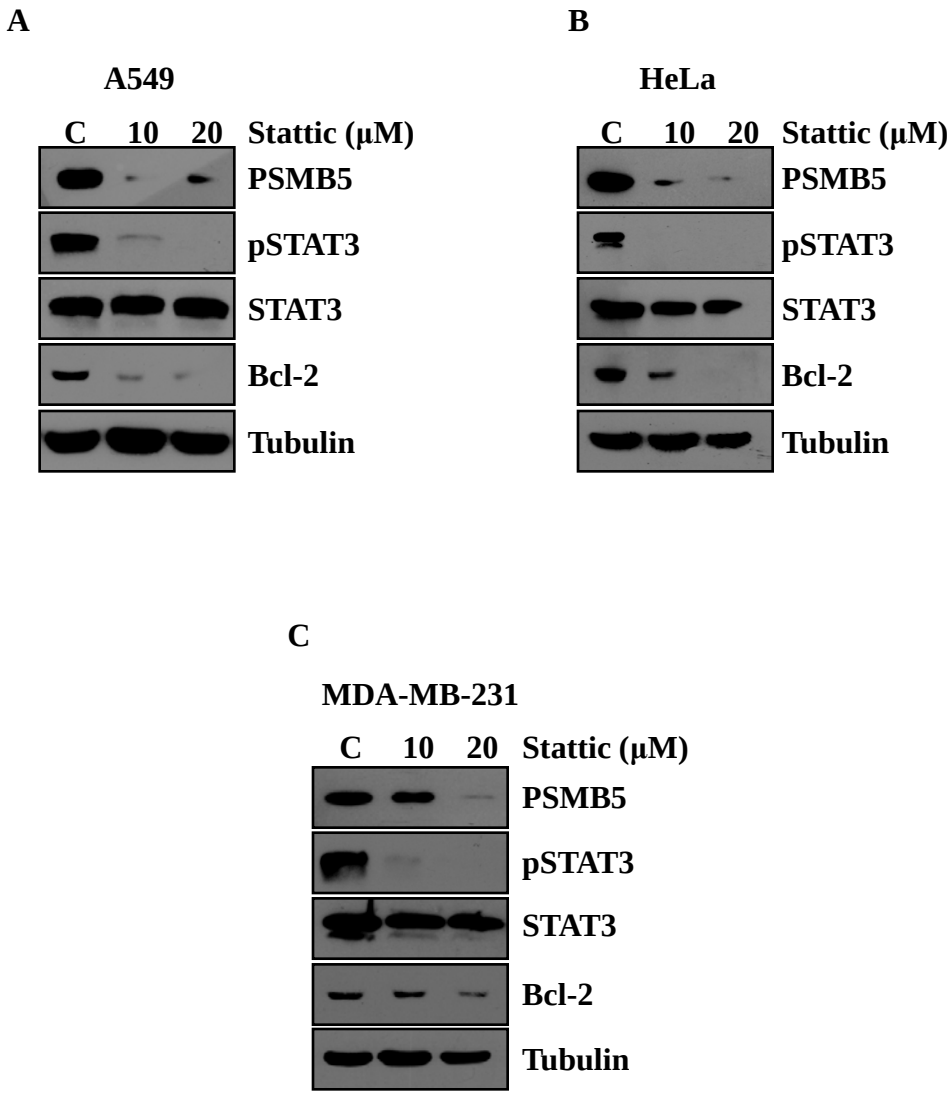

Figure 3.7: Stattic down regulated PSMB5 protein levels in pSTAT3 constitutive cell lines.

Panel A, B and C represents 10 μM, 20 μM of Stattic treated A549, HeLa and MDA-MB-231 respectively for 24 h. Immunoblot analysis was performed for PSMB5, Bcl-2, pSTAT3 and STAT3. Tubulin was used as a loading control.

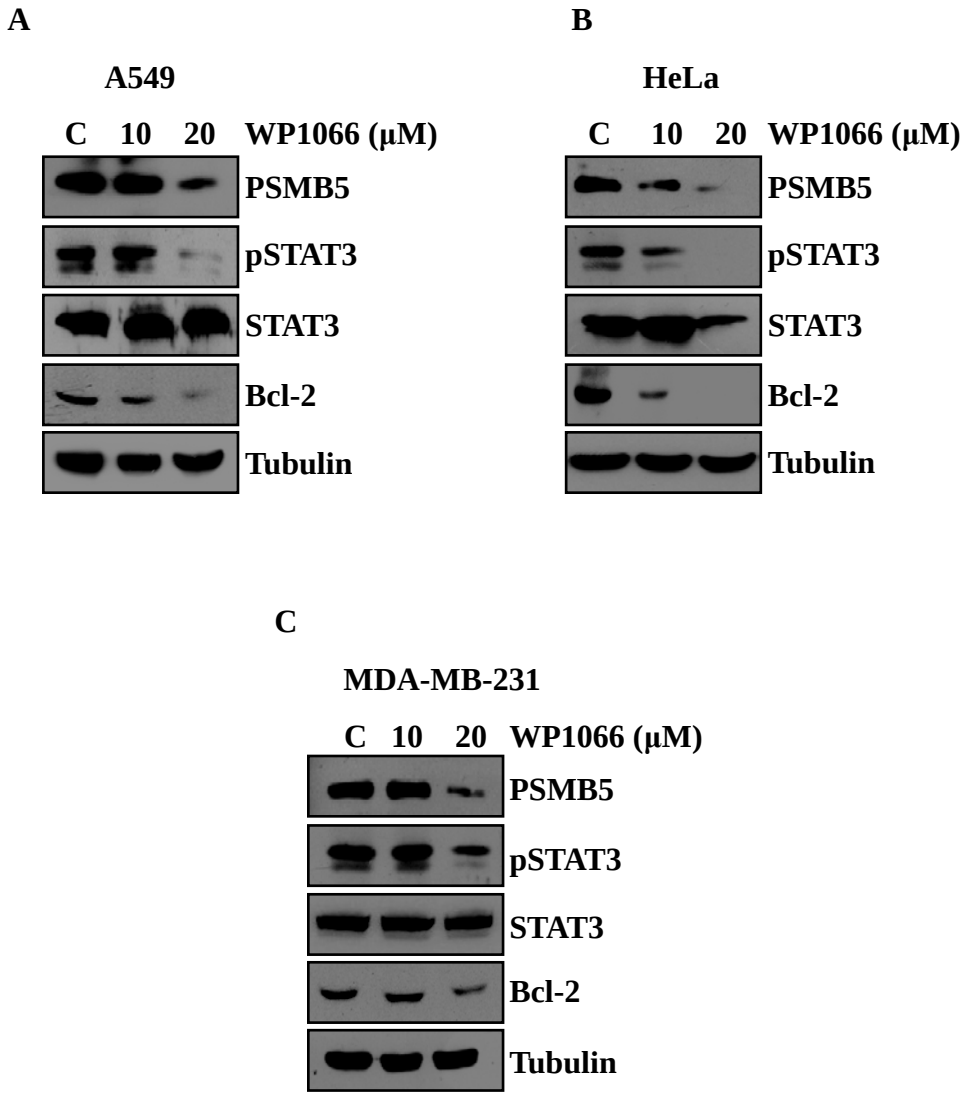

Figure 3.8: WP1066 decreases protein levels of PSMB5 in STAT3 constitutively active cell lines.

Panel A, B, and C represents A549, HeLa and MDA-MB-231 cells respectively treated with 10 μM, 20 μM concentrations of WP1066 for 24 h. Total cell lysates were probed for PSMB5, pSTAT3, STAT3 and Bcl-2 using specific antibodies. Tubulin was served as loading control.

suppression of STAT3 phosphorylation could affect PSMB5 protein levels as observed in DU 145 (Fig.3.1- Fig.3.4). Consequently, all these cell lines were treated with Stattic 10 μM, 20 μM for a period of 24 h. Stattic down-regulated PSMB5 protein to negligible levels at 10 μM and 20 μM in A549, HeLa cell lines. Reduced levels of PSMB5 protein were observed at 10 μM followed by a further decreased levels at 20 μM in Stattic treated MDA-MB-231 cells. It was observed that, concomitant with a decrease of pSTAT3-Y705 levels in Stattic-treated cells, PSMB5 and Bcl-2 protein levels were reduced, whereas, total STAT3 and tubulin levels remained unaffected (Fig. 3.7A-C).

Further, to validate the observations of Stattic treatments, the cell lines were treated with another STAT3 inhibitor, WP1066 at 10 μM, 20 μM for 24 h. Dose dependent decrease of PSMB5 protein levels was evident at 10 μM followed by a further decreased levels at 20 μM of WP1066 in HeLa cells, whereas, total STAT3 and tubulin levels remained unaffected. The decrease in PSMB5 correlates with the observed decrease in pSTAT3 and Bcl-2 levels (Fig. 3.8B). Decreased expression of PSMB5 protein levels were also observed at 20 μM of WP1066 in A549, MDA-MB-231 cells. Though PSMB5 levels were moderately affected at 10 μM of WP1066 in A549, MDA-MB-231 cells, a significant decrease in PSMB5 protein was observed at 20 μM of WP1066 and corroborates with reduced levels of pSTAT3 along with Bcl-2. Under similar treatment conditions the total STAT3 and tubulin levels remained constant (Fig. 3.8A-C).

Hence, the above observations suggest that inhibition of pSTAT3 down-regulates the expression of PSMB5 in cell lines expressing constitutively active STAT3.

3.2.4 Proteasome subunits expression was unaltered by STAT3 inhibition in prostate normal cells and cancer cells devoid of constitutive pSTAT3

Results of the present study suggest that suppression of pSTAT3 down-regulated the mRNA and protein levels of PSMB5 in pSTAT3 constitutive DU 145, A549, HeLa and MDA-MB-231 cell lines. Various subunits of 20S proteasome were also down-regulated by inhibition of pSTAT3-Y705 in DU 145 cells (Fig. 3.5- Fig. 3.6). Among all these pSTAT3 constitutive cells, pSTAT3 suppression dependent down-regulation of proteasome subunits was profound in prostate cancer DU 145 cells. Several lines of

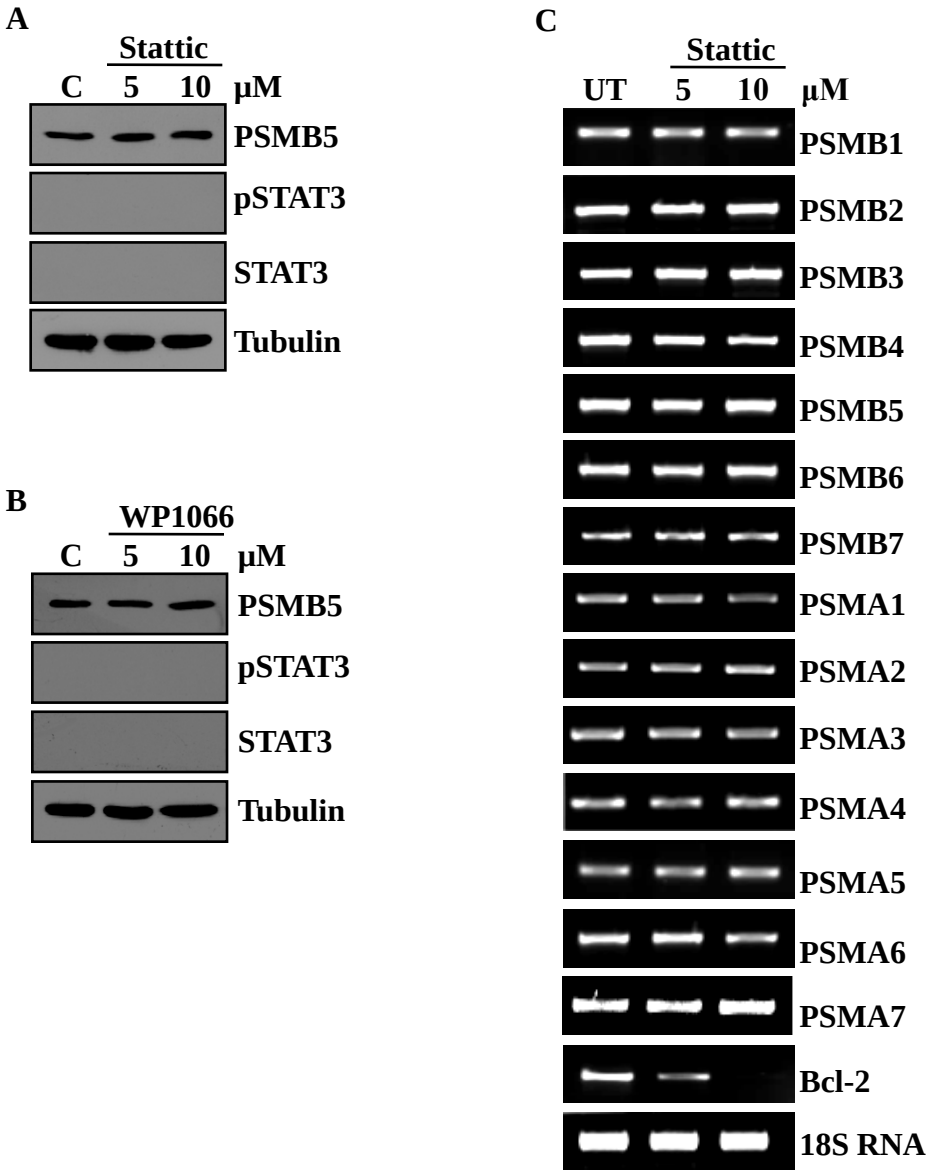

Figure 3.9: 20S proteasome subunits were unaltered by STAT3 inhibitors in PC-3.

Cells were treated with Stattic (5, 10 µM) for 24 h. *Panel A and Panel B,* Whole cell lysates of Stattic and WP1066 (5, 10 µM) respectively were analyzed by immunoblotting for PSMB5, pSTAT3, STAT3, Bcl-2 and Tubulin. *Panel C,* Semi quantitative RT-PCR was employed after total RNA isolation from Stattic treated cells to analyze the expression of 20S proteasome subunits, Bcl-2. 18S was used as loading control.

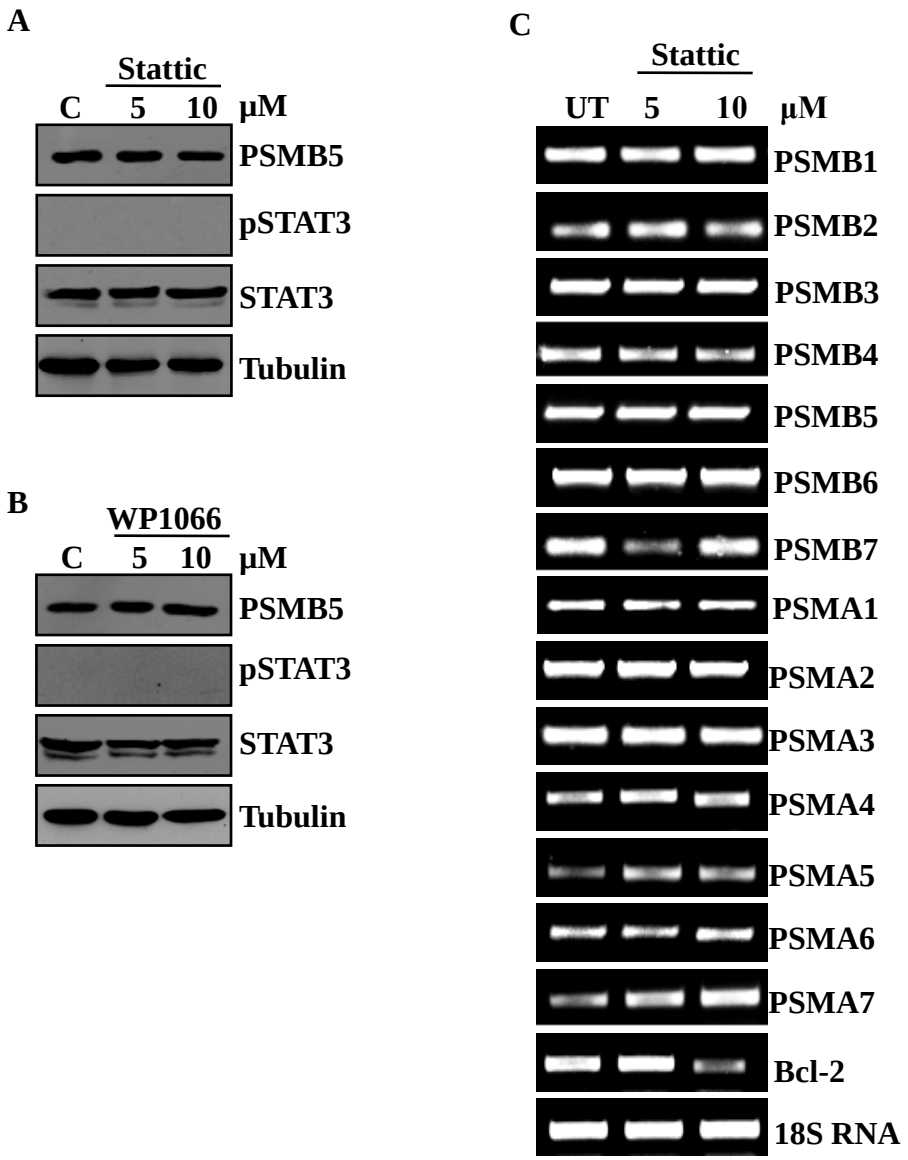

Figure 3.10: Inhibition of pSTAT3 unaffected the 20S proteasome subunits in LNCaP.

Cells were treated with Stattic (5, 10 µM) for 24 h. *Panel A and Panel B,* Immunoblot analysis was performed for PSMB5, pSTAT3, STAT3 and Tubulin of cells treated with Stattic, WP1066 treatments respectively as indicated. *Panel C,* Total RNA was isolated and mRNA levels of 20S proteasome subunits, Bcl-2 were checked by semi quantitative RT-PCR in Stattic treatments. 18S RNA was used as loading control.

evidence reported the indispensible role of proteasome in cell survival and various cellular functions (Kisselev *et al*., 2012). In addition expression of proteasomes in cell lines irrelevant with levels of pSTAT3 were reported (Bazzaro *et al*., 2006; Chen & Madura, 2005; Kraus *et al*., 2007; Kumatori *et al*., 1990; Ren *et al*., 2000; Wyke *et al*., 2004). To further clarify the role of pSTAT3 in proteasome expression in constitutive pSTAT3 cells, we next analyzed the effect of pSTAT3 inhibition on the expression of various subunits of 20S proteasome in cells possessing different levels of pSTAT3. To examine this, we have chosen prostate normal cells WPMY-1A, prostate cancer cells, LNCaP which possess low levels of pSTAT3 and PC-3 cells which does not possess STAT3, pSTAT3 (Abdulghani *et al*., 2008; Yuan *et al*., 2005).

PC-3 cells were treated with Stattic at 5 μM, 10 μM for 24 h. PSMB5 protein levels remain unaffected by Stattic treatments similar to tubulin, whereas, levels of STAT3 and pSTAT3 were decreased to undetectable levels (Fig. 3.9A). To further validate these results, PC-3 cells were treated with WP1066 at 5 μM, 10 μM for 24 h. Corroborating with Stattic treatments (Fig. 3.9A), expression levels of PSMB5 in WP1066 treatments did not change as compared to control. Equal amount of protein in all samples was indicated by the loading control, tubulin (Fig. 3.9B). To verify these observations, we next explored the mRNA levels of 20S proteasome subunits in PC-3 cells treated with similar concentrations of Stattic. Semi quantitative RT-PCR analysis exhibited similar mRNA levels of various α (PSMA1-7) and β (PSMB1-7) subunits of 20S proteasome in both control and Stattic treatments along with 18S RNA, which served as loading control (Fig. 3.9C).

Based on the above observations, we next explored whether suppression of pSTAT3 effects the expression of proteasome subunits. To pursue this, we treated LNCaP cells (prostate cancer cells possessing low levels of STAT3) with STAT3 inhibitors (Stattic; WP1066) at 5 μM, 10 μM for 24 h. Similar to earlier observations (Fig. 3.9), PSMB5 protein levels were not altered by STAT3 inhibition in LNCaP cells, even the levels of STAT3 and tubulin were also unaffected which corroborates the obtained results. Further, the pSTAT3 levels were reduced to undetectable levels (Fig. 3.10 A&B). Next, we determined the mRNA levels of various subunits of 20S proteasome under similar conditions of Stattic treatments in LNCaP cells by employing

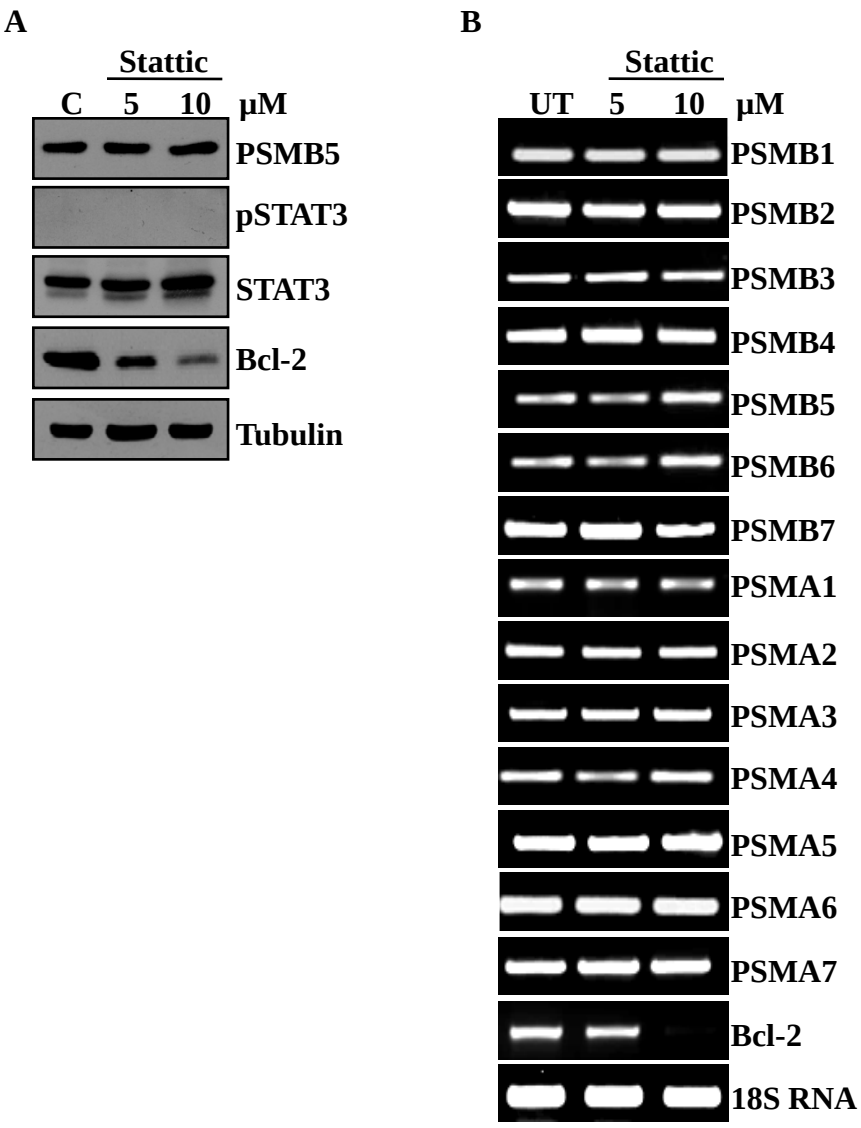

Figure 3.11: Inhibition of pSTAT3 don't effect the expression of 20S proteasome subunits in WPMY-1A.

Normal prostate (WPMY-1A) cells were treated with Stattic (5, 10 µM) for 24 h. *Panel A,* Subsequently total protein extracts were employed to detect the expression levels of PSMB5, pSTAT3, STAT3 and Bcl2 by Western blotting. Tubulin was employed as loading control. *Panel B,* Under similar experimental conditions total RNA was isolated and semi quantitative RT-PCR was performed to analyze the expression levels of 20S proteasome subunits, Bcl-2. 18S was used as loading control.

semi quantitative RT-PCR. No significant changes were observed in the mRNA levels of 20S proteasome subunits, whereas, Bcl-2, a target of STAT3 was reduced by treatment with Stattic (Fig. 3.10C). Under similar experimental conditions, no changes were apparent in 18S RNA levels which was used as a loading control.

Previous studies reported that constitutive activation of pSTAT3 alone is sufficient for malignant transformation of cells (Bromberg *et al*., 1999). Since results of the present study demonstrated down-regulation of PSMB5 along with other proteasome subunits in prostate cancer (DU 145) cells by constitutive pSTAT3 inhibition (Fig. 3.1- Fig. 3.6), we investigated whether suppression of pSTAT3 in normal prostate cells would result in the down-regulation of 20S proteasome subunits. To examine this, we opted for WPMY-1A cell line (normal prostate) and treated with Stattic at 5 μM, 10 μM concentrations for 24 h. Stattic treatments reduced the levels of Bcl-2 at both 5 μM and 10 μM, while protein levels of STAT3 and tubulin remain unaffected. Also, PSMB5 protein levels at 5 μM and 10 μM of Stattic remained same as untreated control cells (Fig. 3.11A) Further, mRNA levels of 20S proteasome subunits were analyzed under similar conditions of Stattic treatments in WPMY-1A. Similar to protein levels, PSMB5 mRNA levels remained unaffected. In addition, mRNA levels of other α- and β-subunits of 20S proteasome were neither down-regulated nor up-regulated in Stattic treated cells as compared to the control (Fig. 3.11B).

The obtained results suggest that expression of 20S proteasome subunits, especially PSMB5, was not regulated by STAT3 in prostate normal and cancer cells either with low levels or devoid of pSTAT3.

3.2.5 Suppression of pSTAT3 abrogated proteasome activities and cell viability in cells expressing constitutively active STAT3

Previous studies in yeast showed that loss of one of the proteasome genes reduced the proteasome assembly and activity (Wang *et al*., 2008). Since, inhibition of pSTAT3 down-regulated protein levels of PSMB5 (a catalytic subunit responsible for chymotrypsin-like activity) in STAT3 constitutively active cell lines (Fig. 3.1- Fig. 3.8). Also, other catalytic subunits (PSMB6, PSMB7 posessing caspase-like and trypsin-like activities respectively) and non catalytic subunits of 20S proteasome were also down-

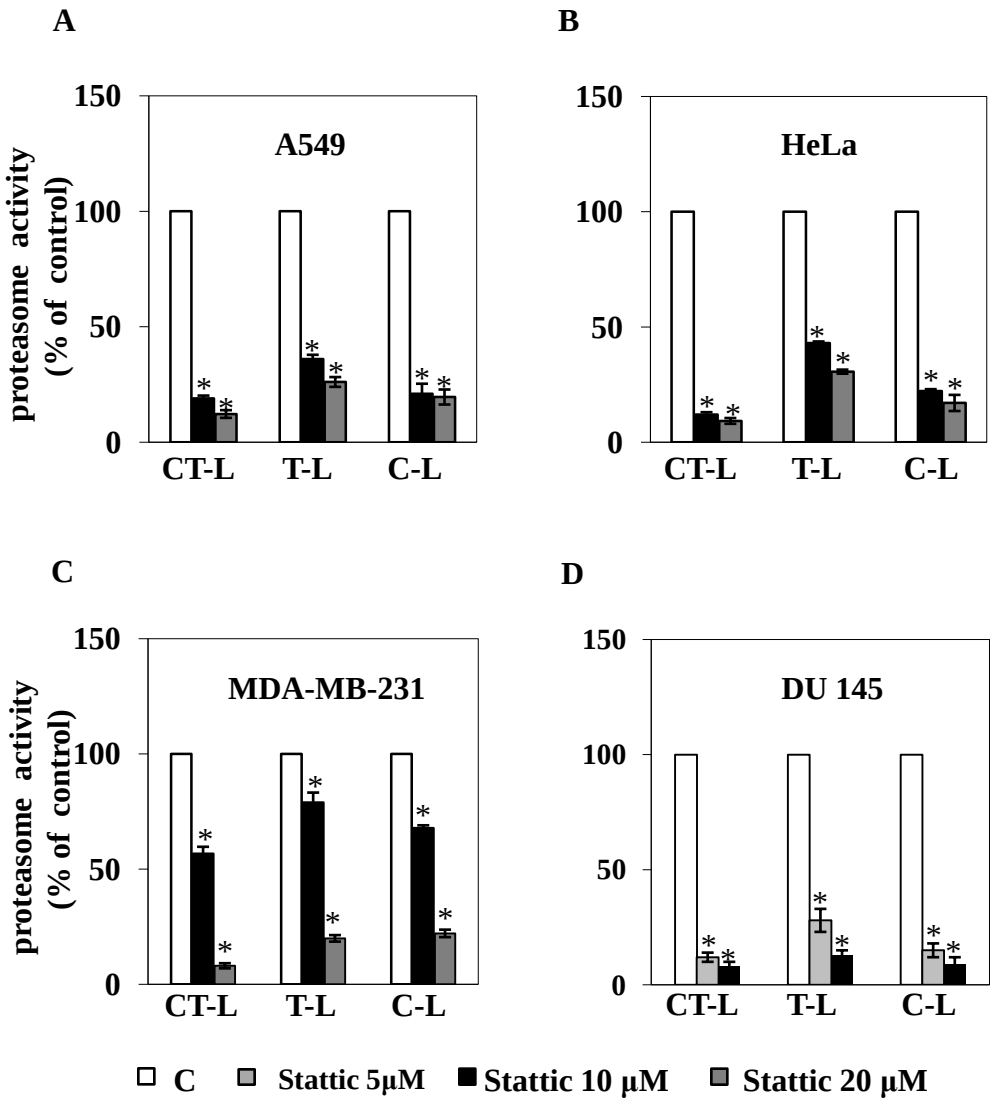

Figure 3.12: Inhibition of pSTAT3 abrogates proteasome activity in pSTAT3 constitutive cell lines.

Panel A, B and C represents proteasome activities A549, HeLa and MDA-MB-231 respectively treated with Stattic (10 μM, 20 μM) for 24 h. *Panel D* represents proteasome activities of DU145 cells treated with Stattic (5 μM, 10 μM). Peptidase activities of 20S proteasome were measured by incubating cell lysates with assay buffer containing fluorogenic substrates (50 μM each) for 30 min at 360nm/460nm excitation and emission respectively. Values are normalized to protein and represented as percentage of activity relative to DMSO control(n=3). *$p<0.01$ compared to control.

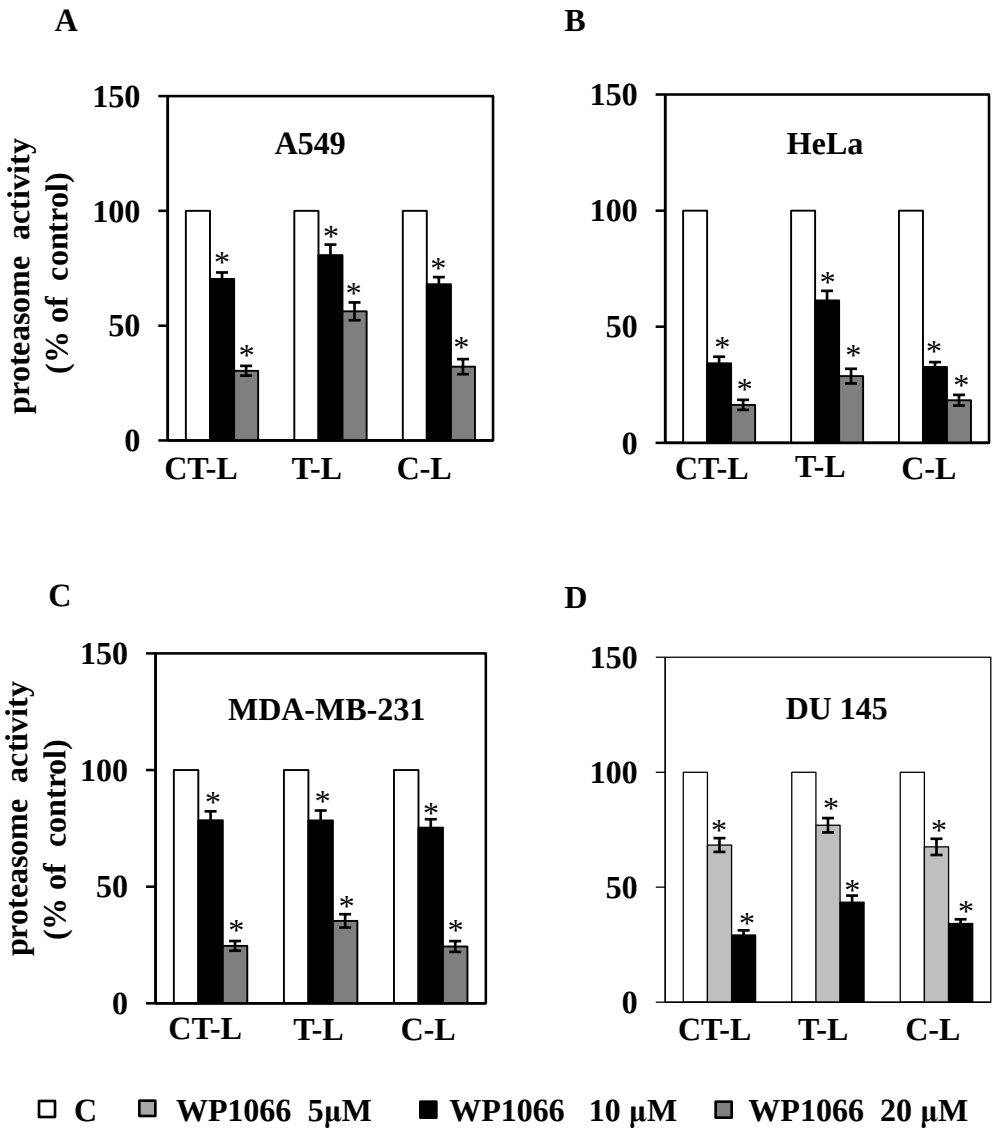

Figure 3.13: Inhibition of pSTAT3 decreases proteasome activity in STAT3 constitutively active cell lines.

Panel A, B and C, A549, HeLa and MDA-MB-231 were treated with WP1066 (10, 20 μM); *Panel D,* DU145 cells treated with WP1066 (5 μM, 10 μM) for 24 h. Peptidase activities of 20S proteasome were measured as described in materials and methods. Values are normalized to protein concentration and expressed as percentage of activities relative to DMSO control (n=3). *p<0.01 compared to control.

regulated in DU 145 cells (Fig. 3.5- Fig. 3.6), we proposed to examine even the other catalytic activities of the proteasome, in addition to the chymotrypsin-like activity. Towards this end, we monitored the proteasome activities in cells that harbor constitutively active STAT3 after treating with Stattic for 24 h.

All the three catalytic activities of proteasome were inhibited significantly in a dose dependent manner by pSTAT3 inhibition in these cells. However, chymotrypsin-like and caspase-like activities have exhibited greater sensitivity than trypsin-like activity of proteasome in all these cell lines. Among these cell lines, Stattic potently inhibited proteasome activities in DU 145 cells. Nearly 90 % and 85 % inhibition of chymotrypsin-like and caspase-like activities was observed at 5 μM in DU 145 cells followed by even a higher rate of inhibition at 10 μM of Stattic (Fig. 3.12D). Nearly 90 % of chymotrypsin-like activity inhibition was achieved at 20 μM in MDA-MB-231 (Fig. 3.12C), however, A549 and HeLa cells reflected these values following treatment with 10 μM Stattic (Fig. 3.12A&B). The caspase-like activity was inhibited to ~ 80 % in A549, HeLa at both 10 μM, 20 μM of Stattic (Fig. 3.12A&B), in case of MDA-MB-231 ~ 30 % and ~ 80 % inhibition was observed at 10 μM and 20 μM of Stattic respectively (Fig. 3.12C). Inhibition of trypsin-like activity was achieved to ~ 70 % and ~ 90 % in DU 145 by 5 μM and 10 μM of Stattic (Fig. 3.12D), whereas, ~ 70 % of inhibition was observed at 20 μM in A549, HeLa and MDA-MB-231 cell lines (Fig. 3.12).

Further, we validated the above results by treating pSTAT3 constitutive cell lines with another pSTAT3 inhibitor WP1066 for 24 h. Similar to Stattic, inhibition of proteasome activities were more pronounced in DU 145 cells. ~ 70 % and ~ 60% decrease in chymotrypsin-like and caspase-like activities were observed at 10 μM and ~ 50 % decrease of trypsin-like activity achieved at 10 μM in DU 145 cells (Fig. 3.13D). A549, HeLa and MDA-MB-231 cells exhibited dose dependent reduction in all the proteasome activities by Stattic treatments. Chymotrypsin-like and caspase-like activities of proteasome were reduced to ~ 33 % in A549, ~ 25 % in MDA-MB-231 and ~ 20 % in HeLa at 20 μM of WP1066. Trypsin-like activity was reduced to ~ 60 % in A549, ~ 40 % in MDA-MB-231 and ~ 30 % in HeLa at 20 μM of WP1066 (Fig. 3.13).

Several earlier studies provided evidence that proteasome function is crucial for cell survival and inhibition of this would lead to induction of apoptosis (Kisselev *et al*.,

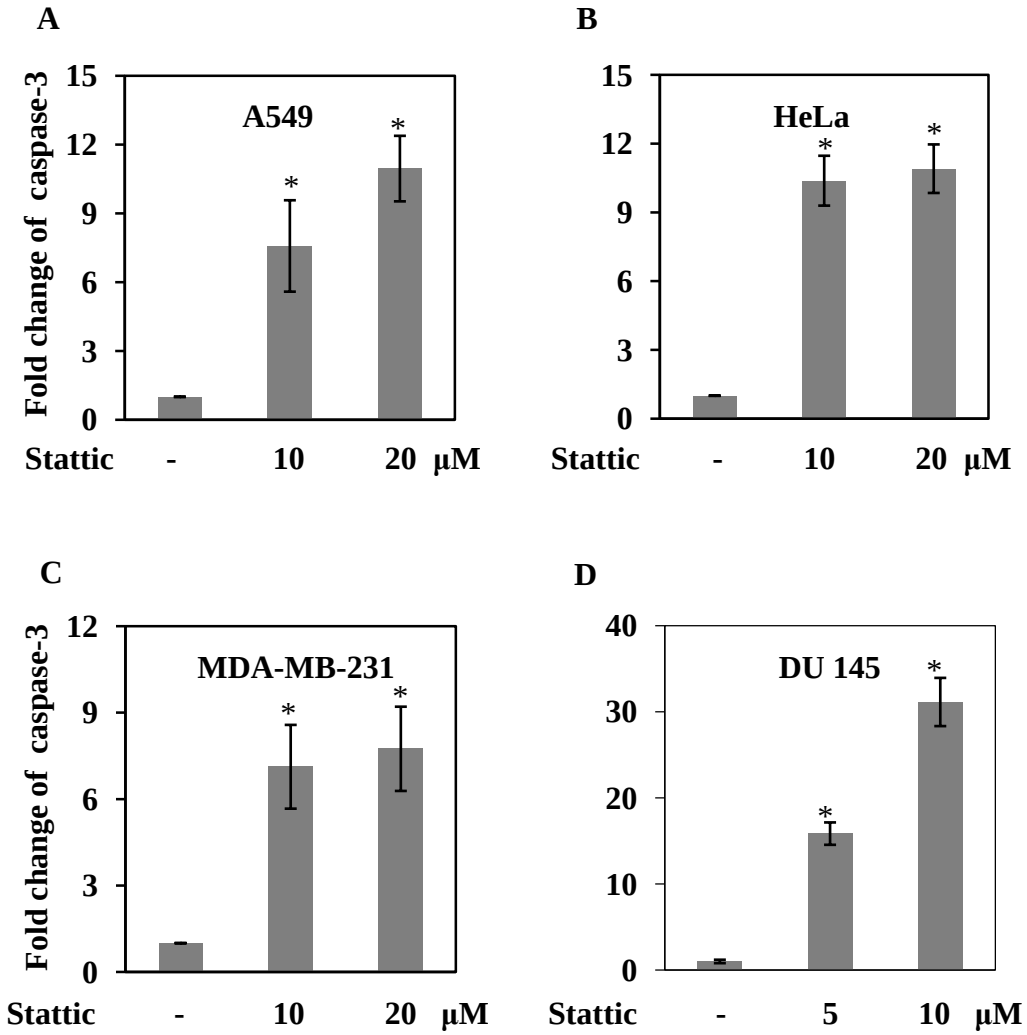

Figure 3.14: Inhibition of pSTAT3 induced Caspase-3 activity in pSTAT3 constitutive cells.

A549, HeLa, MDA-MB-231 cells were treated with Stattic (10, 20 µM); DU 145 cells with 5 µM, 10 µM of Stattic for 24 h. Caspase-3 activity was measured by incubating cell lysates in an assay buffer containing Z-DEVD-AMC for 1 h. Released AMC was measured with an excitation and emission of 360nm/460nm respectively. Values are normalized to protein concentration and expressed as fold change of activity relative to DMSO control (n=3). *p<0.01 compared to control. *Panel A, B, C and D* represents caspase-3 activities of A549, HeLa, MDA-MB-231 and DU 145 respectively.

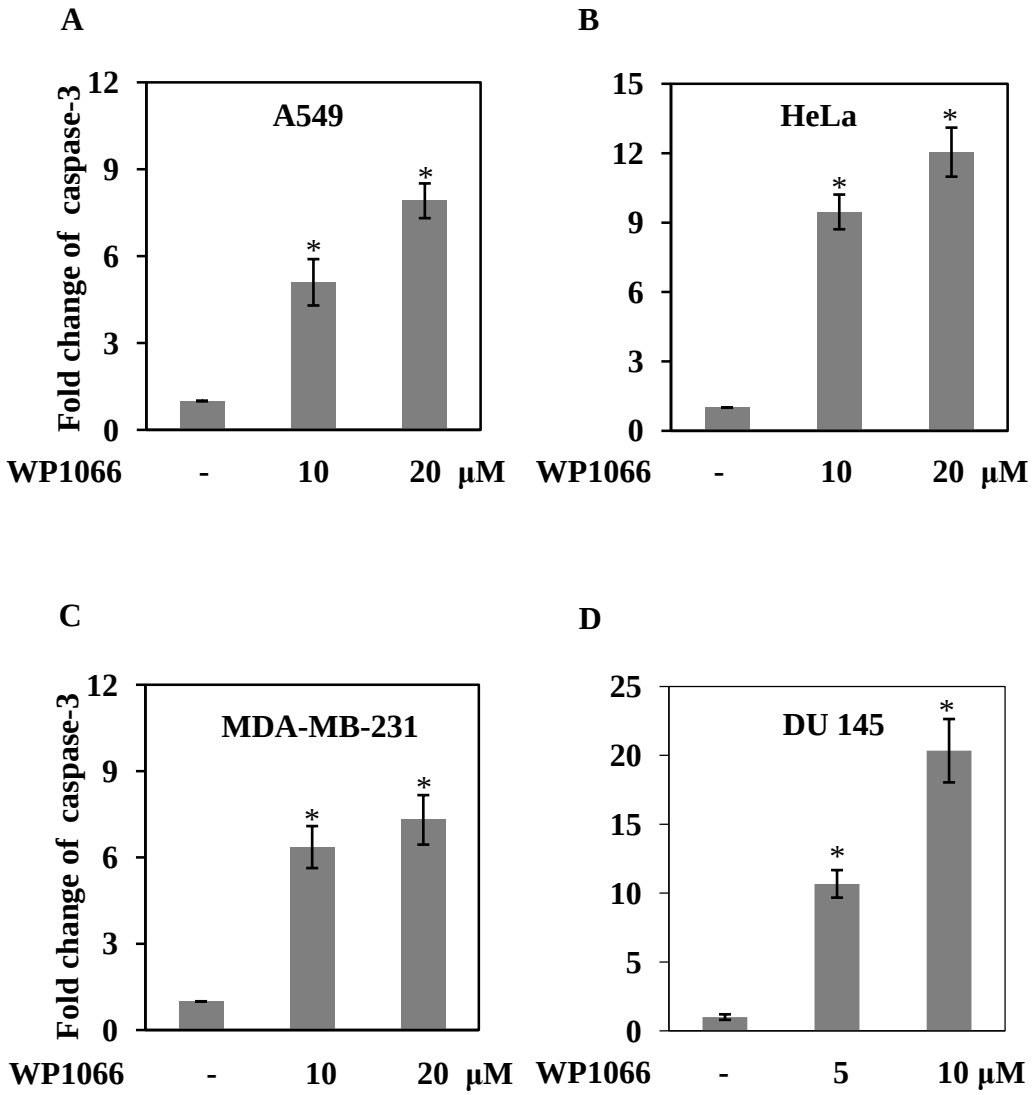

Figure 3.15: WP1066 induced caspase-3 activity in pSTAT3 constitutive cells.

Caspase-3 activities were measured in WP1066 (10, 20 µM) treated A549 (*Panel A*), HeLa (*Panel B*), MDA-MB-231 (*Panel C*); WP1066 (5, 10 µM) treated DU 145 (*Panel D*) cells after 24 h. Caspase-3 activity values are normalized to protein concentration and expressed as fold change of activity relative to DMSO control (n=3). *p<0.01 compared to control.

2012). In addition, suppression of pSTAT3 has been shown to induce apoptosis (Frank, 2007). We next analyzed the caspase-3 activity in STAT3 inhibited cells as an indicator for apoptosis. As expected, a 15-fold induction of caspase-3 was observed in DU 145 with Stattic (5 μM) and the values were further increased to ~ 30 fold at 10 μM (Fig. 3.14D). A549, HeLa cells exhibited 10 fold increase and MDA-MB-231 cells have shown 8 fold increase of caspase-3 activity at 20 μM of Stattic (Fig. 3.14).

Further, caspase-3 activity induction was also observed in WP1066 treated cells with a maximum of 20-fold increase over controls in DU 145 at 10 μM (Fig. 3.15D), 12-fold in MDA-MB-231, 8-fold in A549 and HeLa cells (Fig. 3.15).

Overall, inhibition of pSTAT3 decreased proteasome activities and induced caspase-3 in all pSTAT3 constitutive cell lines with different potency.

3.2.6 Inhibition of pSTAT3 unaltered proteasome activities in prostate cells lacking constitutively active STAT3

The above observations from prostate cells either with low levels or devoid of pSTAT3 suggest that 20S proteasome subunit expression was unaffected following inhibition of pSTAT3 (Fig. 3.9- Fig. 3.11). Next, to validate these findings, we measured the proteasome activities and caspase-3 activity in Stattic treated (5, 10 μM) prostate cells after 24 h. Similar to the expression levels of 20S proteasome subunits, no gross changes were evident in the chymotrypsin-like, trypsin-like and caspase-like activities of proteasome in Stattic treated WPMY-1A, LNCaP and PC-3 cell lines as compared to untreated cells (Fig. 3.16A-C). Surprisingly, a significant increase in the apoptosis as measured by dose-dependent caspase-3 activation was observed in these cell lines following Stattic treatments. Increased caspase-3 activity was observed in low levels pSTAT3 containing WPMY-1A and LNCaP followed by STAT3 negative PC-3 cells in Stattic treatments (Fig. 3.17A-C). Despite of absence or low levels of pSTAT3, the observed increase in caspase-3 by Stattic could be due to the non specific off-target effects or/ inhibition of other SH2 domain containing proteins involved in cell survival by Stattic.

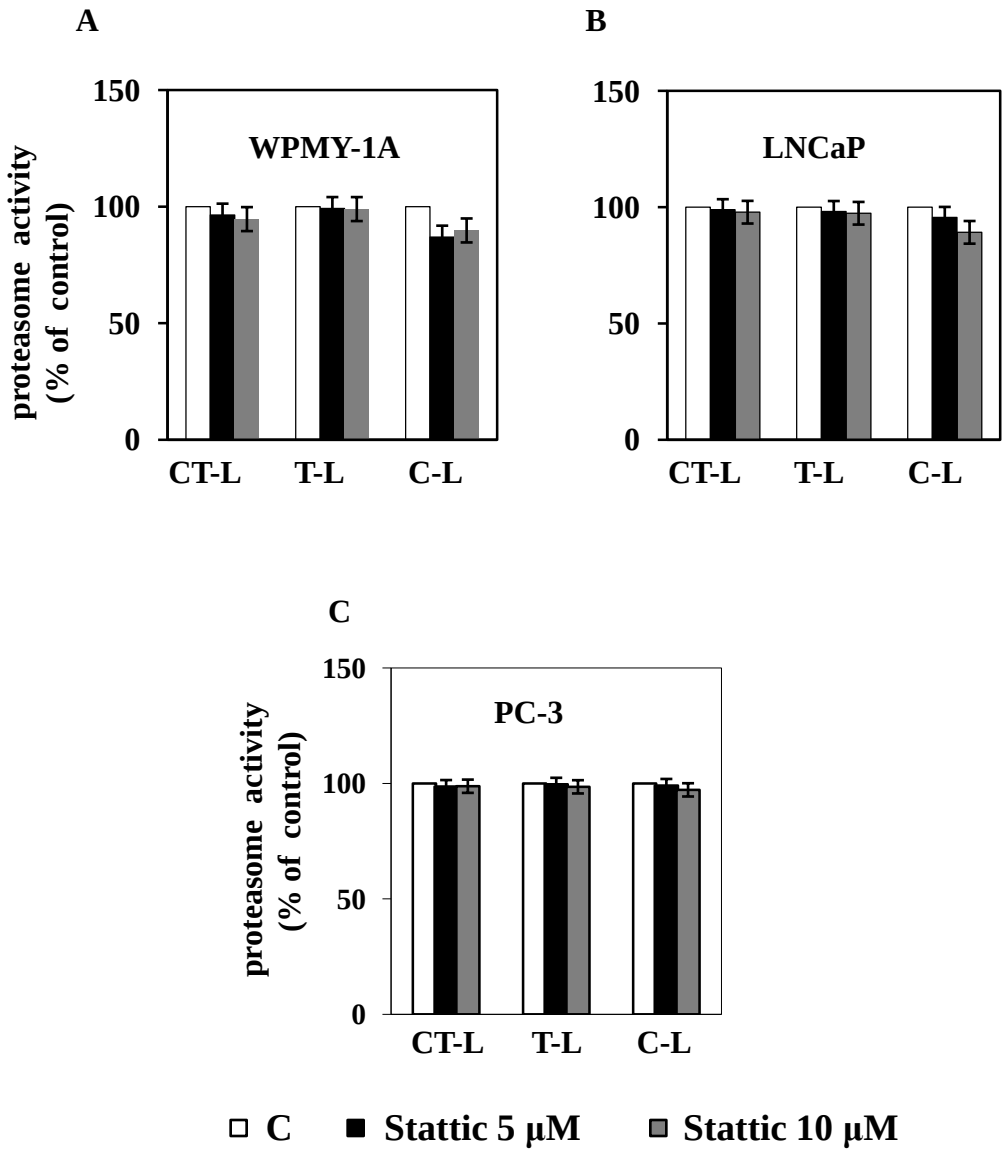

Figure 3.16: Proteasome activities were unaltered due to pSTAT3 inhibition in prostate cells.

WPMY-1A, LNCaP and PC-3 cells were treated with Stattic (5, 10 µM) for 24 h. *Panel A, B and C* represents peptidase activities of WPMY-1A, LNCaP and PC-3 respectively. Values are normalized to protein concentration and expressed as percentage of activities relative to DMSO control (n=3).

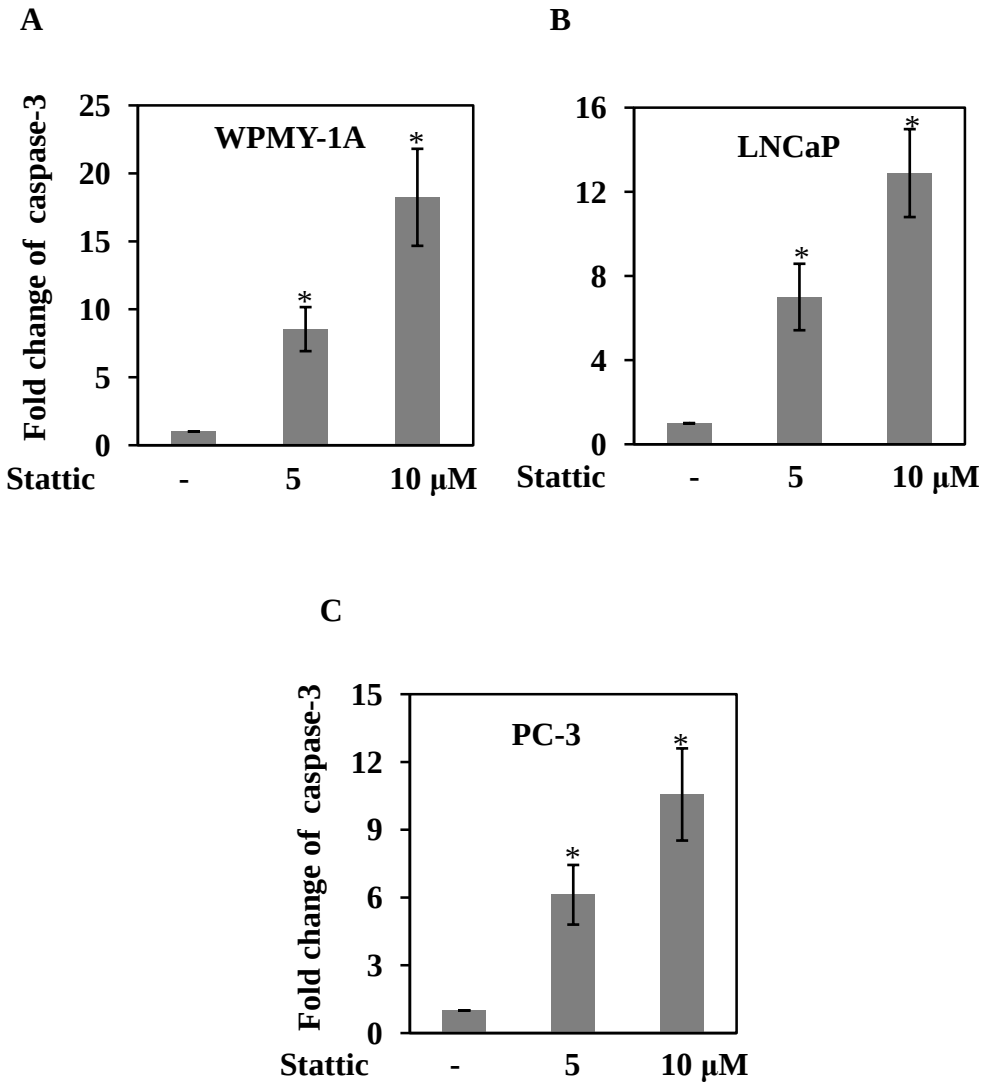

Figure 3.17: Stattic induced Caspase-3 activity in prostate cells.

WPMY-1A, LNCaP and PC-3 cells were treated with Stattic (5, 10 µM) for 24 h. Caspase-3 activity was measured by incubating cell lysates in an assay buffer containing Z-DEVD-AMC for 1 h. Released AMC was measured with an excitation and emission of λ360/λ460 respectively. *Panel A, B and C* represents caspase-3 activities of WPMY-1A, LNCaP and PC-3 respectively. Values are normalized to protein concentration and expressed as fold change of activity relative to DMSO control (n=3). *p<0.01 compared to control.

3.2.7 Proteasome inhibitor induced apoptosis unaltered PSMB5 expression

Proteasome inhibition is known to elicit a feedback-dependent induction of proteasome subunit gene expression (Kwak *et al*., 2006; Meiners *et al*., 2003; Radhakrishnan *et al*., 2010; Steffen *et al*., 2010). In addition, treatment of cells with of bortezomib also induced the activation of STAT3 in head and neck squamous cell carcinoma cell lines (Li *et al*., 2009). Hence, we analyzed whether proteasome inhibitors induce pSTAT3 and PSMB5 protein levels. To test this possibility, DU 145 cells were treated with bortezomib (100 nM), MG132 (1 µM) and epoxomicin (250 nM) for 24 h. All these inhibitors primarily inhibit chymotrypsin-like activity of proteasome. In response to proteasome inhibition, p-STAT3 and PSMB5 protein levels were unaffected and remained similar to control levels (Fig. 3.18A). Even the mRNA levels of PSMB5 remained unchange following treatment with all the three proteasome inhibitors (Fig. 3.18B).

Under similar experimental conditions, the chymotrypsin-like activity was inhibited significantly to 90% in cells treated with bortezomib when compared with the control. In addition, 86% and 58% inhibition of chymotrypsin-like activity was observed in epoxomicin and MG-132-treated cells respectively (Fig. 3.18C). Since, inhibition of proteasome resulted in the induction of apoptosis in several cancer cells (Adams, 2004), we next analyzed the caspase-3 activity. Nevertheless, bortezomib induced a robust 8-fold increase in caspase 3, however, the values were 6-fold and 5-fold in cells treated with MG132 and Epoxomicin respectively (Fig. 3.18D).

Thus, DU 145 cells were susceptible to proteasome inhibitors, although the protein levels of PSMB5 and p-STAT3 remained unaltered.

3.2.8 Levels of proteasome activity and PSMB5 expression in cancer cell lines

3.2.8a PSMB5 expression correlates with intracellular levels of pSTAT3

Since decreased levels of activated STAT3 down-regulated PSMB5 expression, we next examined the interdependency between the endogenous levels of phospho-STAT3-Y705 and PSMB5 protein expression. In order to perform this, we opted for human prostate cancer cell lines, DU 145, LNCaP and PC-3 which possess different levels of either phosphorylated or total STAT3 proteins (Abdulghani *et al*., 2008; Yuan *et*

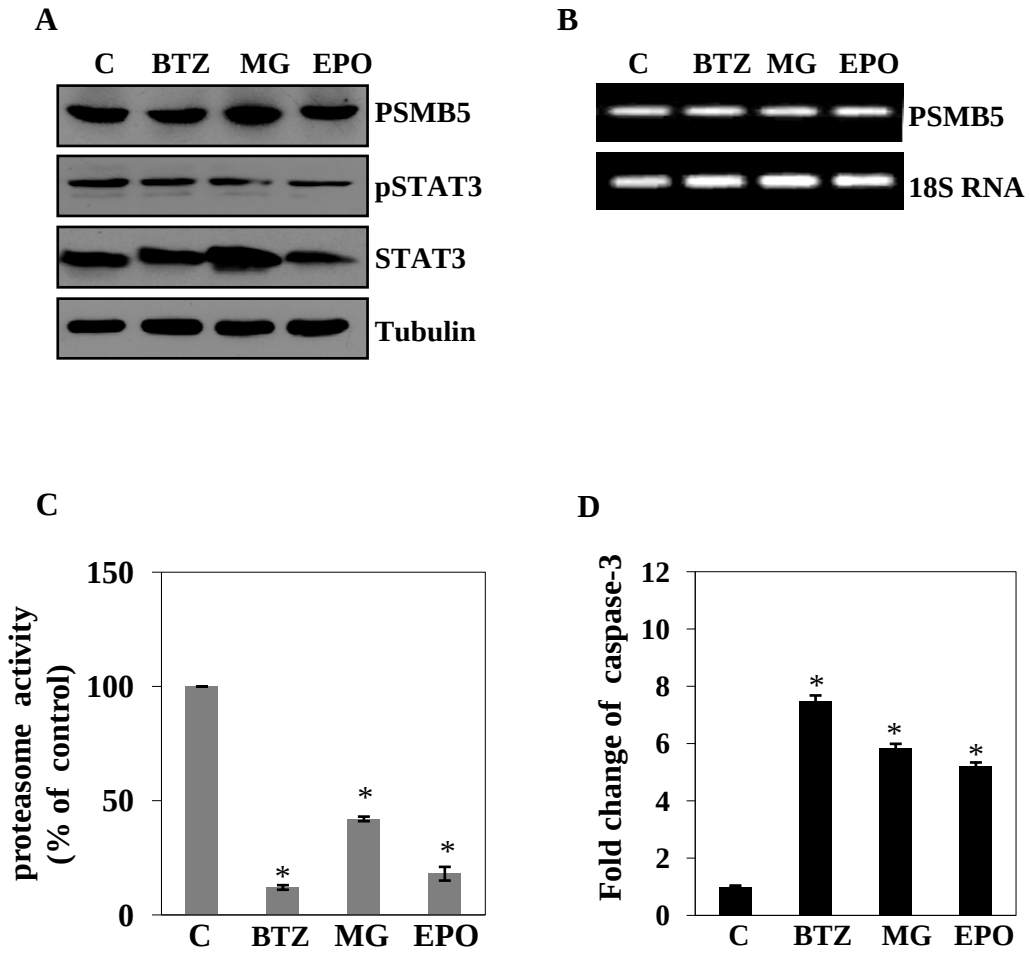

Figure 3.18: Effect of proteasome inhibition on PSMB5 expression.

DU 145 cells were treated with Bortezomib (100 nM), MG-132 (1 μM), Epoxomicin (250 nM) for 24 h. *Panel A*, Immunoblot analysis was conducted for PSMB5, pSTAT3, STAT3 and Tubulin from whole cell extracts after termination of treatment. *Panel B,* Semi quantitative RT-PCR analysis was performed to analyze the mRNA levels of PSMB5. *Panel C and Panel D* represents chymotrypsin-like activity of 20S proteasome and caspase-3 activity respectively under similar conditions of treatments. The obtained activity values are normalized to protein concentration and expressed as relative to DMSO control (n=3). values shown are the mean ± SD of three independent experiments. *$p < 0.01$ as compared to controls.

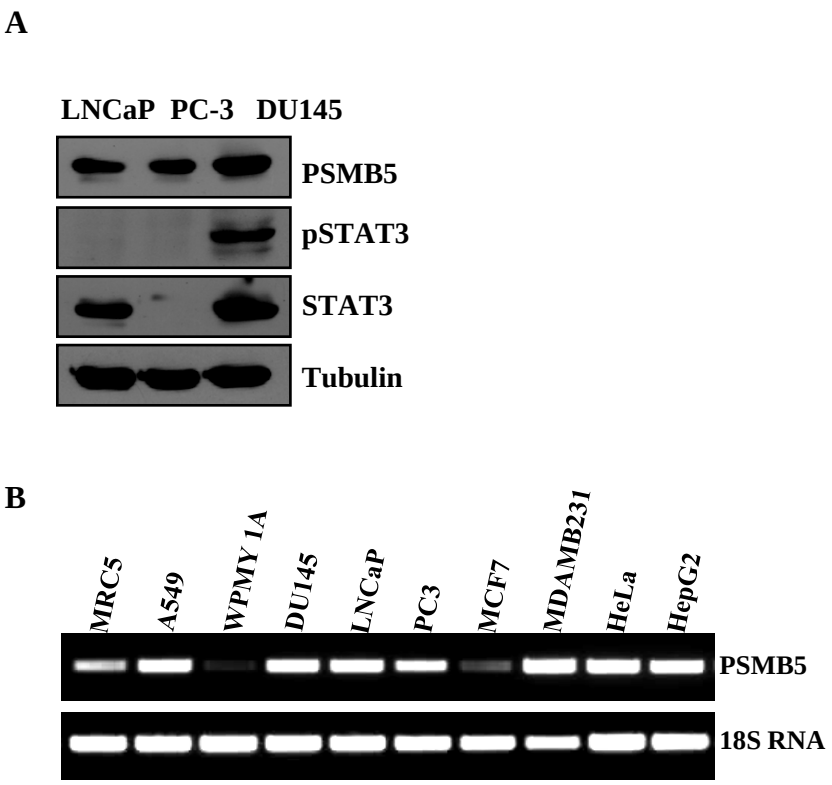

Figure 3.19: H**igh levels of PSMB5 in constitutively active STAT3 cells.** *Panel A,* Prostate cancer cells consists of low, devoid and constitutive pSTAT3 LNCaP, PC-3 and DU145 respectively were lysed. 20 µg of each lysate was analyzed for the expression of PSMB5, STAT3 and pSTAT3 by immunoblotting. Tubulin was used as loading control. *Panel B,* mRNA levels of PSMB5 in various cell lines was analyzed with semi quantitative RT-PCR after total RNA isolation. 18S RNA was used as loading control.

al., 2005). DU 145, which possess higher levels of phospho-Stat3-Y705 (constitutively active STAT3) exhibited high endogenous levels of PSMB5 protein. In contrast, LNCaP and PC-3 cells which possess either undetectable or no phospho-Stat3-Y705 levels, but, still basal levels of PSMB5 protein were observed in these cell lines. Under similar experimental conditions, no gross change was noticed in tubulin levels, which was used as a loading control (Fig. 3.19A).

Further, analysis of the relative mRNA levels of PSMB5 in prostate cancer and other cell lines as measured by semi quantitative RT-PCR revealed high levels of PSMB5 mRNA in cancer cells as compared to normal cells. However, highest level of PSMB5 expression was found in DU 145 while lowest in WPMY-1A cells which correlates with the expression levels of pSTAT3 (Fig. 3.19B).

3.2.8b Proteasome activities are higher in cells possessing constitutively active STAT3

In order to validate the relationship between the expression of pSTAT3 to that of cellular proteasome activity, we analyzed both 20S and 26S proteasome activities in a panel of normal and cancer cells. High levels of proteasome activities were observed in cancer cells as compared to their normal cell counterparts. All the cancer cells examined demonstrated more than 2 fold high chymotrypsin-like activity when compared to trypsin-like and caspase-like activities of proteasome. Amongst cancer cells, the chymotrypsin-like activity was more in cell lines in the order, DU 145 > MDAMB231 > HeLa > A549 > LNCaP > PC-3 > HepG2 > MCF7 in both 20S and 26S proteasome activities. Nearly 3-4 fold lower levels of chymotrypsin-like activity was observed in MRC5 and WPMY1A, which are the normal counterparts of A549 and DU 145 cells respectively. No significant changes were noticed in the trypsin-like and caspase-like activities of both 20S and 26S proteasomes (Fig. 3.20A&B).

Taken together, these results suggest a strong correlation between the endogenous levels of tyrosine phosphorylated STAT3, PSMB5 expression and Proteasome activity.

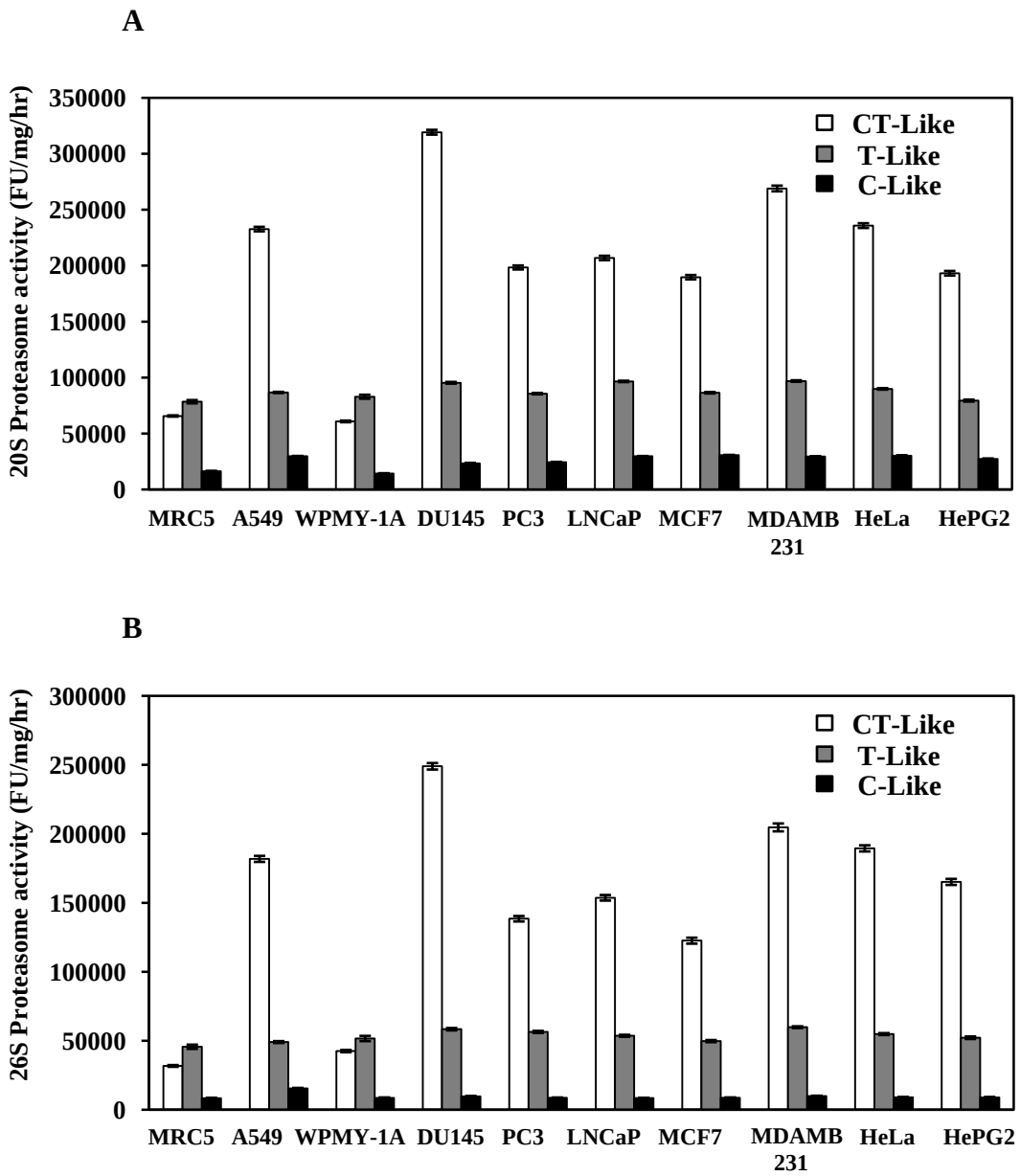

Figure 3.20: Increased proteasomal activities in cancer cells.

Peptidase activities of proteasome were measured by incubating cell supernatants with fluorogenic substrates (50 µM) at 360nm/460nm excitation and emission respectively. Values are normalized to protein concentrations and represented as fluoroscence units/mg/hr. *Panel A* and *Panel B* represents 20S and 26S proteasome activities respectively (n=3).

3.2.9 Effect of exogenous expression of STAT3 on proteasome

3.2.9a Overexpression of STAT3 increased PSMB5 mRNA and protein levels

Results of the previous sections suggested that inhibition of pSTAT3 down-regulated the expression of PSMB5 mRNA and protein levels. We hypothesized that overexpression of STAT3 would increase the expression of PSMB5. To examine this possibility, we have opted for PC-3 cell line which does not express endogenous STAT3 and pSTAT3. PC-3 cells were infected with adenoviruses expressing control, wild type STAT3 protein at a multiplicity of infection that allows 70% transduction in 48 h as visualized by the expression of GFP (Fig. 3.21A). PC-3 cells were fixed after 48 h of infection and analyzed by immunocytochemical staining for FLAG. As expected FLAG expression was observed only in Ad-STAT3 infected cells both in the cytosol and nucleus (Fig. 3.21B). Neither endogenous nor overexpressed STAT3 and pSTAT3 protein levels were observed in uninfected and control infected cells. Accumulation of phospho-STAT3-Y705 protein levels in Ad-STAT3 infected PC-3 cells resulted in a 2-fold increase in the levels of PSMB5 protein. Bcl-2 protein levels have also increased while the levels of tubulin, which was used as loading control remained the same (Fig. 3.21C). Furthermore, mRNA levels of PSMB5 were increased significantly in response to overexpression of Ad-STAT3 cells as compared to control infected cells (Fig. 3.21D). This finding corroborates with the observed increase in the protein levels of PSMB5, suggesting the transcriptional regulation of PSMB5 by STAT3.

3.2.9b Enhanced proteasome activity by overexpression of STAT3

Next, in order to examine whether induction of PSMB5 protein levels would affect the cellular proteasome activities, PC-3 cells were transiently transfected with pRC-STAT3 plasmid for 48 h. Results indicate that all the three catalytic activities of the proteasome were significantly increased by STAT3 overexpression, whereas, no apparent changes were noticed in the proteasome activities of control plasmid and untransfected cells. STAT3 overexpression resulted in a significant increase in the chymotrypsin-like activity (nearly 2.3 fold), trypsin-like (1.5-fold) and caspase-like (1.4-fold) activities (Fig. 3.22C).

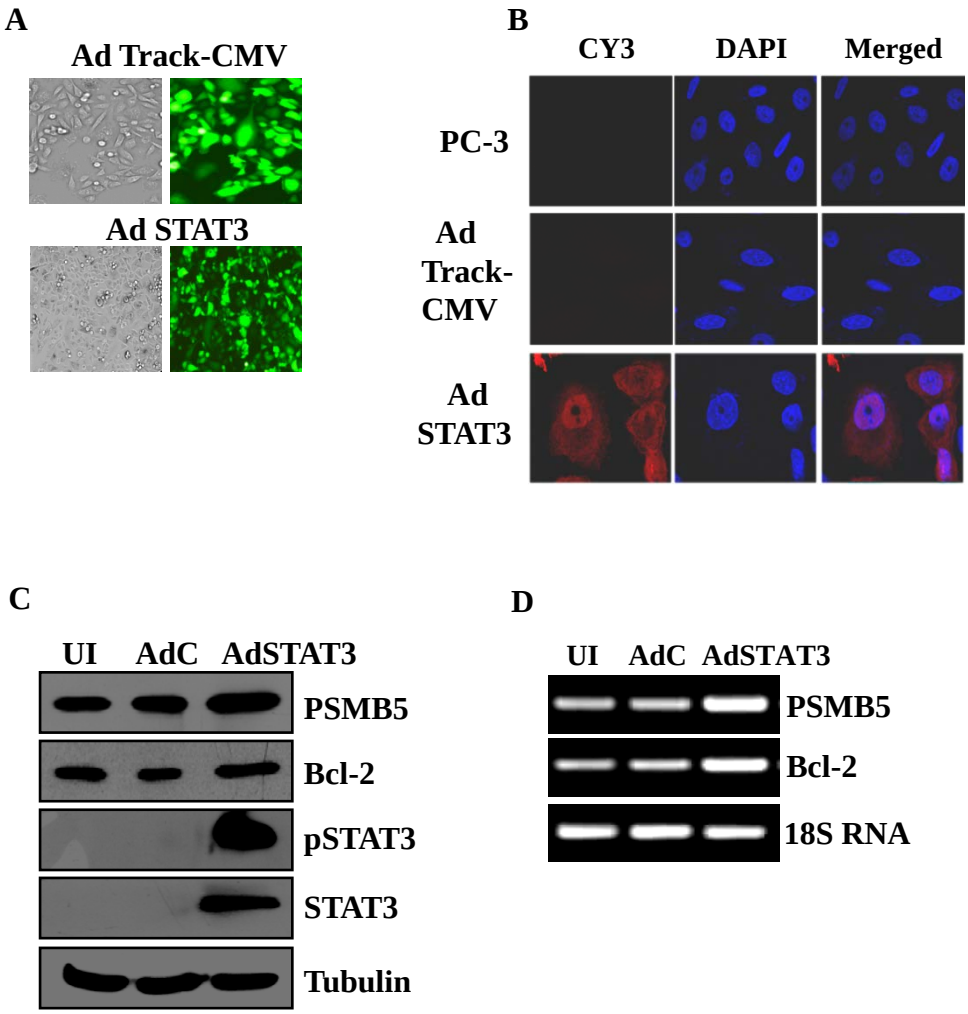

Figure 3.21: Exogenous expression of STAT3 induced PSMB5 expression. PC-3 cells were transduced with control adenovirus (AdC) or adenovirus expressing STAT3 (AdSTAT3) and uninfected cells (UI) for 48 h. *Panel A*, GFP is a marker for infection. *Panel B*, PC-3 cells of uninfected, infected with Ad Con, Ad STAT3 were used for immunostaining with FLAG antibody. Cy3 was used for FLAG, DAPI is for nucleus. *Panel C*, Immunoblot analysis was performed for PSMB5, pSTAT3, STAT3 and Bcl2. Tubulin was employed as loading control. *Panel D*, Semi quantitative anlaysis of PSMB5, Bcl2 mRNA levels is shown. 18S RNA used as loading control.

3.2.9c STAT3 dependent transactivation of PSMB5 promoter

In order to examine whether the regulation of PSMB5 by STAT3 is by virtue of promoter activation or direct transcriptional regulation, a 965 bp promoter for PSMB5 containing TATA box, 294 bp of 5'-untranslated region and 108 bp of exon1 which was predicted by MatInspector was subsequently cloned in to pGL3-basic vector. A STAT3-negative PC-3 cells were employed for experimentation to eliminate any background / basal regulation by STAT3. Consequently, cells were transfected with the PSMB5 promoter-reporter together with STAT3 plasmid of 250 ng, 500 ng and analyzed for basal and STAT3 induced promoter activity. STAT3 dose-dependently increased the PSMB5 promoter activity to a maximum of 4.2-fold. In addition, basal promoter activity of PSMB5 was observed in PC-3 cells as compared to the promoter less vector (Fig. 3.22A). Furhter, promoter assay lysates showed marked expression of tyrosine phosphorylated and total STAT3 proteins (Fig. 3.22B).

Collectively, the observed findings clearly demonstrate that forced expression of STAT3 leads to the induction of PSMB5 protein and proteasomal activities.

3.2.10 Identification of STAT3 responsive sites in the consensus promoters of proteasome subunits

Results from previous sections suggest a STAT3 dependent regulation of PSMB5 by virtue of its promoter activation resulting in the enhanced transcription (Fig. 3.21- Fig. 3.22). We further reasoned that the presence of putative STAT3 responsive sites in the promoter or proximal regions of PSMB5 and other subunits of 20S proteasome might be responsible for the concerted down-regulation by pSTAT3 inhibition. DNA sequence up to -2 kb from TSS of all the 20S proteasome subunits was analyzed for consensus sequence for STAT3 protein binding, TTN (4-6)AA (Bard *et al*., 2009). We found that most of the subunits of 20S proteasome contains one or more TTN (4-6)AA sites in their promoter regions (Fig. 3.23).

Discussion

STAT3 is activated persistently in various malignancies and induces oncogenic processes through expression of various prosurvival genes (Yu *et al*., 2009). Hence,

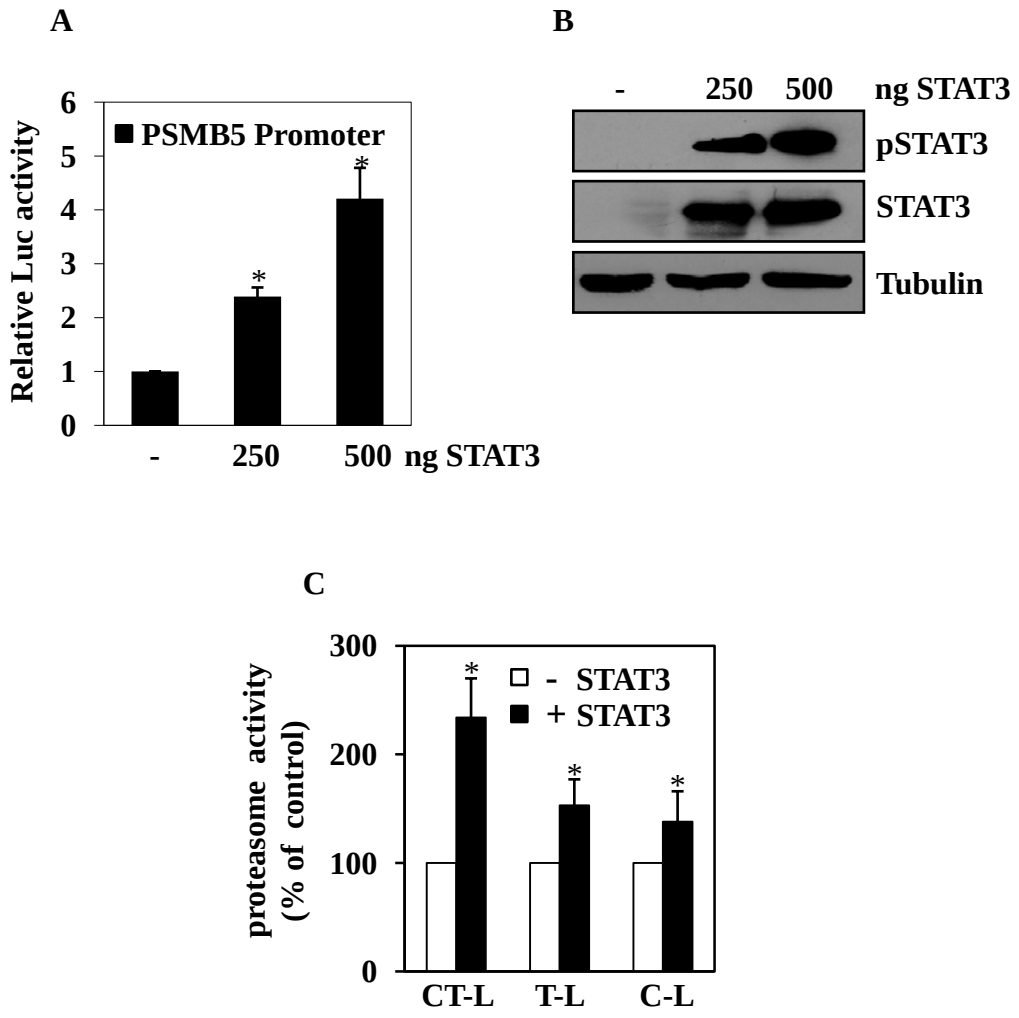

Figure 3.22: Increased PSMB5 promoter and activity by pSTAT3.

Panel A, PC-3 cells in 24 well plates were transfected with wild type promoter reporter construct of pWT-PSMB5 (100 ng), along with pCMV.SPORT-βGal plasmid (100 ng) and pRC-CMV-STAT3 plasmid (250, 500 ng) or control plasmids for 30 h. Cell lysates were prepared for reporter assays. Luciferase activities were measured by normalizing β-gal and were shown as relative to control (n=3). *Panel B,* Lysates employed in reporter assay were analyzed for p-STAT3, STAT3 and tubulin proteins using specific antibodies. *Panel C,* Peptidase activities of proteasome transfected with 1 µg of pRC-CMV-STAT3 for 30 h is shown. values shown are the mean ± SD of three independent experiments. *$p < 0.01$ as compared to controls.

	STAT3(5-TTN(4-6)AA-3) (-bp to TSS)
Gene Name/Subunit	**STAT3**
α- Subunits	
PSMA1/α6	
PSMA2/α2	103, 955
PSMA3/α7	486
PSMA4/α3	319, 522
PSMA5/α5	92, 287, 319
PSMA6/α1	333
PSMA7/α4	
β- Subunits	
PSMB1/β6	233, 742
PSMB2/β4	321
PSMB3/β3	257, 925
PSMB4/β7	657
PSMB5/β5	439, 769
PSMB6/β1	677, 700, 915
PSMB7/β2	647, 703, 713, 933

Figure 3.23: Putative STAT3 binding sites in the promoter regions of 20S proteasome subunits:

small-molecule inhibitors of tyrosine-phosphorylated STAT3 are explored actively for tumor therapy. The inhibition of constitutively active STAT3 induced apoptosis in DU 145 cells (Mora *et al*., 2002). In the present study, STAT3 inhibitors reduced PSMB5 expression and induced apoptosis (Fig. 3.1-3.4; Fig. 3.12&3.13). Similarly, proteasome inhibitors also triggered apoptosis, corroborated by increased caspase 3 activity (Fig. 3.18). However, under similar experimental conditions, PSMB5 or phospho-STAT3-Tyr-705 levels remained unaffected, suggesting that the decrease in the levels of PSMB5 is not a general feature of apoptosis. Thus, lower levels of transcriptionally active STAT3 resulted in decreased levels of PSMB5 protein. The possibility of STAT1-dependent regulation of PSMB5 was ruled out because Stattic selectively binds the SH2 domain of STAT3 over STAT1 (Schust *et al*., 2006). In addition, phospho-STAT1 levels were undetectable in DU 145 cells (Fig. 3.1E), which is in accordance with an earlier report (Patterson *et al*., 2006).

A reduction in the mRNA levels of PSMB5 by STAT3 inhibitors further substantiates STAT3-dependent regulation of PSMB5 (Fig. 3.1-3.4). Moreover, the mRNA and protein levels of Bcl-2, a known STAT3 target, concomitantly decreased with PSMB5, suggesting a transcriptional role of STAT3 (Fig. 3.1-3.4). Furthermore, the promoter analysis of PSMB5 revealed putative STAT3 binding sites with the canonical TT(N) 4–6 AA at –439 bp,+87 bp, and +230 bp relative to TSS (Bard *et al*., 2009). Accordingly, the PSMB5 promoter was activated in a dose-dependent manner by STAT3. In addition, exogenous expression of STAT3 in PC-3 cells resulted in the induction of PSMB5 expression and proteasome activity (Fig. 3.21-3.22). Hence, it is likely that STAT3 transcriptionally activates the gene expression and promoter activity of PSMB5 through the STAT3-responsive sites. Earlier studies revealed the transcription factor binding sites in the promoter regions of proteasome genes mediates the feedback or basal regulation (Kwak *et al*., 2006; Meiners *et al*., 2003; Radhakrishnan *et al*., 2010; Steffen *et al*., 2010; Xu *et al*., 2012). Further, presence of more than one putative STAT3 sites in the promoter regions of various subunits of 20S proteasome except PSMA1 substantiates the concerted regulation by STAT3 (Fig. 3.23). Although putative STAT3 were not detected in PSMA7 the down regulation is probably due to indirect regulation or co activator activity of STAT3.

Induction of apoptosis unaltered expression and activity of proteasome or its subunits followed by inhibition of STAT3 in WPMY-1A, LNCaP and PC-3 cells substantiate the STAT3-dependent regulation of proteasome expression and activity in pSTAT3 constitutive cells and also apoptosis independent regulation of proteasome in all these cells (Fig. 3.9-3.11 & Fig. 3.16-3.17). Intriguingly, LNCaP and PC-3 cells expressed basal levels of PSMB5 protein when compared to DU 145 cells (Fig. 3.19). An abundance of proteasome is important for normal cell survival and indispensable for malignancies (Kisselev *et al*., 2012). Other oncogenic transcription factors may regulate the expression of PSMB5 in cell types lacking constitutive STAT3 levels.

Malignant conditions are often associated with high rates of protein synthesis. Hence, a wide range of cancers exhibit either higher proteasome activity or subunit expression or both to overcome this predicament (Bazzaro *et al*., 2006; Chen & Madura, 2005; Kraus *et al*., 2007; Ren *et al*., 2000; Wyke *et al*., 2004). However, the molecular determinants responsible for the regulation of proteasome activity remained unclear. Accordingly, cancer cells shown high levels of proteasome activities and PSMB5 expression when compared to normal cells (Fig. 3.19-3.20). The results of this study demonstrate, for the first time, that activated STAT3 modulates the proteasome activities through the regulation of PSMB5 and other α and β-subunits. Hence, decreased protein levels of α and β-subunits resulted in reduced proteasome activities in STAT3-suppressed cells (Fig. 3.12-3.13). However, proteasome inhibitors reduced proteasome activity in DU 145 cells without affecting the endogenous levels of PSMB5 (Fig. 3.18). This was probably due to the presence of copious amounts of constitutive STAT3 regulating the basal expression of PSMB5. Overall, persistently activated STAT3 levels function as an important determinant of proteasome activity in cell lines harboring constitutive pSTAT3.

Conclusions

Overall the results presented in this chapter show that

(1) pSTAT3 induces or regulates the expression of PSMB5 in pSTAT3 constitutive cells.

(2) STAT3 also activates promoter of PSMB5.

(3) pSTAT3 regulates the expression of various subunits of 20S proteasome.

(4) Induction of apoptosis do not regulate the expression of PSMB5.

(5) Cells with low levels or devoid of pSTAT3 regulates proteasome in STAT3 independent manner.

6) pSTAT3 constitutive cells exhibit high levels of proteasome activities and PSMB5.

CHAPTER 4

EGF-INDUCED ACTIVATION OF PROTEASOME SUBUNITS THROUGH STAT3

4.1 Introduction

EGFR/ErbB1 is a member of ErbB family of receptor tyrosine kinases (RTKs). Elevated levels of EGFR expression was widely noticed in several different human cancers including breast, head and neck, gastric, prostate, NSCL, ovarian, bladder, colorectal carcinomas and glioblastomas (Yewale *et al*., 2013). In general, overexpression of EGFR is associated with advanced disease, poor prognosis and resistance to hormonal and radio therapies (Akimoto *et al*., 1999; Chen *et al*., 2000). Increased expression of EGFR and its ligands have been identified in prostate tumors. Autocrine activation of EGFR signaling regulates the growth of androgen independent prostate cancer cell line, such as, DU145. High levels of EGFR have also been identified even in androgen independent prostate tumors and is associated with development of castration resistant prostate tumors (Traish & Morgentaler, 2009). Activation of EGFR by autocrine pathway in cancer cells could be attributed to several mechanisms, such as, overexpression of the EGFR, increased concentration of ligand(s), decreased phosphatase activity, decreased receptor turnover and the presence of aberrant receptors, including EGFR gene alterations (Yewale *et al*., 2013).

Activated EGFR results in the activation of several down-stream signaling pathways, such as, Ras-Raf-MAPK, PI3K-Akt, JAK2-STAT3 that are important for tumor growth, progression and survival (Nyati *et al*., 2006). Enhanced EGFR expression in prostate tumors is associated with the elevated levels of STAT3. In addition to this, nuclear EGFR has been shown to be associated with STAT3 and involved in the activation of various genes (Lo & Hung, 2007). Inhibition of proteasome also resulted in the enhanced expression of EGFR in prostate cancer cells by decreasing receptor mediated down-regulation. Studies in pulmonary epithelial cells demonstrated an EGF dependent regulation of Nrf2, a known regulator of proteasome expression (Papaiahgari *et al*., 2006). Further, EGF-induced enhancement of ubiquitn proteasome system was observed in C.elegans (Liu *et al*., 2011).

Previous studies reported that prostate cancers possess enhanced levels of EGF/EGFR. Also, STAT3 activation was also found to be dependent on EGF/EGFR. Even, our observations in the previous chapter also suggest a STAT3 dependent

regulation of proteasome subunit expression. Hence, in the present study we sought to delineate the role of EGF/EGFR pathway in the regulation of mammalian proteasome.

4.2 Results

4.2.1 EGF up-regulates the expression of PSMB5

Elevated levels of epidermal growth factor receptor (EGFR) are associated with loss of androgen regulation resulting in the androgen-independent growth of DU-145 cells (Traish *et al*., 2009). In addition, aberrant EGFR levels are found to be frequently associated with activated STAT3 (Yu *et al*., 2009). Hence, we investigated whether EGF or VEGF regulates PSMB5 in DU-145 cells. To examine this possibility, serum starved cells were treated with EGF (100 ng/ml) and VEGF (100 ng/ml) for 24 h. Although mRNA levels of PSMB5 were induced by both the growth factors, relatively high induction of PSMB5 was observed in EGF treatments compared to 0, 24 h controls (Fig. 4.1A). Since induction of PSMB5 mRNA was more by EGF, we next investigated whether EGF induces PSMB5 protein. In order to pursue this, serum starved DU-145 cells were treated with EGF for various time-points till 24 h. Induction of PSMB5 protein levels were observed by 3 h and gradually reached to a maximum expression of 2-fold by 24 h (Fig. 4.1B). Based on our earlier results of this thesis (chapter 3) on pSTAT3 dependent up-regulation of PSMB5 expression, we analyzed the expression levels of pSTAT3 and STAT3 following EGF treatment. The maximal level of PSMB5 protein was associated with higher phospho-STAT3-Y705 levels, while total STAT3 and tubulin remained unchanged (Fig. 4.1B). Similar to the protein levels mRNA levels of PSMB5 were also increased from 3h (Fig. 4.1C).

Taken together, these results demonstrate that treatment of DU-145 cells with EGF induces the mRNA and protein levels of PSMB5 and pSTAT3 levels.

4.2.2 EGF/ EGFR induced expression of PSMB5 requires STAT3 activation

In continuation to the above studies, we hypothesized whether STAT3 would play a pivotal role in EGF-induced expression of PSMB5. To elucidate this possibility, serum starved DU-145 cells were pre-treated with inhibitors of EGFR (324674 (EI)) or STAT3 (Stattic and WP1066) for 2 h. Subsequently, cells were treated with EGF for 24 h. Similar

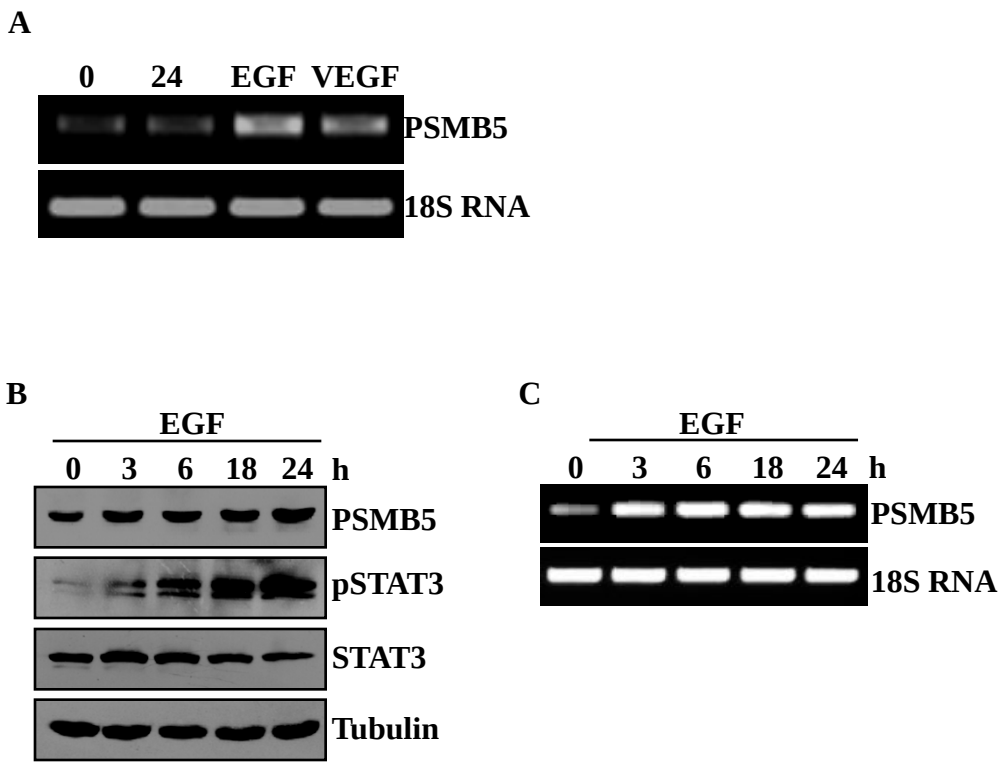

Figure 4.1: EGF induces the expression of PSMB5.

24 h serum starved DU 145 cells were washed thrice with serum free medium and treated with EGF (100 ng/ml), VEGF (100 ng/ml). *Panel A,* After 24 h of treatment, total RNA was isolated and mRNA expression levels of PSMB5 were analyzed with semi quantitative RT-PCR. 18S RNA was used as loading control. Cells were treated with EGF (100 ng/ml) in a time-dependent manner for 24 h. *Panel B,* Whole cell lysates were analyzed for PSMB5, p-STAT3 and STAT3 proteins by immunoblotting. Tubulin used as a loading control. *Panel C,* mRNA levels of PSMB5 was examined by semi quantitative RT-PCR.

to earlier observations, EGF-induced PSMB5, pSTAT3, pEGFR protein levels (Fig. 4.2A), which corroborating with earlier observations (Fig. 4.1). Inhibitors of STAT3 down-regulated both basal and EGF induced expression of PSMB5 more profoundly in Stattic treatments. In addition, inhibition of EGFR also abolished the expression of PSMB5. The specificity of inhibitors was validated by monitoring the expression of their down-stream targets, such as, phospho-EGFR and pSTAT3. Under similar experimental conditions, no gross changes were noticed in the expression levels of EGFR, total STAT3 as well as tubulin, which served as a loading control (Fig. 4.2A).

Previous studies reported that EGF/EGFR can activate down-stream JAK/STAT, PI3K/Akt and MEK/ERK signaling pathways (Mizoguchi *et al*., 2006). In order to identify the precise down-stream pathway of EGF/EGFR responsible for the regulation of PSMB5, serum starved cells were pre-incubated with inhibitors of PI3K/Akt (LY294002) and MEK/ERK (PD98059) for 2 h and then with EGF for 24 h. In agreement with previous reports, treatment of cells with EGF induced pAkt, pERK1/2, pEGFR levels. Interestingly, EGF-induced PSMB5 levels were unaltered by treatments with inhibitors of PI3K/Akt and MEK/ERK. EGFR inhibitor down-regulated both the basal and EGF induced PSMB5 protein levels. Efficacy of the individual inhibitor was verified by monitoring the suppression of their respective down-stream targets, such as, pAkt, pERK1/2 and pEGFR while panAkt, ERK1/2 and EGFR levels were unaltered by EGF treatments. Tubulin was employed as a loading control (Fig. 4.3A).

In agreement with protein levels, inhibitors of PI3K/Akt (LY294002) and MEK/ERK (PD98059) had no effect on the EGF induced mRNA levels of PSMB5 (Fig. 4.3B). However, PSMB5 mRNA levels were significantly inhibited in cells treated with either EGFR or STAT3 inhibitors, which substantiates our early observations on the transcriptional regulation of PSMB5 by STAT3 and EGF (Fig. 4.2B).

Taken together, EGF induced PSMB5 mRNA and protein levels were mediated by pSTAT3 although other down-stream targets of EGF, such as, PI3K/Akt, MEK/ERK are activated in DU-145 cells.

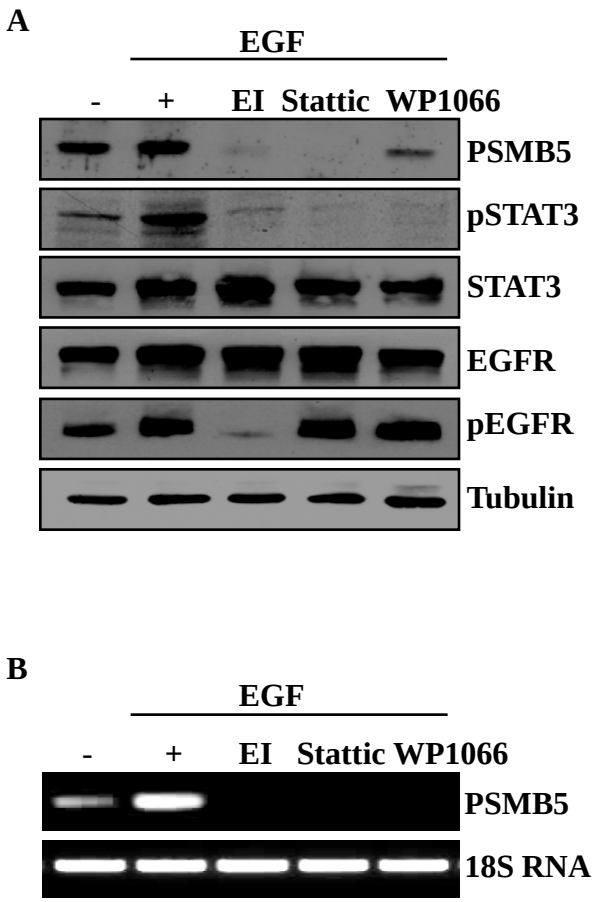

Figure 4.2: Blockade of EGFR, STAT3 down-regulates EGF induced PSMB5 expression.

Serum starved DU145 cells were washed and pre-treated for 2 h in the presence or absence of inhibitors of EGFR (324674 (EI) ; 10 μM), STAT3 (Stattic and WP1066; 10 μM). Later, cells were stimulated with EGF (100 ng/ml) for 24 h. *Panel A,* Whole cell lysates were subjected to western blot analysis using specific antibodies of PSMB5, pSTAT3, STAT3, pEGFR, EGFR. Tubulin was used as loading control. *Panel B,* mRNA levels of PSMB5 were examined by semi quantitative RT-PCR.

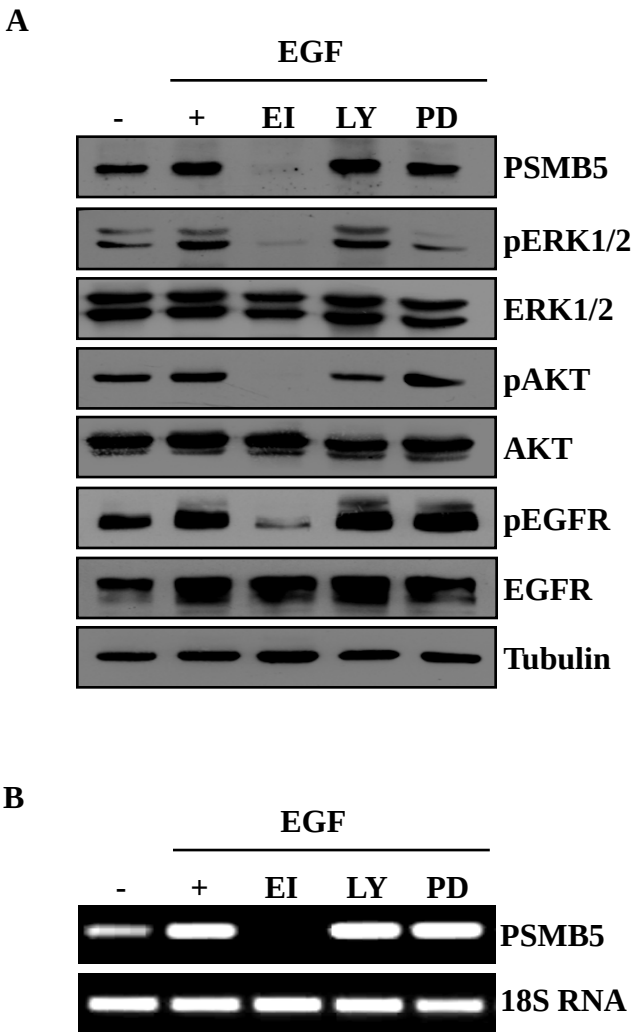

Figure 4.3: EGF induced PSMB5 protein levels were unvaried due to ERK/MAP and PI3K/Akt inhibition.

After serum starvation for 24 h, DU 145 cells were washed and pre-incubated for 2 h in the presence or absence of inhibitors of EGFR (324674 (EI); 10 μM), MEK/ERK (PD98059; 50 μM), Akt (LY294002; 20 μM). Subsequently, cells were stimulated with EGF (100 ng/ml) for 24 h. *Panel A*, Immunoblot analysis of various proteins expression form whole cell lysates is shown. All phospho forms served as positive control and non phospho forms served as loading control along with Tubulin. *Panel B*, represents mRNA levels of PSMB5 and 18S RNA.

4.2.3 Blockade of EGFR coordinately down-regulated the expression of proteasome subunits

Since EGF/EGFR induced expression of PSMB5 requires pSTAT3 (Result: 4.2.2) and the results of previous chapter of this thesis (Result: 3.2.3) demonstrated a concerted down-regulation of 20S proteasome subunits by pSTAT3 inhibition. We surmised whether EGF also induces the expression of other 20S proteasome subunits. Towards this end, DU-145 cells were pretreated for 2 h with or without EGFR inhibitor (324674) and exposed to EGF for 24 h (Fig. 4.4). Although EGF induced the protein levels of various PSMA (α) and PSMB (β) subunits, high levels of induction was observed in case of catalytic subunits. EGF induced the expression of PSMB5, PSMB6 and PSMB7 to nearly 2.5 fold, whereas, the expression of PSMB1, PSMB2, PSMB3, PSMB4 and PSMA4 were found to be between 1.5-2-fold. No gross changes were apparent in the PSMA1 protein levels. In accordance with the previous results (Fig. 4.2&4.3), EI (324674) significantly down-regulated both basal and EGF induced catalytic subunits, whereas, PSMB1, PSMB2, PSMB 3, PSMB4 and PSMA4 were down-regulated by 0.3- 0.5 fold. However, the levels of PSMA1 protein remained unchanged. Even, EGF-induced pEGFR, pSTAT3 were also abrogated by EI and under similar treatment conditions, the levels of EGFR and STAT3 were unaffected. Bcl-2, a known target of STAT3 (hence the target of EGF) was also induced by EGF and its expression was abolished by EGFR inhibition (EI) corroborating the observation that EGF regulates proteasomal subunits through a STAT3 dependent mechanism (Fig. 4.4).

Next, we analyzed the mRNA levels of 20S proteasome subunits in DU-145 cells treated with EGF in the presence or absence of EGFR inhibitor (Fig. 4.5). Similar to changes in protein levels, it was observed that mRNA levels of all PSMB1-7 subunits, PSMA4 of 20S proteasome are up-regulated by EGF treatments, which could be inhibited following pretreatment of cells with EGFR inhibitor. PSMA1 was relatively unaffected by EGF or EGFR inhibitor treatments. In addition, EGF induced mRNA levels of PSMA2, PSMA3, PSMA5, PSMA6 and PSMA7 were also down-regulated by EGFR inhibitor (Fig. 4.5).

The obtained results suggest that EGF or EGFR induced concerted increase in the protein levels of 20S proteasome subunits is STAT3 dependent.

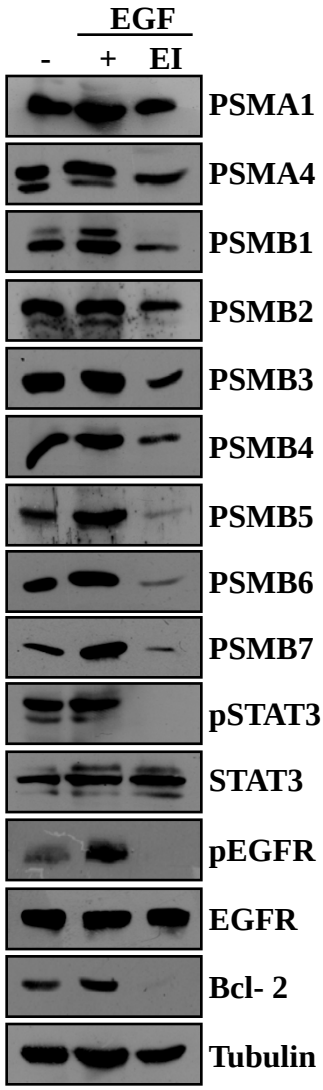

Figure 4.4: Blockade of EGFR down-regulates the expression of EGF induced various 20S proteasome subunits. Serum starved DU145 cells were pre-treated in the presence or absence of EGFR inhibitor (324674 (EI); 10 μM) for 2 h, subsequently treated with EGF (100 ng/ml) for 24 h. Cells were harvested and lysates were analyzed with specific antibodies for various PSMA (α) and PSMB (β) subunits of 20S proteasome, pSTAT3, STAT3, pEGFR, EGFR and Bcl-2. Tubulin was used as a loading control.

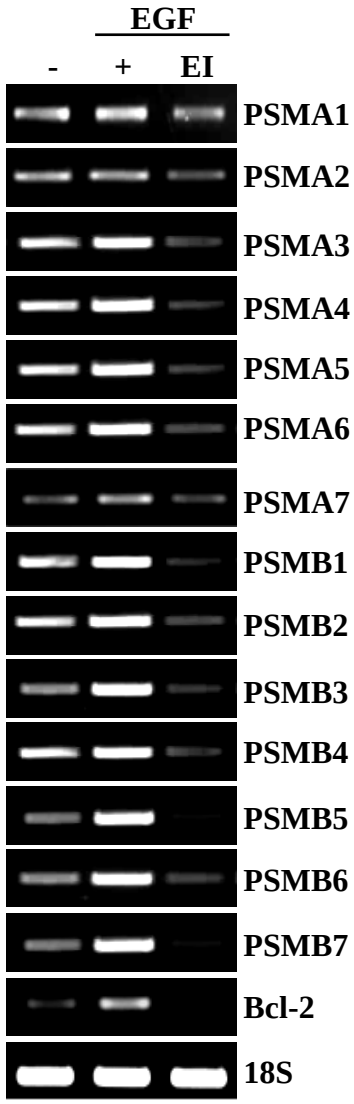

Figure 4.5: Inhibition of EGFR down-regulated mRNAs of various 20S proteasome subunits. Serum starved DU145 cells were pre-treated with or without EGFR inhibitor (324674 (EI); 10 μM) for 2 h, subsequently treated with EGF (100 ng/ml) for 24 h. After termination of treatment, total RNA was isolated from cells. Semi quantitative RT-PCR was employed to analyze the mRNA levels of 20S proteasome subunits, Bcl2. 18S RNA served as loading control.

4.2.4 PSMB5 protein levels are unresponsive to EGF in STAT3-negative PC-3 cells

PC-3 cells display higher levels of endogenous EGFR and are responsive to EGF (Gan *et al*., 2010). Hence, to validate that EGF induced PSMB5 activation requires STAT3, serum-starved PC-3 cells were pre-treated with EGF pathway inhibitors for 2 h. Subsequently, cells were treated with EGF for 24 h. EGF induced the phosphorylation of EGFR (Fig. 4.6A). In contrast, p-STAT3 and STAT3 were undetectable in PC-3 cells. Moreover, phosphorylation of Akt and ERK was also observed with EGF treatment (Fig. 4.6B). Substantiating our results, PSMB5 mRNA and protein levels remain unaffected by EGF or pharmacological inhibition of EGFR, ERK, and Akt proteins (Fig. 4.6B).

Taken together, sustained proteasome activities and loss of EGF-induced PSMB5 expression was due to the absence of STAT3 in PC-3 cells.

4.2.5 Feedback regulation of proteasome subunits in prostate cancer cells

Earlier studies reported a feedback up-regulation of proteasome subunits following proteasome inhibition (Radhakrishnan *et al*., 2010; Steffen *et al*., 2010). We further analyzed whether inhibition of STAT3 would affect the feedback regulation of proteasome subunits in prostate cells. To examine this, DU 145, LNCaP and PC-3 cells were treated with optimal concentration of bortezomib or Stattic for 12 h (Fig. 4.7 – 4.9). Real time-PCR analysis has demonstrated a 2.3-fold induction of PSMB3, 1.5 fold of PSMB5, 2.2 fold of PSMB6 and 1.8 fold of PSMA1 mRNA levels in bortezomib treated PC-3 cells (Fig. 4.7). Proteasome inhibition also induced mRNA of PSMB3 by 1.8 fold, PSMB5 by 2.2, PSMB6 by 2 fold and 1.9 fold of PSMA1 in LNCaP cells (Fig. 4.8). Inhibition of pSTAT3 in LNCaP and PC-3 showed similar expression levels of PSMB3, PSMB5, PSMB6 and PSMA1 which is in agreement with our earlier results (Fig. 4.7 & 4.8). However, Stattic treatment in DU 145 cells reduced the expression levels of PSMB3 to 40 %, PSMB5 to 20 % and PSMB6 to 40 % while PSMA1 levels remained the same as control. Further, no significant changes in the expression levels of PSMB3, PSMB5, PSMB6 and PSMA1 were observed in bortezomib treated DU 145 cells suggesting that compromised feedback response in DU-145 (Fig. 4.9).

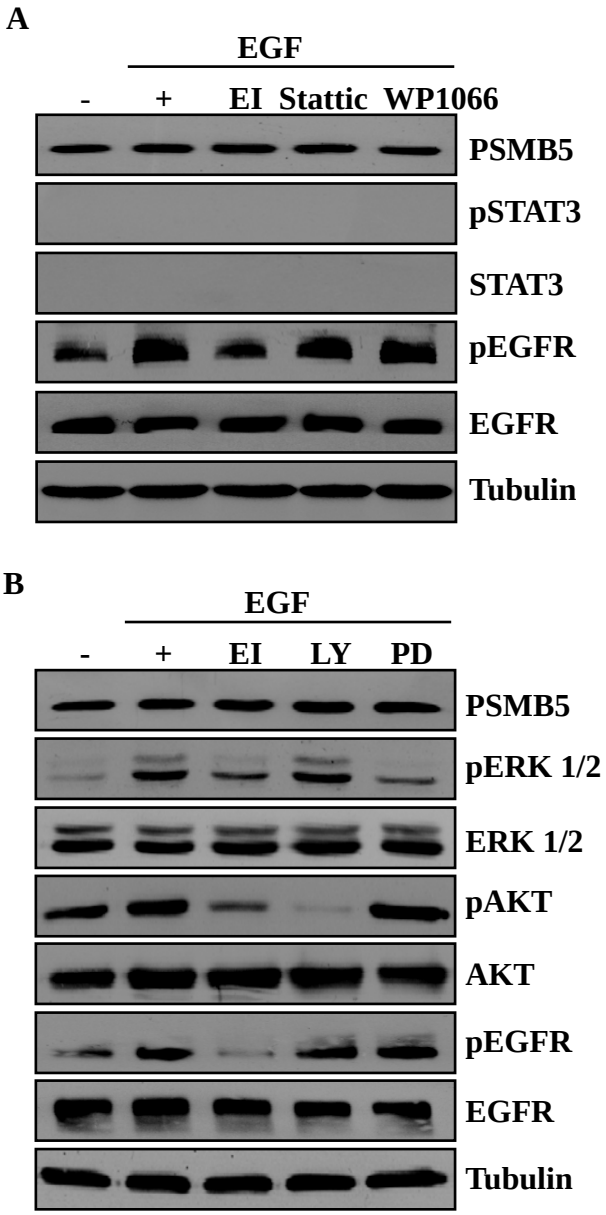

Figure 4.6: Lack of STAT3 impedes EGF-induced PSMB5 expression in PC-3 cells. PC-3 cells after 24 h of serum starvation washed and were pre-incubated for 2 h in the presence or absence of inhibitors of EGFR (324674 (EI); 10 µM), STAT3 (Stattic and WP1066; 10 µM) *Panel A*: Inhibitors of EGFR (324674 (EI); 10 µM), PI3K/AKT (LY294002; 20 µM) and MEK/ERK (PD98059; 50 µM) *Panel B.* Later, cells were stimulated with EGF (100 ng/ml) for 24 h and whole cell lysates were subjected to Western blot analysis using specific antibodies.

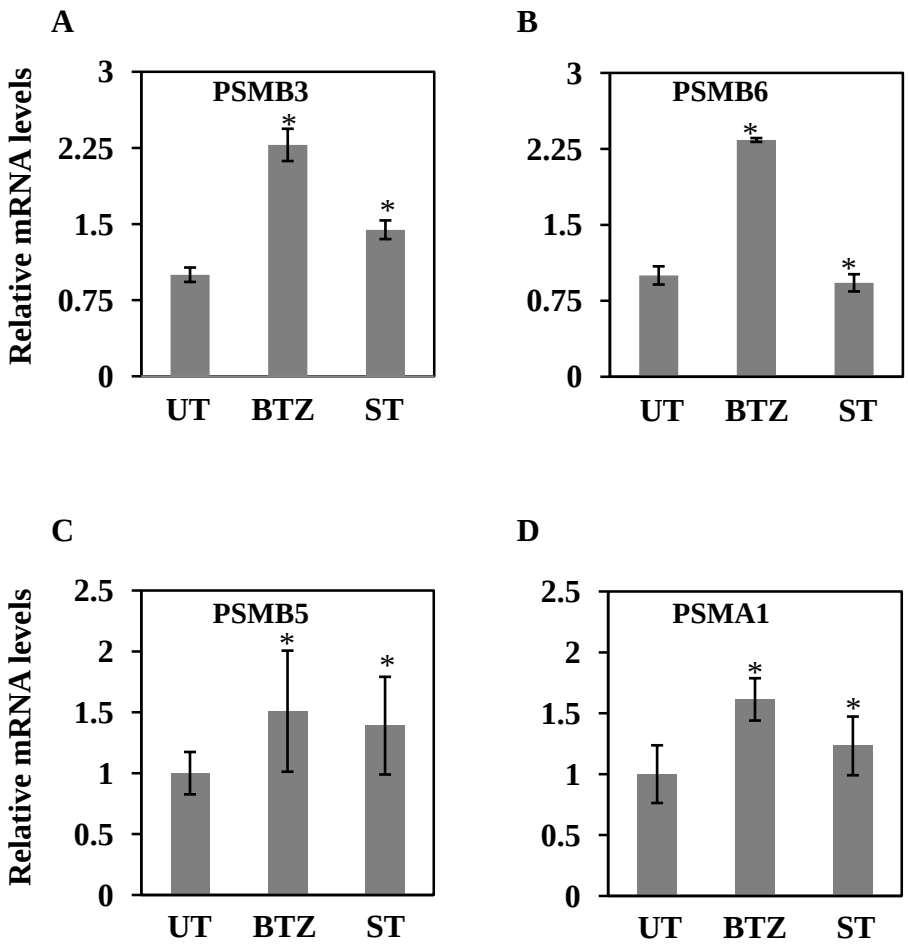

Figure 4.7: Feed back induction of proteasome sub units are not regulated by STAT3.

PC-3 cells were treated with Bortezomib (100 nM), Stattic (2.5 μM) for 12 h. After termination of treatment total RNA was isolated and mRNA levels of PSMB3 (*Panel A*), PSMB5 (*Panel B*), PSMB6 (*Panel C*) and PSMA1 (*Panel D*) were analyzed by Real Time-PCR using 18S RNA as endogenous control. Values represented are at least three independent experiments performed in triplicates and are expressed as fold change of expression relative to control. *$p<0.01$ compared to control.

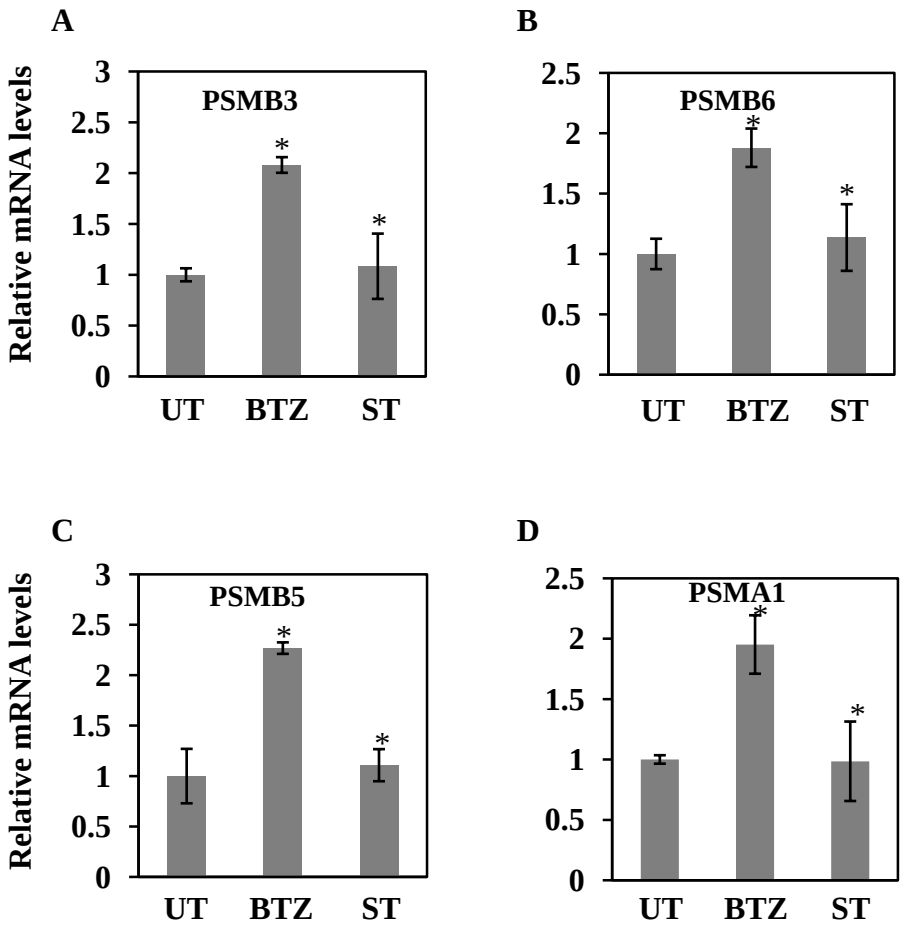

Figure 4.8: Inhibition of pSTAT3 unaltered the feed back induction of proteasome sub units.

LNCaP cells were treated with Bortezomib (100 nM), Stattic (2.5 μM) for 12 h. After termination of treatment total RNA was isolated. Quantitative RT-PCR analysis was performed to analyze the mRNA levels of PSMB3 (*Panel A*), PSMB5 (*Panel B*), PSMB6 (*Panel C*) and PSMA1 (*Panel D*) using 18S as endogenous control. Values represented are at least three independent repeats and are expressed as fold change of expression relative to control. *$p<0.01$ compared to control.

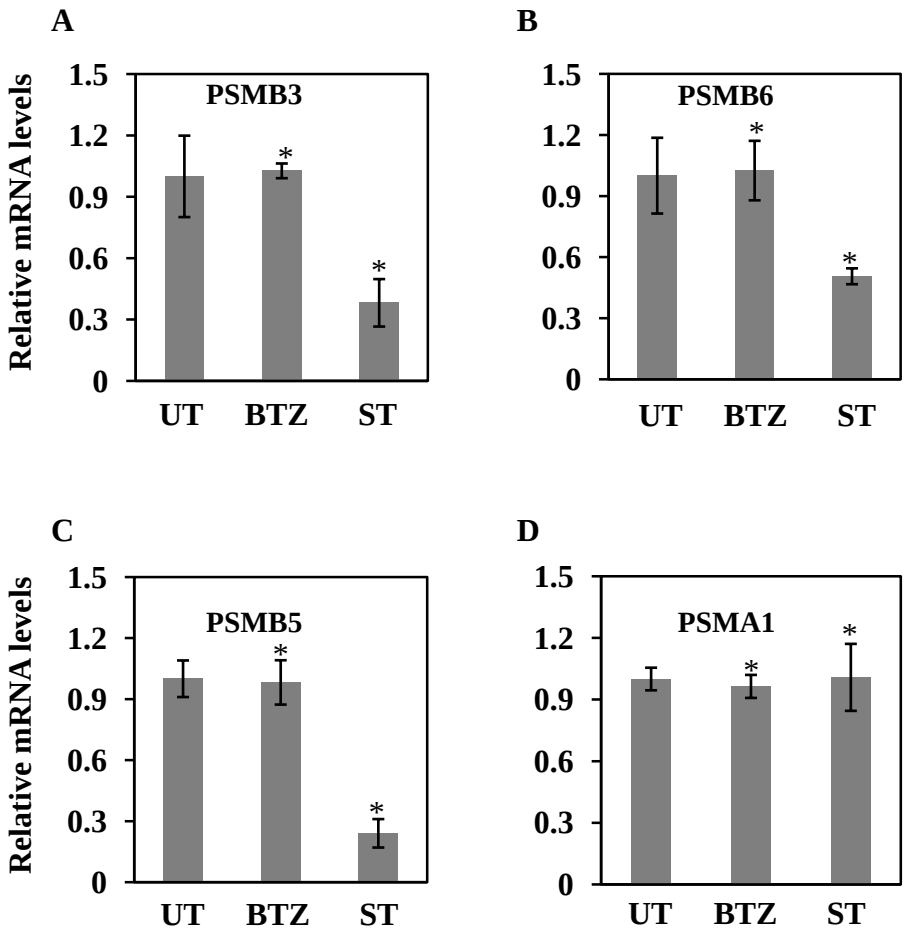

Figure 4.9: Feed back induction of proteasome sub units are regulated by STAT3.

DU145 cells were treated with Bortezomib (100 nM) and Stattic (2.5 μM) for 12 h. Total RNA was isolated and expression of PSMB3 (*Panel A*), PSMB5 (*Panel B*), PSMB6 (*Panel C*) and PSMA1 (*Panel D*) transcripts were analyzed by Real Time-PCR using 18S as endogenous control. Values represented are at least three independent repeats and are expressed as fold change of expression relative to control (n=3). *$p<0.01$ compared to control.

Overall, the present results suggest that feedback up-regulation of proteasome genes was compensated by constitutively activated pSTAT3 in DU-145 cells.

4.2.6 Bortezomib exacerbates STAT3 inhibitor-induced loss of proteasome expression, function and cellular apoptosis

Results of previous chapter demonstrated decreased proteasome subunit expression and activity following inhibition of pSTAT3 in cell lines expressing constitutively active STAT3 (Fig. 3.1-3.8). In comparison, bortezomib treatments also reduced proteasome activity, however, PSMB5 protein levels remained unchanged (Fig. 3.22). Moreover, earlier reports have shown synergistic activation of cell death in response to combined treatments of bortezomib and STAT3 inhibitors in HNSCC cell lines (Li *et al*., 2009). Hence, we reasoned that co-treatments employing bortezomib and STAT3 inhibitor would further reduce the proteasome function and potentiate cell death. To examine this, DU 145 cells were treated with Stattic, WP1066, bortezomib or a combination of STAT3 inhibitors with bortezomib for 18 h (Fig. 4.10A). As expected, chymotrypsin-like activity was decreased to 90% in response to bortezomib. In comparison, the values were reduced to 70% in WP1066 and 98% in Stattic treated cells. However, co-treatments with STAT3 inhibitors and bortezomib completely abolished the chymotrypsin-like activity. In addition, trypsin-like and caspase-like activities of the proteasome were significantly inhibited in co-treatments (Fig. 4.10A). Further, we elucidated whether the decreased proteasome activities were indeed due to down-regulation of proteasome expression by pSTAT3 inhibition. To test this, we determined the chymotrypsin-like activity of purified 20S proteasome with varying concentrations 0.1 µM, 5 µM, 10 µM of bortezomib and STAT3 inhibitors. Neither Stattic nor WP1066 blocked chymotrypsin-like activity of 20S proteasome *in vitro* suggesting that lack of non-specific inhibition of proteasome by both STAT3 inhibitors. In contrast, bortezomib significantly reduced the chymotrypsin-like activity of 20S proteasome (Fig. 4.10B). Next, we analyzed the protein levels of PSMB5, which is responsible for the chymotrypsin-like activity of 20S proteasome. As expected, significantly lower protein levels of PSMB5 and 20S core complex were observed with co-treatments when compared to STAT3 inhibitors. Whereas, no marked change in the protein levels of

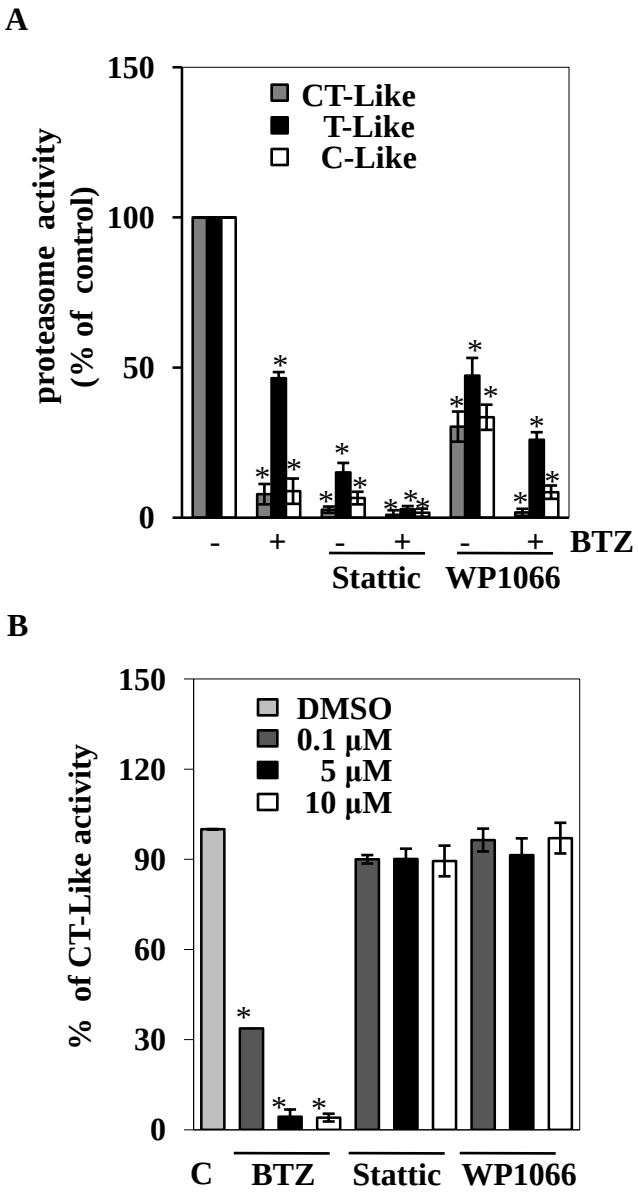

Figure 4.10: Synergistic inhibition of proteasome activities by Co treatments of proteasome and STAT3 inhibitors.

Panel A, DU145 cells were treated with Bortezomib (BTZ, 100 nM) or Stattic (10 µM) or WP1066 (10 µM) or a combination of Bortezomib and STAT3 inhibitors for 18 h. DMSO was used as a vehicle control. Chymotrypsin-like (CT-like), trypsin-like (T-like) and caspase-like (C-like) activities of the proteasome were measured. *Panel B,* Chymotrypsin-like (CT-like) activity of the purified 20S proteasome incubated with different concentrations (0.1 µM, 5 µM, 10 µM) of Bortezomib, Stattic or WP1066. Values represented are atleast three independent repeats (n=3). *$p<0.01$ compared to control.

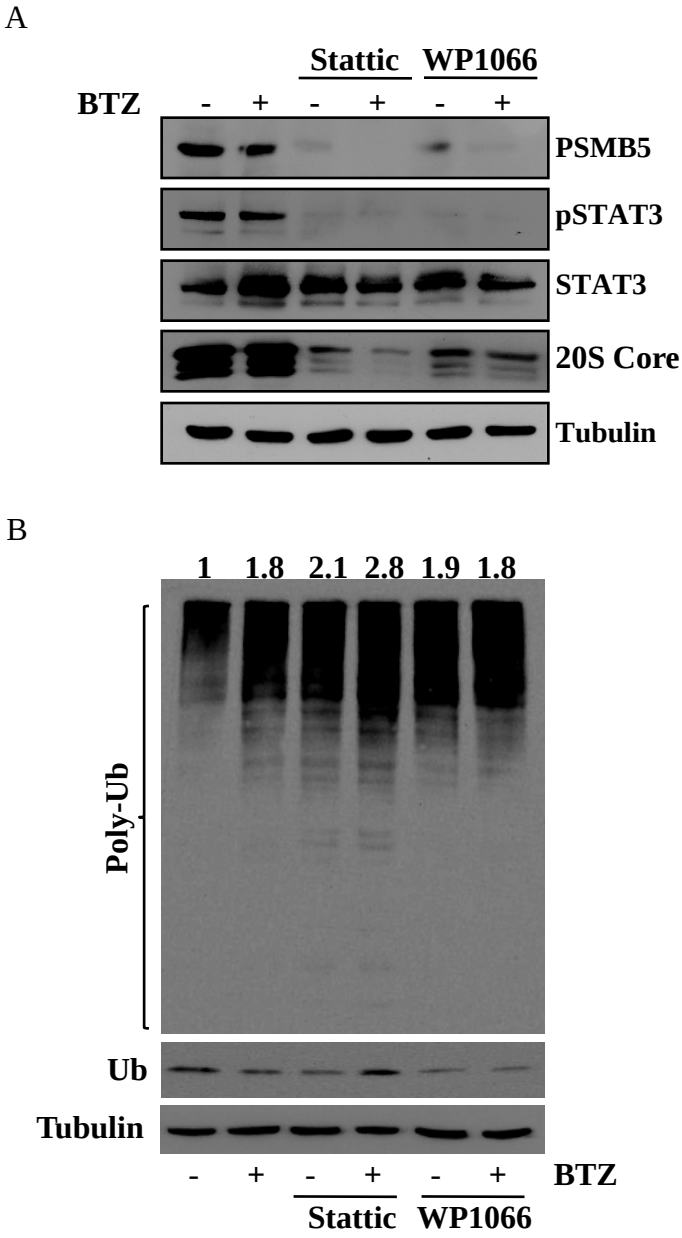

Figure 4.11: Bortezomib enhanced pSTAT3 inhibition induced loss of PSMB5 and proteasome expression and function.

DU-145 cells were treated with Bortezomib (BTZ; 100 nM) or Stattic (10 μM) or WP1066 (10 μM) or a combination of bortezomib and STAT3 inhibitors for 18 h. *Panel A,* Expression levels of PSMB5, pSTAT3, STAT3 and 20S proteasome core complex were analyzed with immunoblotting. Tubulin used as loading control. *Panel B,* Under similar conditions of treatments, levels of poly-ubiquitinated proteins were determined by immunoblot analysis and fold changes were normalized to Tubulin, deduced by densitometry.

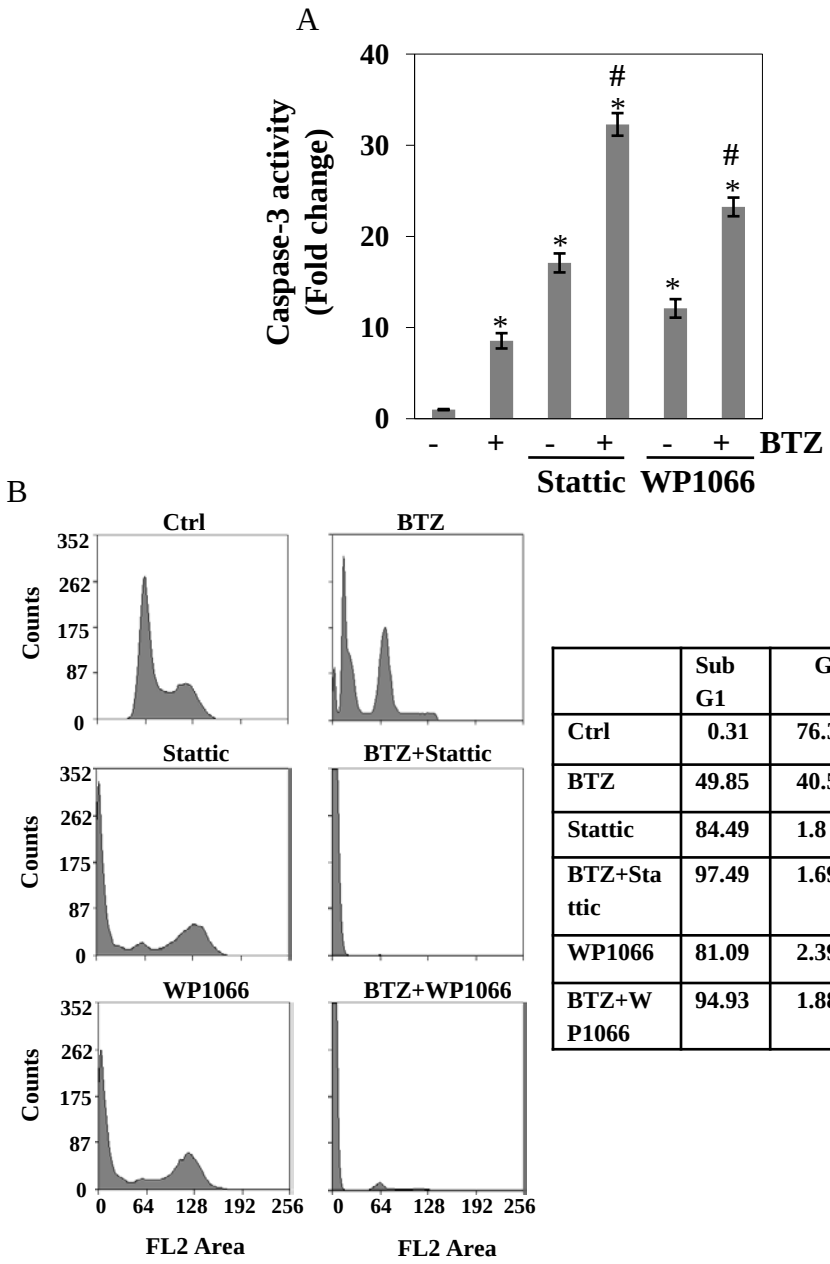

	Sub G1	G1	S	G2/M
Ctrl	0.31	76.33	7.39	15.93
BTZ	49.85	40.50	2.82	6.84
Stattic	84.49	1.8	1.2	12.51
BTZ+Stattic	97.49	1.69	0.17	0.66
WP1066	81.09	2.39	2.9	13.62
BTZ+WP1066	94.93	1.88	0.52	2.67

Figure 4.12: Enhanced activation of apoptosis by pSTAT3 and proteasome inhibition. DU-145 cells were treated with Bortezomib (100 nM) or Stattic (10 μM) or WP1066 (10 μM) or a combination of Bortezomib and STAT3 inhibitors for 18 h. *Panel A* represents caspase-3 activity of treatments. Values represented are at least three independent repeats (n=3). *p<0.01 compared to control, #p<0.01 compared to Bortezomib. *Panel B,* Cell cycle analysis was performed employing propidium iodide as described in Materials and Methods. The percentage of cells in each phase of cell cycle was quantified by flow cytometry.

PSMB5 and 20S proteasome were observed in cells treated with bortezomib alone (Fig. 4.11A). Inhibition of proteasome function is known to result in the accumulation of poly ubiquitinated proteins (De wilt *et al*., 2012), we next examined the poly ubiquitinated protein levels in cells treated either with bortezomib alone or in combination with STAT3 inhibitors. In agreement with our results, co-treatments, individual exposure to STAT3 inhibitors and bortezomib caused an increase in the intracellular levels of poly-ubiquitinated proteins (Fig. 4.11B). Moreover, a combination regimen of bortezomib with Stattic or WP1066 resulted in a significant enhancement of caspase-3 enzyme activity in cells as compared to individual treatments alone. Cellular apoptosis as measured by caspase-3 activation was increased by 8-fold with bortezomib, 15-fold with Stattic, 10-fold with WP1066, whereas, the values increased significantly to nearly 30-fold and 22-fold in co-treatments of bortezomib with Stattic and WP1066 respectively (Fig. 4.12A). The obtained result was further supported by flow cytometric analysis of cells treated with bortezomib and STAT3 inhibitors. Flow cytometry analysis of cell cycle events revealed that the percentage of cells accumulated at sub-G1 phase of cell cycle to be 90%, 82% and 60% in Stattic, WP1066 and bortezomib treated cells respectively. However, nearly 98% of cells were accumulated in sub G1 phase of cell cycle in co-treatments employing bortezomib and STAT3 inhibitors (Fig. 4.12B).

Taken together, co-treatments of bortezomib with inhibitors of STAT3 synergistically increased proteasomal dysfunction and enhanced cellular apoptosis.

Discussion

Androgen-independency of DU 145 cells has been shown to be associated with the higher levels of EGFR. In addition, aberrant EGFR levels are found to be frequently associated with activated STAT3 (Traish *et al*., 2009; Yu *et al*., 2009). Accordingly, EGF-induced expression of PSMB5 mRNA and protein levels correlated with concomitant induction of pSTAT3 in DU 145 cells. This further substantiates the results from the previous chapter of this thesis on STAT3 dependent regulation of PSMB5. STAT3 has been shown as one of the targets of EGF signaling in addition to the PI3K and ERK pathways (Mizoguchi *et al*., 2006). In line with this concept, EGF increased the levels of pERK1/2, pAKT along with pSTAT3 in DU 145 cells. However, EGF induced

activation of the PI3K or ERK pathway did not affect PSMB5 expression in DU 145 (Fig. 4.3). In contrast, EGF-dependent activation of p-STAT3 induced PSMB5 protein in DU 145 cells. Hence, EGF-activated STAT3 possibly regulates the expression of subunits of the 20S proteasome and may contribute to the optimal growth of DU 145 cells through efficient protein homeostasis. In support of these observations, recent studies in *Caenorhabditis elegans* also demonstrated that EGF signaling activates the ubiquitin proteasome system to modulate the life span of the worm (Liu *et al*., 2011). In contrast, activation and inhibition of EGFR did not alter the expression of PSMB5 in PC-3 cells which are STAT3 negative. Further, inhibition of EGF induced activation of the PI3K or ERK pathways did not affect PSMB5 expression in PC-3 cells which corroborates with the earlier results that EGF induced activation requires STAT3 (Fig. 4.6). This would also suggest that proteasomes of PC-3 cells may be regulated by factors other than EGFR or other transcription factors.

Proteasome genes have been shown to be regulated coordinately by Nrf1 and Nrf2 in response to proteasome inhibition (Kwak *et al*., 2006; Meiners *et al*., 2003; Steffen *et al*., 2010; Radhakrishnan *et al*., 2010). In line with this observation, EGF induced various proteasome subunits are concertedly down-regulated by inhibition of EGFR (Fig. 4.4-4.5). This finding further substantiates the results from the previous chapter that inhibition of pSTAT3 coordinately down-regulated various proteasome subunits (Fig. 3.5-3.6) and EGF induced expression of PSMB5 requires STAT3 (Fig. 4.2).

Inhibition of proteasome resulting in the elevated levels of proteasome synthesis by feedback response was reported in LNCaP and other cells (Radhakrishnan *et al*., 2010). In agreement with these results, feedback response of proteasome subunits was observed in LNCaP and PC-3 cells (Fig. 4.7-4.8) with bortezomib but not in Stattic treatments (Fig. 3.9-3.10). Xu *et al*., 2008 demonstrated a diminished feedback expression of proteasome genes in cancer cells in response to proteasome inhibitors due to constitutively active feedback response. Accordingly, no significant feedback induction was observed in DU 145 treatments with bortezomib. In addition, reduced levels of PSMBs by Stattic suggest a compromised feedback response or STAT3 dependent regulation of feedback response (Fig. 4.9).

STAT3 inhibitors impair cellular proteasome activities, leading to accumulation of poly-ubiquitinated proteins similar to proteasome inhibitors (Fig. 4.11B). However, STAT3 inhibitors do not interact with mammalian proteasome subunits because the molecular structures of STAT3 inhibitors differ markedly from known structural classes of proteasome inhibitors. The lack of inhibition by STAT3 inhibitors on chymotrypsin-like activity of the purified 20 S proteasome clearly indicates that there is no cross-reactivity between the STAT3 inhibitors and the proteasome *per se* (Fig. 4.10B). Overall, persistently activated STAT3 levels function as an important determinant of proteasome activity in cell lines harboring constitutive STAT3. PSMB5 is the molecular target of bortezomib, a Food and Drug Administration-approved proteasome inhibitor used clinically to ameliorate relapsed multiple myeloma and mantle cell lymphoma (Fisher *et al*., 2006; Richardson *et al*., 2003). However, bortezomib resistance mechanisms pose a major obstacle in clinical therapy (Chen *et al*., 2011). The status of PSMB5 was elucidated in bortezomib-resistant cell line models. These studies suggested that bortezomib resistance was either due to mutations in or overexpression of the PSMB5 subunit (Lu *et al*., 2009; Ri *et al*., 2010). However, observations from these cell line models remain unverified in clinical samples (Leung *et al*., 2013; Lichter *et al*., 2012; Politou *et al*., 2006). In addition, the feedback regulation of proteasome gene expression also contributes to bortezomib resistance (Xie, 2010). Hence, constitutively activated STAT3 levels in cancers may presumably circumvent the effect of bortezomib regimen through up-regulation of PSMB5 protein. Therefore, co treatment with bortezomib and an inhibitor of STAT3 may suppress bortezomib resistance. Because STAT3 regulates the basal expression of various subunits, blockade of STAT3 activation may, in part, alleviate the feedback response to proteasome inhibition. Moreover, lower expression of proteasome subunits reduces the number of active sites required for proteasome inhibition. In agreement with this hypothesis, knockdown of the 20S core subunits of the proteasome sensitized HCT116 cells to bortezomib (Chen *et al*., 2010). Therefore, co treatment involving bortezomib and STAT3 inhibitors might prove useful to inhibit proteasome function and STAT3 signaling in cancers (Fig. 4.12). Overall, the findings of STAT3 dependent PSMB5 regulation underscore an alternative mechanism for bortezomib insensitivity. Overall, the findings of the present study suggests that the

oncogenic properties of STAT3 regulates the expression of PSMB5 and other subunits and activities of the mammalian proteasome and this feature may be responsible for supporting the malignant progression.

Conclusions:

Overall the results presented in this chapter show that

(1) EGF/EGFR induces the expression of PSMB5.

(2) pSTAT3 is essential for EGF/EGFR induced expression of PSMB5.

(3) EGFR regulates the expression of various 20S proteasome subunits.

(4) Constitutive feedback response was mediated by pSTAT3 in DU 145 cells.

(5) Synergistic abrogation of proteasome and cell viability by co-treatments of proteasome and STAT3 inhibitors.

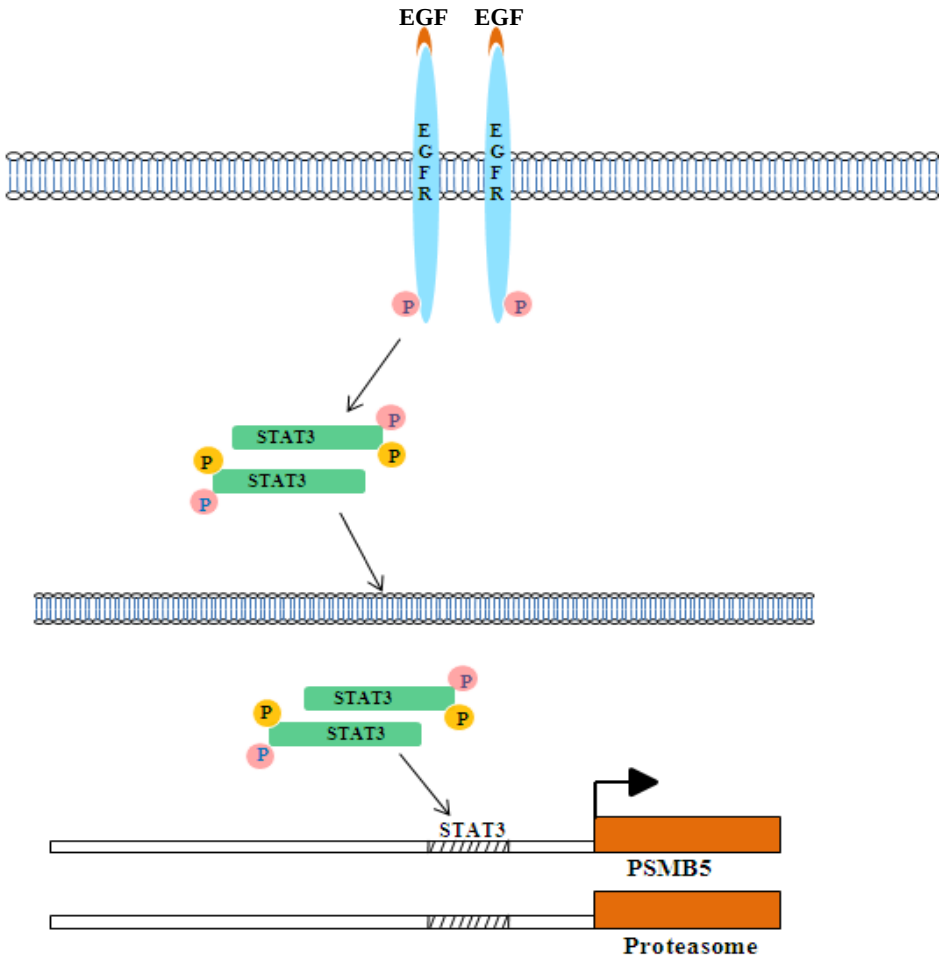

Fig 4.13: Proposed model of EGF/EGFR mediated regulation of PSMB5 and Proteasome.

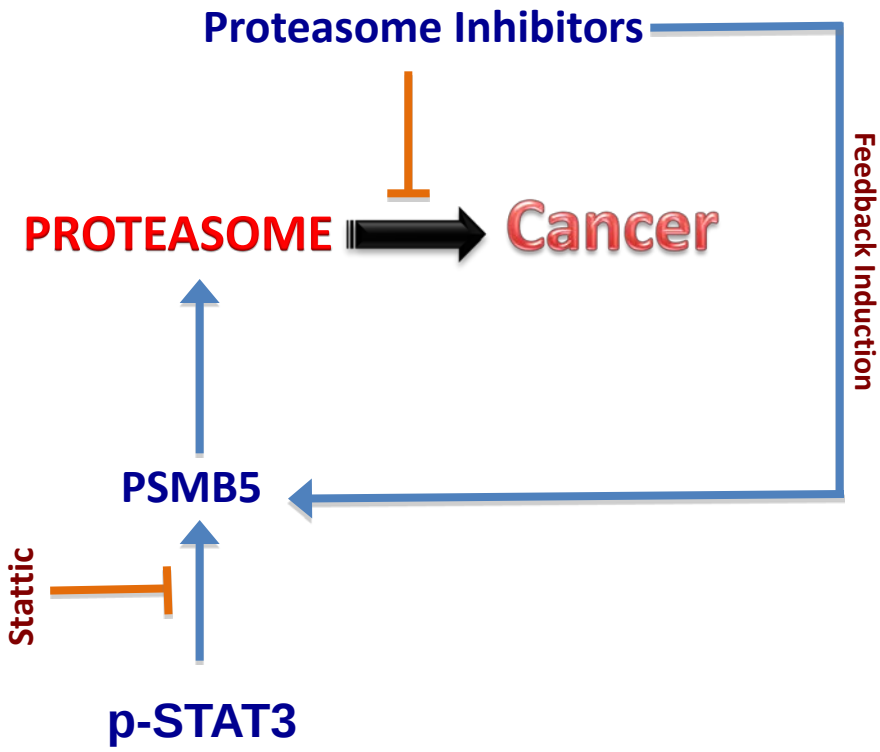

Fig 4.14: Schematic representation on the synergistic role of STAT3 inhibition in enhancing the anticancer effects of the proteasome inhibitors.

SUMMARY OF RESULTS

Overexpressed as well as endogenous pSTAT3 regulates the expression of PSMB5 and cellular proteasome activity.

- pSTAT3 regulates the proteasomal subunits, PSMB5, and cellular proteasome activities in pSTAT3 constitutive cells, as inhibition of pSTAT3 decreased the expression of PSMB5 and proteasome activities.
- Adenoviral mediated expression of pSTAT3 induced the expression of PSMB5 mRNA and protein levels.
- Overexpression of pSTAT3 induced PSMB5 promoter and proteasome activities.
- Apoptosis independent regulation of proteasome was evidenced by the lack of apparent changes in the expression of PSMB5 and proteasome activities by inducers of apoptosis.
- PSMB5 expression is not dependent on STAT3 in cells expressing either low levels or devoid of pSTAT3, as blocking of pSTAT3 unaffected proteasome activities and PSMB5 expression.
- Elevated levels of pSTAT3 directly correlates with the proteasome expression and activities as shown by enhanced expression of PSMB5 and proteasome activities in pSTAT3 constitutive cells.
- pSTAT3 mediates constitutive feedback up-regulation of proteasome, as inhibition of proteasome function diminished up-regulation of proteasome subunits in pSTAT3 constitutive cells, but not, in pSTAT3 negative cells.
- EGF/EGFR induced PSMB5 expression requires pSTAT3 as suppression of pSTAT3, but not, PI3K/Akt, MEK/ERK down-regulated the expression of PSMB5.
- Blockade of EGFR down-regulated the expression of various 20S proteasome subunits.
- Synergistic effects following co-treatments with STAT3 and proteasome inhibitors on proteasomal dysfunction and cell viability suggests that combination treatment with STAT3 inhibitors as a promising approach for improving the therapeutic efficiency of bortezomib in cancer treatment.

REFERENCES

Abdulghani, J., Gu, L., Dagvadorj, A., Lutz, J., Leiby, B., Bonuccelli, G., Lisanti, M. P., Zellweger, T., Alanen, K., Mirtti, T., Visakorpi, T., Bubendorf, L., & Nevalainen, M. T. 2008. Stat3 promotes metastatic progression of prostate cancer. The American Journal of Pathology, 172(6): 1717-1728.

Adams, J. 2004. The development of proteasome inhibitors as anticancer drugs. Cancer Cell, 5(5): 417-421.

Adams, J., Behnke, M., Chen, S., Cruickshank, A. A., Dick, L. R., Grenier, L., Klunder, J. M., Ma, Y. T., Plamondon, L., & Stein, R. L. 1998. Potent and selective inhibitors of the proteasome: dipeptidyl boronic acids. Bioorganic & Medicinal Chemistry Letters, 8(4): 333-338.

Akimoto, T., Hunter, N. R., Buchmiller, L., Mason, K., Ang, K. K., & Milas, L. 1999. Inverse relationship between epidermal growth factor receptor expression and radiocurability of murine carcinomas. Clinical Cancer Research, 5(10): 2884-2890.

Akiyama, K., Kagawa, S., Tamura, T., Shimbara, N., Takashina, M., Kristensen, P., Hendil, K. B., Tanaka, K., & Ichihara, A. 1994. Replacement of proteasome subunits X and Y by LMP7 and LMP2 induced by interferon-gamma for acquirement of the functional diversity responsible for antigen processing. FEBS Letters, 343(1): 85-88.

Aktas, H., Cai, H., & Cooper, G. M. 1997. Ras links growth factor signaling to the cell cycle machinery via regulation of cyclin D1 and the Cdk inhibitor p27KIP1. Molecular and Cellular Biology, 17(7): 3850-3857.

Alroy, I., & Yarden, Y. 1997. The ErbB signaling network in embryogenesis and oncogenesis: signal diversification through combinatorial ligand-receptor interactions. FEBS Letters, 410(1): 83-86.

Arendt, C. S., & Hochstrasser, M. 1997. Identification of the yeast 20S proteasome catalytic centers and subunit interactions required for active-site formation. Proc. Nati. Acad. Scie. USA, 94(14): 7156-7161.

Arlt, A., Bauer, I., Schafmayer, C., Tepel, J., Muerkoster, S. S., Brosch, M., Roder, C., Kalthoff, H., Hampe, J., Moyer, M. P., Folsch, U. R., & Schafer, H. 2009. Increased proteasome subunit protein expression and proteasome activity in colon cancer relate to an enhanced activation of nuclear factor E2-related factor 2 (Nrf2). Oncogene, 28(45): 3983-3996.

Arteaga, C. L. 2002. Overview of epidermal growth factor receptor biology and its role as a therapeutic target in human neoplasia. Seminars in Oncology, 29(5 Suppl 14): 3-9.

Auld, K. L., & Silver, P. A. 2006. Transcriptional regulation by the proteasome as a mechanism for cellular protein homeostasis. Cell Cycle, 5(14): 1503-1505.

Azare, J., Leslie, K., Al-Ahmadie, H., Gerald, W., Weinreb, P. H., Violette, S. M., & Bromberg, J. 2007. Constitutively activated Stat3 induces tumorigenesis and enhances cell motility of prostate epithelial cells through integrin beta 6. Molecular and Cellular Biology, 27(12): 4444-4453.

Baldassarre, G., Boccia, A., Bruni, P., Sandomenico, C., Barone, M. V., Pepe, S., Angrisano, T., Belletti, B., Motti, M. L., Fusco, A., & Viglietto, G. 2000. Retinoic acid induces neuronal differentiation of embryonal carcinoma cells by reducing proteasome-dependent proteolysis of the cyclin-dependent inhibitor p27. Cell Growth & Differentiation, 11(10): 517-526.

Balsas, P., Galan-Malo, P., Marzo, I., & Naval, J. 2012. Bortezomib resistance in a myeloma cell line is associated to PSMbeta5 overexpression and polyploidy. Leukemia Research, 36(2): 212-218.

Bard, J. D., Gelebart, P., Amin, H. M., Young, L. C., Ma, Y., & Lai, R. 2009. Signal transducer and activator of transcription 3 is a transcriptional factor regulating the gene expression of SALL4. FASEB J, 23(5): 1405-1414.

Bartoli, M., Platt, D., Lemtalsi, T., Gu, X., Brooks, S. E., Marrero, M. B., & Caldwell, R. B. 2003. VEGF differentially activates STAT3 in microvascular endothelial cells. FASEB J, 17(11): 1562-1564.

Baumeister, W., Walz, J., Zuhl, F., & Seemuller, E. 1998. The proteasome: paradigm of a self-compartmentalizing protease. Cell, 92(3): 367-380.

Bazzaro, M., Lee, M. K., Zoso, A., Stirling, W. L., Santillan, A., Shih Ie, M., & Roden, R. B. 2006. Ubiquitin-proteasome system stress sensitizes ovarian cancer to proteasome inhibitor-induced apoptosis. Cancer Research, 66(7): 3754-3763.

Bence, N. F., Sampat, R. M., & Kopito, R. R. 2001. Impairment of the ubiquitin-proteasome system by protein aggregation. Science, 292(5521): 1552-1555.

Benedict, C. M., Ren, L., & Clawson, G. A. 1995. Nuclear multicatalytic proteinase alpha subunit RRC3: differential size, tyrosine phosphorylation, and susceptibility to antisense oligonucleotide treatment. Biochemistry, 34(29): 9587-9598.

Bernardi, R., Liebermann, D. A., & Hoffman, B. 2000. Cdc25A stability is controlled by the ubiquitin-proteasome pathway during cell cycle progression and terminal differentiation. Oncogene, 19(20): 2447-2454.

Blanchard, D. A., Mouhamad, S., Auffredou, M. T., Pesty, A., Bertoglio, J., Leca, G., & Vazquez, A. 2000. Cdk2 associates with MAP kinase in vivo and its nuclear translocation is dependent on MAP kinase activation in IL-2-dependent Kit 225 T lymphocytes. Oncogene, 19(36): 4184-4189.

Bose, R., & Zhang, X. 2009. The ErbB kinase domain: structural perspectives into kinase activation and inhibition. Experimental Cell Research, 315(4): 649-658.

Bose, S., Stratford, F.L., Broadfoot, K.I., Mason, G.G., & Rivett, A.J. 2004. gamma-Interferon decreases the level of 26S proteasomes and changes the pattern of phosphorylation. Biochem. J, 353: 291–297.

Bromberg, J. F., & Darnell, J. E., Jr. 1999. Potential roles of Stat1 and Stat3 in cellular transformation. Cold Spring Harbor symposia on quantitative biology, 64: 425-428.

Bromberg, J. F., Horvath, C. M., Besser, D., Lathem, W. W., & Darnell, J. E., Jr. 1998. Stat3 activation is required for cellular transformation by v-src. Molecular and Cellular Biology, 18(5): 2553-2558.

Bromberg, J. F., Wrzeszczynska, M. H., Devgan, G., Zhao, Y., Pestell, R. G., Albanese, C., & Darnell, J. E., Jr. 1999. Stat3 as an oncogene. Cell, 98(3): 295-303.

Bublil, E. M., & Yarden, Y. 2007. The EGF receptor family: spearheading a merger of signaling and therapeutics. Current Opinion in Cell Biology, 19(2): 124-134.

Carrano, A. C., Eytan, E., Hershko, A., & Pagano, M. 1999. SKP2 is required for ubiquitin-mediated degradation of the CDK inhibitor p27. Nature Cell Biology, 1(4): 193-199.

Castagnino, P., Biesova, Z., Wong, W. T., Fazioli, F., Gill, G. N., & Di Fiore, P. P. 1995. Direct binding of eps8 to the juxtamembrane domain of EGFR is phosphotyrosine and SH2-independent. Oncogene, 10(4): 723-729.

Chau, V., Tobias, J. W., Bachmair, A., Marriott, D., Ecker, D. J., Gonda, D. K., & Varshavsky, A. 1989. A multiubiquitin chain is confined to specific lysine in a targeted short-lived protein. Science, 243(4898): 1576-1583.

Chauhan, D., Li, G., Shringarpure, R., Podar, K., Ohtake, Y., Hideshima, T., & Anderson, K. C. 2003. Blockade of Hsp27 overcomes Bortezomib/proteasome inhibitor PS-341 resistance in lymphoma cells. Cancer Research, 63(19): 6174-6177.

Chen, D., Frezza, M., Schmitt, S., Kanwar, J., & Dou, Q. P. 2011. Bortezomib as the first proteasome inhibitor anticancer drug: current status and future perspectives. Current Cancer Drug Targets, 11(3): 239-253.

Chen, L., & Madura, K. 2005. Increased proteasome activity, ubiquitin-conjugating enzymes, and eEF1A translation factor detected in breast cancer tissue. Cancer Research, 65(13): 5599-5606.

Chen, P., & Hochstrasser, M. 1996. Autocatalytic subunit processing couples active site formation in the 20S proteasome to completion of assembly. Cell, 86(6): 961-972.

Chen, S., Blank, J. L., Peters, T., Liu, X. J., Rappoli, D. M., Pickard, M. D., Menon, S., Yu, J., Driscoll, D. L., Lingaraj, T., Burkhardt, A. L., Chen, W., Garcia, K., Sappal, D. S., Gray, J., Hales, P., Leroy, P. J., Ringeling, J., Rabino, C., Spelman, J. J., Morgenstern, J. P., & Lightcap, E. S. 2010. Genome-wide siRNA screen for modulators of cell death induced by proteasome inhibitor bortezomib. Cancer Research, 70(11): 4318-4326.

Chen, Z., Ke, L. D., Yuan, X. H., & Adler-Storthz, K. 2000. Correlation of cisplatin sensitivity with differential alteration of EGFR expression in head and neck cancer cells. Anticancer Research, 20(2A): 899-902.

Chepelev, N. L., Bennitz, J. D., Huang, T., McBride, S., & Willmore, W. G. 2011. The Nrf1 CNC-bZIP protein is regulated by the proteasome and activated by hypoxia. PLoS One, 6(12): e29167.

Chung, C. D., Liao, J., Liu, B., Rao, X., Jay, P., Berta, P., & Shuai, K. 1997a. Specific inhibition of Stat3 signal transduction by PIAS3. Science, 278(5344): 1803-1805.

Chung, J., Uchida, E., Grammer, T. C., & Blenis, J. 1997b. STAT3 serine phosphorylation by ERK-dependent and -independent pathways negatively modulates its tyrosine phosphorylation. Molecular and Cellular Biology, 17(11): 6508-6516.

Ciechanover, A. 2006. The ubiquitin proteolytic system: from a vague idea, through basic mechanisms, and onto human diseases and drug targeting. Neurology, 66(2 Suppl 1): S7-19.

Clifford, S. C., Cockman, M. E., Smallwood, A. C., Mole, D. R., Woodward, E. R., Maxwell, P. H., Ratcliffe, P. J., & Maher, E. R. 2001. Contrasting effects on HIF-1alpha regulation by disease-causing pVHL mutations correlate with patterns of tumourigenesis in von Hippel-Lindau disease. Human Molecular Genetics, 10(10): 1029-1038.

Coux, O., Tanaka, K., & Goldberg, A. L. 1996. Structure and functions of the 20S and 26S proteasomes. Annual Review of Biochemistry, 65: 801-847.

Crawford, H. C., Fingleton, B. M., Rudolph-Owen, L. A., Goss, K. J., Rubinfeld, B., Polakis, P., & Matrisian, L. M. 1999. The metalloproteinase matrilysin is a target of beta-catenin transactivation in intestinal tumors. Oncogene, 18(18): 2883-2891.

Crews, C. M., Alessandrini, A., & Erikson, R. L. 1992. The primary structure of MEK, a protein kinase that phosphorylates the ERK gene product. Science, 258(5081): 478-480.

Croker, B. A., Kiu, H., & Nicholson, S. E. 2008. SOCS regulation of the JAK/STAT signalling pathway. Seminars in Cell & Developmental Biology, 19(4): 414-422.

Daniel, K. G., Chen, D., Orlu, S., Cui, Q. C., Miller, F. R., & Dou, Q. P. 2005. Clioquinol and pyrrolidine dithiocarbamate complex with copper to form proteasome inhibitors and apoptosis inducers in human breast cancer cells. Breast Cancer Research, 7(6): R897-908.

De Wilt, L. H., Jansen, G., Assaraf, Y. G., van Meerloo, J., Cloos, J., Schimmer, A. D., Chan, E. T., Kirk, C. J., Peters, G. J., & Kruyt, F. A. 2012. Proteasome-based mechanisms of intrinsic and acquired bortezomib resistance in non-small cell lung cancer. Biochemical Pharmacology, 83(2): 207-217.

De, M., Jayarapu, K., Elenich, L., Monaco, J. J., Colbert, R. A., & Griffin, T. A. 2003. Beta 2 subunit propeptides influence cooperative proteasome assembly. The Journal of Biological Chemistry, 278(8): 6153-6159.

Dechow, T. N., Pedranzini, L., Leitch, A., Leslie, K., Gerald, W. L., Linkov, I., & Bromberg, J. F. 2004. Requirement of matrix metalloproteinase-9 for the transformation of human mammary epithelial cells by Stat3-C. Proc. Nati. Acad. Scie. USA, 101(29): 10602-10607.

Demartino, G. N., & Gillette, T. G. 2007. Proteasomes: machines for all reasons. Cell, 129(4): 659-662.

DeMartino, G. N., & Slaughter, C. A. 1999. The proteasome, a novel protease regulated by multiple mechanisms. The Journal of Biological Chemistry, 274(32): 22123-22126.

Demasi, M., Silva, G. M., & Netto, L. E. 2003. 20S proteasome from Saccharomyces cerevisiae is responsive to redox modifications and is S-glutathionylated. The Journal of Biological Chemistry, 278(1): 679-685.

Dengjel, J., Akimov, V., Blagoev, B., & Andersen, J. S. 2007. Signal transduction by growth factor receptors: signaling in an instant. Cell Cycle, 6(23): 2913-2916.

Dent, P., Haser, W., Haystead, T. A., Vincent, L. A., Roberts, T. M., & Sturgill, T. W. 1992. Activation of mitogen-activated protein kinase kinase by v-Raf in NIH 3T3 cells and in vitro. Science, 257(5075): 1404-1407.

Di Cunto, F., Topley, G., Calautti, E., Hsiao, J., Ong, L., Seth, P. K., & Dotto, G. P. 1998. Inhibitory function of p21Cip1/WAF1 in differentiation of primary mouse keratinocytes independent of cell cycle control. Science, 280(5366): 1069-1072.

Dick, L. R., Cruikshank, A. A., Destree, A. T., Grenier, L., McCormack, T. A., Melandri, F. D., Nunes, S. L., Palombella, V. J., Parent, L. A., Plamondon, L., & Stein, R. L. 1997. Mechanistic studies on the inactivation of the proteasome by lactacystin in cultured cells. The Journal of Biological Chemistry, 272(1): 182-188.

Dohmen, R. J., Willers, I., & Marques, A. J. 2007. Biting the hand that feeds: Rpn4-dependent feedback regulation of proteasome function. Biochimica Biophysica Acta, 1773(11): 1599-1604.

Emmanouilidou, E., Stefanis, L., & Vekrellis, K. 2010. Cell-produced alpha-synuclein oligomers are targeted to, and impair, the 26S proteasome. Neurobiology of Aging, 31(6): 953-968.

Endo, T. A., Masuhara, M., Yokouchi, M., Suzuki, R., Sakamoto, H., Mitsui, K., Matsumoto, A., Tanimura, S., Ohtsubo, M., Misawa, H., Miyazaki, T., Leonor, N., Taniguchi, T., Fujita, T., Kanakura, Y., Komiya, S., & Yoshimura, A. 1997. A new protein containing an SH2 domain that inhibits JAK kinases. Nature, 387(6636): 921-924.

Evteeva, I. N., Kulichkova, V. A., Mittenberg, A. G., Volkova, I. V., Ermolaeva Iu, B., Teslenko, L. V., Obukhova, A. D., Penniiainen, V. A., Gauze, L. N., & Konstantinova, I. M. 2000. Novel endoribonuclease activity of 26S-proteasomes from A-431 cells. Tsitologiia, 42(7): 675-680.

Ferdous, A., Gonzalez, F., Sun, L., Kodadek, T., & Johnston, S. A. 2001. The 19S regulatory particle of the proteasome is required for efficient transcription elongation by RNA polymerase II. Molecular Cell, 7(5): 981-991.

Firestein, G. S. 2004. NF-kappaB: Holy Grail for rheumatoid arthritis? Arthritis and Rheumatism, 50(8): 2381-2386.

Fisher, R. I., Bernstein, S. H., Kahl, B. S., Djulbegovic, B., Robertson, M. J., de Vos, S., Epner, E., Krishnan, A., Leonard, J. P., Lonial, S., Stadtmauer, E. A., O'Connor, O. A., Shi, H., Boral, A. L., & Goy, A. 2006. Multicenter phase II study of bortezomib in patients with relapsed or refractory mantle cell lymphoma. Journal of Clinical Oncology, 24(30): 4867-4874.

Frank, D. A. 2007. STAT3 as a central mediator of neoplastic cellular transformation. Cancer Letters, 251(2): 199-210.

Franke, N. E., Niewerth, D., Assaraf, Y. G., van Meerloo, J., Vojtekova, K., van Zantwijk, C. H., Zweegman, S., Chan, E. T., Kirk, C. J., Geerke, D. P., Schimmer, A. D., Kaspers, G. J., Jansen, G., & Cloos, J. 2012. Impaired bortezomib binding to mutant

beta5 subunit of the proteasome is the underlying basis for bortezomib resistance in leukemia cells. Leukemia, 26(4): 757-768.

Gan, Y., Shi, C., Inge, L., Hibner, M., Balducci, J., & Huang, Y. 2010. Differential roles of ERK and Akt pathways in regulation of EGFR-mediated signaling and motility in prostate cancer cells. Oncogene, 29(35): 4947-4958.

Gandhi, J., Zhang, J., Xie, Y., Soh, J., Shigematsu, H., Zhang, W., Yamamoto, H., Peyton, M., Girard, L., Lockwood, W. W., Lam, W. L., Varella-Garcia, M., Minna, J. D., & Gazdar, A. F. 2009. Alterations in genes of the EGFR signaling pathway and their relationship to EGFR tyrosine kinase inhibitor sensitivity in lung cancer cell lines. PLoS One, 4(2): e4576.

Gao, M., Labuda, T., Xia, Y., Gallagher, E., Fang, D., Liu, Y. C., & Karin, M. 2004. Jun turnover is controlled through JNK-dependent phosphorylation of the E3 ligase Itch. Science, 306(5694): 271-275.

Garcia, R., Yu, C. L., Hudnall, A., Catlett, R., Nelson, K. L., Smithgall, T., Fujita, D. J., Ethier, S. P., & Jove, R. 1997. Constitutive activation of Stat3 in fibroblasts transformed by diverse oncoproteins and in breast carcinoma cells. Cell Growth & Differentiation, 8(12): 1267-1276.

Gazdar, A. F., & Minna, J. D. 2008. Deregulated EGFR signaling during lung cancer progression: mutations, amplicons, and autocrine loops. Cancer Prevention Research, 1(3): 156-160.

Gillette, T. G., Gonzalez, F., Delahodde, A., Johnston, S. A., & Kodadek, T. 2004. Physical and functional association of RNA polymerase II and the proteasome. Proc. Nati. Acad. Scie. USA, 101(16): 5904-5909.

Glickman, M. H., Rubin, D. M., Coux, O., Wefes, I., Pfeifer, G., Cjeka, Z., Baumeister, W., Fried, V. A., & Finley, D. 1998. A subcomplex of the proteasome regulatory particle required for ubiquitin-conjugate degradation and related to the COP9-signalosome and eIF3. Cell, 94(5): 615-623.

Goldberg, A. L. 2003. Protein degradation and protection against misfolded or damaged proteins. Nature, 426(6968): 895-899.

Grant, S. L., Hammacher, A., Douglas, A. M., Goss, G. A., Mansfield, R. K., Heath, J. K., & Begley, C. G. 2002. An unexpected biochemical and functional interaction between gp130 and the EGF receptor family in breast cancer cells. Oncogene, 21(3): 460-474.

Groettrup, M., van den Broek, M., Schwarz, K., Macagno, A., Khan, S., de Giuli, R., & Schmidtke, G. 2001. Structural plasticity of the proteasome and its function in antigen processing. Critical Reviews in Immunology, 21(4): 339-358.

Groll, M., Ditzel, L., Lowe, J., Stock, D., Bochtler, M., Bartunik, H. D., & Huber, R. 1997. Structure of 20S proteasome from yeast at 2.4 A resolution. Nature, 386(6624): 463-471.

Groll, M., Gotz, M., Kaiser, M., Weyher, E., & Moroder, L. 2006. TMC-95-based inhibitor design provides evidence for the catalytic versatility of the proteasome. Chemistry & Biology, 13(6): 607-614.

Groll, M., Nazif, T., Huber, R., & Bogyo, M. 2002. Probing structural determinants distal to the site of hydrolysis that control substrate specificity of the 20S proteasome. Chemistry & Biology, 9(5): 655-662.

Haas, A. L., Warms, J. V., Hershko, A., & Rose, I. A. 1982. Ubiquitin-activating enzyme. Mechanism and role in protein-ubiquitin conjugation. The Journal of Biological Chemistry, 257(5): 2543-2548.

Hahn, J. S., Neef, D. W., & Thiele, D. J. 2006. A stress regulatory network for co-ordinated activation of proteasome expression mediated by yeast heat shock transcription factor. Molecular Microbiology, 60(1): 240-251.

Han, Y., Amin, H. M., Franko, B., Frantz, C., Shi, X., & Lai, R. 2006. Loss of SHP1 enhances JAK3/STAT3 signaling and decreases proteosome degradation of JAK3 and NPM-ALK in ALK+ anaplastic large-cell lymphoma. Blood, 108(8): 2796-2803.

Hanna, J., & Finley, D. 2007. A proteasome for all occasions. FEBS Letters, 581(15): 2854-2861.

Hartenstein, B., Teurich, S., Hess, J., Schenkel, J., Schorpp-Kistner, M., & Angel, P. 2002. Th2 cell-specific cytokine expression and allergen-induced airway inflammation depend on JunB. The EMBO Journal, 21(23): 6321-6329.

He, T. C., Sparks, A. B., Rago, C., Hermeking, H., Zawel, L., da Costa, L. T., Morin, P. J., Vogelstein, B., & Kinzler, K. W. 1998. Identification of c-MYC as a target of the APC pathway. Science, 281(5382): 1509-1512.

Heinemeyer, W., Fischer, M., Krimmer, T., Stachon, U., & Wolf, D. H. 1997. The active sites of the eukaryotic 20 S proteasome and their involvement in subunit precursor processing. The Journal of Biological Chemistry, 272(40): 25200-25209.

Herrmann, A., Vogt, M., Monnigmann, M., Clahsen, T., Sommer, U., Haan, S., Poli, V., Heinrich, P. C., & Muller-Newen, G. 2007. Nucleocytoplasmic shuttling of persistently activated STAT3. Journal of Cell Science, 120(Pt 18): 3249-3261.

Hirano, Y., Hendil, K. B., Yashiroda, H., Iemura, S., Nagane, R., Hioki, Y., Natsume, T., Tanaka, K., & Murata, S. 2005. A heterodimeric complex that promotes the assembly of mammalian 20S proteasomes. Nature, 437(7063): 1381-1385.

Hirano, Y., Kaneko, T., Okamoto, K., Bai, M., Yashiroda, H., Furuyama, K., Kato, K., Tanaka, K., & Murata, S. 2008. Dissecting beta-ring assembly pathway of the mammalian 20S proteasome. The EMBO Journal, 27(16): 2204-2213.

Hofmann, R. M., & Pickart, C. M. 1999. Noncanonical MMS2-encoded ubiquitin-conjugating enzyme functions in assembly of novel polyubiquitin chains for DNA repair. Cell, 96(5): 645-653.

Hu, M., Li, P., Song, L., Jeffrey, P. D., Chenova, T. A., Wilkinson, K. D., Cohen, R. E., & Shi, Y. 2005a. Structure and mechanisms of the proteasome-associated deubiquitinating enzyme USP14. The EMBO Journal, 24(21): 3747-3756.

Hubbard, S. R. 2009. The juxtamembrane region of EGFR takes center stage. Cell, 137(7): 1181-1183.

Husnjak, K., Elsasser, S., Zhang, N., Chen, X., Randles, L., Shi, Y., Hofmann, K., Walters, K. J., Finley, D., & Dikic, I. 2008. Proteasome subunit Rpn13 is a novel ubiquitin receptor. Nature, 453(7194): 481-488.

Husvik, C., Bryne, M., & Halstensen, T. S. 2009. Epidermal growth factor-induced cyclooxygenase-2 expression in oral squamous cell carcinoma cell lines is mediated through extracellular signal-regulated kinase 1/2 and p38 but is Src and nuclear factor-kappa B independent. European journal of oral sciences, 117(5): 528-535.

Ihle, J. N. 1996. STATs: signal transducers and activators of transcription. Cell, 84(3): 331-334.

Iliopoulos, O., Levy, A. P., Jiang, C., Kaelin, W. G., Jr., & Goldberg, M. A. 1996. Negative regulation of hypoxia-inducible genes by the von Hippel-Lindau protein. Proc. Nati. Acad. Scie. USA, 93(20): 10595-10599.

Imai, J., Maruya, M., Yashiroda, H., Yahara, I., & Tanaka, K. 2003. The molecular chaperone Hsp90 plays a role in the assembly and maintenance of the 26S proteasome. The EMBO Journal, 22(14): 3557-3567.

Itoh, K., Chiba, T., Takahashi, S., Ishii, T., Igarashi, K., Katoh, Y., Oyake, T., Hayashi, N., Satoh, K., Hatayama, I., Yamamoto, M., & Nabeshima, Y. 1997. An Nrf2/small Maf heterodimer mediates the induction of phase II detoxifying enzyme genes through antioxidant response elements. Biochem. Biophys. Rese.Commu, 236(2): 313-322.

Itoh, K., Igarashi, K., Hayashi, N., Nishizawa, M., & Yamamoto, M. 1995. Cloning and characterization of a novel erythroid cell-derived CNC family transcription factor heterodimerizing with the small Maf family proteins. Molecular and Cellular Biology, 15(8): 4184-4193.

Itoh, M., Murata, T., Suzuki, T., Shindoh, M., Nakajima, K., Imai, K., & Yoshida, K. 2006. Requirement of STAT3 activation for maximal collagenase-1 (MMP-1) induction by epidermal growth factor and malignant characteristics in T24 bladder cancer cells. Oncogene, 25(8): 1195-1204.

Ivanov, V. N., Bhoumik, A., Krasilnikov, M., Raz, R., Owen-Schaub, L. B., Levy, D., Horvath, C. M., & Ronai, Z. 2001. Cooperation between STAT3 and c-jun suppresses Fas transcription. Molecular Cell, 7(3): 517-528.

Iwamaru, A., Szymanski, S., Iwado, E., Aoki, H., Yokoyama, T., Fokt, I., Hess, K., Conrad, C., Madden, T., Sawaya, R., Kondo, S., Priebe, W., & Kondo, Y. 2007. A novel inhibitor of the STAT3 pathway induces apoptosis in malignant glioma cells both in vitro and in vivo. Oncogene, 26(17): 2435-2444.

Jaakkola, P., Mole, D. R., Tian, Y. M., Wilson, M. I., Gielbert, J., Gaskell, S. J., von Kriegsheim, A., Hebestreit, H. F., Mukherji, M., Schofield, C. J., Maxwell, P. H., Pugh, C. W., & Ratcliffe, P. J. 2001. Targeting of HIF-alpha to the von Hippel-Lindau ubiquitylation complex by O2-regulated prolyl hydroxylation. Science, 292(5516): 468-472.

Jain, N., Zhang, T., Kee, W. H., Li, W., & Cao, X. 1999. Protein kinase C delta associates with and phosphorylates Stat3 in an interleukin-6-dependent manner. The Journal of Biological Chemistry, 274(34): 24392-24400.

Johnsen, O., Murphy, P., Prydz, H., & Kolsto, A. B. 1998. Interaction of the CNC-bZIP factor TCF11/LCR-F1/Nrf1 with MafG: binding-site selection and regulation of transcription. Nucleic Acids Research, 26(2): 512-520.

Johnsen, O., Skammelsrud, N., Luna, L., Nishizawa, M., Prydz, H., & Kolsto, A. B. 1996. Small Maf proteins interact with the human transcription factor TCF11/Nrf1/LCR-F1. Nucleic Acids Research, 24(21): 4289-4297.

Josefsberg, L. B., Galiani, D., Dantes, A., Amsterdam, A., & Dekel, N. 2000. The proteasome is involved in the first metaphase-to-anaphase transition of meiosis in rat oocytes. Biology of reproduction, 62(5): 1270-1277.

Josefsberg, L. B., Kaufman, O., Galiani, D., Kovo, M., & Dekel, N. 2001. Inactivation of M-phase promoting factor at exit from first embryonic mitosis in the rat is independent of cyclin B1 degradation. Biology of reproduction, 64(3): 871-878.

Ju, D., Wang, L., Mao, X., & Xie, Y. 2004. Homeostatic regulation of the proteasome via an Rpn4-dependent feedback circuit. Biochem. Biophys. Rese.Commu, 321(1): 51-57.

Jura, N., Endres, N. F., Engel, K., Deindl, S., Das, R., Lamers, M. H., Wemmer, D. E., Zhang, X., & Kuriyan, J. 2009. Mechanism for activation of the EGF receptor catalytic domain by the juxtamembrane segment. Cell, 137(7): 1293-1307.

Karni, R., Jove, R., & Levitzki, A. 1999. Inhibition of pp60c-Src reduces Bcl-XL expression and reverses the transformed phenotype of cells overexpressing EGF and HER-2 receptors. Oncogene, 18(33): 4654-4662.

Kawahara, A., & Dawid, I. B. 2000. Expression of the Kruppel-like zinc finger gene biklf during zebrafish development. Mechanisms of development, 97(1-2): 173-176.

Kersting, C., Agelopoulos, K., Schmidt, H., Korsching, E., August, C., Gosheger, G., Dirksen, U., Juergens, H., Winkelmann, W., Brandt, B., Bielack, S., Buerger, H., & Gebert, C. 2008. Biological importance of a polymorphic CA sequence within intron 1 of the epidermal growth factor receptor gene (EGFR) in high grade central osteosarcomas. Genes, chromosomes & cancer, 47(8): 657-664.

Kil, S. J., & Carlin, C. 2000. EGF receptor residues leu(679), leu(680) mediate selective sorting of ligand-receptor complexes in early endosomal compartments. Journal of Cellular Physiology, 185(1): 47-60.

Kim, A., Park, S., Lee, J. E., Jang, W. S., Lee, S. J., Kang, H. J., & Lee, S. S. 2012. The dual PI3K and mTOR inhibitor NVP-BEZ235 exhibits anti-proliferative activity and overcomes bortezomib resistance in mantle cell lymphoma cells. Leukemia Research, 36(7): 912-920.

Kinyamu, H. K., & Archer, T. K. 2007. Proteasome activity modulates chromatin modifications and RNA polymerase II phosphorylation to enhance glucocorticoid receptor-mediated transcription. Molecular and Cellular Biology, 27(13): 4891-4904.

Kisselev, A. F., & Goldberg, A. L. 2001. Proteasome inhibitors: from research tools to drug candidates. Chemistry & Biology, 8(8): 739-758.

Kisselev, A. F., Callard, A., & Goldberg, A. L. 2006. Importance of the different proteolytic sites of the proteasome and the efficacy of inhibitors varies with the protein substrate. The Journal of Biological Chemistry, 281(13): 8582-8590.

Kisselev, A. F., Songyang, Z., & Goldberg, A. L. 2000. Why does threonine, and not serine, function as the active site nucleophile in proteasomes? The Journal of Biological Chemistry, 275(20): 14831-14837.

Kisselev, A. F., van der Linden, W. A., & Overkleeft, H. S. 2012. Proteasome inhibitors: an expanding army attacking a unique target. Chemistry & Biology, 19(1): 99-115.

Kiuchi, N., Nakajima, K., Ichiba, M., Fukada, T., Narimatsu, M., Mizuno, K., Hibi, M., & Hirano, T. 1999. STAT3 is required for the gp130-mediated full activation of the c-myc gene. The Journal of experimental medicine, 189(1): 63-73.

Kloetzel, P. M. 2001. Antigen processing by the proteasome. Nature Reviews. Molecular Cell biology, 2(3): 179-187.

Kojima, H., Sasaki, T., Ishitani, T., Iemura, S., Zhao, H., Kaneko, S., Kunimoto, H., Natsume, T., Matsumoto, K., & Nakajima, K. 2005. STAT3 regulates Nemo-like kinase by mediating its interaction with IL-6-stimulated TGFbeta-activated kinase 1 for STAT3 Ser-727 phosphorylation. Proc. Nati. Acad. Scie. USA, 102(12): 4524-4529.

Kotha, A., Sekharam, M., Cilenti, L., Siddiquee, K., Khaled, A., Zervos, A. S., Carter, B., Turkson, J., & Jove, R. 2006. Resveratrol inhibits Src and Stat3 signaling and induces the apoptosis of malignant cells containing activated Stat3 protein. Mol. Can. Ther, 5(3): 621-629.

Kraft, D. C., Deocaris, C. C., Wadhwa, R., & Rattan, S. I. 2006. Preincubation with the proteasome inhibitor MG-132 enhances proteasome activity via the Nrf2 transcription factor in aging human skin fibroblasts. Annals of the New York Academy of Sciences, 1067: 420-424.

Kraus, M., Ruckrich, T., Reich, M., Gogel, J., Beck, A., Kammer, W., Berkers, C. R., Burg, D., Overkleeft, H., Ovaa, H., & Driessen, C. 2007. Activity patterns of proteasome subunits reflect bortezomib sensitivity of hematologic malignancies and are variable in primary human leukemia cells. Leukemia, 21(1): 84-92.

Krogan, N. J., Lam, M. H., Fillingham, J., Keogh, M. C., Gebbia, M., Li, J., Datta, N., Cagney, G., Buratowski, S., Emili, A., & Greenblatt, J. F. 2004. Proteasome involvement in the repair of DNA double-strand breaks. Molecular Cell, 16(6): 1027-1034.

Kumatori, A., Tanaka, K., Inamura, N., Sone, S., Ogura, T., Matsumoto, T., Tachikawa, T., Shin, S., & Ichihara, A. 1990. Abnormally high expression of proteasomes in human leukemic cells. Proc. Nati. Acad. Scie. USA, 87(18): 7071-7075.

Kupperman, E., Lee, E. C., Cao, Y., Bannerman, B., Fitzgerald, M., Berger, A., Yu, J., Yang, Y., Hales, P., Bruzzese, F., Liu, J., Blank, J., Garcia, K., Tsu, C., Dick, L., Fleming, P., Yu, L., Manfredi, M., Rolfe, M., & Bolen, J. 2010. Evaluation of the proteasome inhibitor MLN9708 in preclinical models of human cancer. Cancer Research, 70(5): 1970-1980.

Kwak, M. K., & Kensler, T. W. 2006. Induction of 26S proteasome subunit PSMB5 by the bifunctional inducer 3-methylcholanthrene through the Nrf2-ARE, but not the AhR/Arnt-XRE, pathway. Biochem. Biophys. Rese.Commu, 345(4): 1350-1357.

Kwak, M. K., Wakabayashi, N., Greenlaw, J. L., Yamamoto, M., & Kensler, T. W. 2003. Antioxidants enhance mammalian proteasome expression through the Keap1-Nrf2 signaling pathway. Molecular and Cellular Biology, 23(23): 8786-8794.

Kyriakis, J. M., App, H., Zhang, X. F., Banerjee, P., Brautigan, D. L., Rapp, U. R., & Avruch, J. 1992. Raf-1 activates MAP kinase-kinase. Nature, 358(6385): 417-421.

Lam, Y. A., Lawson, T. G., Velayutham, M., Zweier, J. L., & Pickart, C. M. 2002. A proteasomal ATPase subunit recognizes the polyubiquitin degradation signal. Nature, 416(6882): 763-767.

Lecomte S, Desmots F, Le Masson F, Le Goff P, Michel D, Christians ES & Le Dréan Y. 2010. Roles of heat shock factor 1 and 2 in response to proteasome inhibition: consequence on p53 stability. Oncogene, 2010 Jul 22;(29):4216-4224

Lee CS., Ho DV., & Chan JY.2013. Nuclear factor-erythroid 2-related factor 1 regulates expression of proteasome genes in hepatocytes and protects against endoplasmic reticulum stress and steatosis in mice. FEBS J. 280:3609–3620.

Lee, C. S., Lee, C., Hu, T., Nguyen, J. M., Zhang, J., Martin, M. V., Vawter, M. P., Huang, E. J., & Chan, J. Y. 2011. Loss of nuclear factor E2-related factor 1 in the brain leads to dysregulation of proteasome gene expression and neurodegeneration. Proc. Nati. Acad. Scie. USA, 108(20): 8408-8413.

Leung-Hagesteijn, C., Erdmann, N., Cheung, G., Keats, J. J., Stewart, A. K., Reece, D. E., Chung, K. C., & Tiedemann, R. E. 2013. Xbp1s-negative tumor B cells and pre-plasmablasts mediate therapeutic proteasome inhibitor resistance in multiple myeloma. Cancer Cell, 24(3): 289-304.

Li, C., Zang, Y., Sen, M., Leeman-Neill, R. J., Man, D. S., Grandis, J. R., & Johnson, D. E. 2009. Bortezomib up-regulates activated signal transducer and activator of transcription-3 and synergizes with inhibitors of signal transducer and activator of transcription-3 to promote head and neck squamous cell carcinoma cell death. Mol. Can. Ther, 8(8): 2211-2220.

Li, X., Kusmierczyk, A. R., Wong, P., Emili, A., & Hochstrasser, M. 2007. beta-Subunit appendages promote 20S proteasome assembly by overcoming an Ump1-dependent checkpoint. The EMBO Journal, 26(9): 2339-2349.

Li, X., Lonard, D. M., Jung, S. Y., Malovannaya, A., Feng, Q., Qin, J., Tsai, S. Y., Tsai, M. J., & O'Malley, B. W. 2006. The SRC-3/AIB1 coactivator is degraded in a ubiquitin- and ATP-independent manner by the REGgamma proteasome. Cell, 124(2): 381-392.

Liang, H., Venema, V. J., Wang, X., Ju, H., Venema, R. C., & Marrero, M. B. 1999. Regulation of angiotensin II-induced phosphorylation of STAT3 in vascular smooth muscle cells. The Journal of Biological Chemistry, 274(28): 19846-19851.

Liang, J., Zubovitz, J., Petrocelli, T., Kotchetkov, R., Connor, M. K., Han, K., Lee, J. H., Ciarallo, S., Catzavelos, C., Beniston, R., Franssen, E., & Slingerland, J. M. 2002. PKB/Akt phosphorylates p27, impairs nuclear import of p27 and opposes p27-mediated G1 arrest. Nature Medicine, 8(10): 1153-1160.

Lichter, D. I., Danaee, H., Pickard, M. D., Tayber, O., Sintchak, M., Shi, H., Richardson, P. G., Cavenagh, J., Blade, J., Facon, T., Niesvizky, R., Alsina, M., Dalton, W., Sonneveld, P., Lonial, S., van de Velde, H., Ricci, D., Esseltine, D. L., Trepicchio, W. L., Mulligan, G., & Anderson, K. C. 2012. Sequence analysis of beta-subunit genes of the 20S proteasome in patients with relapsed multiple myeloma treated with bortezomib or dexamethasone. Blood, 120(23): 4513-4516.

Lipford, J. R., Smith, G. T., Chi, Y., & Deshaies, R. J. 2005. A putative stimulatory role for activator turnover in gene expression. Nature, 438(7064): 113-116.

Liu, C. W., Corboy, M. J., DeMartino, G. N., & Thomas, P. J. 2003a. Endoproteolytic activity of the proteasome. Science, 299(5605): 408-411.

Liu, C. W., Li, X., Thompson, D., Wooding, K., Chang, T. L., Tang, Z., Yu, H., Thomas, P. J., & DeMartino, G. N. 2006. ATP binding and ATP hydrolysis play distinct roles in the function of 26S proteasome. Molecular Cell, 24(1): 39-50.

Liu, G., Rogers, J., Murphy, C. T., & Rongo, C. 2011. EGF signalling activates the ubiquitin proteasome system to modulate C. elegans lifespan. The EMBO Journal, 30(15): 2990-3003.

Liu, H., Ma, Y., Cole, S. M., Zander, C., Chen, K. H., Karras, J., & Pope, R. M. 2003b. Serine phosphorylation of STAT3 is essential for Mcl-1 expression and macrophage survival. Blood, 102(1): 344-352.

Liu, J. J., Chao, J. R., Jiang, M. C., Ng, S. Y., Yen, J. J., & Yang-Yen, H. F. 1995. Ras transformation results in an elevated level of cyclin D1 and acceleration of G1 progression in NIH 3T3 cells. Molecular and Cellular Biology, 15(7): 3654-3663.

Lo, H. W. 2010. Nuclear mode of the EGFR signaling network: biology, prognostic value, and therapeutic implications. Discovery medicine, 10(50): 44-51.

Lo, H. W., Ali-Seyed, M., Wu, Y., Bartholomeusz, G., Hsu, S. C., & Hung, M. C. 2006a. Nuclear-cytoplasmic transport of EGFR involves receptor endocytosis, importin beta1 and CRM1. Journal of cellular biochemistry, 98(6): 1570-1583.

Loda, M., Cukor, B., Tam, S. W., Lavin, P., Fiorentino, M., Draetta, G. F., Jessup, J. M., & Pagano, M. 1997. Increased proteasome-dependent degradation of the cyclin-dependent kinase inhibitor p27 in aggressive colorectal carcinomas. Nature Medicine, 3(2): 231-234.

Lorick, K. L., Jensen, J. P., Fang, S., Ong, A. M., Hatakeyama, S., & Weissman, A. M. 1999. RING fingers mediate ubiquitin-conjugating enzyme (E2)-dependent ubiquitination. Proc. Nati. Acad. Scie. USA, 96(20): 11364-11369.

Lu, S. Q., Yang, J. M., Huang, C. M., Xu, X. Q., Zhou, H., Song, N. X., & Wang, J. M. 2011. Comparison of protein expression profiles between bortezomib-resistant JurkatB cells with PSMB5 mutation and their parent cells. Journal of experimental hematology / Chinese Association of Pathophysiology, 19(4): 869-873.

Lu, S., Yang, J., Chen, Z., Gong, S., Zhou, H., Xu, X., & Wang, J. 2009. Different mutants of PSMB5 confer varying bortezomib resistance in T lymphoblastic lymphoma/leukemia cells derived from the Jurkat cell line. Experimental hematology, 37(7): 831-837.

Lu, S., Yang, J., Song, X., Gong, S., Zhou, H., Guo, L., Song, N., Bao, X., Chen, P., & Wang, J. 2008. Point mutation of the proteasome beta5 subunit gene is an important mechanism of bortezomib resistance in bortezomib-selected variants of Jurkat T cell lymphoblastic lymphoma/leukemia line. The Journal of pharmacology and experimental therapeutics, 326(2): 423-431.

Lundgren, J., Masson, P., Mirzaei, Z., & Young, P. 2005. Identification and characterization of a Drosophila proteasome regulatory network. Molecular and Cellular Biology, 25(11): 4662-4675.

Madhurima Biswas and Jefferson Y Chan. 2010. Role of Nrf1 in antioxidant response element- mediated gene expression and beyond. Toxicol Appl Pharmacol. 2010 April 1; 244(1): 16–20

Mahboubi, K., Li, F., Plescia, J., Kirkiles-Smith, N. C., Mesri, M., Du, Y., Carroll, J. M., Elias, J. A., Altieri, D. C., & Pober, J. S. 2001. Interleukin-11 up-regulates survivin expression in endothelial cells through a signal transducer and activator of transcription-3 pathway. Laboratory investigation, 81(3): 327-334.

Mannhaupt, G., Schnall, R., Karpov, V., Vetter, I., & Feldmann, H. 1999. Rpn4p acts as a transcription factor by binding to PACE, a nonamer box found upstream of 26S proteasomal and other genes in yeast. FEBS Letters, 450(1-2): 27-34.

Marmor, M. D., Skaria, K. B., & Yarden, Y. 2004. Signal transduction and oncogenesis by ErbB/HER receptors. International journal of radiation oncology, biology, physics, 58(3): 903-913.

Marques, A. J., Glanemann, C., Ramos, P. C., & Dohmen, R. J. 2007. The C-terminal extension of the beta7 subunit and activator complexes stabilize nascent 20S proteasomes and promote their maturation. The Journal of Biological Chemistry, 282(48): 34869-34876.

Masuda, M., Toh, S., Koike, K., Kuratomi, Y., Suzui, M., Deguchi, A., Komiyama, S., & Weinstein, I. B. 2002. The roles of JNK1 and Stat3 in the response of head and neck cancer cell lines to combined treatment with all-trans-retinoic acid and 5-fluorouracil. Japanese Journal of Cancer Research, 93(3): 329-339.

McConkey, D. J., & Zhu, K. 2008. Mechanisms of proteasome inhibitor action and resistance in cancer. Drug resistance updates, 11(4-5): 164-179.

Meiners, S., Heyken, D., Weller, A., Ludwig, A., Stangl, K., Kloetzel, P. M., & Kruger, E. 2003. Inhibition of proteasome activity induces concerted expression of proteasome genes and de novo formation of Mammalian proteasomes. The Journal of Biological Chemistry, 278(24): 21517-21525.

Minamoto, S., Ikegame, K., Ueno, K., Narazaki, M., Naka, T., Yamamoto, H., Matsumoto, T., Saito, H., Hosoe, S., & Kishimoto, T. 1997. Cloning and functional analysis of new members of STAT induced STAT inhibitor (SSI) family: SSI-2 and SSI-3. Biochem. Biophys. Rese.Commu, 237(1): 79-83.

Mittenberg, A. G., Kulichkova, V. A., Gauze, L. N., & Konstantinova, I. M. 2002. Properties of endoribonuclease activity of proteasomes from K562 cells. III. The specific endonuclease activity of ribonucleoprotein particles (alpha-RNP) tightly bound to chromatin and containing 20S proteosomes. Tsitologiia, 44(4): 364-368.

Mittenberg, A. G., Moiseeva, T. N., Pugacheva, I. V., Kulichkova, V. A., Tsimokha, A. S., Gauze, L. N., & Konstantinova, I. M. 2007.Regulation of the 26S proteasome's endoribonuclease activity specificity in k562 cells under effect of differentiation and apoptosis inductors. Tsitologiia, 49(2): 142-148.

Miyoshi, Y., Nagase, H., Ando, H., Horii, A., Ichii, S., Nakatsuru, S., Aoki, T., Miki, Y., Mori, T., & Nakamura, Y. 1992. Somatic mutations of the APC gene in colorectal tumors: mutation cluster region in the APC gene. Human Molecular Genetics, 1(4): 229-233.

Mizoguchi, M., Betensky, R. A., Batchelor, T. T., Bernay, D. C., Louis, D. N., & Nutt, C. L. 2006. Activation of STAT3, MAPK, and AKT in malignant astrocytic gliomas: correlation with EGFR status, tumor grade, and survival. Journal of neuropathology and Experimental Neurology, 65(12): 1181-1188.

Moller, M. B. 2000. P27 in cell cycle control and cancer. Leukemia & lymphoma, 39(1-2): 19-27.

Momand, J., Jung, D., Wilczynski, S., & Niland, J. 1998. The MDM2 gene amplification database. Nucleic Acids Research, 26(15): 3453-3459.

Mora, L. B., Buettner, R., Seigne, J., Diaz, J., Ahmad, N., Garcia, R., Bowman, T., Falcone, R., Fairclough, R., Cantor, A., Muro-Cacho, C., Livingston, S., Karras, J., Pow-Sang, J., & Jove, R. 2002. Constitutive activation of Stat3 in human prostate tumors and cell lines: direct inhibition of Stat3 signaling induces apoptosis of prostate cancer cells. Cancer Research, 62(22): 6659-6666.

Morandell, S., Stasyk, T., Skvortsov, S., Ascher, S., & Huber, L. A. 2008. Quantitative proteomics and phosphoproteomics reveal novel insights into complexity and dynamics of the EGFR signaling network. Proteomics, 8(21): 4383-4401.

Motohashi, H., & Yamamoto, M. 2004. Nrf2-Keap1 defines a physiologically important stress response mechanism. Trends in Molecular Medicine, 10(11): 549-557.

Murata, S., Sasaki, K., Kishimoto, T., Niwa, S., Hayashi, H., Takahama, Y., & Tanaka, K. 2007. Regulation of CD8+ T cell development by thymus-specific proteasomes. Science, 316(5829): 1349-1353.

Murata, S., Takahama, Y., & Tanaka, K. 2008. Thymoproteasome: probable role in generating positively selecting peptides. Current Opinion in Immunology, 20(2): 192-196.

Murata, S., Yashiroda, H., & Tanaka, K. 2009. Molecular mechanisms of proteasome assembly. Nature Reviews. Molecular Cell biology, 10(2): 104-115.

Myhrstad, M. C., Husberg, C., Murphy, P., Nordstrom, O., Blomhoff, R., Moskaug, J. O., & Kolsto, A. B. 2001. TCF11/Nrf1 overexpression increases the intracellular glutathione level and can transactivate the gamma-glutamylcysteine synthetase (GCS) heavy subunit promoter. Biochimica Biophysica Acta, 1517(2): 212-219.

Naviglio, S., Di Gesto, D., Illiano, F., Chiosi, E., Giordano, A., Illiano, G., & Spina, A. 2010. Leptin potentiates antiproliferative action of cAMP elevation via protein kinase A down-regulation in breast cancer cells. Journal of Cellular Physiology, 225(3): 801-809.

Nederlof, P. M., Wang, H. R., & Baumeister, W. 1995. Nuclear localization signals of human and Thermoplasma proteasomal alpha subunits are functional in vitro. Proc. Nati. Acad. Scie. USA, 92(26): 12060-12064.

Negishi, Y., Ui, N., Nakajima, M., Kawashima, K., Maruyama, K., Takizawa, T., & Endo, H. 2001. p21Cip-1/SDI-1/WAF-1 gene is involved in chondrogenic differentiation of ATDC5 cells in vitro. The Journal of Biological Chemistry, 276(35): 33249-33256.

Nguyen, D. X., Bos, P. D., & Massague, J. 2009. Metastasis: from dissemination to organ-specific colonization. Nature Reviews. Cancer, 9(4): 274-284.

Nicholson, K. M., & Anderson, N. G. 2002. The protein kinase B/Akt signalling pathway in human malignancy. Cellular Signalling, 14(5): 381-395.

Nicola, N. A., Nicholson, S. E., Metcalf, D., Zhang, J. G., Baca, M., Farley, A., Willson, T. A., Starr, R., Alexander, W., & Hilton, D. J. 1999. Negative regulation of cytokine signaling by the SOCS proteins. Cold Spring Harbor Symposia on Quantitative Biology, 64: 397-404.

Niu, G., Wright, K. L., Huang, M., Song, L., Haura, E., Turkson, J., Zhang, S., Wang, T., Sinibaldi, D., Coppola, D., Heller, R., Ellis, L. M., Karras, J., Bromberg, J., Pardoll, D., Jove, R., & Yu, H. 2002. Constitutive Stat3 activity up-regulates VEGF expression and tumor angiogenesis. Oncogene, 21(13): 2000-2008.

Niu, G., Wright, K. L., Ma, Y., Wright, G. M., Huang, M., Irby, R., Briggs, J., Karras, J., Cress, W. D., Pardoll, D., Jove, R., Chen, J., & Yu, H. 2005. Role of Stat3 in regulating p53 expression and function. Molecular and Cellular Biology, 25(17): 7432-7440.

Nyati, M. K., Morgan, M. A., Feng, F. Y., & Lawrence, T. S. 2006. Integration of EGFR inhibitors with radiochemotherapy. Nature Reviews. Cancer, 6(11): 876-885.

Oerlemans, R., Franke, N. E., Assaraf, Y. G., Cloos, J., van Zantwijk, I., Berkers, C. R., Scheffer, G. L., Debipersad, K., Vojtekova, K., Lemos, C., van der Heijden, J. W., Ylstra, B., Peters, G. J., Kaspers, G. L., Dijkmans, B. A., Scheper, R. J., & Jansen, G. 2008. Molecular basis of bortezomib resistance: proteasome subunit beta5 (PSMB5) gene mutation and overexpression of PSMB5 protein. Blood, 112(6): 2489-2499.

Orlowski, M., Cardozo, C., & Michaud, C. 1993. Evidence for the presence of five distinct proteolytic components in the pituitary multicatalytic proteinase complex. Properties of two components cleaving bonds on the carboxyl side of branched chain and small neutral amino acids. Biochemistry, 32(6): 1563-1572.

Oved, S., & Yarden, Y. 2002. Signal transduction: molecular ticket to enter cells. Nature, 416(6877): 133-136.

Pagano, M., Tam, S. W., Theodoras, A. M., Beer-Romero, P., Del Sal, G., Chau, V., Yew, P. R., Draetta, G. F., & Rolfe, M. 1995. Role of the ubiquitin-proteasome pathway in regulating abundance of the cyclin-dependent kinase inhibitor p27. Science, 269(5224): 682-685.

Papaiahgari, S., Yerrapureddy, A., Hassoun, P. M., Garcia, J. G., Birukov, K. G., & Reddy, S. P. 2007. EGFR-activated signaling and actin remodeling regulate cyclic stretch-induced NRF2-ARE activation. American Journal of Respiratory Cell and Molecular Biology, 36(3): 304-312.

Patterson, S. G., Wei, S., Chen, X., Sallman, D. A., Gilvary, D. L., Zhong, B., Pow-Sang, J., Yeatman, T., & Djeu, J. Y. 2006. Novel role of Stat1 in the development of docetaxel resistance in prostate tumor cells. Oncogene, 25(45): 6113-6122.

Petit, F., Jarrousse, A. S., Boissonnet, G., Dadet, M. H., Buri, J., Briand, Y., & Schmid, H. P. 1997. Proteasome (prosome) associated endonuclease activity. Molecular Biology Reports, 24(1-2): 113-117.

Piva, R., Ruggeri, B., Williams, M., Costa, G., Tamagno, I., Ferrero, D., Giai, V., Coscia, M., Peola, S., Massaia, M., Pezzoni, G., Allievi, C., Pescalli, N., Cassin, M., di Giovine, S., Nicoli, P., de Feudis, P., Strepponi, I., Roato, I., Ferracini, R., Bussolati, B., Camussi, G., Jones-Bolin, S., Hunter, K., Zhao, H., Neri, A., Palumbo, A., Berkers, C., Ovaa, H., Bernareggi, A., & Inghirami, G. 2008. CEP-18770: A novel, orally active proteasome inhibitor with a tumor-selective pharmacologic profile competitive with bortezomib. Blood, 111(5): 2765-2775.

Politou, M., Karadimitris, A., Terpos, E., Kotsianidis, I., Apperley, J. F., & Rahemtulla, A. 2006. No evidence of mutations of the PSMB5 (beta-5 subunit of proteasome) in a case of myeloma with clinical resistance to Bortezomib. Leukemia Research, 30(2): 240-241.

Powell, S. M., Zilz, N., Beazer-Barclay, Y., Bryan, T. M., Hamilton, S. R., Thibodeau, S. N., Vogelstein, B., & Kinzler, K. W. 1992. APC mutations occur early during colorectal tumorigenesis. Nature, 359(6392): 235-237.

Que, W., Chen, J., Chuang, M., & Jiang, D. 2012. Knockdown of c-Met enhances sensitivity to bortezomib in human multiple myeloma U266 cells via inhibiting Akt/mTOR activity. APMIS, 120(3): 195-203.

Rabl, J., Smith, D. M., Yu, Y., Chang, S. C., Goldberg, A. L., & Cheng, Y. 2008. Mechanism of gate opening in the 20S proteasome by the proteasomal ATPases. Molecular Cell, 30(3): 360-368.

Radha, V., Nambirajan, S., & Swarup, G. 1994. Subcellular localization of a protein-tyrosine phosphatase: evidence for association with chromatin. The Biochemical Journal, 299 (Pt 1): 41-47.

Radhakrishnan, S. K., Lee, C. S., Young, P., Beskow, A., Chan, J. Y., & Deshaies, R. J. 2010. Transcription factor Nrf1 mediates the proteasome recovery pathway after proteasome inhibition in mammalian cells. Molecular Cell, 38(1): 17-28.

Ramos, P. C., Hockendorff, J., Johnson, E. S., Varshavsky, A., & Dohmen, R. J. 1998. Ump1p is required for proper maturation of the 20S proteasome and becomes its substrate upon completion of the assembly. Cell, 92(4): 489-499.

Rape, M., & Jentsch, S. 2004. Productive RUPture: activation of transcription factors by proteasomal processing. Biochimica Biophysica Acta, 1695(1-3): 209-213.

Rechsteiner, M., Realini, C., & Ustrell, V. 2000. The proteasome activator 11 S REG (PA28) and class I antigen presentation. The Biochemical Journal, 345 Pt 1: 1-15.

Reid, J., & Svejstrup, J. Q. 2004. DNA damage-induced Def1-RNA polymerase II interaction and Def1 requirement for polymerase ubiquitylation in vitro. The Journal of Biological Chemistry, 279(29): 29875-29878.

Ren, S., Smith, M. J., Louro, I. D., McKie-Bell, P., Bani, M. R., Wagner, M., Zochodne, B., Redden, D. T., Grizzle, W. E., Wang, N., Smith, D. I., Herbst, R. A., Bardenheuer, W., Opalka, B., Schutte, J., Trent, J. M., Ben-David, Y., & Ruppert, J. M. 2000. The p44S10 locus, encoding a subunit of the proteasome regulatory particle, is amplified during progression of cutaneous malignant melanoma. Oncogene, 19(11): 1419-1427.

Reverte, C. G., Ahearn, M. D., & Hake, L. E. 2001. CPEB degradation during Xenopus oocyte maturation requires a PEST domain and the 26S proteasome. Developmental Biology, 231(2): 447-458.

Ri, M., Iida, S., Nakashima, T., Miyazaki, H., Mori, F., Ito, A., Inagaki, A., Kusumoto, S., Ishida, T., Komatsu, H., Shiotsu, Y., & Ueda, R. 2010. Bortezomib-resistant myeloma cell lines: a role for mutated PSMB5 in preventing the accumulation of unfolded proteins and fatal ER stress. Leukemia, 24(8): 1506-1512.

Richardson, P. G., Barlogie, B., Berenson, J., Singhal, S., Jagannath, S., Irwin, D., Rajkumar, S. V., Srkalovic, G., Alsina, M., Alexanian, R., Siegel, D., Orlowski, R. Z., Kuter, D., Limentani, S. A., Lee, S., Hideshima, T., Esseltine, D. L., Kauffman, M., Adams, J., Schenkein, D. P., & Anderson, K. C. 2003. A phase 2 study of bortezomib in relapsed, refractory myeloma. The New England Journal of Medicine, 348(26): 2609-2617.

Rivett, A. J., Palmer, A., & Knecht, E. 1992. Electron microscopic localization of the multicatalytic proteinase complex in rat liver and in cultured cells. The Journal of Histochemistry and Cytochemistry, 40(8): 1165-1172.

Rock, K. L., York, I. A., Saric, T., & Goldberg, A. L. 2002. Protein degradation and the generation of MHC class I-presented peptides. Advances in Immunology, 80: 1-70.

Rushmore, T. H., Morton, M. R., & Pickett, C. B. 1991. The antioxidant responsive element. Activation by oxidative stress and identification of the DNA consensus sequence required for functional activity. The Journal of Biological Chemistry, 266(18): 11632-11639.

Saeki, Y., & Tanaka, K. 2007. Unlocking the proteasome door. Molecular Cell, 27(6): 865-867.

Saeki, Y., & Tanaka, K. 2008. Cell biology: two hands for degradation. Nature, 453(7194): 460-461.

Sano, S., Itami, S., Takeda, K., Tarutani, M., Yamaguchi, Y., Miura, H., Yoshikawa, K., Akira, S., & Takeda, J. 1999. Keratinocyte-specific ablation of Stat3 exhibits impaired skin remodeling, but does not affect skin morphogenesis. The EMBO Journal, 18(17): 4657-4668.

Sarbassov, D. D., Guertin, D. A., Ali, S. M., & Sabatini, D. M. 2005. Phosphorylation and regulation of Akt/PKB by the rictor-mTOR complex. Science, 307(5712): 1098-1101.

Scheffner, M., Huibregtse, J. M., Vierstra, R. D., & Howley, P. M. 1993. The HPV-16 E6 and E6-AP complex functions as a ubiquitin-protein ligase in the ubiquitination of p53. Cell, 75(3): 495-505.

Schlessinger J. 2002. Ligand-induced, receptor-mediated dimerization and activation of EGF receptor. Cell.110(6):669-672.

Schlessinger, J. 2000. Cell signaling by receptor tyrosine kinases. Cell, 103(2): 211-225.

Schreiner, P., Chen, X., Husnjak, K., Randles, L., Zhang, N., Elsasser, S., Finley, D., Dikic, I., Walters, K. J., & Groll, M. 2008. Ubiquitin docking at the proteasome through a novel pleckstrin-homology domain interaction. Nature, 453(7194): 548-552.

Schuh, S. M., Newberry, E. P., Dalton, M. A., & Pike, L. J. 1994. Mutation of proline-1003 to glycine in the epidermal growth factor (EGF) receptor enhances responsiveness to EGF. Molecular Biology of the Cell, 5(7): 739-746.

Schust, J., Sperl, B., Hollis, A., Mayer, T. U., & Berg, T. 2006. Stattic: a small-molecule inhibitor of STAT3 activation and dimerization. Chemistry & Biology, 13(11): 1235-1242.

Seidel, H. M., Milocco, L. H., Lamb, P., Darnell, J. E., Jr., Stein, R. B., & Rosen, J. 1995. Spacing of palindromic half sites as a determinant of selective STAT (signal transducers and activators of transcription) DNA binding and transcriptional activity. Proc. Nati. Acad. Scie. USA, 92(7): 3041-3045.

Sharma, S. V., & Settleman, J. 2009. ErbBs in lung cancer. Experimental Cell Research, 315(4): 557-571.

Shinde, U., & Inouye, M. 2000. Intramolecular chaperones: polypeptide extensions that modulate protein folding. Seminars in cell & Developmental Biology, 11(1): 35-44.

Shirane, M., Harumiya, Y., Ishida, N., Hirai, A., Miyamoto, C., Hatakeyama, S., Nakayama, K., & Kitagawa, M. 1999. Down-regulation of p27(Kip1) by two mechanisms, ubiquitin-mediated degradation and proteolytic processing. The Journal of Biological Chemistry, 274(20): 13886-13893.

Shirogane, T., Fukada, T., Muller, J. M., Shima, D. T., Hibi, M., & Hirano, T. 1999. Synergistic roles for Pim-1 and c-Myc in STAT3-mediated cell cycle progression and antiapoptosis. Immunity, 11(6): 709-719.

Shringarpure, R., Catley, L., Bhole, D., Burger, R., Podar, K., Tai, Y. T., Kessler, B., Galardy, P., Ploegh, H., Tassone, P., Hideshima, T., Mitsiades, C., Munshi, N. C.,

Chauhan, D., & Anderson, K. C. 2006. Gene expression analysis of B-lymphoma cells resistant and sensitive to bortezomib. British Journal of Haematology, 134(2): 145-156.

Shtiegman, K., Kochupurakkal, B. S., Zwang, Y., Pines, G., Starr, A., Vexler, A., Citri, A., Katz, M., Lavi, S., Ben-Basat, Y., Benjamin, S., Corso, S., Gan, J., Yosef, R. B., Giordano, S., & Yarden, Y. 2007. Defective ubiquitinylation of EGFR mutants of lung cancer confers prolonged signaling. Oncogene, 26(49): 6968-6978.

Shuai, K., & Liu, B. 2005. Regulation of gene-activation pathways by PIAS proteins in the immune system. Nature Reviews. Immunology, 5(8): 593-605.

Siemeister, G., Weindel, K., Mohrs, K., Barleon, B., Martiny-Baron, G., & Marme, D. 1996. Reversion of deregulated expression of vascular endothelial growth factor in human renal carcinoma cells by von Hippel-Lindau tumor suppressor protein. Cancer Research, 56(10): 2299-2301.

Sieradzan, K. A., Mechan, A. O., Jones, L., Wanker, E. E., Nukina, N., & Mann, D. M. 1999. Huntington's disease intranuclear inclusions contain truncated, ubiquitinated huntingtin protein. Experimental Neurology, 156(1): 92-99.

Slingerland, J., & Pagano, M. 2000. Regulation of the cdk inhibitor p27 and its deregulation in cancer. Journal of Cellular Physiology, 183(1): 10-17.

Smith, D. M., Chang, S. C., Park, S., Finley, D., Cheng, Y., & Goldberg, A. L. 2007. Docking of the proteasomal ATPases' carboxyl termini in the 20S proteasome's alpha ring opens the gate for substrate entry. Molecular Cell, 27(5): 731-744.

Somesh, B. P., Reid, J., Liu, W. F., Sogaard, T. M., Erdjument-Bromage, H., Tempst, P., & Svejstrup, J. Q. 2005. Multiple mechanisms confining RNA polymerase II ubiquitylation to polymerases undergoing transcriptional arrest. Cell, 121(6): 913-923.

Sorokin, A. V., Selyutina, A. A., Skabkin, M. A., Guryanov, S. G., Nazimov, I. V., Richard, C., Th'ng, J., Yau, J., Sorensen, P. H., Ovchinnikov, L. P., & Evdokimova, V. 2005. Proteasome-mediated cleavage of the Y-box-binding protein 1 is linked to DNA-damage stress response. The EMBO Journal, 24(20): 3602-3612.

Sparks, A. B., Morin, P. J., Vogelstein, B., & Kinzler, K. W. 1998. Mutational analysis of the APC/beta-catenin/Tcf pathway in colorectal cancer. Cancer Research, 58(6): 1130-1134.

Spinella, M. J., Freemantle, S. J., Sekula, D., Chang, J. H., Christie, A. J., & Dmitrovsky, E. 1999. Retinoic acid promotes ubiquitination and proteolysis of cyclin D1 during induced tumor cell differentiation. The Journal of Biological Chemistry, 274(31): 22013-22018.

Starr, R., Willson, T. A., Viney, E. M., Murray, L. J., Rayner, J. R., Jenkins, B. J., Gonda, T. J., Alexander, W. S., Metcalf, D., Nicola, N. A., & Hilton, D. J. 1997. A family of cytokine-inducible inhibitors of signalling. Nature, 387(6636): 917-921.

Steffen, J., Seeger, M., Koch, A., & Kruger, E. 2010. Proteasomal degradation is transcriptionally controlled by TCF11 via an ERAD-dependent feedback loop. Molecular Cell, 40(1): 147-158.

Stephen, A. G., Trausch-Azar, J. S., Ciechanover, A., & Schwartz, A. L. 1996. The ubiquitin-activating enzyme E1 is phosphorylated and localized to the nucleus in a cell cycle-dependent manner. The Journal of Biological Chemistry, 271(26): 15608-15614.

Suiqing, C., Min, Z., & Lirong, C. 2005. Overexpression of phosphorylated-STAT3 correlated with the invasion and metastasis of cutaneous squamous cell carcinoma. The Journal of Dermatology, 32(5): 354-360.

Sullivan, M. L., & Vierstra, R. D. 1991. Cloning of a 16-kDa ubiquitin carrier protein from wheat and Arabidopsis thaliana. Identification of functional domains by in vitro mutagenesis. The Journal of Biological Chemistry, 266(35): 23878-23885.

Sutterluty, H., Chatelain, E., Marti, A., Wirbelauer, C., Senften, M., Muller, U., & Krek, W. 1999. p45SKP2 promotes p27Kip1 degradation and induces S phase in quiescent cells. Nature Cell Biology, 1(4): 207-214.

Suzuki, E., Demo, S., Deu, E., Keats, J., Arastu-Kapur, S., Bergsagel, P. L., Bennett, M. K., & Kirk, C. J. 2011. Molecular mechanisms of bortezomib resistant adenocarcinoma cells. PLoS One, 6(12): e27996.

Tai, H. C., & Schuman, E. M. 2008. Ubiquitin, the proteasome and protein degradation in neuronal function and dysfunction. Nature Reviews. Neuroscience, 9(11): 826-838.

Tanahashi, N., Yokota, K., Ahn, J. Y., Chung, C. H., Fujiwara, T., Takahashi, E., DeMartino, G. N., Slaughter, C. A., Toyonaga, T., Yamamura, K., Shimbara, N., & Tanaka, K. 1997. Molecular properties of the proteasome activator PA28 family proteins and gamma-interferon regulation. Genes to Cells, 2(3): 195-211.

Tanaka, K. 2009. The proteasome: overview of structure and functions. Proceedings of the Japan Academy. Series B, Physical and biological sciences, 85(1): 12-36.

Tanaka, K., & Kasahara, M. 1998. The MHC class I ligand-generating system: roles of immunoproteasomes and the interferon-gamma-inducible proteasome activator PA28. Immunological reviews, 163: 161-176.

Tetsu, O., & McCormick, F. 1999. Beta-catenin regulates expression of cyclin D1 in colon carcinoma cells. Nature, 398(6726): 422-426.

Thrower, J. S., Hoffman, L., Rechsteiner, M., & Pickart, C. M. 2000. Recognition of the polyubiquitin proteolytic signal. The EMBO Journal, 19(1): 94-102.

Traish, A. M., & Morgentaler, A. 2009. Epidermal growth factor receptor expression escapes androgen regulation in prostate cancer: a potential molecular switch for tumour growth. British Journal of Cancer, 101(12): 1949-1956.

Tsao, P. W., Suzuki, T., Totsuka, R., Murata, T., Takagi, T., Ohmachi, Y., Fujimura, H., & Takata, I. 1997. The effect of dexamethasone on the expression of activated NF-kappa B in adjuvant arthritis. Clinical immunology and immunopathology, 83(2): 173-178.

Tsimokha, A. S., Mittenberg, A. G., Evteeva, I. N., Kulichkova, V. A., Kozhukharova, I. V., Ermolaeva Iu, B., & Konstantinova, I. M. 2007. Reprogramming of nuclear proteasomes in K562 cells undergoing apoptosis. II. Effect of anticancer drug doxorubicin. Tsitologiia, 49(7): 552-560.

Tsimokha, A. S., Mittenberg, A. G., Kulichkova, V. A., Evteeva, I. N., Vatazhok, I., Moiseeva, T. N., Ermolaeva Iu, B., Vashukova, E. S., Volkova, I. V., Kozhukharova, I. V., Gauze, L. N., & Konstantinova, I. M. 2006. Specificity of changes in proteasome properties in diethylmaleate-induced apoptosis of K562 cells. Tsitologiia, 48(2): 133-141.

Tsvetkov, L. M., Yeh, K. H., Lee, S. J., Sun, H., & Zhang, H. 1999. p27(Kip1) ubiquitination and degradation is regulated by the SCF(Skp2) complex through phosphorylated Thr187 in p27. Current Biology, 9(12): 661-664.

Turkson, J., Bowman, T., Adnane, J., Zhang, Y., Djeu, J. Y., Sekharam, M., Frank, D. A., Holzman, L. B., Wu, J., Sebti, S., & Jove, R. 1999. Requirement for Ras/Rac1-mediated p38 and c-Jun N-terminal kinase signaling in Stat3 transcriptional activity induced by the Src oncoprotein. Molecular and Cellular Biology, 19(11): 7519-7528.

Turkson, J., Bowman, T., Garcia, R., Caldenhoven, E., De Groot, R. P., & Jove, R. 1998. Stat3 activation by Src induces specific gene regulation and is required for cell transformation. Molecular and Cellular Biology, 18(5): 2545-2552.

Turner, K. J., Crew, J. P., Wykoff, C. C., Watson, P. H., Poulsom, R., Pastorek, J., Ratcliffe, P. J., Cranston, D., & Harris, A. L. 2002. The hypoxia-inducible genes VEGF and CA9 are differentially regulated in superficial vs invasive bladder cancer. British Journal of Cancer, 86(8): 1276-1282.

Unno, M., Mizushima, T., Morimoto, Y., Tomisugi, Y., Tanaka, K., Yasuoka, N., & Tsukihara, T. 2002. Structure determination of the constitutive 20S proteasome from bovine liver at 2.75 A resolution. Journal of biochemistry, 131(2): 171-173.

Uthoff, S. M., Eichenberger, M. R., McAuliffe, T. L., Hamilton, C. J., & Galandiuk, S. 2001. Wingless-type frizzled protein receptor signaling and its putative role in human colon cancer. Molecular Carcinogenesis, 31(1): 56-62.

Varshavsky, A. 2005. Ubiquitin fusion technique and related methods. Methods in Enzymology, 399: 777-799.

Venuprasad, K., Elly, C., Gao, M., Salek-Ardakani, S., Harada, Y., Luo, J. L., Yang, C., Croft, M., Inoue, K., Karin, M., & Liu, Y. C. 2006. Convergence of Itch-induced ubiquitination with MEKK1-JNK signaling in Th2 tolerance and airway inflammation. The Journal of Clinical Investigation, 116(4): 1117-1126.

Verma, R., Aravind, L., Oania, R., McDonald, W. H., Yates, J. R., 3rd, Koonin, E. V., & Deshaies, R. J. 2002. Role of Rpn11 metalloprotease in deubiquitination and degradation by the 26S proteasome. Science, 298(5593): 611-615.

Vijay-Kumar, S., Bugg, C. E., Wilkinson, K. D., & Cook, W. J. 1985. Three-dimensional structure of ubiquitin at 2.8 A resolution. Proc. Nati. Acad. Scie. USA, 82(11): 3582-3585.

Wada, M., Kosaka, M., Saito, S., Sano, T., Tanaka, K., & Ichihara, A. 1993. Serum concentration and localization in tumor cells of proteasomes in patients with hematologic malignancy and their pathophysiologic significance. The Journal of Laboratory and Clinical Medicine, 121(2): 215-223.

Wang, H. R., Kania, M., Baumeister, W., & Nederlof, P. M. 1997. Import of human and Thermoplasma 20S proteasomes into nuclei of HeLa cells requires functional NLS sequences. European Journal of Cell Biology, 73(2): 105-113.

Wang, T., Niu, G., Kortylewski, M., Burdelya, L., Shain, K., Zhang, S., Bhattacharya, R., Gabrilovich, D., Heller, R., Coppola, D., Dalton, W., Jove, R., Pardoll, D., & Yu, H. 2004. Regulation of the innate and adaptive immune responses by Stat-3 signaling in tumor cells. Nature Medicine, 10(1): 48-54.

Wang, X. J., Yu, J., Wong, S. H., Cheng, A. S., Chan, F. K., Ng, S. S., Cho, C. H., Sung, J. J., & Wu, W. K. 2013. A novel crosstalk between two major protein degradation systems: regulation of proteasomal activity by autophagy. Autophagy, 9(10): 1500-1508.

Wang, X., Chen, C. F., Baker, P. R., Chen, P. L., Kaiser, P., & Huang, L. 2007. Mass spectrometric characterization of the affinity-purified human 26S proteasome complex. Biochemistry, 46(11): 3553-3565.

Wang, X., Xu, H., Ju, D., & Xie, Y. 2008. Disruption of Rpn4-induced proteasome expression in Saccharomyces cerevisiae reduces cell viability under stressed conditions. Genetics, 180(4): 1945-1953.

Wei, D., Le, X., Zheng, L., Wang, L., Frey, J. A., Gao, A. C., Peng, Z., Huang, S., Xiong, H. Q., Abbruzzese, J. L., & Xie, K. 2003. Stat3 activation regulates the expression of vascular endothelial growth factor and human pancreatic cancer angiogenesis and metastasis. Oncogene, 22(3): 319-329.

Wells, A. 1999. EGF receptor. The international Journal of Biochemistry & Cell biology, 31(6): 637-643.

Wen, Z., Zhong, Z., & Darnell, J. E., Jr. 1995. Maximal activation of transcription by Stat1 and Stat3 requires both tyrosine and serine phosphorylation. Cell, 82(2): 241-250.

Wilkinson, K. D., & Audhya, T. K. 1981. Stimulation of ATP-dependent proteolysis requires ubiquitin with the COOH-terminal sequence Arg-Gly-Gly. The Journal of Biological Chemistry, 256(17): 9235-9241.

Wilson, K. J., Gilmore, J. L., Foley, J., Lemmon, M. A., & Riese, D. J. 2009. Functional selectivity of EGF family peptide growth factors: implications for cancer. Pharmacology & Therapeutics, 122(1): 1-8.

Witt, E., Zantopf, D., Schmidt, M., Kraft, R., Kloetzel, P. M., & Kruger, E. 2000. Characterisation of the newly identified human Ump1 homologue POMP and analysis of LMP7(beta 5i) incorporation into 20S proteasomes. Journal of molecular biology, 301(1): 1-9.

Wojcik, C., Tanaka, K., Paweletz, N., Naab, U., & Wilk, S. 1998. Proteasome activator (PA28) subunits, alpha, beta and gamma (Ki antigen) in NT2 neuronal precursor cells and HeLa S3 cells. European Journal of Cell Biology, 77(2): 151-160.

Woolson, H. D., Thomson, V. S., Rutherford, C., Yarwood, S. J., & Palmer, T. M. 2009. Selective inhibition of cytokine-activated extracellular signal-regulated kinase by cyclic AMP via Epac1-dependent induction of suppressor of cytokine signalling-3. Cellular Signalling, 21(11): 1706-1715.

Wormald, S., & Hilton, D. J. 2004. Inhibitors of cytokine signal transduction. The Journal of Biological Chemistry, 279(2): 821-824.

Wyke, S. M., Russell, S. T., & Tisdale, M. J. 2004. Induction of proteasome expression in skeletal muscle is attenuated by inhibitors of NF-kappaB activation. British Journal of Cancer, 91(9): 1742-1750.

Xie, T. X., Huang, F. J., Aldape, K. D., Kang, S. H., Liu, M., Gershenwald, J. E., Xie, K., Sawaya, R., & Huang, S. 2006. Activation of stat3 in human melanoma promotes brain metastasis. Cancer Research, 66(6): 3188-3196.

Xie, T. X., Wei, D., Liu, M., Gao, A. C., Ali-Osman, F., Sawaya, R., & Huang, S. 2004. Stat3 activation regulates the expression of matrix metalloproteinase-2 and tumor invasion and metastasis. Oncogene, 23(20): 3550-3560.

Xie, Y. 2010. Feedback regulation of proteasome gene expression and its implications in cancer therapy. Cancer Metastasis Reviews, 29(4): 687-693.

Xie, Y., & Varshavsky, A. 2001. RPN4 is a ligand, substrate, and transcriptional regulator of the 26S proteasome: a negative feedback circuit. Proc. Nati. Acad. Scie. USA, 98(6): 3056-3061.

Xu H., Ju D., Jarois T., & Xie Y. 2008. Diminished feedback regulation of proteasome expression and resistance to proteasome inhibitors in breast cancer cells. Breast Cancer Res Treat. 107(2):267-274

Xu, H., Fu, J., Ha, S. W., Ju, D., Zheng, J., Li, L., & Xie, Y. 2012. The CCAAT box-binding transcription factor NF-Y regulates basal expression of human proteasome genes. Biochimica Biophysica Acta, 1823(4): 818-825.

Xu, J. M., Han, Y., Duan, H. Q., Gao, E. M., Zhang, Y., Liu, X. Q., Zhang, J. S., Toschi, L., Galetta, D., Azzariti, A., & Paradiso, A. 2009. EGFR mutations and HER2/3 protein expression and clinical outcome in Chinese advanced non-small cell lung cancer patients treated with gefitinib. Journal of Cancer Research and Clinical Oncology, 135(6): 771-782.

Yahata, Y., Shirakata, Y., Tokumaru, S., Yamasaki, K., Sayama, K., Hanakawa, Y., Detmar, M., & Hashimoto, K. 2003. Nuclear translocation of phosphorylated STAT3 is essential for vascular endothelial growth factor-induced human dermal microvascular endothelial cell migration and tube formation. The Journal of Biological Chemistry, 278(41): 40026-40031.

Yarden, Y., & Shilo, B. Z. 2007. SnapShot: EGFR signaling pathway. Cell, 131(5): 1018.

Yeom, S. Y., Lee, S. J., Kim, W. S., & Park, C. 2012. Rad knockdown induces mitochondrial apoptosis in bortezomib resistant leukemia and lymphoma cells. Leukemia Research, 36(9): 1172-1178.

Yewale C., Baradia D., Vhora I., Patil S., & Misra A. 2013. Epidermal growth factor receptor targeting in cancer: a review of trends and strategies. Biomaterials. 34(34):8690-8707

Yokogami, K., Wakisaka, S., Avruch, J., & Reeves, S. A. 2000. Serine phosphorylation and maximal activation of STAT3 during CNTF signaling is mediated by the rapamycin target mTOR. Current Biology, 10(1): 47-50.

Yu, H., Pardoll, D., & Jove, R. 2009. STATs in cancer inflammation and immunity: a leading role for STAT3. Nature Reviews. Cancer, 9(11): 798-809.

Yu, J. Y., DeRuiter, S. L., & Turner, D. L. 2002. RNA interference by expression of short-interfering RNAs and hairpin RNAs in mammalian cells. Proc. Nati. Acad. Scie. USA, 99(9): 6047-6052.

Yuan, Z. L., Guan, Y. J., Chatterjee, D., & Chin, Y. E. 2005. Stat3 dimerization regulated by reversible acetylation of a single lysine residue. Science, 307(5707): 269-273.

Zhang, F., Su, K., Yang, X., Bowe, D. B., Paterson, A. J., & Kudlow, J. E. 2003. O-GlcNAc modification is an endogenous inhibitor of the proteasome. Cell, 115(6): 715-725.

Zhang, N. Y., Tang, Z., & Liu, C. W. 2008a. alpha-Synuclein protofibrils inhibit 26S proteasome-mediated protein degradation: understanding the cytotoxicity of protein protofibrils in neurodegenerative disease pathogenesis. The Journal of Biological Chemistry, 283(29): 20288-20298.

Zhang, Z., & Zhang, R. 2008. Proteasome activator PA28 gamma regulates p53 by enhancing its MDM2-mediated degradation. The EMBO Journal, 27(6): 852-864.

Zhao, M., Gao, F. H., Wang, J. Y., Liu, F., Yuan, H. H., Zhang, W. Y., & Jiang, B. 2011. JAK2/STAT3 signaling pathway activation mediates tumor angiogenesis by upregulation of VEGF and bFGF in non-small-cell lung cancer. Lung Cancer, 73(3): 366-374.

Zhou, J., Ong, C. N., Hur, G. M., & Shen, H. M. 2010. Inhibition of the JAK-STAT3 pathway by andrographolide enhances chemosensitivity of cancer cells to doxorubicin. Biochemical Pharmacology, 79(9): 1242-1250.

Zhou, Z. D., & Lim, T. M. 2009. Dopamine (DA) induced irreversible proteasome inhibition via DA derived quinones. Free radical research, 43(4): 417-430.

Zong, C., Gomes, A. V., Drews, O., Li, X., Young, G. W., Berhane, B., Qiao, X., French, S. W., Bardag-Gorce, F., & Ping, P. 2006. Regulation of murine cardiac 20S proteasomes: role of associating partners. Circulation Research, 99(4): 372-380.

Zushi, S., Shinomura, Y., Kiyohara, T., Miyazaki, Y., Kondo, S., Sugimachi, M., Higashimoto, Y., Kanayama, S., & Matsuzawa, Y. 1998. STAT3 mediates the survival signal in oncogenic ras-transfected intestinal epithelial cells. International Journal of Cancer, 78(3): 326-330.

Zwang, Y., & Yarden, Y. 2009. Systems biology of growth factor-induced receptor endocytosis. Traffic, 10(4): 349-363.

List of Publications:

- **Vangala JR**, Dudem S, Jain N, Kalivendi SV. "Regulation of PSMB5 and β-Subunits of Mammalian Proteasome by Constitutively Activated STAT3: Potential Role in Bortezomib Mediated Anticancer Therapy". ***J Biol Chem***. 2014 May 2; 289(18):12612-22.

Publications from Collaborations:

- Rekha K, Rao RR, Pandey R, Prasad KR, Babu KS, **Vangala JR**, Kalivendi SV, Rao JM. "Two new sesquiterpenoids from the rhizomes of *Nardostachys jatamansi"*. ***J Asian Nat Prod Res***. 2013; 15(2): 111-6.

- Reddy MA, Jain N, Yada D, Kishore C, **Vangala JR**, P Surendra R, Addlagatta A, Kalivendi SV, Sreedhar B. "Design and synthesis of resveratrol-based nitrovinylstilbenes as antimitotic agents". ***J Med Chem***. 2011; 54(19): 6751-60.

- Yadav JS, Boyapelly K, Alugubelli SR, Pabbaraja S, **Vangala JR**, Kalivendi SV. "Stereoselective total synthesis of (+)-oploxyne A, (-)-oploxyne B, and their C-10 epimers and structure revision of natural oploxyne B". ***J Org Chem***. 2011; 76(8): 2568-76.

THE JOURNAL OF BIOLOGICAL CHEMISTRY VOL. 289, NO. 18, pp. 12612–12622, May 2, 2014

Regulation of PSMB5 Protein and β Subunits of Mammalian Proteasome by Constitutively Activated Signal Transducer and Activator of Transcription 3 (STAT3)

*POTENTIAL ROLE IN BORTEZOMIB-MEDIATED ANTICANCER THERAPY**

Received for publication, December 12, 2013, and in revised form, March 11, 2014 Published, JBC Papers in Press, March 13, 2014, DOI 10.1074/jbc.M113.542829

Janakiram Reddy Vangala, Srikanth Dudem, Nishant Jain[1], and Shasi V. Kalivendi[2]

From the Centre for Chemical Biology, CSIR-Indian Institute of Chemical Technology, Uppal Road, Tarnaka, Hyderabad 500-607, Andhra Pradesh, India

Background: Malignancies are frequently associated with altered abundance of proteasome and elevated proteasome activity.
Results: EGF-induced PSMB5 expression requires STAT3 activation.
Conclusion: The catalytic subunits and activities of the mammalian proteasome are regulated by STAT3.
Significance: Proteasome function is regulated by oncogenic signaling.

The ubiquitin-proteasome system facilitates the degradation of ubiquitin-tagged proteins and performs a regulatory role in cells. Elevated proteasome activity and subunit expression are found in several cancers. However, the inherent molecular mechanisms responsible for increased proteasome function in cancers remain unclear despite the well investigated and defined role of the mammalian proteasome. This study was initiated to elucidate the mechanisms involved in the regulation of β subunits of the mammalian proteasome. Suppression of STAT3 tyrosine phosphorylation coordinately decreased the mRNA and protein levels of the β subunits of the 20 S core complex in DU145 cells. Notably, PSMB5, a molecular target of bortezomib, was shown to be a target of STAT3. Knockdown of STAT3 decreased PSMB5 protein. Inhibition of phospho-STAT3 substantially reduced PSMB5 protein levels in cells expressing constitutively active-STAT3. Accumulation of activated STAT3 resulted in the induction of PSMB5 promoter and protein levels. In addition, a direct correlation was observed between the endogenous levels of PSMB5 and constitutively active STAT3. PSMB5 and STAT3 protein levels remained unaltered following the inhibition of proteasome activity. The EGF-induced concerted increase of β subunits was blocked by inhibition of the EGF receptor or STAT3 but not by the PI3K/AKT or MEK/ERK pathways. Decreased proteasome activities were due to reduced protein levels of catalytic subunits of the proteasome in STAT3-inhibited cells. Combined treatments with bortezomib and inhibitor of STAT3 abrogated proteasome activity and enhanced cellular apoptosis. Overall, we demonstrate that aberrant activation of STAT3 regulates the expression of β subunits, in particular PSMB5, and the catalytic activity of the proteasome.

The ubiquitin-proteasome system facilitates the degradation of regulatory and abnormal proteins. Polyubiquitinated proteins are targeted for degradation by the 26 S proteasome. The 19 S regulatory complex recognizes polyubiquitinated proteins, whereas proteolytic activity resides within the 20 S catalytic core of the 26 S proteasome. The 20 S proteasome is comprised of two outer α and two inner β rings (αββα). Each of the α and β rings consists of seven subunits, termed α1-α7 and β1-β7. The α subunits maintain the structure, whereas the core β rings contains proteolytically active subunits such as PSMB5 (β5, chymotrypsin-like), PSMB6 (β1, caspase-like), and PSMB7 (β2, trypsin-like). The proteasome activity is controlled stringently and attuned to cellular requirements. Aberrations of this pathway lead to pleiotropic defects in all aspects of cell function. Because of their indispensable role, inhibitors of the proteasome are routinely used as antineoplastic agents in clinics (1–4). Most of the proteasome inhibitors target the chymotrypsin-like activity of PSMB5, although they coinhibit the caspase-like and/or trypsin-like activity at higher concentrations. Bortezomib, a peptide boronic acid congener, is used clinically as a frontline therapy for multiple myeloma as a single agent or in combination with standard therapies. Bortezomib binds and inhibits the chymotrypsin-like activity of the PSMB5 subunit. However, resistance to bortezomib develops in a majority of patients, thereby limiting its clinical efficacy (5–7). Hence, elucidation of the mechanism of regulation of PSMB5 is imperative to identify the molecular basis of bortezomib resistance.

Suppression of the proteasome activity or autophagy in mammalian cells by pharmacological inhibitors results in the induction of PSMB5 and other proteasome genes in a concerted manner (8, 9). Nrf1 and Nrf2 are key transcription factors involved in the up-regulation of proteasome genes in response

* This work was supported by the Department of Science and Technology, India (to S. V. K.); by Council of Scientific and Industrial Research (CSIR) SMiLE Project CSC-0111, India (to S. V. K.); and by a senior research fellowship from the Indian Council of Medical Research (to V. J. R.).
[1] To whom correspondence may be addressed: Centre for Chemical Biology, CSIR-Indian Institute of Chemical Technology, Uppal Rd., Tarnaka, Hyderabad 500-607, AP, India. Tel.: 91-40-27191862; Fax: 91-40-27191816; E-mail: nishant@iict.res.in.
[2] To whom correspondence may be addressed: Centre for Chemical Biology, CSIR-Indian Institute of Chemical Technology, Uppal Road, Tarnaka, Hyderabad 500-607, AP, India. Tel.: 91-40-27191865; Fax: 91-40-27191816; E-mail: kalivendi@iict.res.in.

to proteasome inhibition. Under normal conditions, Nrf1 undergoes endoplasmic reticulum-mediated degradation, whereas Keap1-bound Nrf2 is degraded by the ubiquitin-proteasome system. In response to proteasome inhibition, these transcription factors translocate to the nucleus and form heterodimers with Maf proteins. The Nrf1/Maf or Nrf2/Maf heterodimers transactivate proteasome genes through the antioxidant response elements in the promoters (10–12). Brain-specific, conditional knockout mice of Nrf1 exhibit a coordinated down-regulation of the basal levels of various proteasomal genes (13). Conversely, endogenous levels of proteasome subunits remain unaltered in mouse embryonic fibroblasts of *nrf1*- and *nrf2*-disrupted mice (11). Therefore, on the basis of these observations, Nrf1 or Nrf2 largely regulate the feedback response to proteasome inhibition and contribute minimally to the basal expression of proteasome genes. However, the transcription factors that regulate the basal level expression of proteasome subunits are largely unknown (14).

Neoplastic growth is frequently associated with increased proteasome activity and subunit expression to maintain protein homeostasis (15–19). Because of their stringent mode of activation, Nrf1 and Nrf2 are unlikely to promote the increased proteasome subunit expression in malignancies unless they are deregulated. Accordingly, colon tumors showed a gain of proteasome activity because of increased nuclear localization of Nrf2 (20). Thus, to cope with increased proteasome function in malignancies, it is plausible that the proteasome genes are regulated coordinately by oncogenic transcription factor(s). In this study, we investigated the mechanisms underlying increased proteasome subunit expression and activity in cell lines harboring oncogenic STAT3 protein. Importantly, PSMB5 has been shown to be a STAT3 target.

EXPERIMENTAL PROCEDURES

Cell Culture and Transfections—All cell lines were purchased from the ATCC and maintained at 37 °C in a humidified incubator with 5% CO_2. DU145, A549, HeLa, MDA-MB-231, and LNCaP cells were cultured in DMEM with 10% FBS. HEK293T and PC-3 cells were grown in minimal essential medium and F12, respectively, supplemented with 10% FBS. Transfections were carried out using Lipofectamine 2000 reagent (Invitrogen) according to the instructions of the manufacturer. All plasmids for transfection were prepared using Qiagen columns (Hilden, Germany). DU145 cells were washed three times with medium without serum following 24 h of serum starvation. Human EGF (catalog no. 324831, Calbiochem, Darmstadt, Germany) was added whenever required at a final concentration of 100 ng/ml.

Chemicals, Expression Vectors, and Antibodies—Stattic (catalog no. 573099), WP1066 (catalog no. 573097), EGFR inhibitor 324674 (EI)[3] (catalog no. D00067055), PI3K/AKT inhibitor LY294002 (catalog no. 440202), and MEK/ERK inhibitor PD98059 (catalog no. 513000) were obtained from Calbiochem. Bortezomib was from Natco Pharma, India. The pRC/CMV/STAT3-FLAG expression construct was a gift from Dr. Vijay Gupta (Scripps Research Institute). Resveratrol (catalog no. R5010); epoxomicin (catalog no. E3652); MG-132 (catalog no. C2211); a purified fraction of 20 S proteasome (catalog no. P3988); and antibodies for PSMB5 (catalog no. SAB2101895), GFP (catalog no. G1546), ubiquitin (catalog no. U5379), and tubulin (catalog no. T5168) were from Sigma-Aldrich. Bcl-2 (catalog no. sc-492) antibody was from Santa Cruz Biotechnology. AKT (catalog no. 4691), phospho-AKT-Ser-473 (catalog no. 4060), ERK1/2 (catalog no. 4695), phospho-ERK1/2 (catalog no. 4370), EGFR (catalog no. 4267), phospho-EGFR-Tyr-1068 (catalog no. 3777), STAT1 (catalog no. 9175), phospho-STAT1-Tyr-701 (catalog no. 9167), STAT3 (catalog no. 9132), and phospho-STAT3-Tyr-705 (catalog no. 9145) were from Cell Signaling Technology (Danvers, MA). The antibodies for the β subunits and 20 S proteasome core (catalog no. PW 8905) were from Enzo Life Sciences. The secondary antibodies anti-mouse IgG HRP (catalog no. NA9310) and anti-rabbit IgG HRP (catalog no. NA9340) were from Amersham Biosciences Pharmacia.

Construction of shRNA—The shRNAs targeting STAT3 were constructed using a U6 promoter-based vector as described previously (21). The desired synthetic oligonucleotides targeting the nucleotide sequences of STAT3 (NM_139276.2) were annealed and cloned into the BbsI-XbaI-digested mU6 pro vector. The two sequences of oligonucleotides cloned were STAT3sh1 (5′-tttgCAATGGAGTACGTGCAGAAGAttcaagaga TCTTCTGCACGTACTCCATTGttttt-3′); and STAT3sh2 (5′-tttgAGGAGGAGGCATTTGGAA AGTttcaagagaACTT-TCCAAATGCCTCCTCCTtt ttt-3′). This vector expressed the sense, 9 bp of hairpin, and antisense sequence. The mU6pro vector expressing shRNA of an unrelated sequence of the same length was used as a control (21).

Measurement of Caspase 3 Activity—Following treatment, cell pellets were washed twice with phosphate-buffered saline and suspended in lysis buffer (50 mM HEPES (pH 7.4) containing 5 mM CHAPS and 5 mM DTT) for 15 min on ice. Subsequently, cells were centrifuged for 15 min at 14,000 × *g* under cold conditions, and clear supernatant was collected. The supernatant was added to assay buffer (20 mM HEPES (pH 7.4), 2 mM EDTA, 0.1% CHAPS, and 5 mM DTT) containing caspase 3 substrate (Ac-DEVD-AMC, 40 μM) in a final volume of 100 μl as described earlier (22). The incubation was performed for 1 h at 37 °C with readings recorded at 5-min intervals. Fluorescence released by AMC was measured at 360-nm and 460-nm excitation and emission wavelengths, respectively. Values were normalized to protein concentration and expressed as fold change of activity relative to DMSO control.

Construction of Adenoviral Vectors—Adenoviral vectors were generated using the AdEasy™ adenoviral vector system from Stratagene. The cDNA was isolated from the pRC-CMV-FLAG-mSTAT3 plasmid by PCR and cloned into the Not1/Xho1 site of pAdtrack-CMV plasmid coexpressing green fluorescent protein as a marker to monitor infection efficiency. The cDNA was under the control of the CMV promoter terminated by the simian virus 40 (SV40) polyadenylation signal, resulting in pAdSTAT3. The pAdtrack-CMV plasmid was utilized as a control vector. The adenoviruses were generated as described previously (23).

[3] The abbreviations used are: EI, EGFR inhibitor; DMSO, dimethyl sulfoxide; p-STAT3, tyrosine 705-phosphorylated STAT3; EGFR, EGF receptor; Ac, acetyl; AMC, 7-amino-4-methyl coumarin.

Cloning of the PSMB5 Promoter and Luciferase Assays—Genomatix software predicted a 965-bp PSMB5 promoter. The sequence was amplified by PCR employing human genomic DNA with sequence-specific primers (PSMB5, 5′-GGGGTACCTGGTACATATTTATGCAGTCTC AACCGTC-3′ (forward) and 5′-CCGCTCGA GACTGAGACTCCCTGGACCTAGATCCAG-3′ (reverse)). Subsequently, the PSMB5 promoter was cloned into the pGL3-basic luciferase vector and sequenced to ensure the absence of mutations. The sequence matched with *Homo sapiens* chromosome 14 with sequence identification NC_000014.8 from nucleotides 23,503,983–23,504,947. Putative transcription factor binding sites were determined by using MatInspector from Genomatix software. To determine the promoter activity, PC-3 cells plated in 12-well plates were transfected with 100 ng of pWT-PSMB5 promoter-reporter construct and required concentrations of STAT3 plasmids. The plasmid concentrations were kept constant at 1 μg by the addition of control plasmids. 30 h post-transfection, cellular lysates were prepared for luciferase activity assays according to protocols described by Promega. Relative luciferase activities were calculated after normalizing the values with β-galactosidase enzyme activities (24).

Measurement of Proteasome Activities—Peptidase activities of the proteasome were measured in cellular lysates by the addition of 50 μM fluorogenic peptide substrates, Suc-Leu-Leu-Val-Tyr-AMC (for chymotrypsin-like), Z-Ala-Arg-Arg-AMC (for trypsin-like) and Z-Leu-Leu-Glu-AMC (for caspase-like activity) in assay buffer (50 mM Tris-HCl (pH 7.8), 20 mM KCl, 5 mM $MgCl_2$, and 1 mM dithiothreitol). The reaction mixture was incubated for 20 min at 37 °C. Later, the reaction was stopped by the addition of 125 mM sodium borate buffer (pH 9.0) containing 7.5% ethanol, as described previously (12). Fluorescence released by AMC was measured at 360-nm and 460-nm excitation and emission wavelengths, respectively, in an EnSpire multimode plate reader (PerkinElmer Life Sciences). Enzymatic activities were normalized to protein concentration and expressed as a percentage of activities relative to the DMSO control.

RT-PCR—Total RNA was isolated using TRIzol reagent (Invitrogen). Semiquantitative RT-PCR was carried out as described previously (21). RNA was reverse-transcribed using reagents from the first-strand cDNA synthesis kit (Invitrogen). The PCR conditions for PSMB1-PSMB7 were one cycle of 3 min at 95 °C, 1 min at 95 °C, 1 min at 56 °C, and 1 min at 72 °C and one cycle of 7 min final extension at 72 °C. The primers employed for the amplification of individual subunits were as follows: PSMB1, 5′-TTTCGCCCTACGTTTTCAAC-3′ (forward) and 5′-TACAGCCCCCTTTCCTTCTT-3′ (reverse); PSMB2, 5′-AAGGCCCCGACTATGTTCTT-3′ (forward) and 5′-AGGTTGGCAGATTCAGGATG-3′ (reverse); PSMB3, 5′-GAAGGGGAAGAACTGTGTGG-3′ (forward) and 5′-CCTGGTGGTGATTTTGTCCT-3′ (reverse); PSMB4, 5′-TCAGTCCTCGGCGTTAAGTT-3′ (forward) and 5′-GCTTAGCACTGGCTGCTTCT-3′ (reverse); PSMB5, 5′-CCATACCTGCTAGGCACCAT-3′ (forward) and 5′-GCACCTCCTGAGTAGGCATC-3′ (reverse); PSMB6, 5′-CCTATTCACGACCGCATTTT-3′ (forward) and 5′-TCCCGGTAGGTAGCATCAAC-3′ (reverse); PSMB7, 5′-GCAACTGAAGGGATGGTTGT-3′ (forward) and 5′-AAACTAGGGCTGCACCAATG-3′ (reverse); 18 S, 5′-CCTGCGGCTTAATTTGACTC-3′ (forward) and 5′-ATGCCAGAGTCTCGTTCGTT-3′ (reverse); and Bcl2, 5′-CTACGAGTGGGATGCGGGAGATGT-3′ (forward) and 5′-GGTGCCGGTTCAGGTACT CAGTCATC-3′ (reverse). PSMB1, 3, and 4 were amplified for 27 cycles. PSMB2 and 5 were amplified for 25 cycles. PSMB6 and 7 were amplified for 22 cycles. Bcl-2 and 18 S RNA were amplified for 28 and 18 cycles, respectively, in 25-μl volumes of PCR mixture (Fermentas) in an Eppendorf Master Cycler®.

Western Blot Analysis—Following treatments, cells were washed twice with PBS and lysed in 1× SDS sample buffer. Proteins were separated on 10% SDS-polyacrylamide gels and transferred onto nitrocellulose membranes. The membranes were washed twice with Tween Tris-buffered saline before blocking nonspecific binding with 5% nonfat dry milk (Blotto, Santa Cruz Biotechnology) or 3% bovine serum albumin. The primary antibodies were used at 1:1000 dilutions, and the membrane was incubated for 2 h at room temperature. The phosphoproteins were detected using primary antibodies at 1:500 dilution and incubation of 2 h at room temperature in 0.3% BSA containing Tween-Tris-buffered saline. The membranes were washed three times, and the detection was performed by using horseradish peroxidase-conjugated secondary antibody as described previously (21).

Statistical Analysis—Statistical differences were calculated using Student's *t* test. When significant differences were observed, *p* values for pairwise comparisons were calculated by employing a two-tailed *t* test. $p < 0.01$ was considered significant.

RESULTS

Suppression of Activated STAT3 Down-regulated PSMB5 Expression—Bortezomib treatment of head and neck squamous cell carcinoma cell lines lead to a significant up-regulation of total and phosphorylated STAT3 (25). In another study, bortezomib-resistant clones of human monocytic cells (THP1 cell line) manifested a marked increase in PSMB5 protein levels (26). These observations suggest a possible role of STAT3 in the regulation of PSMB5 expression. To explore this, we opted for DU145 cells, which harbor aberrantly high levels of activated STAT3 (27). DU145 cells were treated with Stattic, an inhibitor of STAT3, at 10 μM concentrations for various time periods (28). Stattic treatment resulted in the down-regulation of STAT3 tyrosine phosphorylation (p-STAT3) from 3 h onwards, whereas total STAT3 protein levels remained unaffected. The protein levels of Bcl-2, a target of STAT3, also decreased significantly by 3 h of treatment. Similar to p-STAT3 and Bcl-2, PSMB5 protein levels also decreased correspondingly. Moreover, PSMB5 protein levels were undetectable from 12 h of treatment (Fig. 1*A*). To validate the observations with Stattic, we employed another STAT3 inhibitor, WP1066 (29). Treatment with WP1066 resulted in a significant reduction of PSMB5 protein levels by 18 h. p-STAT3 levels also concomitantly decreased from 18 h of treatment. Similar to Stattic, STAT3 protein levels remain unchanged in WP1066-treated cells (Fig. 1*B*). The difference in the inhibition of p-STAT3 protein levels in Stattic- and WP1066-treated cells was probably due to differences in the efficacy of the inhibitors. Previous

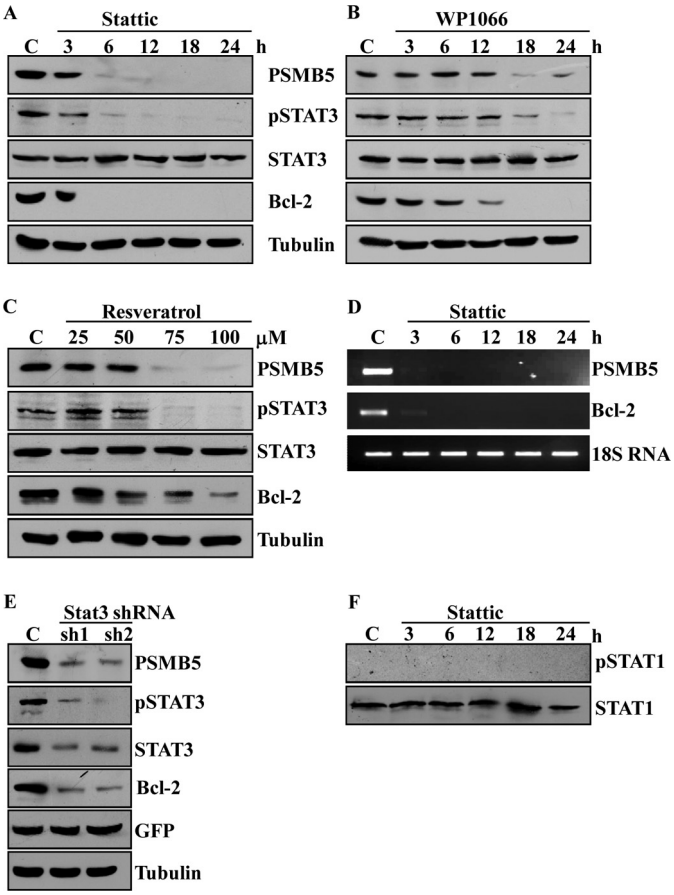

FIGURE 1. **STAT3 inhibitors reduce PSMB5 expression in DU145 cells.** *A* and *B*, DU145 cells were treated with Stattic (10 μM) or WP1066 (10 μM) for different time periods. DMSO was used as a vehicle control (*C*). Following termination of treatment, cells were harvested and subjected to Western blot analysis employing specific antibodies for PSMB5, p-STAT3, STAT3, and Bcl-2. The p-STAT3/STAT3 antibodies detect the α and β isoforms of STAT3. Tubulin was used as a loading control. *C*, DU145 cells were treated with different concentrations of resveratrol (25–100 μM) for 24 h, and an immunoblot analysis was performed for proteins. *D*, DU145 cells were treated with Stattic (10 μM) for 3–24 h. Following treatment, total RNA was isolated. PSMB5 and Bcl-2 mRNA levels were examined by semiquantitative RT-PCR. 18 S RNA was used as a loading control. *E*, DU145 cells were transfected with 2 μg of STAT3 shRNA constructs for 30 h. Scrambled shRNA was employed as control. GFP and tubulin were used as transfection and loading controls. Cells were harvested 30 h after transfection and probed for PSMB5, p-STAT3, STAT3, and Bcl-2 proteins. *F*, p-STAT1 and STAT1 protein levels were analyzed in DU145 cells treated with Stattic (10 μM) for the indicated time intervals. RT-PCR analysis and Western blot images were from pooled samples of triplicate cultures, and data are representative of three independent experiments.

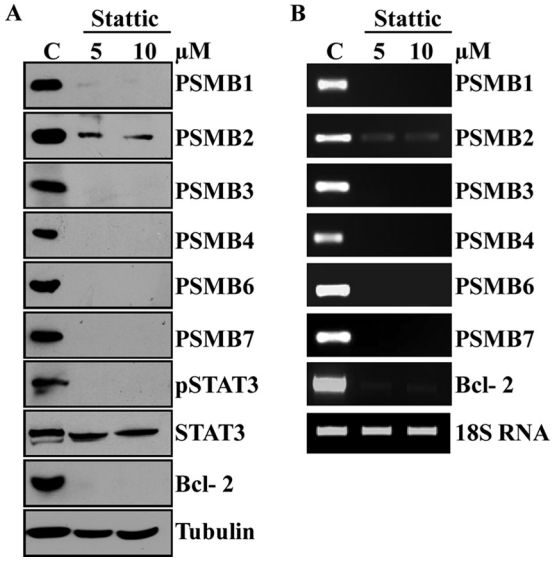

FIGURE 2. **Suppression of p-STAT3 reduces mRNA and protein levels of β subunits of the 20 S core complex.** *A*, DU145 cells were treated with Stattic at 5 μM and 10 μM concentrations for 24 h. DMSO was used as a vehicle control (*C*). Total proteins from control- and Stattic-treated cells were subjected to Western blotting using antibodies against β subunits, p-STAT3, STAT3, Bcl-2, and tubulin. *B*, DU145 cells were treated with Stattic (5 μM and 10 μM) for 24 h. Later, semiquantitative RT-PCR analysis was performed for the mRNA levels of β subunits, Bcl-2, and 18 S RNA. Data are representative of three separate experiments.

studies report that resveratrol inhibits Src tyrosine kinase activity and, thereby, blocks STAT3 phosphorylation in DU145 cells (30). To further confirm STAT3-dependent PSMB5 subunit expression, we employed resveratrol. Treatment of DU145 cells with resveratrol suppressed p-STAT3 levels in a dose-dependent manner. The reduction in p-STAT3 levels was associated with decreased PSMB5 protein levels in resveratrol-treated cells (Fig. 1*C*). Further, STAT3 inhibition drastically reduced the mRNA levels of PSMB5 (Fig. 1*D*). The decrease in protein levels was preceded by reduced mRNA levels of PSMB5 in Stattic-treated cells. To provide further evidence for the requirement of STAT3 in the regulation of PSMB5, we employed a STAT3-directed shRNA. Both constructs of STAT3 shRNA significantly knocked down total STAT3 and p-STAT3 protein levels. In accordance with our earlier observations, knockdown of STAT3 protein resulted in lower PSMB5 protein levels (Fig. 1*E*). To validate the specificity of STAT3 inhibitors, Stattic-treated DU145 cells were analyzed for p-STAT1 levels. Notably, the tyrosine-phosphorylated STAT1 levels were undetectable in DU145 cells, and total STAT1 levels also remained unchanged (Fig. 1*F*). Overall, pharmacological inhibition and shRNA-mediated down-regulation of STAT3 levels decreased PSMB5 protein in DU145 cells. Thus, STAT3 activation is essential for PSMB5 expression.

Coordinated Decrease of β Subunits of Proteasome because of STAT3 Inhibition—Previous reports demonstrated that proteasome genes are regulated coordinately through a common transcription factor (10–12). Because the expression of PSMB5 is regulated by STAT3, we analyzed whether the other β subunits are also regulated coordinately by STAT3. To test this assumption, we treated DU145 cells dose-dependently with Stattic for 24 h. It was observed that, like PSMB5, protein levels of PSMB6, PSMB7, and other β subunits decreased significantly in a concerted manner in STAT3-inhibited cells (Fig. 2*A*). Stattic also decreased the levels of p-STAT3 and Bcl-2 protein levels. Next, under similar treatment conditions, we examined the mRNA levels of other β subunits. Similar to protein levels, the mRNA levels of β subunits decreased substantially in Stattic-treated cells (Fig. 2*B*). Thus, blockade of activated STAT3 coordinately reduced the mRNA and protein levels of the β subunits of the proteasome in DU145 cells.

Stattic Down-regulated PSMB5 Protein Levels and Decreased Proteasome Activities—In addition to DU145, other cancer cell types, such as the A549, HeLa, and MDA-MB-231 cell lines, display constitutively active STAT3 (31, 32). Hence, we analyzed whether suppression of p-STAT3 affects PSMB5 protein

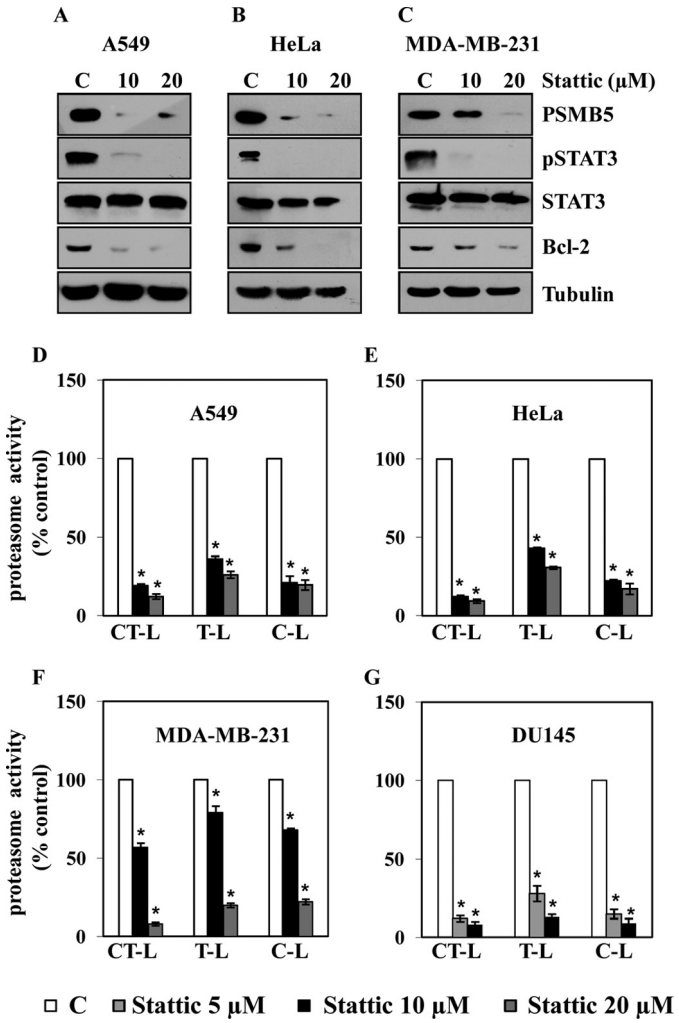

FIGURE 3. **STAT3 inhibition decreases PSMB5 protein levels and proteasome activities in cell lines possessing constitutively active STAT3.** *A–C*, panels of cell lines harboring constitutively active STAT3 were treated with Stattic at 10 μM and 20 μM concentrations for 24 h. Whole-cell lysates of A549, HeLa, and MDA-MB-231 cells were analyzed for PSMB5, p-STAT3, STAT3, Bcl-2, and tubulin by Western blotting. DMSO served as vehicle control (*C*). Data are representative of three separate experiments. *D–F*, chymotrypsin-like (*CT-L*), trypsin-like (*T-L*), and caspase-like (*C-L*) activities of the 20 S proteasome in A549, HeLa, and MDA-MB-231 cells under similar conditions of treatment as in *A–C*. *G*, DU145 cells were treated with Stattic (5 μM and 10 μM) for 24 h, and 20 S proteasome activities were measured as described under "Experimental Procedures." The obtained activities were normalized to protein concentration and expressed as a percentage of activities relative to the DMSO control ($n = 3$). *D–G*, data are mean ± S.D. of three independent experiments. *, $p < 0.01$ compared with controls.

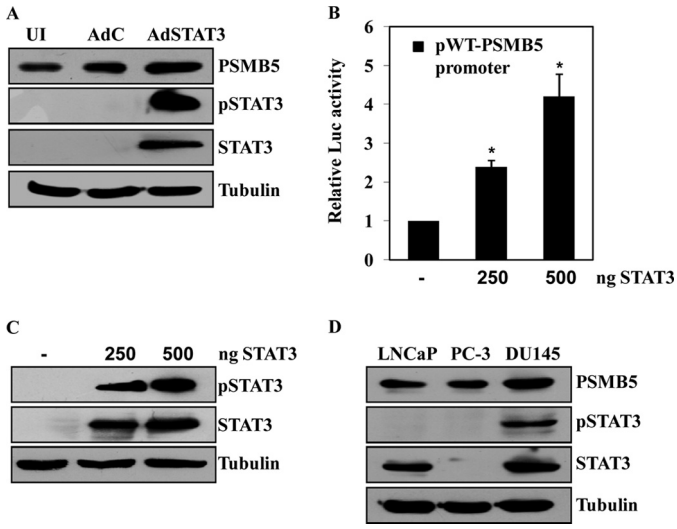

FIGURE 4. **Overexpression of STAT3-induced PSMB5 promoter and protein.** *A*, PC-3 cells were infected with control adenovirus (*AdC*) or adenovirus expressing the STAT3 gene (*AdSTAT3*) and uninfected cells (*UI*). Following 48 h of infection, Western blotting was performed from cell lysates with antibodies of PSMB5, p-STAT3, STAT3, and tubulin. The fold induction of PSMB5 was analyzed by densitometry relative to the control adenovirus. *B*, PC-3 cells were transfected with the wild-type pWT-PSMB5 promoter-reporter construct (100 ng) along with the pCMV.SPORT-βGal plasmid (100 ng) and pWT-STAT3 (250 and 500 ng) for 30 h. Luciferase activities relative to the control are shown. *C*, lysates employed in the reporter assay were analyzed for p-STAT3, STAT3, and tubulin proteins using specific antibodies. *D*, endogenous protein levels of PSMB5, p-STAT3, and STAT3 in three different human prostate cancer cell lines with tubulin as a loading control. *A*, *C*, and *D*, data are representative of three separate experiments. In each experiment, pooled samples from triplicate cultures were used for Western blot analysis. *B*, data are mean ± S.D. of four independent experiments. *, $p < 0.01$ compared with the control.

levels as observed in DU145 cells. Consequently, these cell lines were treated in a dose-dependent manner with Stattic for 24 h. Concomitant with a decrease of p-STAT3 levels in Stattic-treated A549 cells, PSMB5 and Bcl-2 protein levels were also reduced (Fig. 3*A*). PSMB5 protein levels also decreased in the HeLa and MDA-MB-231 cell lines because of compromised activation of p-STAT3 (Fig. 3, *B* and *C*). Previous studies in yeast showed that loss of one of the proteasome genes reduced proteasome assembly and activity (33). Because PSMB5 protein levels decreased due to inhibition of p-STAT3, we hypothesized that chymotrypsin-like activity would reflect the reduction of subunit expression. Hence, we monitored the proteasome activities in cells that harbor constitutively active STAT3. Chymotrypsin-like activity significantly decreased to 90% in A549 cells. In comparison, the same activity was reduced to 78 and 85% at 10 μM concentrations of Stattic in the HeLa and MDA-MB-231 cell lines, respectively (Fig. 3, *D–F*). Similarly, chymotrypsin-like activity was reduced significantly to 92% in DU145 cells (Fig. 3*G*). In addition, trypsin-like and caspase-like activities were also reduced significantly in STAT3-inhibited cells (Fig. 3, *D–G*). Taken together, suppression of p-STAT3 levels decreased PSMB5 protein and reduced proteasome activities in cell lines possessing constitutively activated STAT3.

PSMB5 Expression Is Induced by STAT3—Compromised STAT3 activation leads to decreased PSMB5 protein. Therefore, we examined whether increased levels of activated STAT3 induce PSMB5 expression. To investigate this possibility, we used a human prostate cancer cell line, PC-3, that does not express endogenous STAT3 (34). PC-3 cells were infected with adenovirus expressing wild-type STAT3 protein for 48 h. Endogenous or overexpressed STAT3 protein levels were absent in uninfected and control-infected cells. Accumulation of p-STAT3 protein levels in PC-3 cells resulted in a significant increase of PSMB5 protein levels to 1.8-fold relative to control-infected cells (Fig. 4*A*). Next, we analyzed whether STAT3 enhanced expression of PSMB5 through promoter activation. A bioinformatics analysis predicted a 965-bp promoter for PSMB5, with a TATA box harboring 294 bp of the 5′ untranslated region and 108 bp of exon 1. Consequently, the cloned promoter in the pGL3-basic vector was analyzed for basal and

STAT3-induced promoter activity in STAT3-negative PC-3 cells. Wild-type STAT3 dose-dependently increased the PSMB5 promoter activity to a maximum of 4.2-fold (Fig. 4*B*). In addition, basal promoter activity was observed in PC-3 cells compared with a promoterless vector. Promoter assay lysates showed a marked expression of tyrosine-phosphorylated and total STAT3 proteins (Fig. 4*C*). Because increased levels of p-STAT3 induced PSMB5 protein and its promoter, we examined the interdependency between the endogenous levels of p-STAT3 and PSMB5 proteins. The human prostate cancer cell lines DU145, LNCaP, and PC-3 displayed dissimilar levels of either phosphorylated or total STAT3 proteins (35). DU145 cells with constitutive levels of p-STAT3 exhibited high levels of PSMB5 protein. p-STAT3 levels were undetectable in LNCaP and PC-3 cells (Fig. 4*D*). However, basal levels of PSMB5 protein were observed in LNCaP and PC-3 cells when compared with DU145 cells. Collectively, overexpression of STAT3 leads to the induction of the PSMB5 promoter and protein. Moreover, a strong correlation exists between the endogenous levels of p-STAT3 and PSMB5.

EGF-induced Up-regulation of PSMB5 Is Mediated by STAT3 Activation—The elevated levels of epidermal growth factor receptor (EGFR) in association with loss of androgen regulation results in androgen-independent growth of DU145 cells (36). In addition, aberrant EGFR levels are found to be frequently associated with activated STAT3 (37). Hence, we investigated whether EGF regulates PSMB5 protein in DU145 cells. To examine this possibility, cells were serum-starved for 24 h and later treated with EGF (100 ng/ml) for various time points until 24 h. PSMB5 protein levels were increased by 3 h and gradually reached a maximum by 24 h. The maximal levels of PSMB5 protein were associated with higher p-STAT3 levels (Fig. 5*A*). Next, we analyzed whether EGF-induced PSMB5 expression requires STAT3. To elucidate this, serum-starved DU145 cells were pretreated with inhibitors of EGFR (324674) and STAT3 (Stattic and WP1066) for 2 h. Subsequently, cells were treated with EGF for 24 h. EGF-induced STAT3 activation and PSMB5 protein levels were decreased significantly either by EI or STAT3 inhibitors (Fig. 5*B*). EGF/EGFR can activate the PI3K and MEK/ERK signaling pathways (38). Next, we investigated whether these downstream pathways were also responsible for PSMB5 induction. However, treatment with inhibitors of PI3K/AKT (LY294002) and MEK/ERK (PD98059) did not prevent EGF-induced PSMB5 expression (Fig. 5*C*). The efficacy of all inhibitors was substantiated by suppression of their target kinases. Because β subunits are coordinately regulated by STAT3, we determined whether EGF also induced the expression of β subunits. EGF was added to cells pretreated with or without EGFR inhibitor for 24 h. EGF-induced concerted increases in the protein levels of β subunits were reduced in EGFR inhibitor-treated cells (Fig. 5*D*). Taken together, these results suggest that EGF induced the expression of β subunits and, in particular, that the induction of the PSMB5 subunit was through STAT3 activation.

PSMB5 Protein Levels Are Unresponsive to EGF in STAT3-negative PC-3 Cells—PC-3 cells display overexpressed EGFR and are responsive to EGF (39). Hence, to validate that EGF-induced PSMB5 activation requires STAT3, serum-starved

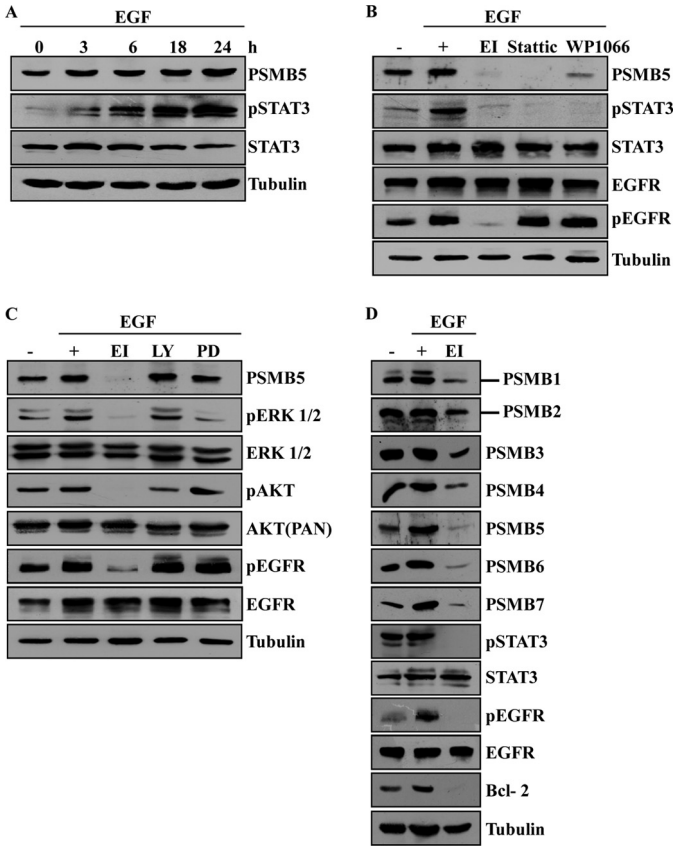

FIGURE 5. **EGF induced PSMB5 expression by activation of STAT3.** *A*, DU145 cells were serum-starved for 24 h, and, subsequently, cells were treated with EGF (100 ng/ml) in a time-dependent manner for 24 h. Later, whole-cell lysates were analyzed for PSMB5, p-STAT3, and STAT3 proteins. *B* and *C*, serum-starved DU145 cells were pretreated for 2 h in the presence or absence of inhibitors of EGFR (EI) (324674, 10 μM), STAT3 (Stattic and WP1066, 10 μM), PI3K/AKT (LY294002 (*LY*), 20 μM), and MEK/ERK (PD98059 (*PD*), 50 μM). Later, cells were stimulated with EGF (100 ng/ml) for 24 h, and whole-cell lysates were subjected to Western blot analysis using specific antibodies. The Akt (pan) antibody detects total Akt proteins. The efficiencies of various inhibitors against their target kinases were analyzed by reduced phosphorylation status of EGFR (EI, 324674), STAT3 (Stattic and WP1066), AKT (LY294002), and ERK1/2 (PD98059). *D*, serum-starved DU145 cells were pretreated with or without EGFR inhibitor (324674, 10 μM) for 2 h and subsequently treated with EGF for 24 h. Cells were harvested, and lysates were analyzed for β subunits, p-STAT3, STAT3, Bcl-2, pEGFR-Tyr-1068, and EGFR by Western blotting. Bands corresponding to PSMB1 and PSMB2 are indicated. Tubulin was used as a loading control. The Western blots shown were from pooled samples of triplicate cultures and are representative of three independent experiments.

PC-3 cells were pretreated with EGF pathway inhibitors for 2 h. Subsequently, cells were treated with EGF for 24 h. EGF induced the phosphorylation of EGFR (Fig. 6*A*). In contrast, p-STAT3 and STAT3 were undetectable in PC-3 cells. Moreover, phosphorylation of AKT and ERK proteins was also observed with EGF treatment. Notably, PSMB5 protein levels remained unaffected by EGF or pharmacological inhibition of EGFR, ERK, and AKT proteins (Fig. 6, *A* and *B*). Blockade of p-STAT3 decreased PSMB5 protein levels and proteasome activities in STAT3-activated cells (Fig. 3, *A*–*G*). We analyzed whether PC-3 cells respond similarly to STAT3 inhibition. Treatments of cells with STAT3 inhibitors did not alter the protein levels of PSMB5 in PC-3 cells that lack endogenous STAT3 (Fig. 6, *C* and *D*). Correspondingly, chymotrypsin-like, trypsin-like, and caspase-like activities of the proteasome remained unaltered in Stattic-treated cells (Fig. 6*E*). Taken

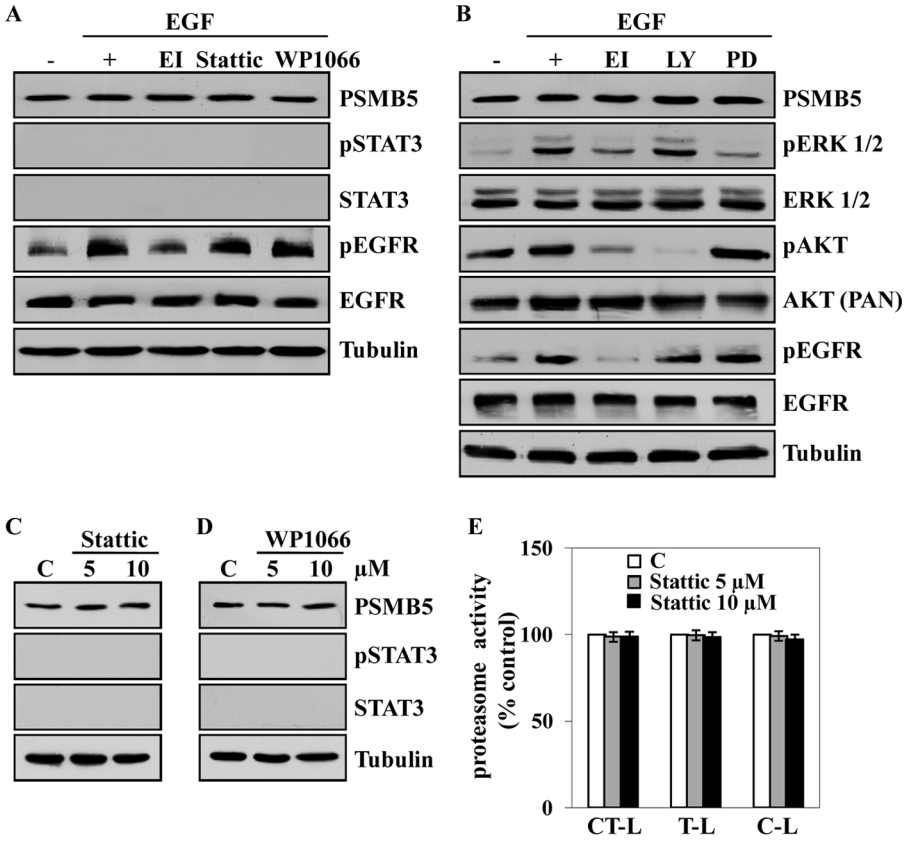

FIGURE 6. **Lack of STAT3 impedes EGF-induced PSMB5 expression in PC-3 cells.** *A* and *B*, PC-3 cells were serum-starved for 24 h. Subsequently, cells were pretreated for 2 h with inhibitors of EGFR (324674, 10 μM), STAT3 (Stattic and WP1066, 10 μM), PI3K/AKT (LY294002 (*LY*), 20 μM), and MEK/ERK (PD98059 (*PD*), 50 μM). Later, cells were stimulated with EGF (100 ng/ml) for 24 h, and whole-cell lysates were subjected to Western blot analysis. The phosphorylation statuses of EGFR (EI, 324674), STAT3 (Stattic and WP1066), AKT (LY294002), and ERK1/2 (PD98059) were analyzed for the efficacy of the inhibitors. *C* and *D*, PC-3 cells were treated with Stattic and WP1066 (5 μM and 10 μM) for 24 h. Following treatment, whole cell lysates were probed for PSMB5, p-STAT3, STAT3, and tubulin by Western blotting. *C*, control. *E*, 20 S proteasome activities were measured in PC-3 cells treated with Stattic (5 μM and 10 μM) for 24 h ($n = 3$). *CT-L*, chymotrypsin-like; *T-L*, trypsin-like; *C-L*, caspase-like. *A–D*, data are representative of three separate experiments. In each experiment, pooled samples from triplicate cultures were used for Western blot analysis. *E*, data are mean ± S.D. of three independent experiments.

together, sustained proteasome activities in STAT3 inhibitor-treated cells and loss of EGF-induced PSMB5 expression was due to the absence of STAT3 in PC-3 cells.

PSMB5 and STAT3 Protein Levels Are Not Altered by Proteasome Inhibitors—Proteasome inhibition elicits a feedback-dependent induction of PSMB5 gene expression (8, 10–12). In addition, bortezomib also induced the activation of STAT3 in head and neck squamous cell carcinoma cell lines (25). Hence, we analyzed whether proteasome inhibitors activate STAT3 and PSMB5. To test this possibility, DU145 cells were treated with bortezomib, epoxomicin, and MG-132 for 24 h. In response to proteasome inhibition, p-STAT3 and PSMB5 protein levels were unaffected and remained similar to control levels (Fig. 7*A*). Because the protein levels of PSMB5 and STAT3 were unaltered, we analyzed whether cells exhibit resistance to proteasome inhibitors by examining the chymotrypsin-like and caspase 3 enzyme activities. Chymotrypsin-like activity was inhibited significantly to 90% in cells treated with bortezomib when compared with the control. In addition, chymotrypsin-like activity in epoxomicin- and MG-132-treated cells was reduced to 86 and 58%, respectively (Fig. 7*B*). Nevertheless, bortezomib induced a robust caspase 3 response compared with the other two inhibitors (Fig. 7*C*). Thus, DU145 cells were susceptible to proteasome inhibitors, although the protein levels of PSMB5 or p-STAT3 remain unaltered.

Combination Treatment of Bortezomib and STAT3 Inhibitors Exacerbates Proteasome Dysfunction and Cellular Apoptosis—Abrogation of p-STAT3 was found to decrease proteasome subunit expression and activity in DU145 cells (Figs. 2*A* and 3*G*). In comparison, bortezomib treatment reduced proteasome activity. However, PSMB5 protein levels remained unchanged (Fig. 7, *A* and *B*). Furthermore, synergistic activation of cell death in response to combined treatment of bortezomib and STAT3 inhibitors was observed in head and neck squamous cell carcinoma cell lines (25). Hence, we reasoned that cotreatment would further reduce proteasome function and potentiate cell death. To examine this, DU145 cells were treated with Stattic, WP1066, bortezomib, or a combination of STAT3 inhibitors with bortezomib for 18 h. Chymotrypsin-like activity was decreased to 90% in response to bortezomib. In comparison, the same activity was reduced to 70% in WP1066-treated and 98% in Stattic-treated cells (Fig. 8*A*). However, cotreatment with STAT3 inhibitors and bortezomib completely abolished chymotrypsin-like activity. In addition, trypsin-like and caspase-like activities of the proteasome were inhibited significantly in cotreatment (Fig. 8*A*). We also exam-

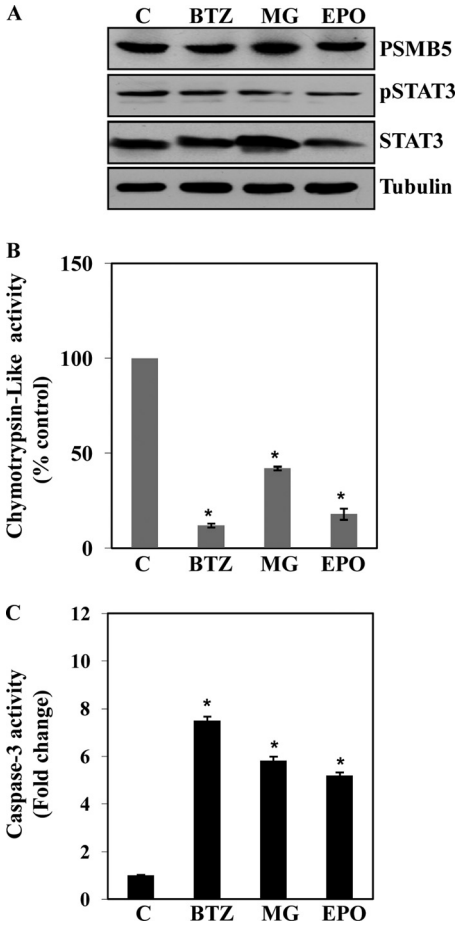

FIGURE 7. **Proteasome activity inhibitors do not alter the endogenous levels of PSMB5 and p-STAT3/STAT3.** *A*, DU145 cells were treated with proteasome inhibitors (bortezomib (*BTZ*), 100 nM; MG-132 (*MG*), 1 μM; and epoxomicin (*EPO*), 250 nM) for 24 h. Later, an immunoblot analysis was performed for PSMB5, p-STAT3, STAT3, and tubulin employing specific antibodies. Data are representative of three separate experiments. *C*, control. *B*, the chymotrypsin-like activity of proteasome inhibitor-treated DU145 cell lysates was measured employing fluorogenic substrate ($n = 3$). *C*, DU145 cells were treated with different proteasome inhibitors, and cellular caspase 3 enzyme activity was determined as described under "Experimental Procedures" ($n = 3$). *, $p < 0.01$ compared with the control.

ined whether the decreased proteasome activities were due to STAT3 inhibitors. To test this, purified 20 S proteasome was incubated with varying concentrations of bortezomib and STAT3 inhibitors. Neither Stattic nor WP1066 inhibited the chymotrypsin-like activity of purified 20 S proteasome *in vitro*. In contrast, bortezomib significantly inhibited the chymotrypsin-like activity of the purified 20 S proteasome (Fig. 8*B*). Furthermore, significantly lower protein levels of PSMB5 and the 20 S core complex were observed with STAT3 inhibitors and cotreatment compared with bortezomib treatment alone (Fig. 8*C*). Because inhibition of proteasome function is known to result in the accumulation of polyubiquitinated proteins (40), we next examined the polyubiquitinated protein levels in cells treated either with bortezomib alone or in combination with STAT3 inhibitors. Cotreatment, STAT3 inhibitors, and bortezomib caused an increase in the intracellular levels of polyubiquitinated proteins (Fig. 8*D*). Moreover, cotreatment employing bortezomib with Stattic or WP1066 caused a significant increase in caspase 3 activity compared with bortezomib treatment alone (Fig. 8*E*). Taken together, cotreatment of bortezomib with inhibitors of STAT3 synergistically increased proteasomal dysfunction and enhanced apoptotic cell death.

DISCUSSION

In this study, we report that PSMB5 is a target of STAT3. Suppression of STAT3 tyrosine phosphorylation by either chemical inhibitors or shRNA-mediated knockdown of STAT3 reduced PSMB5 protein levels. Blockade of p-STAT3 resulted in the concerted down-regulation of mRNA and protein levels of β subunits, leading to reduced proteasome activities. PSMB5 promoter and protein levels were induced by p-STAT3. EGF-induced expression of PSMB5 requires STAT3 activation. PSMB5 and STAT3 protein levels were unresponsive to proteasome inhibition. Bortezomib-induced loss of chymotrypsin-like activity and cell viability was potentiated by STAT3 inhibitors.

STAT3 is activated persistently in various malignancies and induces oncogenic processes through expression of various prosurvival genes (37). Hence, small-molecule inhibitors of tyrosine-phosphorylated STAT3 are explored actively for tumor therapy. The inhibition of constitutively active STAT3 induced apoptosis in DU145 cells (27). In our study, STAT3 inhibitors reduced PSMB5 expression and induced apoptosis. Similarly, proteasome inhibitors also triggered apoptosis, corroborated by increased caspase 3 activity. However, under similar experimental conditions, PSMB5 or phospho-STAT3-Tyr-705 levels remained unaffected, suggesting that the decreased levels of PSMB5 were not a general feature of apoptosis. Thus, lower levels of transcriptionally active STAT3 resulted in decreased levels of PSMB5 protein. The possibility of STAT1-dependent regulation of PSMB5 was ruled out because Stattic selectively binds the SH2 domain of STAT3 over STAT1 (28). In addition, phospho-STAT1 levels were undetectable in DU145 cells, which is in accordance with an earlier report (41). A reduction in the mRNA levels of PSMB5 by STAT3 inhibitors further substantiates STAT3-dependent regulation of PSMB5 (Fig. 1*D*). Moreover, the mRNA and protein levels of Bcl-2, a known STAT3 target, concomitantly decreased with PSMB5, suggesting a transcriptional role of STAT3. Furthermore, a promoter analysis of PSMB5 revealed putative STAT3 binding sites with the canonical TT (N) $_{4-6}$AA at -439 bp, + 87 bp, and + 230 bp relative to TSS (42). Accordingly, the PSMB5 promoter was activated in a dose-dependent manner by STAT3. In addition, exogenous expression of STAT3 in PC-3 cells resulted in the induction of PSMB5 protein. Hence, it is likely that STAT3 transcriptionally activates the gene expression and promoter activity of PSMB5 through the STAT3-responsive sites. Intriguingly, LNCaP and PC-3 cells expressed basal levels of PSMB5 protein when compared with DU145 cells. An abundance of proteasome is important for normal cell survival and indispensable for malignancies (6). Other oncogenic transcription factors may regulate the expression of PSMB5 in cell types lacking constitutive STAT3 levels.

Malignant conditions are often associated with high rates of protein synthesis. Hence, a wide range of cancers exhibit either higher proteasome activity or subunit expression or both to overcome this predicament (15–19). However, the molecular

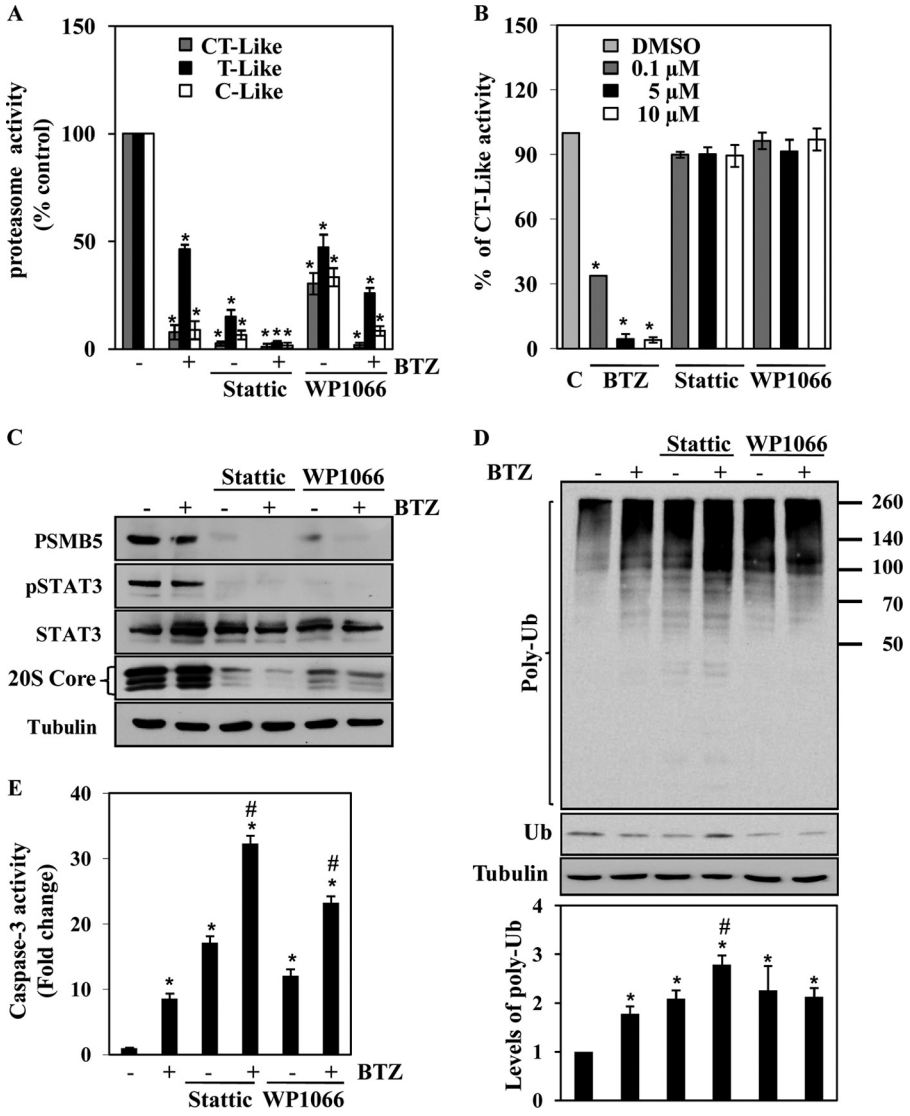

FIGURE 8. **The synergistic effect of bortezomib and STAT3 inhibitors on proteasome dysfunction and apoptosis.** *A*, DU145 cells were treated with bortezomib (*BTZ*, 100 nM), Stattic (10 μM), or WP1066 (10 μM) or a combination of bortezomib and STAT3 inhibitors for 18 h. DMSO was used as a vehicle control. Chymotrypsin-like (*CT-like*), trypsin-like (*T-like*), and caspase-like (*C-like*) activities of the proteasome were measured. *B*, the chymotrypsin-like activity of the purified 20 S proteasome incubated with different concentrations (0.1, 5, and 10 μM) of bortezomib, Stattic, or WP1066. *C*, control. *C*, Under similar treatment conditions as in *A*, cell lysates were analyzed for PSMB5, p-STAT3, STAT3, 20 S core, and tubulin by Western blotting. *D*, levels of polyubiquitinated (*Poly-Ub*) proteins were determined by immunoblot analysis, and tubulin was employed as loading control. The *bottom panel* demonstrates the densitometric analysis of polyubiquitinated proteins. *E*, caspase 3 activity of cells treated with Stattic (10 μM) or WP1066 (10 μM) in the presence or absence of bortezomib for 18 h ($n = 3$). *, $p < 0.01$ compared with controls; #, $p < 0.01$ compared with the BTZ-treated group. Western blot images are the pooled samples from triplicate cultures. Data are representative of three independent experiments.

determinants responsible for the regulation of proteasome activity remain unclear. The results of this study demonstrate, for the first time, that activated STAT3 modulates the proteasome activities through the regulation of PSMB5 and other β subunits. Hence, decreased protein levels of β subunits resulted in reduced proteasome activities in STAT3-suppressed cells. However, proteasome inhibitors reduced proteasome activity in DU145 cells without affecting the endogenous levels of PSMB5. This was probably due to the presence of copious amounts of constitutive STAT3 regulating the basal expression of PSMB5. Thus, STAT3 inhibitors impair cellular proteasome activities, leading to accumulation of polyubiquitinated proteins similar to proteasome inhibitors. However, STAT3 inhibitors do not interact with mammalian proteasome subunits because the molecular structures of STAT3 inhibitors differ markedly from known structural classes of proteasome inhibitors. The lack of inhibition by STAT3 inhibitors on chymotrypsin-like activity of the purified 20 S proteasome clearly indicates that there is no cross-reactivity between the STAT3 inhibitors and the proteasome *per se*. Overall, persistently activated STAT3 levels function as an important determinant of proteasome activity in cell lines harboring constitutive STAT3.

Proteasome genes are regulated coordinately by Nrf1 and Nrf2 in response to proteasome inhibition (8, 10–12). Similarly, the expression levels of other β subunits were reduced concertedly because of EGFR or STAT3 inhibition. It is likely that promoters of β subunits may contain STAT3-responsive sites. STAT3 has been shown as one of the targets of EGF signaling in

addition to the PI3K and ERK pathways (38). However, EGF-induced activation of the PI3K or ERK pathway did not affect PSMB5 expression in DU145 and PC-3 cells. Further, PSMB5 protein levels remained unchanged in response to EGF in STAT3-negative PC-3 cells. In contrast, EGF-dependent activation of p-STAT3 induced PSMB5 protein in DU145 cells. Hence, EGF-activated STAT3 possibly regulates the expression of β subunits of the 20 S proteasome and may contribute to the optimal growth of DU145 cells through efficient protein homeostasis. In support of these observations, recent studies in *Caenorhabditis elegans* also demonstrated that EGF signaling activates the ubiquitin proteasome system to modulate the life span of the worm (43).

PSMB5 is the molecular target of bortezomib, a Food and Drug Administration-approved proteasome inhibitor used clinically to ameliorate relapsed multiple myeloma and mantle cell lymphoma (44, 45). However, bortezomib resistance mechanisms pose a major obstacle in clinical therapy (7). The status of PSMB5 was elucidated in bortezomib-resistant cell line models. These studies suggested that bortezomib resistance was either due to mutations in or overexpression of the PSMB5 subunit (46, 47). However, observations from these cell line models remain unverified in clinical samples (48–50). In addition, the feedback regulation of proteasome gene expression also contributes to bortezomib resistance (14). Hence, constitutively activated STAT3 levels in cancers may presumably circumvent the effect of bortezomib regimen through up-regulation of PSMB5 protein. Therefore, cotreatment with bortezomib and an inhibitor of STAT3 may suppress bortezomib resistance. Because STAT3 regulates the basal expression of β subunits, blockade of STAT3 activation may, in part, alleviate the feedback response to proteasome inhibition. Moreover, lower expression of proteasome subunits reduces the number of active sites required for proteasome inhibition. In agreement with this hypothesis, knockdown of the 20 S core subunits of the proteasome sensitized HCT116 cells to bortezomib (51). Therefore, cotreatment involving bortezomib and STAT3 inhibitors might prove useful to inhibit proteasome function and STAT3 signaling in cancers (Fig. 8, *A–E*). Overall, the present findings on STAT3 dependent PSMB5 regulation underscore an alternative mechanism for bortezomib insensitivity. Finally, the oncogenic properties of STAT3 regulate the expression of PSMB5, β subunits, and activities of the mammalian proteasome to support malignant progression.

Acknowledgments—We thank Ananthamurthy Nagabhushana for critical reading of the manuscript.

REFERENCES

1. Coux, O., Tanaka, K., and Goldberg, A. L. (1996) Structure and functions of the 20 S and 26 S proteasomes. *Annu. Rev. Biochem.* **65,** 801–847
2. Goldberg, A. L. (2003) Protein degradation and protection against misfolded or damaged proteins. *Nature* **426,** 895–899
3. Demartino, G. N., and Gillette, T. G. (2007) Proteasomes: machines for all reasons. *Cell* **129,** 659–662
4. Tanaka, K. (2009) The proteasome: overview of structure and functions. *Proc. Jpn. Acad. Ser. B Phys. Biol. Sci.* **85,** 12–36
5. Adams, J. (2004) The development of proteasome inhibitors as anticancer drugs. *Cancer Cell* **5,** 417–421
6. Kisselev, A. F., van der Linden, W. A., and Overkleeft, H. S. (2012) Proteasome inhibitors: an expanding army attacking a unique target. *Chem. Biol.* **19,** 99–115
7. Chen, D., Frezza, M., Schmitt, S., Kanwar, J., and Dou, Q. P. (2011) Bortezomib as the first proteasome inhibitor anticancer drug: current status and future perspectives. *Curr. Cancer Drug Targets* **11,** 239–253
8. Meiners, S., Heyken, D., Weller, A., Ludwig, A., Stangl, K., Kloetzel, P. M., and Krüger, E. (2003) Inhibition of proteasome activity induces concerted expression of proteasome genes and *de novo* formation of mammalian proteasomes. *J. Biol. Chem.* **278,** 21517–21525
9. Wang, X. J., Yu, J., Wong, S. H., Cheng, A. S., Chan, F. K., Ng, S. S., Cho, C. H., Sung, J. J., and Wu, W. K. (2013) A novel crosstalk between two major protein degradation systems: regulation of proteasomal activity by autophagy. *Autophagy* **9,** 1500–1508
10. Steffen, J., Seeger, M., Koch, A., and Krüger, E. (2010) Proteasomal degradation is transcriptionally controlled by TCF11 via an ERAD-dependent feedback loop. *Mol. Cell* **40,** 147–158
11. Radhakrishnan, S. K., Lee, C. S., Young, P., Beskow, A., Chan, J. Y., and Deshaies, R. J. (2010) Transcription factor Nrf1 mediates the proteasome recovery pathway after proteasome inhibition in mammalian cells. *Mol. Cell* **38,** 17–28
12. Kwak, M. K., Wakabayashi, N., Greenlaw, J. L., Yamamoto, M., and Kensler, T. W. (2003) Antioxidants enhance mammalian proteasome expression through the Keap1-Nrf2 signaling pathway. *Mol. Cell. Biol.* **23,** 8786–8794
13. Lee, C. S., Lee, C., Hu, T., Nguyen, J. M., Zhang, J., Martin, M. V., Vawter, M. P., Huang, E. J., and Chan, J. Y. (2011) Loss of nuclear factor E2-related factor 1 in the brain leads to dysregulation of proteasome gene expression and neurodegeneration. *Proc. Natl. Acad. Sci. U.S.A.* **108,** 8408–8413
14. Xie, Y. (2010) Feedback regulation of proteasome gene expression and its implications in cancer therapy. *Cancer Metastasis Rev.* **29,** 687–693
15. Ren, S., Smith, M. J., Louro, I. D., McKie-Bell, P., Bani, M. R., Wagner, M., Zochodne, B., Redden, D. T., Grizzle, W. E., Wang, N., Smith, D. I., Herbst, R. A., Bardenheuer, W., Opalka, B., Schütte, J., Trent, J. M., Ben-David, Y., and Ruppert, J. M. (2000) The p44S10 locus, encoding a subunit of the proteasome regulatory particle, is amplified during progression of cutaneous malignant melanoma. *Oncogene* **19,** 1419–1427
16. Chen, L., and Madura, K. (2005) Increased proteasome activity, ubiquitin-conjugating enzymes, and eEF1A translation factor detected in breast cancer tissue. *Cancer Res.* **65,** 5599–5606
17. Bazzaro, M., Lee, M. K., Zoso, A., Stirling, W. L., Santillan, A., Shih, I. M., and Roden, R. B. (2006) Ubiquitin-proteasome system stress sensitizes ovarian cancer to proteasome inhibitor-induced apoptosis. *Cancer Res.* **66,** 3754–3763
18. Wyke, S. M., Russell, S. T., and Tisdale, M. J. (2004) Induction of proteasome expression in skeletal muscle is attenuated by inhibitors of NF-κB activation. *Br. J. Cancer* **91,** 1742–1750
19. Kraus, M., Rückrich, T., Reich, M., Gogel, J., Beck, A., Kammer, W., Berkers, C. R., Burg, D., Overkleeft, H., Ovaa, H., and Driessen, C. (2007) Activity patterns of proteasome subunits reflect bortezomib sensitivity of hematologic malignancies and are variable in primary human leukemia cells. *Leukemia* **21,** 84–92
20. Arlt, A., Bauer, I., Schafmayer, C., Tepel, J., Müerköster, S. S., Brosch, M., Röder, C., Kalthoff, H., Hampe, J., Moyer, M. P., Fölsch, U. R., and Schäfer, H. (2009) Increased proteasome subunit protein expression and proteasome activity in colon cancer relate to an enhanced activation of nuclear factor E2-related factor 2 (Nrf2). *Oncogene* **28,** 3983–3996
21. Jain, N., Gupta, S., Sudhakar, C., Radha, V., and Swarup, G. (2005) Role of p73 in regulating human caspase-1 gene transcription induced by interferon-γ and cisplatin. *J. Biol. Chem.* **280,** 36664–36673
22. Kalivendi, S. V., Konorev, E. A., Cunningham, S., Vanamala, S. K., Kaji, E. H., Joseph, J., and Kalyanaraman, B. (2005) Doxorubicin activates nuclear factor of activated T-lymphocytes and Fas ligand transcription: role of mitochondrial reactive oxygen species and calcium. *Biochem. J.* **389,** 527–539
23. Jain, N., Sudhakar, C., and Swarup, G. (2007) Tumor necrosis factor-α-induced caspase-1 gene expression. Role of p73. *FEBS J.* **274,** 4396–4407
24. Sudhakar, C., Nagabhushana, A., Jain, N., and Swarup, G. (2009) NF-κB

mediates tumor necrosis factor α-induced expression of optineurin, a negative regulator of NF-κB. *PLoS ONE* **4,** e5114
25. Li, C., Zang, Y., Sen, M., Leeman-Neill, R. J., Man, D. S., Grandis, J. R., and Johnson, D. E. (2009) Bortezomib up-regulates activated signal transducer and activator of transcription-3 and synergizes with inhibitors of signal transducer and activator of transcription-3 to promote head and neck squamous cell carcinoma cell death. *Mol. Cancer Ther.* **8,** 2211–2220
26. Oerlemans, R., Franke, N. E., Assaraf, Y. G., Cloos, J., van Zantwijk, I., Berkers, C. R., Scheffer, G. L., Debipersad, K., Vojtekova, K., Lemos, C., van der Heijden, J. W., Ylstra, B., Peters, G. J., Kaspers, G. L., Dijkmans, B. A., Scheper, R. J., and Jansen, G. (2008) Molecular basis of bortezomib resistance: proteasome subunit β5 (PSMB5) gene mutation and overexpression of PSMB5 protein. *Blood* **112,** 2489–2499
27. Mora, L. B., Buettner, R., Seigne, J., Diaz, J., Ahmad, N., Garcia, R., Bowman, T., Falcone, R., Fairclough, R., Cantor, A., Muro-Cacho, C., Livingston, S., Karras, J., Pow-Sang, J., and Jove, R. (2002) Constitutive activation of STAT3 in human prostate tumors and cell lines: direct inhibition of STAT3 signaling induces apoptosis of prostate cancer cells. *Cancer Res.* **62,** 6659–6666
28. Schust, J., Sperl, B., Hollis, A., Mayer, T. U., and Berg, T. (2006) Stattic: a small-molecule inhibitor of STAT3 activation and dimerization. *Chem. Biol.* **13,** 1235–1242
29. Iwamaru, A., Szymanski, S., Iwado, E., Aoki, H., Yokoyama, T., Fokt, I., Hess, K., Conrad, C., Madden, T., Sawaya, R., Kondo, S., Priebe, W., and Kondo, Y. (2007) A novel inhibitor of the STAT3 pathway induces apoptosis in malignant glioma cells both *in vitro* and *in vivo*. *Oncogene* **26,** 2435–2444
30. Kotha, A., Sekharam, M., Cilenti, L., Siddiquee, K., Khaled, A., Zervos, A. S., Carter, B., Turkson, J., and Jove, R. (2006) Resveratrol inhibits Src and STAT3 signaling and induces the apoptosis of malignant cells containing activated STAT3 protein. *Mol. Cancer Ther.* **5,** 621–629
31. Zhao, M., Gao, F. H., Wang, J. Y., Liu, F., Yuan, H. H., Zhang, W. Y., and Jiang, B. (2011) JAK2/STAT3 signaling pathway activation mediates tumor angiogenesis by upregulation of VEGF and bFGF in non-small-cell lung cancer. *Lung Cancer* **73,** 366–374
32. Zhou, J., Ong, C. N., Hur, G. M., and Shen, H. M. (2010) Inhibition of the JAK-STAT3 pathway by andrographolide enhances chemosensitivity of cancer cells to doxorubicin. *Biochem. Pharmacol.* **79,** 1242–1250
33. Wang, X., Xu, H., Ju, D., and Xie, Y. (2008) Disruption of Rpn4-induced proteasome expression in *Saccharomyces cerevisiae* reduces cell viability under stressed conditions. *Genetics* **180,** 1945–1953
34. Yuan, Z. L., Guan, Y. J., Chatterjee, D., and Chin, Y. E. (2005) STAT3 dimerization regulated by reversible acetylation of a single lysine residue. *Science* **307,** 269–273
35. Abdulghani, J., Gu, L., Dagvadorj, A., Lutz, J., Leiby, B., Bonuccelli, G., Lisanti, M. P., Zellweger, T., Alanen, K., Mirtti, T., Visakorpi, T., Bubendorf, L., and Nevalainen, M. T. (2008) STAT3 promotes metastatic progression of prostate cancer. *Am. J. Pathol.* **172,** 1717–1728
36. Traish, A. M., and Morgentaler, A. (2009) Epidermal growth factor receptor expression escapes androgen regulation in prostate cancer: a potential molecular switch for tumour growth. *Br. J. Cancer* **101,** 1949–1956
37. Yu, H., Pardoll, D., and Jove, R. (2009) STATs in cancer inflammation and immunity: a leading role for STAT3. *Nat. Rev. Cancer* **9,** 798–809
38. Mizoguchi, M., Betensky, R. A., Batchelor, T. T., Bernay, D. C., Louis, D. N., and Nutt, C. L. (2006) Activation of STAT3, MAPK, and AKT in malignant astrocytic gliomas: correlation with EGFR status, tumor grade, and survival. *J. Neuropathol. Exp. Neurol.* **65,** 1181–1188
39. Gan, Y., Shi, C., Inge, L., Hibner, M., Balducci, J., and Huang, Y. (2010) Differential roles of ERK and Akt pathways in regulation of EGFR-mediated signaling and motility in prostate cancer cells. *Oncogene* **29,** 4947–4958
40. de Wilt, L. H., Jansen, G., Assaraf, Y. G., van Meerloo, J., Cloos, J., Schimmer, A. D., Chan, E. T., Kirk, C. J., Peters, G. J., and Kruyt, F. A. (2012) Proteasome-based mechanisms of intrinsic and acquired bortezomib resistance in non-small cell lung cancer. *Biochem. Pharmacol.* **83,** 207–217
41. Patterson, S. G., Wei, S., Chen, X., Sallman, D. A., Gilvary, D. L., Zhong, B., Pow-Sang, J., Yeatman, T., and Djeu, J. Y. (2006) Novel role of Stat1 in the development of docetaxel resistance in prostate tumor cells. *Oncogene* **25,** 6113–6122
42. Bard, J. D., Gelebart, P., Amin, H. M., Young, L. C., Ma, Y., and Lai, R. (2009) Signal transducer and activator of transcription 3 is a transcriptional factor regulating the gene expression of SALL4. *FASEB J.* **23,** 1405–1414
43. Liu, G., Rogers, J., Murphy, C. T., and Rongo, C. (2011) EGF signalling activates the ubiquitin proteasome system to modulate *C. elegans* lifespan. *EMBO J.* **30,** 2990–3003
44. Richardson, P. G., Barlogie, B., Berenson, J., Singhal, S., Jagannath, S., Irwin, D., Rajkumar, S. V., Srkalovic, G., Alsina, M., Alexanian, R., Siegel, D., Orlowski, R. Z., Kuter, D., Limentani, S. A., Lee, S., Hideshima, T., Esseltine, D. L., Kauffman, M., Adams, J., Schenkein, D. P., and Anderson, K. C. (2003) A phase 2 study of bortezomib in relapsed, refractory myeloma. *N. Engl. J. Med.* **348,** 2609–2617
45. Fisher, R. I., Bernstein, S. H., Kahl, B. S., Djulbegovic, B., Robertson, M. J., de Vos, S., Epner, E., Krishnan, A., Leonard, J. P., Lonial, S., Stadtmauer, E. A., O'Connor, O. A., Shi, H., Boral, A. L., and Goy, A. (2006) Multicenter phase II study of bortezomib in patients with relapsed or refractory mantle cell lymphoma. *J. Clin. Oncol.* **24,** 4867–4874
46. Ri, M., Iida, S., Nakashima, T., Miyazaki, H., Mori, F., Ito, A., Inagaki, A., Kusumoto, S., Ishida, T., Komatsu, H., Shiotsu, Y., and Ueda, R. (2010) Bortezomib-resistant myeloma cell lines: a role for mutated PSMB5 in preventing the accumulation of unfolded proteins and fatal ER stress. *Leukemia* **24,** 1506–1512
47. Lü, S., Yang, J., Chen, Z., Gong, S., Zhou, H., Xu, X., and Wang, J. (2009) Different mutants of PSMB5 confer varying bortezomib resistance in T lymphoblastic lymphoma/leukemia cells derived from the Jurkat cell line. *Exp. Hematol.* **37,** 831–837
48. Politou, M., Karadimitris, A., Terpos, E., Kotsianidis, I., Apperley, J. F., and Rahemtulla, A. (2006) No evidence of mutations of the PSMB5 (β-5 subunit of proteasome) in a case of myeloma with clinical resistance to bortezomib. *Leuk. Res.* **30,** 240–241
49. Lichter, D. I., Danaee, H., Pickard, M. D., Tayber, O., Sintchak, M., Shi, H., Richardson, P. G., Cavenagh, J., Bladé, J., Façon, T., Niesvizky, R., Alsina, M., Dalton, W., Sonneveld, P., Lonial, S., van de Velde, H., Ricci, D., Esseltine, D. L., Trepicchio, W. L., Mulligan, G., and Anderson, K. C. (2012) Sequence analysis of β-subunit genes of the 20 S proteasome in patients with relapsed multiple myeloma treated with bortezomib or dexamethasone. *Blood* **120,** 4513–4516
50. Leung-Hagesteijn, C., Erdmann, N., Cheung, G., Keats, J. J., Stewart, A. K., Reece, D. E., Chung, K. C., and Tiedemann, R. E. (2013) Xbp1s-negative tumor B cells and pre-plasmablasts mediate therapeutic proteasome inhibitor resistance in multiple myeloma. *Cancer Cell* **24,** 289–304
51. Chen, S., Blank, J. L., Peters, T., Liu, X. J., Rappoli, D. M., Pickard, M. D., Menon, S., Yu, J., Driscoll, D. L., Lingaraj, T., Burkhardt, A. L., Chen, W., Garcia, K., Sappal, D. S., Gray, J., Hales, P., Leroy, P. J., Ringeling, J., Rabino, C., Spelman, J. J., Morgenstern, J. P., and Lightcap, E. S. (2010) Genome-wide siRNA screen for modulators of cell death induced by proteasome inhibitor bortezomib. *Cancer Res.* **70,** 4318–4326

Journal of Asian Natural Products Research, 2013
Vol. 15, No. 2, 111–116, http://dx.doi.org/10.1080/10286020.2012.738673

Two new sesquiterpenoids from the rhizomes of *Nardostachys jatamansi*

K. Rekha[a], R. Ranga Rao[a], Richa Pandey[a], Kothakonda Rajendra Prasad[a], Katragadda Suresh Babu[a]*, Janakiram R. Vangala[ab], Sashi V. Kalivendi[ab] and Janaswamy Madhusudana Rao[a]*.

[a]*Division of Natural Product Chemistry, Natural Product Laboratory, CSIR-Indian Institute of Chemical Technology, Tarnaka, Hyderabad 500 607, India;* [b]*Division of Pharmacology, Center for Chemical Biology, CSIR- Indian Institute of Chemical Technology, Tarnaka, Hyderabad 500 607, India*

(*Received 26 April 2012; final version received 8 October 2012*)

Phytochemical investigation of $CHCl_3$:MeOH (1:1) extract from the rhizomes of *Nardostachys jatamansi* led to the isolation of two new sesquiterpenoids (**5** and **6**), along with six known compounds (**1**–**4**, **7**, and **8**). The structures of two new compounds were established using IR, MS, 1D, and 2D NMR techniques. In addition, all the isolates were tested for their cytotoxicities against the A549 (lung cancer), DU-145 (prostate cancer), MCF-7 (breast cancer), and SK-N-SH (neuroblastoma).

Keywords: *Nardostachys jatamansi*; Valerianaceae; sesquiterpenoids; cytotoxicity

1. Introduction

Nardostachys jatamansi, a plant belonging to the family Valerianaceae, is commonly known as Indian spikenard or muskroot. It is an erect perennial herb, 10–60 m high with long stout, woody rootstock found in the alpine Himalayas from Punjab to Sikkim and Bhutan at altitude of 3000–5000 m. Its rhizomes and roots are used as anti-stress agents in traditional medicines and marketed in India as an anticonvulsant Ayurvedic drug Ayush 56 [1]. The rhizomes are used as aromatic adjunct in the preparation of medicinal oils, to promote growth of hair and also impart blackness [2]. In Ayurveda, *N. jatamansi* is used for nervous headache, excitement, menopausal symptoms, flatulence, epilepsy, and intestinal colic. Previous studies on this species have shown the plant to be particularly rich in sesquiterpenoids [3], though other classes of compounds such as sterols [4], alkaloids [5], neolignans, and lignans [6] have also been reported. As a part of our continuing efforts in the isolation of structurally interesting and biologically active compounds from the Indian medicinal plants [7–10], an initial screening procedure was conducted using the cancer cell lines. It was found that $CHCl_3$:MeOH (1:1) extract of *N. jatamansi* showed cytotoxic activity against lung cancer (A-549), prostate cancer (DU-145), breast cancer (MCF-7), and neuroblastoma (SK-N-SH) cell lines. Bioassay-guided fractionation of active extract of *N. jatamansi* led to the isolation of two new sesquiterpenoids (**5**, **6**), along with six known compounds (**1**–**4** and **7**–**8**). Herein, we report the isolation and structural elucidation of two new compounds, along with their biological activities against

*Corresponding authors. Email: suresh@iict.res.in; janaswamy@iict.res.in

Journal of Medicinal Chemistry

ARTICLE

pubs.acs.org/jmc

Design and Synthesis of Resveratrol-Based Nitrovinylstilbenes as Antimitotic Agents

M. Amarnath Reddy,[†,∥] Nishant Jain,[‡,∥] Deepthi Yada,[†] Chandan Kishore,[‡] Vangala Janakiram Reddy,[‡] P. Surendra Reddy,[†] Anthony Addlagatta,[*,‡] Shasi V. Kalivendi,[*,‡] and Bojja Sreedhar[*,†]

[†]Inorganic and Physical Chemistry Division and [‡]Centre for Chemical Biology, Indian Institute of Chemical Technology (Council of Scientific and Industrial Research), Hyderabad 500607, India

Supporting Information

ABSTRACT: A new series of resveratrol analogues was designed, synthesized, and demonstrated to be tubulin polymerization inhibitors. Most of these compounds exhibited antiproliferative activity and inhibited in vitro tubulin polymerization effectively at concentrations of 4.4−68.1 and 17−62 μM, respectively. Flow cytometry studies showed that compounds **7c**, **7e**, and **7g** arrested cells in the G2/M phase of the cell cycle. Immunocytochemistry revealed loss of intact microtubule structure in cells treated with **7c** and **7e**. Docking of compounds **7c** and **7e** with tubulin suggested that the A-ring of the compounds occupies the colchicine binding site of tubulin, which coordinates with Cys241, Leu242, Ala250, Val318, Val328, and I378, and that the nitrovinyl side chain forms two hydrogen bonds with the main loop of the β-chain at Asn249 and Ala250.

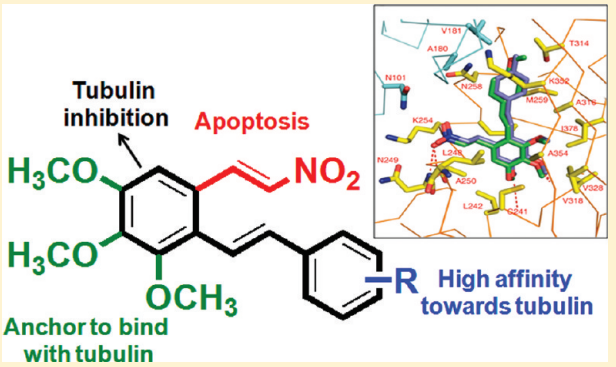

INTRODUCTION

Microtubules are cytoskeletal filaments consisting of α,β-tubulin heterodimers and are involved in a wide range of cellular functions that are critical to the life cycle of the cell.[1] In the mitotic phase of the cell cycle, microtubules are in dynamic equilibrium with tubulin dimers as tubulin is assembled into microtubules, which are disassembled to tubulin. Because inhibition of tubulin polymerization increases the number of cells in metaphase arrest,[2] the interference with the dynamics of tubulin and cell division has been proven to be clinically useful for designing anticancer agents such as paclitaxel,[3] vinblastine,[4] and docetaxel and vincristine.[5]

Resveratrol, **1** ((*E*)-3,5, 4′-trihydroxystilbene, Figure 1), a polyphenolic stilbene found in the skin of red grapes, various other fruits, and root extract of the plant *Polygonum cuspidatum*, has been an important constituent of Chinese and Japanese folk medicine.[6] Resveratrol has been extensively investigated as a cardioprotective, anti-inflammatory, and antiaging agent.[7] Recent studies have shown that resveratrol has potent anticancer effects. This was evidenced by its in vitro and in vivo inhibitory effects on the growth of a number of tumor cell lines including lymphoma, myeloma, melanoma, breast, pancreatic, colorectal, hepatocellular, and prostate carcinoma.[8] Resveratrol has been reported to have diverse effects on signaling molecules, such as downregulation of the expression of angiogenesis-associated genes, activation of the apoptotic mechanisms,[9] and induction of cell cycle arrest.[10] Resveratrol was also found to sensitize resistant tumor cell lines to a variety of chemotherapeutic agents, such as paclitaxel, thalidomide, and bortezomib.[9]

In view of the great potential of resveratrol as a potent chemotherapeutic agent against a wide variety of cancers, the trihydroxystilbene scaffold of resveratrol has been the subject of synthetic manipulations with the aim of generating novel resveratrol analogues with improved anticancer activity. The *trans*-3,4,5,4′-tetramethoxystilbene analogue, **3** (Figure 1), of **1** has been shown to possess stronger antiproliferative properties than resveratrol in HeLa cervical cancer cells, LnCaP prostate cancer cells, and HepG2 hepatoma cells, as well as HCA-7, HCEC, and HT-29 colon cancer cells.[11]

Compounds having a nitrovinyl side chain attached to the aromatic ring (β-nitrostyrenes) have been reported as pro-apoptotic anticancer agents, and the nitrovinyl moiety was identified as the pharmacophore for this activity.[12] These compounds have also been described as highly potent and selective inhibitors of human telomerase, by which the essential telomeres that protect chromosomes from exonucleolytic degradation are added to the end of eukaryotic chromosomes.[13] Recently, we have reported nitrovinylbiphenyls as potent cytotoxic agents against a wide range of cancer cell lines.[14] In the present study we report the synthesis and antitumor evaluation of nitrovinylstilbenes that are resveratrol analogues. The *trans*-stilbene

Received: May 19, 2011
Published: August 18, 2011

dx.doi.org/10.1021/jm200639r | *J. Med. Chem.* 2011, 54, 6751–6760

JOC The Journal of Organic Chemistry

ARTICLE

pubs.acs.org/joc

Stereoselective Total Synthesis of (+)-Oploxyne A, (−)-Oploxyne B, and Their C-10 Epimers and Structure Revision of Natural Oploxyne B

J. S. Yadav,*[,†,‡] Kumaraswamy Boyapelly,[†] Sathish Reddy Alugubelli,[†] Srihari Pabbaraja,[†] Janakiram R Vangala,[§] and Shasi V Kalivendi*[,§]

[†]Organic Division-I, Indian Institute of Chemical Technology, CSIR, Hyderabad-500 607, India

[‡]King Saud University, Riyadh-11451, Saudi Arabia

[§]Chemical Biology, Indian Institute of Chemical Technology, CSIR, Hyderabad-500 607, India

Supporting Information

ABSTRACT: The first total synthesis of recently isolated diacetylene alcohols oploxyne A, oploxyne B, and their C-10 epimers was accomplished. The structure of natural oploxyne B has been revised. The key steps involved are base-induced double elimination of a carbohydrate-derived β-alkoxy chloride to generate the chiral acetylenic alcohol and Cadiot−Chodkiewicz cross-coupling reaction. The target compounds displayed potent cytotoxicity against neuroblastoma and prostate cancer cell lines.

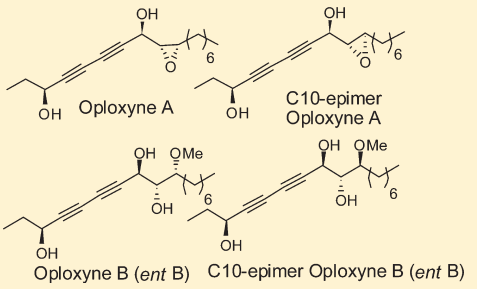

INTRODUCTION

Polyacetylene containing molecules attract significant attention due to their impressive biological properties such as antitumor, antiinflammatory, antimicrobial, antiviral, cytotoxic, and phytotoxic activities.[1] For example, the diacetylene panaxydol **1** (Figure 1) displayed antiproliferative effects against malignant cells[2] and panaxytriol **2**, obtained from Red ginseng, was found to show inhibitory activity against MK-1 cells with IC_{50} 8.5 ng/mL and suppress the growth of B16 melanoma cells in mice.[3] Recently, investigations on the inhibitors for the formation of NO and prostaglandin E_2 (PGE_2) in lipopolysaccharide (LPS)-induced murine macrophage RAW 267.7 cells resulted in isolation of two new diynes oploxynes A and B from the CH_2Cl_2 extract of the stem of *Oplopanax elatus*.[4] The structures of oploxyne A **3** and oploxyne B **4** were established based on NMR spectroscopy through chiral derivatization. Oploxyne A was found to display inhibition of NO and PGE_2 production with an IC_{50} of 1.90 ± 0.28 and 3.08 ± 0.37 mg/mL. In continuation to our program toward the development of new protocols and their applications in the total synthesis of biologically potent natural products,[5] we herein describe the first total synthesis of oploxyne A, oploxyne B, and their C-10 epimers **5** and **6**, wherein a strategy that allows facile access to all four molecules (**3**−**6**) has been employed. These target compounds when screened against cancer cell lines were found to display potent cytotoxicity.

We initially focused on the total synthesis of oploxynes A and B and also accomplished the total synthesis of their C-10 epimers. Retrosynthetically, oploxyne A and oploxyne B were envisaged to be obtained in a convergent fashion wherein two fragments **10** and **11** are coupled together by Cadiot−Chodkiewicz cross-coupling to give the key intermediate **9**. The intermediate **9** can be easily maneuvered to synthesize the final targets involving two steps: tosylation to obtain **7**, one-pot PMB cleavage, acetonide deprotection, and epoxide formation to yield the target oploxyne A or methylation of **9** to obtain methyl ether **8** followed by PMB and acetonide deprotection to yield oploxyne B **4**. While the fragment **10** can be obtained from readily available sugar D-mannitol, the other key fragment **11** could be obtained from D-ribose (Scheme 1).

RESULTS AND DISCUSSION

Our synthesis of fragment **10** is delineated in Scheme 2, which departs from the prior work at the readily available secondary alcohol **12** obtained from D-mannitol.[6] PMB protection of compound **12** yielded the corresponding PMB ether **13**, which was treated with 1 M HCl to obtain the diol **14**. The diol **14** upon treatment with $NaIO_4$ yielded the corresponding aldehyde,[7] which was converted to alkyne **16** by employing Ohira−Bestmann reagent **15**.[8] The free terminal acetylene was converted to the key intermediate bromo alkyne **10** by using NBS and catalytic silver nitrate in 98% yield (Scheme 2).

For the synthesis of fragment **11**, we started with the mixture of esters **18** and **19** synthesized from D-ribose following the known procedures.[9] The mixture of esters **18** and **19** was reduced to a mixture of aldehydes **20** and **21** and subjected to a Wittig reaction with *n*-pentyltriphenylphosphonium bromide in the presence of $NaNH_2$ to afford diastereomers **22** and **23** in 68.5:31.5 ratio (diastereomers **22**, **23** were in turn a mixture of

Received: December 10, 2010
Published: March 17, 2011

